

**AN EXPERIMENTAL AND EMPIRICAL INVESTIGATION OF
CONVECTIVE HEAT TRANSFER FOR GAS-LIQUID
TWO-PHASE FLOW IN VERTICAL
AND HORIZONTAL PIPES**

By

DONGWOO KIM

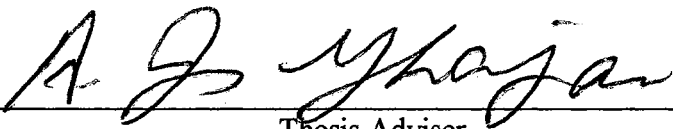
**Bachelor of Science
Soongsil University
Seoul, Korea
1988**

**Master of Science
Oklahoma State University
Stillwater, Oklahoma
1994**

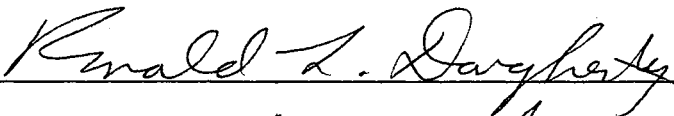
**Submitted to the Faculty of the
Graduate College of the
Oklahoma State University
in partial fulfillment of
the requirements for
the Degree of
DOCTOR OF PHILOSOPHY
July, 2000**

**AN EXPERIMENTAL AND EMPIRICAL INVESTIGATION OF
CONVECTIVE HEAT TRANSFER FOR GAS-LIQUID
TWO-PHASE FLOW IN VERTICAL
AND HORIZONTAL PIPES**

Thesis Approved:

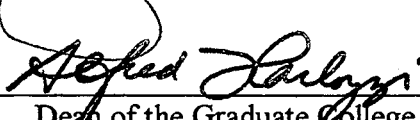


Thesis Adviser









Dean of the Graduate College

ACKNOWLEDGMENTS

I wish to express my sincere appreciation to my major advisor, Dr. Afshin Ghajar for his intelligent supervision, constructive guidance, inspiration and endless patience. My sincere appreciation extends to my other committee members Dr. Ronald Dougherty, Dr. Frank Chambers, and Dr. Jan Wagner, whose guidance, assistance, encouragement, and friendship are also invaluable. I would like to thank Dr. Afshin Ghajar and the School of Mechanical and Aerospace Engineering for providing me with this research opportunity and their generous financial support.

Moreover, I wish to express my sincere gratitude to those who provided suggestions and assistance for this study, Dr. Chung-Shin Park, Dr. Eun-Soo Choi, Dr. Seoung-Jhin Choi, Mr. Venkata Ryali, and Mr. Jae-Yong Kim.

I would also like to give my special appreciation to my beloved wife, Miyoung, for her precious suggestions to my research, her strong encouragement at times of difficulty, love and understanding throughout this whole process. Thanks also go to my mother who supported me emotionally, monetarily, and spiritually.

Finally, I would like to thank Jesus and the Korean Baptist Church of Stillwater for the spiritual supports during the years of this study.

TABLE OF CONTENTS

Chapter	Page
I. INTRODUCTION.....	1
1.1 Definitions of Variables Used in Two-Phase Flow.....	2
1.1.1 Flow Rates and Void Fraction (α).....	3
1.1.2 Velocities.....	7
1.2 Flow Patterns.....	8
1.2.1 Upward Vertical Flow.....	10
1.2.2 Horizontal Flow.....	16
1.3 Literature Survey.....	21
1.3.1 Extended Sieder-Tate Type Correlation for Two-Phase Heat Transfer.....	21
1.3.2 Lockhart-Martinelli Type Correlation for Heat Transfer	33
1.3.3 Explicit Void Fraction Parameters in Two-Phase Flow Heat Transfer Correlation.....	36
1.3.4 Simplified Numerical/Analytical Approach.....	40
1.3.5 Two-Phase Heat Transfer Experimental Data.....	44
1.4 Preliminary Comparisons.....	51
1.4.1 Introduction of Preliminary Comparisons.....	52
1.4.2 Water-Air Data of Vijay (1978).....	56
1.4.3 Glycerin-Air Data of Vijay (1978).....	60
1.4.4 Silicone-Air Data of Rezkallah (1986).....	60
1.4.5 Water-Air Data of Pletcher (1966) and King (1952).....	66
1.4.6 Summary and Conclusions of the Preliminary Comparisons.....	66
1.5 Shortcomings of the Previous Work.....	72
1.6 Objectives.....	75
II. DEVELOPMENT OF A GENERAL TWO-PHASE HEAT TRANSFER CORRELATION FOR VERTICAL PIPES.....	77
2.1 Comparison of 20 Two-Phase Heat Transfer Correlations with Seven Sets of Experimental Data, Including Flow Pattern and Tube Inclination Effects.....	78
2.1.2 Introduction.....	78
2.1.2 Results from Comparison with Correlation Limitations..	81

Chapter	Page
2.1.3 Results from Comparison without Correlation	
Limitations.....	83
2.1.4 Summary and Conclusions.....	89
2.2 Development of Improved Two-Phase Two-Component Pipe	
Flow Heat Transfer Correlations from Existing Correlations	
and Published Data.....	94
2.2.1 Introduction.....	94
2.2.2 Results and Discussion.....	96
2.2.3 Summary and Conclusions.....	108
2.3 A General Heat Transfer Correlation for Turbulent Gas-Liquid	
Two-Phase Flow in Vertical Pipes.....	110
2.3.1 Introduction.....	111
2.3.2 Development of A New General Correlation.....	112
2.3.3 Prediction Results and Discussion.....	118
2.3.4 Summary and Conclusions.....	124
 III. EXPERIMENTAL SETUP AND DATA REDUCTION.....	 126
3.1 Description of the Experimental Setup and Equipments.....	126
3.1.1 Test Section.....	128
3.1.2 Thermocouples.....	129
3.1.3 Pressure Taps and Pressure Transducers.....	132
3.1.4 Gas-Liquid Mixer and Calming Section.....	134
3.1.5 Mixing Well.....	139
3.1.6 Voltmeter and DC Ammeter.....	139
3.1.7 Heat Exchanger.....	140
3.1.8 Pumps.....	140
3.1.9 Liquid Turbine Meters and Frequency Meter.....	141
3.1.10 Gas Flowmeter and Absolute Pressure Transducer.....	143
3.1.11 Water Reservoirs.....	144
3.1.12 Data Acquisition System.....	144
3.2 Experimental Calibration.....	145
3.2.1 Thermocouples.....	145
3.2.2 Calibration of Liquid Turbine Meter.....	150
3.2.3 Calibration of Gas Flow Meter.....	152
3.2.4 Calibration of System Pressure Transducer.....	154
3.2.5 Calibration of Differential Pressure Transducer.....	154
3.2.6 Calibration of Gas Pressure Transducer.....	157
3.3 Data Reduction Programs.....	157
3.3.1 Input Data.....	160
3.3.2 Finite-Difference Formulations.....	161
3.3.3 Physical Properties of the Fluids.....	166
3.3.4 Output.....	167

Chapter	Page
3.4 Experimental Procedures.....	169
3.4.1 Testing the Loop.....	169
3.4.2 Warm Up.....	169
3.4.3 Data Collection and Shut Down.....	170
 IV. RESULTS AND DISCUSSION.....	 173
4.1 Single-Phase Heat Transfer Results.....	173
4.1.1 Nusselt Numbers Along the Test Section.....	174
4.1.2 Comparison of Available Correlations with Experimental Data.....	 174
4.2 Presentation of Flow Patterns.....	185
4.2.1 Flow Pattern Observation.....	186
4.2.2 Experimental Data on Taitel and Dukler (1976) Flow Pattern Map.....	 191
4.2.3 Flow Pattern Classification Using the Mass Flow Rates of Air and Water.....	 202
4.3 Two-Phase Heat Transfer Results.....	207
4.3.1 Two-Phase Air-Water Experimental Data.....	207
4.3.2 Prediction of Air-Water Two-Phase Heat Transfer Experimental Data.....	 221
 V. SUMMARY, CONCLUSIONS AND RECOMMENDATIONS.....	 229
5.1 Summary and Conclusions.....	229
5.2 Recommendations.....	237
 REFERENCES.....	 241
 APPENDIX A— UNCERTAINTY ANALYSIS.....	 248
 APPENDIX B— COMPUTER CODE LISTING FOR RHt99F.....	 253
 APPENDIX C—AIR-WATER EXPERIMENTAL DATA.....	 280

LIST OF TABLES

Table		Page
1.1	Values of Constants Suggested by the Various Models and Correlations.....	7
1.2	Extended Sieder-Tate Type Correlations for Two-Phase Heat Transfer.....	22
1.3	Lockhart-Martinelli Type Correlations for Two-Phase Heat Transfer..	34
1.4	Explicit Void Fraction Parameters in Two-Phase Heat Transfer Correlations.....	37
1.5	Resources with Experimental Data.....	44
1.6	Heat Transfer Correlations Chosen for the Preliminary Comparisons...	53
1.7	Limitations of the Heat Transfer Correlations Used in the Preliminary Comparisons.....	54
1.8	Ranges of the Experimental Data Used in the Preliminary Comparisons.....	55
1.9	Comparison of Water-Air Experimental Data (139 Data Points) of Vijay (1978) with the Suggested Correlations.....	57
1.10	Comparison of Glycerin-Air Experimental Data (57 Data Points) of Vijay (1978) with the Suggested Correlations.....	61
1.11	Comparison of Silicone-Air Experimental Data (162 Data Points) of Rezkallah (1986) with the Suggested Correlations.....	63
1.12	Comparison of 48 Water-Air Experimental Data Points of Pletcher (1966) and 21 Water-Air Experimental Data Points of King (1952) with the Suggested Correlations.....	67

Table		Page
1.13	Recommended Correlations from the Preliminary Comparisons with Regard to Pipe Orientation, Fluids, and Flow Patterns.....	69
1.14	Available Experimental Data Points.....	74
2.1	Ranges of the Experimental Data Used in this Study.....	80
2.2	Comparison of Water-Air Experimental Data (139 Data Points) of Vijay (1978) with the Studied Correlations.....	82
2.3	Comparison of Water-Air Experimental Data (139 Data Points) of Vijay (1978) with the Studied Correlations.....	86
2.4	Recommended Correlations from the General Comparisons with Regard to Pipe Orientation, Fluids, and Major Flow Patterns.....	90
2.5	Recommended Correlations from the General Comparisons with Regard to Pipe Orientation, Fluids, and Transition Flow Patterns.....	91
2.6	Different Values for the Exponent of the Key Parameters of Six Two-Phase Heat Transfer Correlations.....	97
2.7	Recommended Modified Two-Phase Heat Transfer Correlations for Five Fluid Combinations and Four Major Flow Patterns in a Vertical Pipe.....	103
2.8	Recommended Simplified Two-Phase Heat Transfer Correlations for Five Fluid Combinations and Four Major Flow Patterns in a Vertical Pipe.....	103
2.9	Simplified Two-Phase Heat Transfer Correlations, with Recommendations, Predicting all Five Fluid Combinations for Each of the Four Major Flow Patterns in a Vertical Pipe.....	106
2.10	Results of the Predictions for Available Experimental Data Using the Recommended Correlations by Kim et al. (1999a).....	112
2.11	Ranges of the Experimental Data for Vertical Tubes Used in this Study.....	113
2.12	Results of the Predictions for Available Two-Phase Heat Transfer Experimental Data Using the Recommended General Correlation.....	120

Table		Page
2.13	Summary of the Values of the Leading Coefficient (C) and Exponents (m, n, p, q) in the General Heat Transfer Coefficients Correlation (h_{TP}) and the Prediction Results.....	120
3.1	Physical Properties of the Fluids Used in this Study.....	166
4.1	Ranges of Reynolds, Prandtl, and Nusselt Numbers, and % Deviations for Colburn (1933) Correlation.....	179
4.2	Ranges of Reynolds, Prandtl, and Nusselt Numbers, and % Deviations for Sieder and Tate (1936) Correlation.....	180
4.3	Ranges of Reynolds, Prandtl, and Nusselt Numbers, and % Deviations for Ghajar and Tam (1994) Correlation.....	181
4.4	Ranges of Reynolds, Prandtl, and Nusselt Numbers, and % Deviations for Gnielinski [1] (1976) Correlation.....	183
4.5	Ranges of Reynolds, Prandtl, and Nusselt Numbers, and % Deviation for Gnielinski [3] (1976) Correlation.....	184
4.6	Summary of the Two-Phase Flow Pattern Experimental Data.....	188
4.7	Minimum and Maximum Values of the Air and Water Mass Flow Rates According to the Different Flow Patterns and Number of Experimental Data Points Taken.....	206
4.8	Summary of the Air-Water Experimental Data.....	208
4.9	Summary of the Values of the Leading Coefficient (C) and Exponents (m, n, p, q) in the Recommended Heat Transfer Coefficient Correlation (h_{TP}), the Results of Prediction, and the Parameter Range of the Correlation.....	227

LIST OF FIGURES

Figure		Page
1.1	Idealized Model of Two-Phase Gas-Liquid Flow in an Inclined Tube.....	4
1.2	Schematic Representations of Flow Regimes Observed in Vertical Upward Gas-Liquid Two-Phase Flow.....	12
1.3	Flow Regime Map of the Type Proposed by Hewitt & Roberts (1979).....	13
1.4	Schematic Representations of Flow Regimes Observed in Horizontal Gas-Liquid Flow.....	18
1.5	Flow Regime Map for Horizontal Gas-Liquid Flow of the Type Proposed by Taitel & Dukler (1976).....	20
1.6	Comparison of Knott et al. (1959) Correlation with Vijay's (1978) Water-Air Experimental Data.....	58
1.7	Comparison of Ravipudi & Godbold (1978) Correlation with Vijay's (1978) Water-Air Experimental Data.....	58
1.8	Comparison of Aggour (1978) Correlation with Vijay's (1978) Water-Air Experimental Data.....	59
1.9	Comparison of Aggour (1978) Correlation with Vijay's (1978) Glycerin-Air Experimental Data.....	62
1.10	Comparison of Rezkallah & Sims (1987) Correlation with Rezkallah's (1986) Silicone-Air Experimental Data.....	64
1.11	Comparison of Ravipudi & Godbold (1978) Correlation with Rezkallah's (1986) Silicone-Air Experimental Data.....	64

Figure		Page
1.12	Comparison of Shah (1981) Correlation with Rezkallah's (1986) Silicone-Air Experimental Data.....	65
1.13	Comparison of Shah (1981) Correlation with Pletcher's (1966) Water-Air Experimental Data.....	68
1.14	Comparison of Correlations of Chu & Jones (1980), King (1952), Kudirka et al. (1965), Martin & Sims (1971), and Ravipudi & Godbold (1978) with King's (1952) Water-Air Experimental Data.....	68
2.1	Comparison of Chu & Jones (1980) Correlation with Vijay's (1978) Water-Air Experimental Data.....	84
2.2	Comparison of Ravipudi & Godbold (1978) Correlation with Vijay's (1978) Water-Air Experimental Data.....	85
2.3	Comparison of Knott et al. (1959) Correlation with Vijay's (1978) Water-Air Experimental Data.....	88
2.4	Comparison of Knott et al. (1959) Original and Modified Correlation with Aggour [1] Water-Helium Experimental Data in a Vertical Pipe	105
2.5	Comparison of the Modified Shah (1981), Aggour (1978), Rezkallah & Sims (1987), and Ravipudi & Godbold (1978) Correlations with the Experimental Data of Four Major Flow Patterns in a Vertical Pipe.....	107
2.6	Comparison of the General Correlation (Equation 2.11) with All of the Two-Phase Heat Transfer Experimental Data (255 Data Points) in Table 2.11.....	121
3.1	Schematic Diagram of the Experimental Setup.....	127
3.2	Copper Plate and Electrode Cables.....	130
3.3	Thermocouples and Pressure Tap Locations Along the Test Section..	131
3.4	Schematic Diagram of the Gas-Liquid Mixer.....	135
3.5	Flange Connection between Stainless Steel Pipe and Calming Section	137
3.6	Mixer, Calming Section, and Flange Connection to Stainless Steel Test Section.....	138

Figure		Page
3.7	Pumps and By-pass Line.....	142
3.8	Calibration Curve for Thermocouple 1.....	147
3.9	Trend of Temperature Difference between Thermocouple and Bath vs. Bath Temperature.....	147
3.10(a)	Temperature Readings from 40 Thermocouples along the Test Section Based on the Time Variation.....	149
3.10(b)	Temperatures of Bulk Inlet (T_{B_in}) and Outlet (T_{B_out}) of the Fluid and Water Temperature of the Storage Tank (T_{Tank}).....	149
3.11(a)	Temperature Readings from 40 Thermocouples along the Test Section Based on the Time Variation.....	151
3.11(b)	Averaged Wall Temperatures of the Thermocouple Stations and Bulk Inlet (T_{B_in}) and Outlet (T_{B_out}) Temperatures of the Fluid.....	151
3.12	Calibration of Liquid Turbine Meters.....	153
3.13	Calibration of Gas Flow Meter.....	155
3.14	Calibration of System Pressure Transducer.....	156
3.15	Calibration of Differential Pressure Transducer.....	158
3.16	Calibration of Gas Absolute Pressure Transducer.....	159
3.17	Finite-Difference Grid Arrangement.....	162
3.18	A Sample Output Data File from the Computer Program RHt99F.....	168
4.1	Experimental Nusselt Number vs. Dimensionless Axial Distance for All Types of the Test Runs.....	175
4.2	Comparison of Nu_{exp} vs. Nu_{cal} from Selected Correlations at Thermocouple Station No. 6 ($3,000 < Re < 30,000$).....	177
4.3	Deviations of Nu_{cal} Referenced to Nu_{exp} vs. Reynolds Number at Thermocouple Station No. 6 ($3,000 < Re < 30,000$).....	178

Figure		Page
4.4	Nu_{EXP} vs. Nu_{CAL} – Colburn (1933) Correlation.....	179
4.5	Nu_{EXP} vs. Nu_{CAL} - Sieder and Tate (1936) Correlation.....	181
4.6	Nu_{EXP} vs. Nu_{CAL} - Ghajar and Tam (1994) Correlation.....	182
4.7	Nu_{EXP} vs. Nu_{CAL} - Gnielinski [1] (1976) Correlation.....	183
4.8	Nu_{EXP} vs. Nu_{CAL} - Gnielinski [3] (1976) Correlation.....	185
4.9	Photographs of Representative Flow Patterns.....	189
4.10	Comparison of Taitel & Dukler Map with Stratified Flow Pattern Data.....	194
4.11	Comparison of Taitel & Dukler Map with Wavy Flow Pattern Data...	195
4.12	Comparison of Taitel & Dukler Map with Wavy/Slug Transition Flow Pattern Data.....	197
4.13	Comparison of Taitel & Dukler Map with Slug Flow Pattern Data....	198
4.14	Comparison of Taitel & Dukler Map with Annular/Wavy Transition Flow Pattern Data.....	200
4.15	Comparison of Taitel & Dukler Map with Annular/Bubbly and Annular/Bubbly/Slug Flow Pattern Data.....	201
4.16	Comparison of Taitel & Dukler Map with Bubbly/Slug Flow Pattern Data.....	203
4.17	Observed Flow Pattern Data as a Function of the Corresponding Mass Flow Rates of Air and Water.....	205
4.18(a)	Variation in Bulk Inlet (T_{B_in}) and Outlet (T_{B_out}) Temperatures of the Fluid and Water Temperature of the Storage Tank (T_{Tank}) During the Measurement Period.....	211
4.18(b)	Variation of Temperature Difference between Bulk Inlet (T_{B_in}) and Outlet (T_{B_out}) of the Fluid with the Measurement Time.....	211

Figure		Page
4.19(a)	Averaged Wall Temperatures of the Thermocouple Stations and Bulk Inlet (T_{B_in}) and Outlet (T_{B_out}) Temperatures of the Fluids.....	212
4.19(b)	Temperature Difference between the Averaged Wall (T_{wall}) and Fluid Bulk (T_B) of the Test Section.....	212
4.20	Local Heat Transfer Coefficients Along the Test Section for Test Runs Listed in Table 4.8.....	214
4.21	Variation of Mean Heat Transfer Coefficients with Superficial Reynolds Numbers (Re_{SL} and Re_{SG}) for All Flow Patterns Listed in Table 4.8.....	215
4.22(a)	Air-Water Two-Phase Heat Transfer Coefficients in Wavy Flow Pattern (20 Data Points).....	218
4.22(a)	Air-Water Two-Phase Heat Transfer Coefficients in Wavy/Annular Transitional Flow Pattern (41 Data Points).....	218
4.22(c)	Air-Water Two-Phase Heat Transfer Coefficients in Slug Flow Pattern (53 Data Points).....	219
4.22(d)	Air-Water Two-Phase Heat Transfer Coefficients in Bubbly/Slug or Annular/Bubbly/Slug Transitional Flow Pattern (36 Data Points).....	219
4.23	Comparison of Kim et al. (2000) Vertical Pipe Correlation with Current Horizontal Pipe Experimental Data (150 pts.) and King's (1952) Horizontal Pipe Data (21 pts.).....	223
4.24	Comparison of Recommended Correlation for Slug Flow and Bubbly-Slug or Annular-Bubbly-Slug Transitional Flow with Current Horizontal Pipe Experimental Data (89 pts.) and King's (1952) Horizontal Pipe Data (21 pts.).....	223
4.25	Comparison of Recommended Correlations with Wavy Flow Data (20 pts.) and Wavy-Annular Transitional Flow Data (41 pts.) from Current Study.....	228
4.26	Comparison of Recommended Correlations with Data from Current Study (150 pts.).....	228

NOMENCLATURE

English Letters

A	cross sectional area, ft ² or m ²
c	specific heat at constant pressure, Btu/(lbm-°F) or kJ/(kg-K)
D	inside diameter of the tube, ft or m
G _t	mass velocity of total flow (= ρV), lbm/(hr-ft ²) or kg/(s-m ²)
h	heat transfer coefficient, Btu/(hr-ft ² -°F) or W/(m ² -K)
k	thermal conductivity, Btu/(hr-ft-°F) or W/(m-K)
k _s	thermal conductivity of stainless steel, Btu/(hr-ft-°F) or W/(m-K)
L	length of the heated test section, ft or m
ṁ	mass flow rate, lbm/hr or kg/s
Nu	Nusselt number (= hD/k), dimensionless
P	mean system pressure, psi or Pa
Pa	atmospheric pressure, psi or Pa
ΔP _M	momentum pressure drop, psf or Pa
ΔP/ΔL	total pressure drop per unit length, lbf/ft ³ or Pa/m
Pr	Prandtl number (= c _p μ/k), dimensionless
Q	volumetric flow rate, ft ³ /min or m ³ /s
q̇"	heat flux per unit area, Btu/(hr-ft ²) or W/m ²
Re _M	mixture Reynolds number (= ρ _L U _M *D/μ _L in [Ueda & Hanaoka, 1967]), dimensionless, where $U_M^* = V_L + 1.2(Re_S)^{-0.25} V_S - 12 F_{TED} V_{ED} + 16(F_{TS})^{1.25} V_S,$ $Re_S = \rho_L V_S D (1 - \sqrt{\alpha}) / \mu_L, V_{ED} = V_{SL} + V_{SG}, F_{TED} = \alpha D (1 - \sqrt{\alpha}) / V_{ED}^2,$ $F_{TS} = D(1 - \sqrt{\alpha}) / V_S^2, V_L = V_{SL} / (1 - \alpha), V_G = V_{SG} / \alpha,$ $V_S = \text{slip velocity} = V_G - V_L$
Re _{TP}	two-phase flow Reynolds number, dimensionless = Re _{SL} /(1-α) in [Chu & Jones, 1980] = G _F D/μ _F where G _F = mass flow rate of froth and μ _F = (μ _w +μ _A)/2 in [Dusseau, 1968] = Re _{SL} + Re _{SG} in [Elamvaluthi & Srinivas, 1984] and [Groothuis & Hendaal, 1959]
R _L	liquid volume fraction (= 1-α), dimensionless
T	temperature, °F or °C
V	average velocity in the test section, ft/s or m/s
x	flow quality, dimensionless
X _{TT}	Martinelli parameter [= $\left(\frac{1-x}{x}\right)^{0.9} \left(\frac{\rho_G}{\rho_L}\right)^{0.5} \left(\frac{\mu_L}{\mu_G}\right)^{0.1}$], dimensionless

Abbreviations

A	air or annular flow
B	bubbly flow
B-S	bubbly-slug transitional flow (other combinations with dashes are also transitional flows)
C	churn flow
F	froth flow
H	horizontal
M	mist flow
S	slug flow
V	vertical
W	water

Greek Symbols

α	void fraction [= $A_G/(A_G+A_L)$], dimensionless
μ	dynamic viscosity, lbm/(hr-ft) or Pa-s
ρ	density, lbm/ft ³ or kg/m ³
ϕ_g, ϕ_l	Lockhart-Martinelli (1949) two-phase gas and liquid multipliers, dimensionless

Subscripts

A	air
B	bulk
CAL	predicted
EXP	experimental
G	gas
L	liquid
MIX	gas-liquid mixture
TP	two-phase
TPF	two-phase frictional
SG	superficial gas
SL	superficial liquid
W	wall

CHAPTER I

INTRODUCTION

Two-phase flow occurs frequently in the processing industries, and the design of such equipment as condensers, heat exchangers, and reactors depends on a detailed knowledge of two-phase flow to predict heat transfer and pressure drop in conjunction with void fraction and flow pattern. The flow of a liquid and a permanent gas (usually referred to as two-phase, two-component flow) also involves a wide range of industrial applications. Examples are the flow of natural gas in pipelines, oil wells and many chemical processes. The flows in pipes may be vertical, inclined or horizontal, and methods must be available for predicting heat transfer and pressure drop in pipes at any inclination angle. Providing information on the heat transfer coefficient in the fluids in wellbores and pipelines to predict the occurrence of paraffin deposition on the pipe wall is another example of the importance of two-phase flow, which has received considerable attention in recent years due to the growing need for more economical design and optimization of operating conditions.

When a natural gas-paraffinic liquid (or crude oil) mixture flows in wellbores and pipelines, wax precipitation and deposition will take place once the pipe wall temperature becomes lower than the paraffinic cloud point (or wax appearance temperature) and lower

than the bulk fluid temperature. The paraffin deposition problem can cause a loss of millions of dollars per year worldwide through the numerous cost of prevention and remediation, pipeline replacement and abandonment, and extra horsepower requirements. It also becomes increasingly imperative to adequately identify the conditions for paraffin precipitation and predict the paraffin deposition rates to optimize the design and operation of the gas and oil production systems. Therefore, the detailed knowledge of the convective heat transfer from the gas-liquid mixture to the pipe wall before the occurrence of a wax layer deposit on the pipe wall is required to adequately achieve the identification and prediction of the wax deposition in wellbores and pipelines.

The main purpose of this study is to develop a comprehensive model (or correlation) for predicting heat transfer coefficients during gas-liquid two-phase flow in pipes, by evaluating and refining existing models/correlations on the basis of their physical merits and comparisons with the available data from the open literature and the collected data from our own experiments. This chapter is devoted to the descriptions of the background in two-phase flow study including the flow patterns possibly observed in two-phase flow in pipes, the literature survey of related studies, and the objectives of this study.

1.1 Definitions of Variables Used in Two-Phase Flow

In internal gas and liquid mixture flow, the gas and liquid are in simultaneous motion inside the pipe. The resulting two-phase flow is generally more complicated physically than single-phase flow. In addition to the usual inertia, viscous, and pressure

forces present in single-phase flow, two-phase flows are also affected by interfacial tension forces, the wetting characteristics of the liquid on the tube wall, and the exchange of momentum between the liquid and gas phases in the flow. Also, since the flow conditions in a pipe vary along its length, over its cross section, and with time, the gas-liquid flow is an extremely complex three-dimensional transient problem. Thus, most researchers have sought simplified descriptions of the problem which are both capable of analysis and retain important features of the flow. The descriptions, or definitions of variables, presented here is that of one-dimensional flow (the flow conditions in each phase only vary with distance along the tube) and it is perhaps the most important and common method developed for analyzing two-phase pressure drop and heat transfer.

1.1.1 Flow Rates and Void Fraction (α)

Figure 1.1 shows a very simple two-phase flow. Although this simple flow configuration will be specifically referred to, the basic definitions and terminology described here would be applicable to any gas-liquid flow circumstance. The total mass flow rate through the tube \dot{m} is equal to the sum of the mass flow rates of gas \dot{m}_G and liquid \dot{m}_L ,

$$\dot{m} = \dot{m}_G + \dot{m}_L \quad (1.1)$$

The ratio of gas flow to total flow x ,

$$x = \frac{\dot{m}_G}{\dot{m}} \quad (1.2)$$

is sometimes called the dryness fraction or the quality. In similar fashion, the value of

$1 - x = \dot{m}_L / \dot{m}$ is sometimes referred to as the wetness fraction.

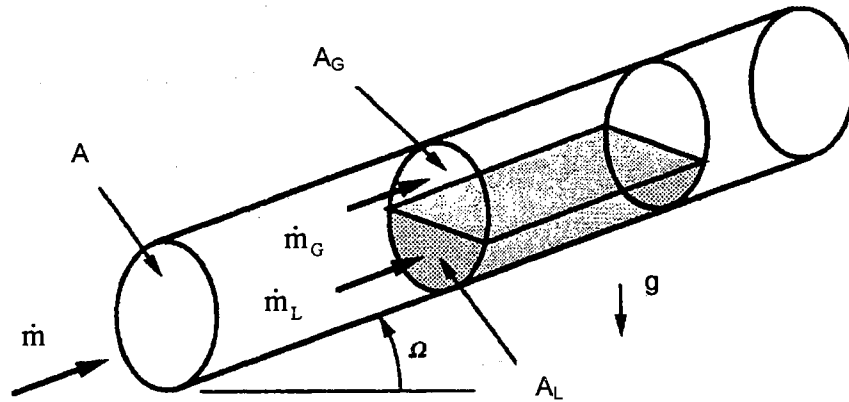


Figure 1.1 Idealized Model of Two-Phase Gas-Liquid Flow in an Inclined Tube
(Adapted from Carey, 1992)

For a tube with cross-sectional area A , the mass flux or mass velocity G is defined as

$$G = \frac{\dot{m}}{A} \quad (1.3)$$

The void fraction α is defined as the ratio of the gas-flow cross sectional area A_G to the total cross-sectional area A ,

$$\alpha = \frac{A_G}{A} \quad (1.4)$$

where A must equal the sum of the cross-sectional areas occupied by the two-phases:

$$A = A_G + A_L \quad (1.5)$$

It follows directly that liquid volume fraction or liquid holdup R_L is given by

$$R_L = 1 - \alpha = \frac{A_L}{A} \quad (1.6)$$

If gas and liquid phases travel at the same velocity (no-slippage); the assumption is no slip between phases, no-slip holdup, sometimes called input liquid content λ_L and is defined as

$$\lambda_L = \frac{Q_L}{Q_L + Q_G} \quad (1.7)$$

where Q_L and Q_G are in-situ liquid and gas volumetric flow rates, respectively.

It is obvious that the difference between the liquid holdup and the no-slip holdup is a measure of the degree of slippage between the gas and liquid phases.

The gas mass flow rate \dot{m}_G is given by

$$\dot{m}_G = \dot{m}x = \int_{A_G} \rho_G V_G dA \quad (1.8)$$

where x is the gas-phase mass flow fraction, ρ_G the gas density, V_G the gas velocity, and \dot{m} the total mass flow rate. Now, since for a one-dimensional flow ρ_G and V_G do not vary over the cross-section A_G , Equation (1.8) becomes

$$\dot{m}x = \rho_G V_G \int_{A_G} dA = \rho_G V_G \alpha A \quad (1.9)$$

Similarly, for the liquid phase

$$\dot{m}_L = \dot{m}(1-x) = \rho_L V_L (1-\alpha)A \quad (1.10)$$

where ρ_L is the liquid density and V_L the liquid velocity.

Dividing Equation (1.9) by Equation (1.10) gives

$$K = \frac{V_G}{V_L} = \left(\frac{x}{1-x} \right) \left(\frac{1-\alpha}{\alpha} \right) \frac{\rho_L}{\rho_G} \quad (1.11)$$

where K is often referred to as the 'slip ratio'. It is usually greater than unity which means that V_G is usually greater than V_L , and the relative velocity $V_G - V_L$ is often referred to as the 'slip velocity'.

If there is no slip between the phases (often referred to as 'homogeneous flow'), i.e.

K is unity; Equation (1.11) becomes

$$\frac{1-\alpha}{\alpha} = \left(\frac{1-x}{x}\right) \frac{\rho_G}{\rho_L} \quad (1.12)$$

There exist several empirical methods for determining the value of α or K and Butterworth (1975) summarized some of the well known empirical equations having the following form:

$$\frac{1-\alpha}{\alpha} = C \left(\frac{1-x}{x}\right)^p \left(\frac{\rho_G}{\rho_L}\right)^q \left(\frac{\mu_L}{\mu_G}\right)^r \quad (1.13)$$

where C is a constant. Explicitly in terms of the void fraction and the slip ratio,

$$\alpha = \frac{1}{1 + C \left(\frac{1-x}{x}\right)^p \left(\frac{\rho_G}{\rho_L}\right)^q \left(\frac{\mu_L}{\mu_G}\right)^r} \quad (1.14)$$

and

$$K = \frac{V_G}{V_L} = C \left(\frac{1-x}{x}\right)^{p-1} \left(\frac{\rho_G}{\rho_L}\right)^{q-1} \left(\frac{\mu_L}{\mu_G}\right)^r \quad (1.15)$$

The values of C, p, q, and r for the different correlations are given in Table 1.1.

Another well known empirical method for K or α is Chisholm's (1973) method as shown below:

$$K = \left(\frac{\rho_L}{\rho_{HOM}}\right)^{1/2} \quad (1.16)$$

where ρ_{HOM} is the homogeneous density and can be determined from

$$\frac{1}{\rho_{\text{HOM}}} = \frac{1-x}{\rho_L} + \frac{x}{\rho_G} \quad (1.17)$$

Table 1.1 Values of Constants Suggested by the Various Models and Correlations
(Adapted from Butterworth, 1975)

Model or Correlation	C	p	q	r
Homogeneous Model	1	1	1	0
Zivi Model (1963)	1	1	0.67	0
Turner & Wallis Model (1965)	1	0.72	0.40	0.08
Lockhart & Martinelli Correlation (1949)	0.28	0.64	0.36	0.07
Thom Correlation (1964)	1	1	0.89	0.18
Baroczy Correlation (1963)	1	0.74	0.65	0.13

1.1.2 Velocities

Many two-phase flow correlations are based on a variable called superficial velocity. The superficial velocity of a fluid phase is defined as the velocity which that phase would exhibit if it flowed through the total cross section of the pipe alone.

The superficial gas velocity, V_{SG} is defined as

$$V_{\text{SG}} = \frac{Gx}{\rho_G} = \frac{Q_G}{A} \quad (1.18)$$

where A is the pipe area. The actual gas velocity, V_G can be calculated from

$$V_G = \frac{Q_G}{A\alpha} \quad (1.19)$$

Similarly, for the superficial liquid velocity, V_{SL} is defined as

$$V_{SL} = \frac{G(1-x)}{\rho_L} = \frac{Q_L}{A} \quad (1.20)$$

$$V_L = \frac{Q_L}{A(1-\alpha)} \quad (1.21)$$

The slip velocity, V_s is defined as the difference in the actual gas and liquid velocities

$$V_s = V_G - V_L = \frac{V_{SG}}{\alpha} - \frac{V_{SL}}{(1-\alpha)} \quad (1.22)$$

Using the above definitions for velocity, the alternate equation for no-slip holdup is

$$\lambda_L = \frac{V_{SL}}{V_{SL} + V_{SG}} \quad (1.23)$$

In this section, some basic definitions of variables used in two-phase flow were introduced. In the next section, basic descriptions and determination of two-phase flow patterns in vertical and horizontal flows will be presented.

1.2 Flow Patterns

Whenever two fluids with different physical properties flow simultaneously in a pipe, there is a wide range of possible flow regimes. The flow pattern is referred to the distribution of each phase in the pipe relative to the other phase. Many investigators have attempted to predict the flow pattern that will exist for various sets of conditions, and many different names have been given to the various patterns.

Predictions of flow patterns for horizontal flow are a more difficult problem than the vertical flow since the phases tend to separate due to differences in density, causing a

form of stratified flow to be very common. When flow occurs in a pipe inclined at some angle other than vertical or horizontal, the flow patterns take other forms. For inclined upward flow, the pattern is known to be almost always slug or mist flow since the effect of gravity on the liquid precludes stratification. For inclined downward flow, the pattern is usually stratified or annular flow.

Because of the multitude of flow patterns and the various interpretations accorded to them by different investigators, no uniform procedure exists at present for describing and classifying them. However, in recent years, some attempts have been made to standardize their description (Wallis, 1965, Hewitt and Hall-Taylor, 1970, Govier and Aziz, 1972, Beggs and Brill, 1973, Taitel and Dukler, 1976, Barnea, 1987). The characterization and description proposed by Hewitt and Hall-Taylor (1970) for a vertical flow and by Taitel and Dukler (1976) for a horizontal flow appear to be among the best and most common.

Although different names of the flow patterns were given by different investigators, the descriptions of the basic main flow patterns were found to be essentially the same. In the following section, the characterizations and descriptions of the flow patterns presented by Carey (1992) and Hewitt and Hall-Taylor (1970), which can be generally accepted in two-phase flow study will be introduced. Carey (1992) used the flow pattern maps of Hewitt and Roberts (1969) for vertical upward flow and Taitel and Dukler (1976) for horizontal flow. The following descriptions, with some modification if necessary, will be adapted to the analysis of the results which will be observed for horizontal two-phase flow in the experimental phase of this study.

1.2.1 Upward Vertical Flow

For gas-liquid two-phase upward flow in a vertical round tube, the possible observed flow regimes are indicated in Figure 1.2. Hewitt & Hall-Taylor (1970) designated four basic patterns for upward flow as follows:

- **Bubbly Flow:** The gas phase is approximately uniformly distributed in the form of discrete bubbles in a continuous liquid phase.
- **Slug Flow:** Most of the gas is located in large bullet shaped bubbles which have a diameter almost equal to the pipe diameter. They move uniformly upward and are sometimes designated as "Taylor bubbles". Taylor bubbles are separated by slugs of continuous liquid which bridge the pipe and contain small gas bubbles. Between the Taylor bubbles and the pipe wall, liquid flows downward in the form of a thin falling film. (This pattern has been designated by others as plug flow at low rates where the gas liquid boundaries are well defined, and as slug flow at higher rates where the boundaries are less clear.)
- **Churn Flow:** Churn flow is somewhat similar to slug flow. It is, however, much more chaotic, frothy and disordered. The bullet-shaped Taylor bubble becomes narrow, and its shape is distorted. The continuity of the liquid in the slug between successive Taylor bubbles is repeatedly destroyed by a high local gas concentration in the slug. As this happens, and liquid slug falls, the liquid accumulates and forms a bridge and is again lifted by the gas. Typical of churn flow is this oscillatory or alternating direction of motion of the liquid. (Some observers refer to a froth flow pattern for higher liquid and gas rates where the system appears more finely dispersed.)

- **Annular Flow:** Annular flow is characterized by the continuity of the gas phase along the pipe in the core. The liquid phase moves upward partly in the form of drops entrained in the gas core. (Annular flow has been described as a wispy-annular pattern when the entrained phase is in the form of large lumps or "wisps". Froth, mist or semi-annular flow patterns have also been used to describe the churn and annular flow patterns.)

In a similar way, Carey (1992) described the churn and wispy-annular pattern flows as follows:

- **Churn Flow:** For intermediate qualities and lower flow rates, the gas shear on the liquid-gas interface may be near the value where it just balances the combined effects of the imposed pressure gradient and the downward gravitational body force on the liquid film. As a result, the liquid flow tends to be unstable and oscillatory. The gas flow in the center of the tube flows continuously upward. Although the mean velocity of the liquid film is upward, the liquid experiences intermittent upward and downward motion. The flow of these conditions is highly agitated, resulting in a highly irregular interface.
- **Wispy-Annular Flow:** At intermediate qualities, if both the liquid and gas flow rates are high, an annular-type flow is observed with heavy "wisps" of entrained liquid flowing in the gas core. Although this is a form of annular flow, it is sometimes designated as a separate regime, referred to as wispy-annular flow.

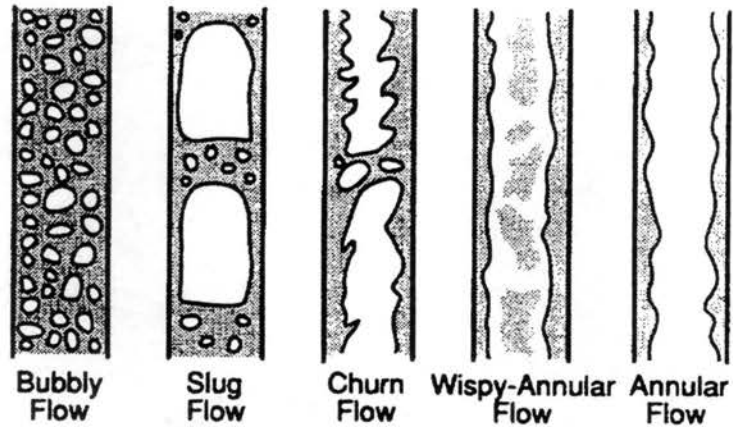


Figure 1.2 Schematic Representations of Flow Regimes Observed in Vertical Upward Gas-Liquid Two-Phase Flow (Adapted from Carey, 1992)

The conditions corresponding to the flow regimes described above can be represented on the flow regime map shown in Figure 1.3. The form of this map was proposed by Hewitt & Roberts (1969). The vertical coordinate is equal to the superficial momentum flux of the gas, and the horizontal coordinate is the superficial momentum flux of liquid through the tube. The boundaries between the flow regimes have been established from visual observation of the two-phase flow in a series of experiments (using a transparent tube) that spanned the entire flow regime map. Since the flow regime for a given set of conditions is a matter of judgment regarding the appearance of the flow, the boundaries should be interpreted as specifying the middle of a transition between two regimes.

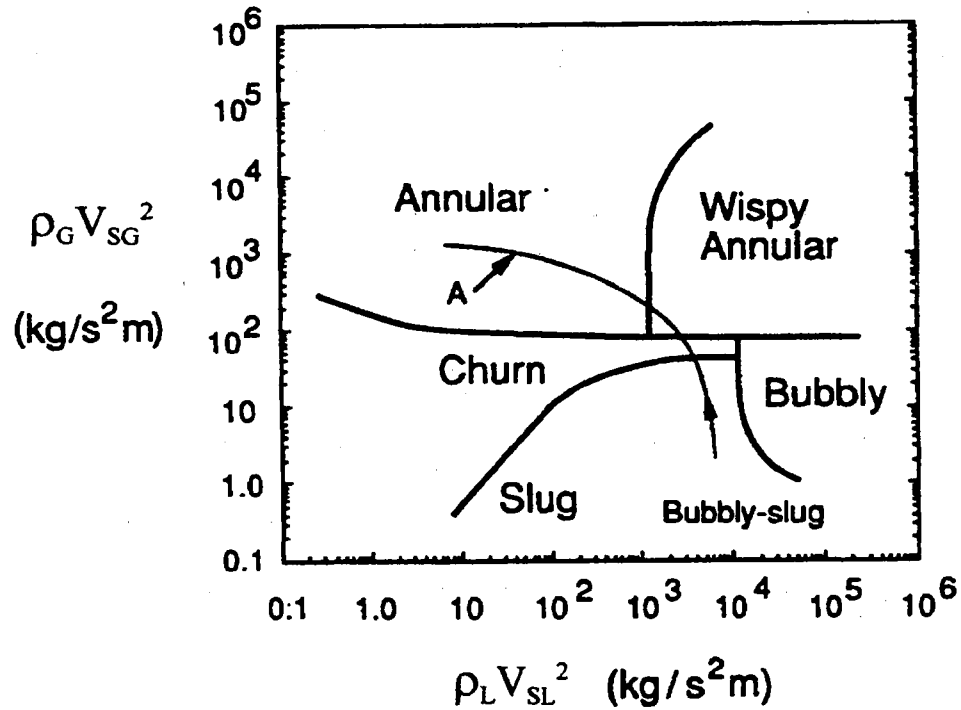


Figure 1.3 Flow Regime Map of the Type Proposed by Hewitt & Roberts (1969)
(Adapted from Carey, 1992)

From the theoretical consideration, analytical expressions for the transition conditions between the two-phase flow regimes have also been obtained. Radovcich & Moissis (1962) presented arguments about the frequency of bubble collisions, which suggest that the transition from bubbly to slug flow is highly probable at void fractions above $\alpha = 0.3$. Based on a more detailed analysis, Taitel & Dukler (1977) proposed the relation

$$\frac{V_{SL}}{V_{SG}} = 2.34 - 1.07 \frac{[g(\rho_L - \rho_G)\sigma]^{1/4}}{V_{SG}\rho_L^{1/2}} \quad (1.24)$$

as defining the incipient conditions for the transition from bubbly to slug flow.

As previously mentioned, increasing quality can lead to a transition from slug flow to churn flow. This breakdown of slug flow is a consequence of the interaction between the rising slug bubble and the liquid film between the slug and the wall. In a flow of this type, this liquid film actually moves downward as the slug moves upward at a velocity higher than the mean velocity of the two-phase flow, due to its buoyancy. As the quality and void fraction increase, this type of counter flow becomes unstable in a manner similar to the Helmholtz instability. This instability leads to the breakup of the large bubbles characteristic of slug flow, initiating a transition to churn flow. Porteus (1969) presented theoretical arguments that suggest that this transition corresponds to conditions defined by the relation

$$\frac{V_{SL}}{V_{SG}} = 0.105 \frac{[gD(\rho_L - \rho_G)]^{1/2}}{V_{SG} \rho_G^{1/2}} - 1 \quad (1.25)$$

where D is the tube diameter. However, Taitel & Dukler (1977) argued that for $(V_{SL} + V_{SG})/(gD)^{1/2}$ greater than 50, the slug-to-churn transition occurs at conditions that correspond to $V_{SL}/V_{SG} = 0.16$.

The transition from churn flow to annular flow occurs at conditions where the upward shear stress of the gas core flow plus the imposed pressure gradient just balances the downward gravitational force on the liquid film. These conditions correspond to the lower gas velocity limit for which steady upward annular flow can be sustained. Wallis (1965) proposed that this transition occurred approximately at conditions specified by the relation

$$\left[\frac{V_{SG}^2 \rho_G}{gD(\rho_L - \rho_G)} \right]^{0.5} = 0.9 \quad (1.26)$$

Taitel & Dukler (1977) suggested the following relation as a means of predicting the transition from churn to annular flow:

$$\frac{V_{SG} \rho_G^2}{[g(\rho_L - \rho_G)\sigma]^{0.25}} = 3.09 \frac{(1 + 20X + X^2)^{0.5} - X}{(1 + 20X + X^2)^{0.5}} \quad (1.27)$$

where X is the Martinelli parameter, defined as

$$X = \left[\frac{(dP/dz)_L}{(dP/dz)_G} \right]^{1/2} \quad (1.28)$$

where $(dP/dz)_L$ and $(dP/dz)_G$ are the frictional pressure gradients for the liquid and gas phases flowing alone in the pipe, respectively. These frictional gradients can be calculated from

$$\left(\frac{dP}{dz} \right)_L = - \frac{2f_L G^2 (1-x)^2}{\rho_L D} \quad (1.29)$$

$$\left(\frac{dP}{dz} \right)_G = - \frac{2f_G G^2 x^2}{\rho_G D} \quad (1.30)$$

$$f_L = B Re_{SL}^{-n}, \quad Re_{SL} = \frac{G(1-x)D}{\mu_L} \quad (1.31)$$

$$f_G = B Re_{SG}^{-n}, \quad Re_{SG} = \frac{GxD}{\mu_G} \quad (1.32)$$

In the above friction-factor relations, for round tubes the constants can be taken to be $B = 16$ and $n = 1$, respectively, for laminar flow (Re_{SL} or $Re_{SG} < 2000$), or $B = 0.079$ and $n = 0.25$ for turbulent flow (Re_{SL} or $Re_{SG} \geq 2000$).

The transition between wispy-annular flow and annular flow is difficult to distinguish precisely since the regimes are quite similar. Wallis (1965) proposed the following correlation for the transition condition based on the experiments that used a probe to detect wispy filaments in the core flow:

$$\frac{V_{SG}}{V_{SL}} = \left(7 + 0.06 \frac{\rho_L}{\rho_G} \right) \quad (1.33)$$

The relation is recommended for $V_{SL}\rho_L^{0.5}[gD(\rho_L-\rho_G)]^{-0.5} > 1.5$.

1.2.2 Horizontal Flow

For two-phase flow in horizontal round tubes, the flow regimes that may occur are shown in Figure 1.4. One of the main differences between the regimes observed for horizontal flow and those for vertical flow is that there is a tendency for stratification of the flow in horizontal flow. Regardless of the flow regime, the gas tends to migrate toward the top of the tube while the lower portion of the tube carries more of the liquid. The descriptions of the flow regimes introduced by Carey (1992) will be presented as follows:

- **Bubbly Flow:** At very low quality, bubbly flow is often observed for horizontal flow. However, as indicated in Figure 1.4, the bubbles, because of their buoyancy, flow mainly in the upper portion of the tube.
- **Plug Flow:** As the quality is increased in the bubbly regime, coalescence of small bubbles produces larger plug-type bubbles, which flow in the upper portion of the tube (see Figure 1.4). This is referred to as the plug flow regime.

- **Stratified Flow:** At low flow rates and somewhat higher qualities, stratified flow may be observed in which liquid flowing in the bottom of the pipe is separated from gas in the upper portion of the pipe by a relatively smooth interface.
- **Wavy Flow:** If the flow rate and/or the quality is increased in the stratified flow regime, eventually the interface becomes Helmholtz-unstable, whereupon the interface becomes wavy. This type of flow is categorized as wavy flow.
- **Slug Flow:** The strong gas shear on the interface for the wavy circumstances, together with the formation and breaking of waves on the interface, may lead to significant entrainment of liquid droplets in the gas core flow. At high liquid flow rates, the amplitude of the waves may grow so that the crests span almost the entire width of the tube, effectively forming large slug-type bubbles. Because of their buoyancy, the slugs of gas flowing along the tube tend to skew toward the upper portion of the tube. In other respects, it is identical to slug flow in vertical tubes, and hence it too is referred to as slug flow.
- **Annular Flow:** At high gas velocities and moderate liquid flow rates, annular flow is observed for gas-liquid flow. For such conditions, buoyancy effects may tend to thin the liquid film on the top portion of the tube wall and thicken it at the bottom. However, at sufficiently high gas flow rates, the gas flow is invariably turbulent, and strong lateral Reynolds stresses and the shear resulting from secondary flows may serve to distribute liquid more evenly around the tube perimeter against the tendency of gravity to stratify the flow. The strong gas shear may also result in significant entrainment of liquid in the gas core. Because gravitational body forces are often small compared to inertial effects and turbulent transport of momentum,

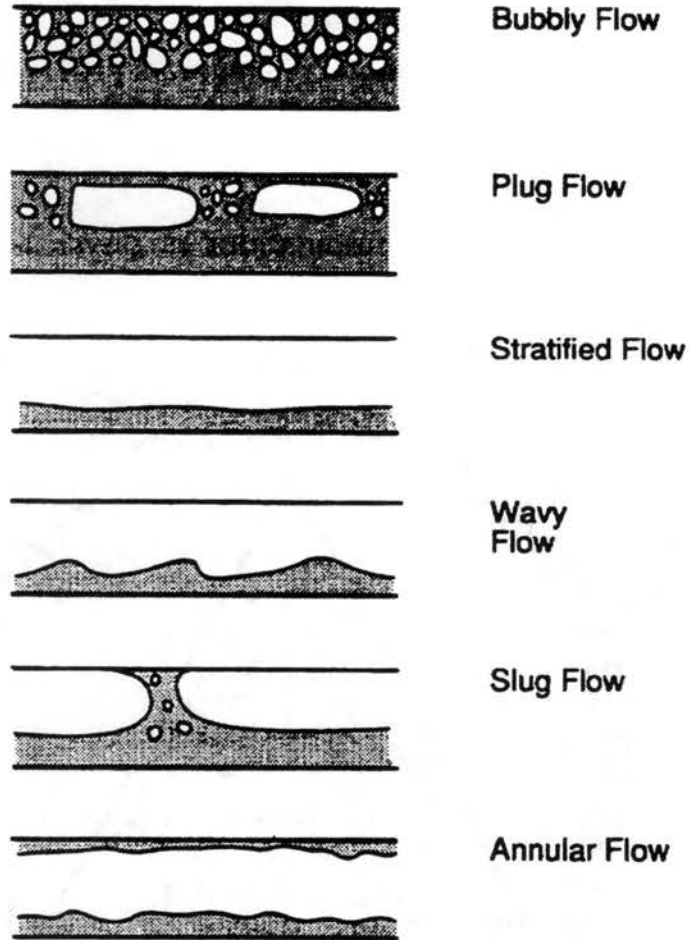


Figure 1.4 Schematic Representations of Flow Regimes Observed in Horizontal Gas-Liquid Flow (Adapted from Carey, 1992)

the resulting flow for these circumstances is generally expected to differ little from annular flow in a vertical tube under similar flow conditions.

Flow regime maps for gas-liquid flow in horizontal or slightly inclined round tubes have been proposed by Baker (1954), Mandhane, Gregory & Aziz (1974), and Taitel & Dukler (1976). Later, Barnea (1987) adapted the same approach of Taitel & Dukler (1976), modified and extended the existing model to form a unified model for the entire pipe inclination angles. Unfortunately, this approach is mathematically complex and its

solution is very involved for design purposes. Thus, the Taitel & Dukler (1976) model which has perhaps the most conceived theoretical basis will be used in this study. The map proposed by Taitel & Dukler (1976), which attempted to account for the different combinations of physical parameters that affect different regime transitions on the map, is shown in Figure 1.5.

The horizontal coordinate on the map (see Figure 1.5) is the Martinelli parameter X defined by Equations (1.28), (1.29) and (1.30). The value of X fixes the horizontal position on the map regardless of the flow regime. However, the vertical coordinate of the dimensionless parameters used to determine the flow regime varies depending on the specific transition being considered as follows:

Stratified flow to wavy flow transition: The vertical position of the corresponding point in Figure 1.5 is specified in terms of the parameter K_{TD} , defined as

$$K_{TD} = \left[\frac{\rho_G V_{SG}^2 V_{SL}}{\nu_L (\rho_L - \rho_G) g \cos \Omega} \right]^{0.5} \quad (1.34)$$

where ν_L is the kinematic viscosity of the liquid and Ω is the angle of inclination between the tube axis and the horizontal.

Wavy to annular and wavy to intermittent (plug or slug) transitions: The transitions in Figure 1.5 are evaluated in terms of X and the parameter F_{TD} , defined as

$$F_{TD} = \left[\frac{\rho_G V_{SG}^2}{(\rho_L - \rho_G) D g \cos \Omega} \right]^{0.5} \quad (1.35)$$

where D is the tube diameter.

Bubbly flow to intermittent flow transition: The transition is specified in terms of X and the parameter T_{TD} , defined as

$$T_{TD} = \left[\frac{-(dP/dz)_L}{(\rho_L - \rho_G)g \cos\Omega} \right]^{0.5} \quad (1.36)$$

where $(dP/dz)_L$ is given by Equation (1.29).

The transition between intermittent and annular flow or bubbly and annular flow is simply corresponded to $X = 1.6$ on the map.

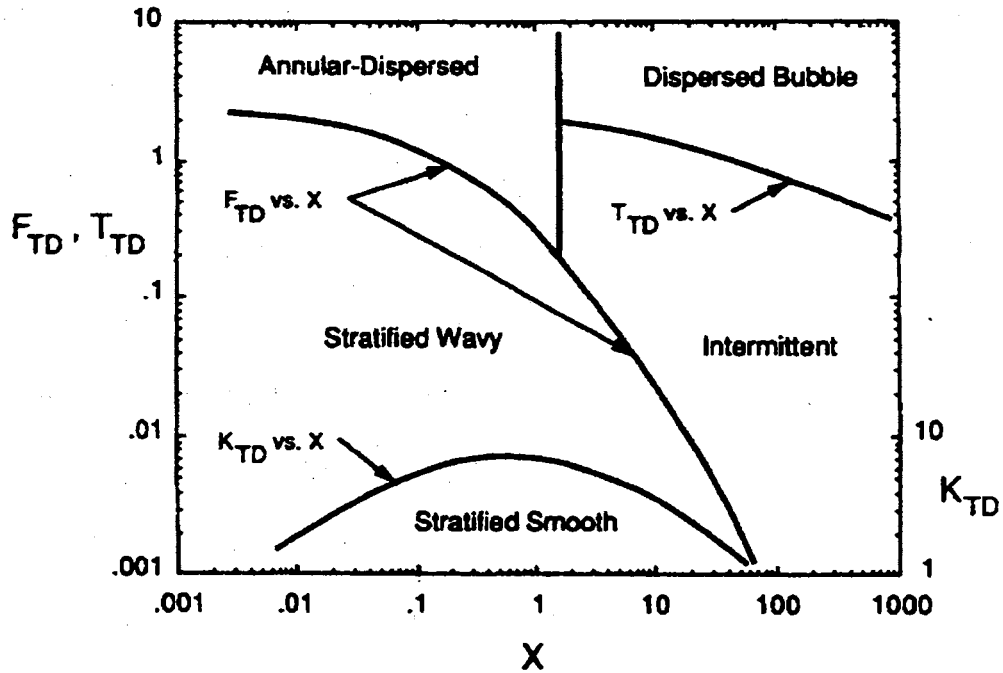


Figure 1.5 Flow Regime Map for Horizontal Gas-Liquid Flow of the Type Proposed by Taitel & Dukler (1976)

In this section, descriptions and determination of flow patterns in vertical and horizontal flows were introduced. In the next section, literature survey for heat transfer in two-phase flow will be presented.

1.3 Literature Survey

Numerous heat transfer correlations and experimental data for forced convective heat transfer during gas-liquid two-phase flow in vertical and horizontal pipes have been published over the past 40 years. Still experimental data are limited in both amount and usefulness, especially for horizontal pipe flow. Several investigators did not mention flow regime in detail, and others performed the experiment in limited simple flow regimes rather than comprehensive flow regimes. No data concerning the comprehensive aspects of the horizontal pipe flow have been yet reported.

In this study, a comprehensive literature search is carried out and studies having two-phase heat transfer correlations are mainly introduced. Attempts to correlate the data of two-phase heat transfer may be classified into four main approaches.

1.3.1 Extended Sieder-Tate Type Correlation for Two-Phase Heat Transfer

A single-phase heat transfer correlation developed by Sieder and Tate (1936) was employed and modified for two-phase heat transfer data, since several researchers assumed that the two-phase flow heat transfer mechanisms are quite similar to that of single-phase flow. Table 1.2 shows those two-phase heat transfer coefficient correlations and the correlation limitations.

During the procedures of adapting the single-phase heat transfer correlation to two-phase heat transfer correlation, additional parameters were introduced by dimensional analysis or a single-phase parameter was modified to two-phase parameter using homogeneous or separated flow model concepts. For the additional parameters for the two-phase heat transfer correlations, dimensionless parameters of (ρ_L/ρ_G) , (μ_G/μ_L) , and (V_{SG}/V_{SL}) were

Table 1.2 Extended Sieder-Tate Type Correlations for Two-Phase Heat Transfer

Source	Heat Transfer Correlations
Groothuis & Heandal (1959)	<p>For water-air</p> $Nu_{TP} = 0.029 (Re_{TP})^{0.87} (Pr_L)^{1/3} (\mu_B/\mu_W)^{0.14}$ $Re_{TP} = Re_{SL} + Re_{SG}$ <p>where μ_B = viscosity of bulk liquid μ_W = viscosity of liquid at wall</p> <p>Valid for $Re_{SL} > 5000$, $Re_{SG} > 0$, and $V_{SG}/V_{SL} > 1$</p> <p>For (gas-oil)-air</p> $Nu_{TP} = 2.6 (Re_{TP})^{0.39} (Pr_L)^{1/3} (\mu_B/\mu_W)^{0.14}$ <p>Valid for $1400 < Re_{SL} < 3500$, $Re_{SG} > 0$, and $V_{SG}/V_{SL} > 1$</p> <p>For single phase</p> $Nu = C Re_{SL}^{0.81} Pr_L^{1/3} (\mu_B/\mu_W)^{0.14}$ <p>where $C = 0.030$ for water where $Re_{SL} > 5000$ $= 0.028$ for gas-oil where $Re_{SL} > 4000$</p>
Knott et al. (1959)	$\frac{\bar{h}_{TP}}{\bar{h}_L} = \left(1 + \frac{V_{SG}}{V_{SL}}\right)^{1/3}$ <p>Valid for $6.7 < Re_{SL} < 162$, $126 < Re_{SG} < 3920$, and $0.1 < V_{SG}/V_{SL} < 40$. \bar{h}_L was calculated from the Sieder-Tate correlation.</p>
Davis & David (1964)	$\frac{hD}{k_L} = 0.060 \left(\frac{\rho_L}{\rho_g}\right)^{0.28} \left(\frac{DG_t \chi}{\mu_L}\right)^{0.87} \left(\frac{C_p \mu}{k}\right)_L^{0.4}$ <p>where h = two-phase heat transfer coefficient G_t = total flow rate χ = vapor mass fraction</p>
Oliver & Wright (1964)	<p>Newtonian liquid:</p> $Nu_{TP} = Nu_{SP} \left(\frac{12}{R_L^{0.36}} - \frac{0.2}{R_L} \right)$ <p>where R_L = liquid holdup = $Q_L/(Q_L + Q_G)$ Q_L = volumetric flow rate of liquid Q_G = volumetric flow rate of gas</p> $Nu_{SP} = 1.615 \left(\frac{\mu_B}{\mu_W}\right)^{0.14} \left(Re_{ACT} Pr \frac{D}{L}\right)^{1/3}$ <p>where</p> $Re_{ACT} = \frac{V_{ACT} D \rho}{\mu}$ <p>V_{ACT} = approximate actual velocity of liquid in two phase flow, $(Q_L + Q_G)/A$</p>

Table 1.2 Extended Sieder-Tate Type Correlations for Two-Phase Heat Transfer - Cont.

Source	Heat Transfer Correlations
Oliver & Wright (1964) - Cont.	<p>Non-Newtonian liquid:</p> $Nu_{TP} = Nu_{SP} \left(\frac{110}{R_L^{0.73}} - \frac{0.10}{R_L^2} \right)$ $Nu_{SP} = 1.75 \left(\frac{\gamma_B}{\gamma_W} \right)^{0.14} \left(\frac{3n^1 + 1}{4n^1} \right)^{1/3} \left(\frac{\pi}{4} Re_{ACT} Pr \frac{D}{L} \right)^{1/3}$ <p>where γ_B = value of γ measured under bulk temperature conditions, $(T_1 + T_2)/2$ γ_W = value of γ measured under wall temperature conditions T_1 = initial temperature of liquid T_2 = final temperature of liquid (or gas/liquid mixture) n^1 = function of non-Newtonian fluid physical properties ranging from 0.5 to 0.8 $\gamma = gK^1 8^{n^1 - 1}$ where g = gravity K^1 was defined as</p> $\frac{D\Delta P}{4L} = K^1 \left(\frac{8V}{D} \right)^{n^1}$ <p>where D = internal diameter of tube ΔP = pressure drop across the tube L = length of heat transfer section V = mean velocity of liquid</p>
Kudirka et al. (1965)	$Nu_{TP} = \frac{h_{TP} D}{k_L} = 125 \left(\frac{V_{SG}}{V_{SL}} \right)^{1/8} (Re_{SL})^{1/4} (Pr_L)^{1/3} \left(\frac{\mu_G}{\mu_L} \right)^{0.6} \left(\frac{\mu_B}{\mu_W} \right)^{0.14}$ <p>Valid for $2.5 \times 10^{-4} < x = \dot{m}_G / (\dot{m}_L + \dot{m}_G) < 0.092$</p>
Ueda & Hanaoka (1967)	$Nu_{TP} = 0.075 (Re_M)^{0.6} \frac{Pr_L}{1 + 0.035(Pr_L - 1)}$ <p>$Re_M = \rho_L U_M^* D / \mu_L$ $U_M^* = V_L + 1.2(Res)^{-0.25} V_S - 12 Fr_{ED} V_{ED} + 16(Fr_S)^{1.25} V_S$ $Res = V_S D (1 - \sqrt{\alpha}) / \nu_L$ $V_{ED} = V_{SL} + V_{SG}$ $Fr_{ED} = g\alpha D (1 - \sqrt{\alpha}) / V_{ED}^2$ $Fr_S = gD(1 - \sqrt{\alpha}) / V_S^2$ $Nu_{SP} = 0.023 Re_{SL}^{0.8} Pr_L^{0.4}$</p> <p>where V_L = mean velocity of liquid phase = $V_{SL}/(1-\alpha)$ V_G = mean velocity of gas phase = V_{SG}/α</p>

Table 1.2 Extended Sieder-Tate Type Correlations for Two-Phase Heat Transfer - Cont.

Source	Heat Transfer Correlations
Ueda & Hanaoka (1967) – Cont.	$V_S = \text{slip velocity} = V_G - V_L$ Correlation was valid for $1.5 \times 10^3 < Re_M < 6 \times 10^4$
Oliver & Young Hoon (1968)	$\frac{h_{TP}}{h_L} = \left(\frac{L}{L_S} \right)^{1/3}$ where $L_S = \text{length of the liquid slug}$ $L = \text{test section length}$
Martin & Sims (1971)	$\frac{h_{TP}}{h_L} = 1 + 0.64 \sqrt{\frac{V_{SG}}{V_{SL}}}$ Valid for $0.08 < V_{SG}/V_{SL} < 276$
Ravipudi & Godbold (1978)	$Nu_{TP} = 0.56 \left(\frac{V_{SG}}{V_{SL}} \right)^{0.3} \left(\frac{\mu_G}{\mu_L} \right)^{0.2} (Re_{SL})^{0.6} (Pr)^{1/3} \left(\frac{\mu_B}{\mu_W} \right)^{0.14}$ Valid for $8554 < Re_{SL} < 89626$ and $1 < V_{SG}/V_{SL} < 90$
Khoze et al. (1976)	$Nu_{TP} = 0.26 Re_{SG}^{0.2} Re_{SL}^{0.55} Pr_L^{0.4}$ Valid for $4 \times 10^3 < Re_{SG} < 3.7 \times 10^4$, $3.5 < Re_{SL} < 210$, and $4.1 < Pr_L < 90$
Chu & Jones (1980)	$Nu_{TP} = C1 (Re_{TP})^{0.55} (Pr_L)^{1/3} \left(\frac{\mu_B}{\mu_W} \right)^{0.14} \left(\frac{Pa}{P} \right)^{0.17}$ $Re_{TP} = Re_{SL} / (1 - \alpha)$ where $Pa = \text{atmospheric system pressure}$ $P = \text{mean system pressure}$ $\alpha = \text{void fraction}$ $C1 = 0.43 \text{ for upward flow}$ $= 0.47 \text{ for downward flow}$
Shah (1981)	$\frac{h_{TP}}{h_L} = \left(1 + \frac{V_{SG}}{V_{SL}} \right)^{1/4}$ The above correlation was valid for $Re_{SL} < 170$. h_L for laminar flow ($Re_{SL} < 170$) was calculated from the Sieder-Tate equation (1936) as $h_L D / k_L = 1.86 (Re_L Pr_L D / L)^{1/3} (\mu_L / \mu_W)^{0.14}$ For $Re_{SL} > 170$, a graphical correlation was given with axes as (h_{TP}/h_L) and (V_{SG}/V_{SL}) and with the liquid Froude number as a parameter. h_L for turbulent flow ($Re_{SL} > 170$) was calculated from the Dittus-Boelter equation $h_L = 0.023 Re_L^{0.8} Pr_L^{0.4} k_L / D$

Table 1.2 Extended Sieder-Tate Type Correlations for Two-Phase Heat Transfer - Cont.

Source	Heat Transfer Correlations
Elamvaluthi & Srinivas (1984)	$\text{Nu}_{\text{TP}} = 0.5 \left(\frac{\mu_{\text{G}}}{\mu_{\text{L}}} \right)^{1/4} (\text{Re}_{\text{TP}})^{0.7} (\text{Pr})^{1/3} \left(\frac{\mu_{\text{B}}}{\mu_{\text{W}}} \right)^{0.14}$ $\text{Re}_{\text{TP}} = (\text{D}V_{\text{SL}}\rho_{\text{L}}/\mu_{\text{L}}) + (\text{D}V_{\text{SG}}\rho_{\text{G}}/\mu_{\text{G}})$ <p>The Nu_{TP} correlation was valid for $300 < \text{Re}_{\text{SL}} < 16500$ and $V_{\text{SG}}/V_{\text{SL}} = 0.3 - 4.6$.</p>

introduced. Also, several researchers considered that the increase of two-phase heat transfer was attributed to the increase of mean mixture velocity, and the mean mixture velocity was defined as the sum of the single-phase liquid and gas velocities based on separated flow model concept. Some of the researchers introduced Re_{TP} or $(1+V_{\text{SG}}/V_{\text{SL}})$ for the two-phase parameters in their suggested two-phase heat transfer correlations.

Groothuis and Hendl (1959) measured heat transfer for two air-liquid mixtures (water and gas-oil) and empirically correlated the results. The authors reported that the tube-wall temperature influenced their results and that the two-phase heat transfer coefficient values were recalculated for wall temperatures of 140°F for air-water and 203°F for air-gas-oil. The authors observed that the introduction of the first amount of air caused a rapid increase in heat transfer, but then the increase in heat transfer was more gradual; further, the influence of air on the heat transfer rate was more pronounced at the lower liquid flow rates. This was explained by noting that resistance to the heat transfer was mainly due to the viscous sublayer at the wall, and the eddies produced in the wake of the rising air bubbles reduced the effective thickness of the film on the wall, thus

enhancing the heat transfer rate. They also developed a criterion for the flow conditions at which the liquid film on the wall was partly and temporarily disintegrated by the shearing stresses exerted by the flow. However, the test section was relatively short (thermal boundary layer not fully developed, Chu,1980) and they did not include flow pattern effects in detail.

Knott et al. (1959) measured the rate of heat transfer to two-phase mixtures of a viscous oil and nitrogen under uniform heat flux. Although the Sieder and Tate equation was applied only when the wall temperature was held constant, it was used for the uniform heat flux condition. Thus the authors obtained unsatisfactory results from a logarithmic mean temperature difference, but the integrated mean temperature difference in the calculation of over-all heat transfer coefficient resulted in satisfactory agreement between the single-phase oil experiments and the Sieder and Tate equation calculations. They applied the single-phase heat transfer theory to two-phase heat transfer and calculated h_{TP} from the equation of Sieder and Tate with the mean velocity of the two-phase flow. The authors attributed the increase in h_{TP} to the increase in the mean velocity of the mixture in the bubbly flow region, and based on this assumption they proposed a correlation for the two-phase heat transfer coefficient using the single-phase, Sieder and Tate equation approach with $V_{TP} = (V_{SL} + V_{SG})$. Although this method generally over-predicted the experimental values of the two-phase heat transfer coefficients, it gave the approximate trend of the data.

Davis and David (1964) used a slip model to suggest an empirical correlation for two-phase gas-liquid heat transfer. The experimental data in the purely convective heat transfer region (no nucleate boiling) corresponded to annular and mist annular regions.

The authors mentioned that the slip ratio (V_G/V_L) should be a function of the gas and liquid flow rates, the system geometry, the physical properties of the system, and the flow pattern, and then they used a gas-liquid density ratio (ρ_G/ρ_L) from the relationship with the slip ratio for their proposed empirical correlation for heat transfer coefficients.

The heat transfer in the horizontal slug flow with emphasis on the laminar flow regime was experimentally studied by Oliver and Wright (1964) using 88% by weight glycol in water, 1.5% sodium carboxymethylcellulose (SCMC) in water, and 0.5% by weight Polyox in water. The first type of liquid was Newtonian and the other two were non-Newtonian liquids. It was suggested that the heat transfer rise obtained during the two-phase slug flow might be regarded as due partly to an increase of liquid velocity and partly to the presence of circulation within the liquid slugs. The authors explained the circulation effect that it was directly dependent on liquid slug length and might be expected to be of greatest importance when the liquid slugs were short enough to permit several cycles of circulation within the heated test section of the tube. It was also observed that the maximum in the two-phase flow heat transfer occurred when the liquid holdup, R_L , was within the range of 0.3 - 0.5. In order to calculate the two-phase heat transfer coefficient, they used an approach that the influences from the actual liquid velocity and the liquid holdup were included as a controlling parameter. However, in order to evaluate the actual liquid velocity, based on homogeneous model concept they assumed that the two-phases of liquid and gas moved at substantially the same velocity, equal to $(Q_L + Q_G)/A$.

Kudirka et al. (1965) investigated the hydrodynamic aspects of two-phase heat transfer in the low quality range by bubbling air (through the wall of a porous tube

preceding the heated test section) into water and ethylene-glycol flowing vertically at atmospheric pressure. As the effect of liquid viscosity (viscosity of ethylene glycol was 17 times that of water) on the results, the author concluded that (a) under the same flow conditions, the higher the viscosity of the liquid, the lower the heat transfer coefficient, (b) for the same liquid velocity, the transitions between the flow patterns for ethylene glycol-air flows occurred at lower values of V_{SG} than for water-air mixtures, and (c) because of the differences in heat transfer behavior at low and high gas-liquid ratios, different heat transfer correlations must be used. They used the liquid temperature range of T_L ($^{\circ}\text{C}$) = 21 - 37 to minimize heat of vaporization effects.

Experimental results of the averaged heat transfer coefficients were presented by Ueda and Hanaoka (1967) for upward flow of air-liquid mixtures in a vertical tube. In this report, the effects of the liquid flow rate, the void fraction and the Prandtl number of the liquid phase on the heat transfer coefficient were investigated. The results showed that for low liquid Prandtl number, h_{TP} values were little affected by the variation of the void fraction at low V_{SG}/V_{SL} (where observations indicated that slug flow was occurring); at the high values of V_{SG}/V_{SL} (where observations indicated that the flow was annular flow) h_{TP} increased sharply with the void fraction. The authors also presented an analytical solution for predicting the h_{TP} in the slug and annular flow regions. However, in their derivations, the followings were assumed: the liquid film consisted of a viscous sublayer and a turbulent sublayer; in the viscous sublayer, the eddy diffusivity was zero while in the turbulent layer, the eddy diffusivity for momentum was much greater than the kinematic viscosity and was equal to the eddy diffusivity for heat. Also during the derivation for the temperature distribution in the liquid film, they assumed that all of the heat transfer was

absorbed in the liquid phase only. They performed graphical integration for their analytical bulk temperature and demonstrated good agreement between the theory and their experimental data.

Oliver and Young Hoon (1968) controlled the length of slugs in their investigation of heat transfer in slug flow using pseudoplastic liquids. In the low Graetz number range, two-phase heat transfer was found to be higher than that predicted by single phase correlation. Over a wide range of slug and wavy flow regimes, the two-phase heat transfer coefficients were almost constant and were lower than the predictions of the single phase correlation using the mixture velocity. This behavior was thought to be due to the non-circulating flow patterns observed during the two-phase flow with non-Newtonian fluids. The small heat transfer benefits gained in slug flow during this study contradict the large heat transfer coefficients in slug flow obtained previously by Oliver and Wright (1964). The possible breakup of liquid slugs might be the reason for higher heat transfer rates in Oliver and Wright's work.

Martin and Sims (1971) investigated the effect of forced convection heat transfer to water and water-air mixtures in a horizontal rectangular duct with air injection through a porous heated wall called "barbotage". The term barbotage was defined as the bubbling of a gas through a drilled or porous heat-transfer surface into a liquid. The main independent variables were the rate of air injection through the porous wall (barbotage rate), the superficial liquid velocity in the duct, and the amount of air mixed with the water upstream of the heated test section (finite inlet quality). With the zero barbotage and finite inlet quality, the experiments might be analogs to non-boiling two-phase horizontal heat transfer experiments. In the zero barbotage rate test, the authors observed that the two-

phase heat transfer coefficient increased as more air was introduced and the coefficient reached a relative maximum in the stratified froth regime and a relative minimum in the slug flow regime. With further increase of air from the upstream mixing, the coefficient increased monotonically into the annular flow regime. With the presence of barbotage rate, they used two additive contributions for two-phase heat transfer coefficient, one for the forced convection flow (h_{MAC}) and the other for bubbling (h_{MIC}):

$$h = h_{MAC} + h_{MIC} = h_{SP}F + h_{bub}\psi$$

with F as an "upstream turbulent factor" accounting for the increased velocity and turbulence in the forced convection flow, h_{bub} as a "bubbling function" due to agitation by barbotage bubbles, and ψ as a "bubble effectiveness factor" accounting for the reduced effectiveness of the bubble agitation process as turbulence in the forced convective flow increases. The F -function was found from the zero barbotage rate experiments.

Ravipudi and Godbold (1978) used a mixture of toluene and air to obtain heat-transfer results at one liquid mass velocity at low vapor pressure in a steam heated vertical tube. The authors measured local h_{TP} at five locations along the test section, and reported overall mean h_{TP} . By employing dimensional analysis, the authors proposed a correlation similar to the one proposed by Kudirka et al. (1965). The h_{TP} was observed to increase as much as 5.8 times h_{SP} . This enhancement in h_{TP} was attributed to the reduction of effective thickness of the viscous sublayer with an increase in gas flow rate (the rate of heat transfer in two-phase flow increased by 200 % over that of liquid flow alone). This suggested that the highly turbulent motion of the gas-liquid mixture with increasing amounts of air caused randomly distributed dry spots to appear on the wall and thereby decreasing the heat transfer rate. The authors found that as the mass transfer rate from liquid to gas increased,

the heat transfer rates increased, but the apparent heat transfer coefficients decreased. The authors also concluded that the small quantity of air into liquid increased the heat transfer coefficient and heat transfer rate significantly.

Khoze et al. (1976) presented three dimensionless correlations for experimental data on heat and mass transfer in rectangular channels carrying two-phase flows of air-water, air-diphenyl oxide, and air-polymethylsiloxane. The viscosity of diphenyl oxide was close to that of water, and the viscosity of polymethylsiloxane was ten times greater than that of water. The experiments were carried out with approximately equal air and liquid temperatures at the inlet to the heated test section. The authors used a method which represented the total heat flux as a sum of heat fluxes involved in the heat transfer to the moving liquid film, transfer of heat from the film surface to the film core, and the mass transfer from the film to the flow core. They reported that the maximum relative error of the experiments did not exceed $\pm 20\%$.

Chu and Jones (1980) studied vertical convective heat transfer in upward and downward two-phase, non-boiling flows. This experimental study demonstrated that the non-boiling two-phase convective heat transfer coefficient in vertical downflow exceeds that in vertical upflow for the same mass flow rates of liquid and gas. In the bubbly and slug flow regimes, they explained that this was attributed to significantly different liquid velocities and velocity profiles for the upward and downward orientations. The authors developed a correlation based on Sieder-Tate type equation having a pressure term which might be from Johnson (1955). Johnson modified Colburn (1933) heat transfer factor based on the following observation: In the normal turbulence region, two-phase heat transfer coefficients follow the equivalent single-phase relationships and the mechanisms

involved are much the same. Two-phase heat transfer coefficient results indicated that values of h_{TP} increased when superficial air velocity were increased for constant superficial water velocity.

Shah (1981) proposed correlations for laminar and turbulent heat transfer coefficients in two-phase flow covering a wide range of parameters. A total of 672 data points from previous other researcher's 18 experimental studies with certain assumptions were correlated with rms error of 15.5%, with 96% of the data predicted to within $\pm 30\%$. The data included heated and cooled horizontal tubes, heated and cooled vertical tubes with up and down flow, heated annuli and a heated vertical channel. The data were 10 liquid gas combinations: air and water, air and oil, nitrogen oil, air and oil, air and n-butyl alcohol, hydrogen and n-butyl alcohol, hydrogen and water, air and ethylene glycol, and nitrogen and glycerin solutions. Only those data in which gas and liquid were mixed before entering the test section were considered in his study. Hence his proposed correlations were generally inapplicable in the case where gas is injected through the walls of the heat transfer channel. Based on the data analysis, he observed that the transition Re_L for gas-liquid flows appeared to be 170 and for $Re_L > 170$, the liquid Froude number (Fr_L) had no significant effect on the heat transfer for horizontal and vertical tubes. Throughout the data analysis the author suggested three correlations for $Re_L < 170$, horizontal tubes with $Re_L > 170$, and vertical tubes with $Re_L > 170$. However those correlations for $Re_L > 170$ were graphical correlations, having some limitations of practical applicability, with axes as (h_{TP}/h_L) and (V_{SG}/V_{SL}) and with Fr_L as a parameter to account for flow pattern effects.

Vertical experimental data of two-phase pressure drop, single phase and two-phase heat transfer was collected by Elamvaluthi and Srinivas (1984) in non-boiling situation.

The two-phase pressure drop data using air-water and air-glycerin agreed with the Lockhart and Martinelli (1949) correlation. Single-phase heat transfer coefficients of water and glycerin were obtained from the energy balance equation using log mean temperature difference and compared with standard correlations of Sieder & Tate type equations for laminar and turbulent flows. These two comparisons confirmed the reliability of the collected two-phase heat transfer data. The authors observed that the addition of air caused a sharp increase in two-phase heat transfer. This increase was not very dominant at high Reynolds number of liquid. Based on the assumption of the separated flow model concept, a two-phase heat transfer coefficient correlation was developed using mixture Reynolds number defined as

$$Re_{TP} = \frac{DV_{SL}\rho_L}{\mu_L} + \frac{DV_{SG}\rho_G}{\mu_G}$$

The suggested correlation was compared with some collected literature values and about 90% of the data points fell within $\pm 25\%$.

1.3.2 Lockhart-Martinelli Type Correlation for Heat Transfer

In this approach, the two-phase heat transfer data were correlated using the relationship between two-phase pressure drop and single-phase pressure drop suggested by Lockhart and Martinelli (1949). This approach can characterize the flow features by two parameters: two-phase to single-phase liquid pressure drop ratio, defined as $\phi = \Delta P_{TP} / \Delta P_L$; ratio of two-phase to single-phase heat transfer coefficient, $\psi = h_{TP} / h_L$. The following researchers tried to predict ψ using the Lockhart-Martinelli multiplier, ϕ , with a leading coefficient and different exponent numbers and Table 1.3 shows those correlations and the correlation limitations.

Table 1.3 Lockhart-Martinelli Type Correlations for Two-Phase Heat Transfer

Source	Heat Transfer Correlations
Fried (1954)	$\psi^2 = \bar{h}_{TP} / \bar{h}_{SP}$ $\phi^2 = \Delta P_{TPF} / \Delta P_{SPF}$ <p>where ΔP_{TPF} = two-phase frictional pressure drop ΔP_{SPF} = single-phase frictional pressure drop of the liquid as if it were flowing alone in the tube</p>
Serizawa et al. (1975)	$\frac{h_{TP}}{h_L} = 1 + 462 \chi_{tt}^{-1.27}$ <p>where χ_{tt} = Lockhart-Martinelli modulus</p> $= \left(\frac{1-x}{x} \right)^{0.9} \left(\frac{\rho_G}{\rho_L} \right)^{0.5} \left(\frac{\mu_L}{\mu_G} \right)^{0.1}$
Vijay et al. (1982)	$h_{TP} / h_L = (\Delta P_{TPF} / \Delta P_L)^{0.451}$ $Nu_L = 1.615 (Re_{SL} Pr_L D / L)^{1/3} (\mu_B / \mu_W)^{0.14} \text{ for } Re_{SL} < 2000$ $Nu_L = 0.0155 Re_{SL}^{0.83} Pr_L^{0.5} (\mu_B / \mu_W)^{0.33} \text{ for } Re_{SL} > 2000$ <p>h_{TP} correlation was valid for $0.005 < V_{SG}/V_{SL} < 7670$, $1.8 < Re_{SL} < 130000$, and $5.5 < Pr_L < 7000$.</p>

Fried (1954) investigated pressure drop and heat transfer for an air-water mixture flowing in a horizontal pipe, where the flow of both phases was always turbulent. The author correlated his heat transfer results by plotting the ratio of the two-phase heat transfer coefficient to the single-phase heat transfer coefficient (ψ^2) against the two-phase frictional pressure drop ratio (ϕ^2). Heat transfer coefficients were computed by use of logarithmic and integrated mean temperature differences and the author concluded that the latter gave the better correlation since the log mean temperature difference was frequently

used with steam heating requiring constant entire pipe wall temperature - a condition which did not exist in the equipment. The integrated-mean heat-transfer coefficients thus found were lower in every case. The author concluded that the Martinelli correlation for isothermal pressure drop was applicable to nonisothermal flow by compensation for kinetic-energy changes in the mixture, however he did not specify the compensation method.

Serizawa et al. (1975) investigated the radial eddy diffusivity of heat in order to evaluate the contribution to heat transfer coefficient of bubbles in the central core region of both single-phase water flow and air-water two-phase flow. The radial eddy diffusivity of heat was obtained by measuring radial temperature distributions at five axial positions downstream of a line heat source located along the pipe diameter. It was found that the diffusivity, varying in the range of $1.2 \sim 1.5 \times 10^{-4} \text{ m}^2/\text{sec}$, increased considerably with quality and also with water flow rate. The ratio of the eddy diffusivity of heat for two-phase flow to that for single-phase water flow was correlated in terms of the Martinelli modulus X_{TT} . They also concluded that the dominant role in the turbulent transport process of heat, momentum, and bubbles was the turbulent velocity component of the liquid phase.

Vijay et al. (1982) conducted two-phase two-component forced convective heat transfer in co-current upward flow in a vertical tube using glycerin-air, water-air, water-helium, and water-Freon 12. They suggested a Lockhart-Martinelli type correlation for their heat transfer data using the combination of coordinates originally suggested by Fried (1954) for horizontal two-phase two-component flow. The correlation was of the form

$$\psi^2 = (\phi^2)^n$$

where n depends slightly on the flow pattern, ψ^2 is a ratio of heat transfer coefficients and ϕ^2 is a ratio of frictional pressure drops. Also they tried to develop a single correlation independent of the flow pattern giving $n = 0.451$ for bubble, slug, froth, and annular flows and concluded that the scheme did not work well for slug flow and the slug-annular transition with pressure drops less than approximately 1000 Pa/m.

1.3.3 Explicit Void Fraction Parameters in Two-Phase Flow Heat Transfer Correlation

Some of this approach were based on the assumption that the introduction of the gas phase into the two-phase heated test section acted only to accelerate the liquid phase, and further the heat was transferred and carried away mainly by the liquid phase only. Thus, the two-phase heat transfer mechanism could be considered as a heat transfer to single-phase liquid flow with the liquid flowing with the actual mean (not the superficial) velocity in the heated test section. Therefore, the void fraction parameter explicitly appeared in the two-phase heat transfer correlation. However, researchers used different single-phase heat transfer correlations in their two-phase heat transfer coefficient correlation which resulted in a little different non-dimensional parameters and exponent values. Also, some researchers assumed that the two-phase heat transfer mechanism was directly related to the instantaneous amount of the ratio of liquid and gas. Thus, they used void fraction or liquid holdup as a two-phase heat transfer correlation parameter. The following researchers explicitly used void fraction or liquid holdup as a parameter for two-phase heat transfer and Table 1.4 shows those correlations and their limitations.

A two-phase heat transfer coefficient correlation for horizontal gas-liquid slug flow was developed by Hughmark (1965) from the relationship of the velocity of the gas slug and the liquid slug Reynolds number. It was assumed that the entire wall is wet with liquid

Table 1.4 Explicit Void Fraction Parameters in Two-Phase Flow Heat Transfer Correlations

Source	Heat Transfer Correlations
Hughmark (1965)	$Nu_{TP} = 1.75 (R_L)^{-1/2} \left(\frac{\dot{m}_L c_L}{R_L k_L L} \right)^{1/3} \left(\frac{\mu_B}{\mu_W} \right)^{0.14}$
Dorresteyn (1970)	$h_{TP} / h_L = (1-\alpha)^{-1/3} \text{ for } Re_{SL} < 2000$ $h_{TP} / h_L = (1-\alpha)^{-0.8} \text{ for } Re_{SL} > 2000$ <p>where $Nu_L = 0.0123 Re_{SL}^{0.9} Pr_L^{0.33} (\mu_B / \mu_W)^{0.14}$ Correlations were valid for $0.004 < V_{SG}/V_{SL} < 4500$ and $300 < Re_{SL} < 66000$</p>
Aggour (1978)	$h_{TP} / h_L = (1-\alpha)^{-1/3} \text{ for } Re_{SL} < 2000$ <p>where $Nu_L = 1.615 (Re_{SL} Pr_L D / L)^{1/3} (\mu_B / \mu_W)^{0.14}$ $h_{TP} / h_L = (1-\alpha)^{-0.83} \text{ for } Re_{SL} > 2000$ <p>where $Nu_L = 0.0155 Re_{SL}^{0.83} Pr_L^{0.5} (\mu_B / \mu_W)^{0.33}$ Correlations were valid for $7.5 \times 10^{-5} < \dot{m}_G / \dot{m}_L < 5.72 \times 10^{-2}$, $0.02 < V_{SG}/V_{SL} < 470$, $13.95 < Re_{SG} < 2.09 \times 10^5$, and $5.42 < Pr_L < 6.36$.</p> </p>
Rezkallah & Sims (1987)	<p>For laminar flow ($Re_{SL} < 2000$)</p> $\frac{h_{TP}}{h_L} = 1 + C \left(\frac{V_{SG}}{V_{SL}} \right)^{0.25} (Pr_L)^{-0.23}$ <p>The correlation was valid for $1.8 < Re_{SL} < 1960$; $4.2 < Pr_L < 7000$; $0.06 < V_{SG}/V_{SL} < 7030$; $12.8 < D < 70$; $19.7 \times 10^{-3} < \sigma < 72 \times 10^{-3}$ where D = pipe diameter, mm σ = surface tension, N/m and $C = 4.0$.</p> <p>For turbulent flow ($Re_{SL} > 2000$)</p> $\frac{h_{TP}}{h_L} = \left(\frac{1}{1-\alpha} \right)^{0.9}$ <p>where α is the void fraction predicted from the correlation of Chisholm (1973). The range of variables included in the data was $2400 < Re_{SL} < 1.3 \times 10^5$; $4.2 < Pr_L < 220$; $0.01 < V_{SG}/V_{SL} < 265$; $2 \times 10^{-4} < \rho_G/\rho_L < 10^{-2}$; $12.8 < D < 70$; $19.7 \times 10^{-3} < \sigma < 72 \times 10^{-3}$</p> <p>$h_L$ used was either the measured value where this was reported with the data or that predicted by the relevant Sieder-Tate correlation.</p>

and there is a continuous liquid phase in the region of the wall to the liquid phase, thus the heat transfers between the wall and the slug only. The author used the momentum-heat transfer analogy based on the two-phase friction factor. The friction factor was calculated using the assumed average liquid velocity instead of the actual slug velocity. The suggested correlation was compared with the experimental data of Oliver and Wright (1964) for air-88.5% glycerin in water, and the correlation agreed with 8.4% average absolute deviation.

Dorresteyn (1970) experimentally investigated the forced convective heat transfer coefficients in a non-boiling, gas oil/air two-phase vertical flow system for both upward and downward flow directions in an electrically heated 70 mm diameter coil. The unique feature of this test was that it consisted of a U-shaped downer and riser with a heat transfer section halfway down the tubes. The gas/liquid mixture first passed through an upward section, then through the downer and the riser and finally discharged through a downflow section. Liquid velocities varied from 0.02 to 4.64 m/s, corresponding to Reynolds numbers from 300 to 66000. For liquid velocities above 1.0 m/s, h_{TP} first remained almost constant and then increased slightly with increasing air velocity. The flow regimes were bubbly or froth. No difference in h_{TP} between upflow and downflow was observed.

However, for liquid velocities lower than 1.0 m/s, h_{TP} for downflow with gas velocities lower than 0.2 m/s was even lower than h_L for single-phase liquid flow, which was quite in contrast to the other researchers' findings. This difference was attributed to the disturbance caused by the 180° bend tube couplings between the downflow and

upflow tubes. In the downflow tube, the values of h_{TP} were lower than those for upflow tube at the same gas and liquid velocities. As the gas velocities ranged from 0.5 to 5.0 m/s upflow, h_{TP} reached a relative maximum of about 800 to 1000 $W/m^2\text{-}^\circ C$ which was about 3 to 15 times greater than the measured single-phase liquid coefficients. The absolute h_{TP} was found to be independent of the liquid velocity for the case of liquid velocities below 1 m/s with the upflow tube. The author also compared his results with those of Groofhuis & Hendal (1959) and concluded that for a larger tube size, h_{TP} was much lower compared to other data for smaller tube sizes.

Aggour (1978) studied the effect of gas-phase density (by changing the type of gas being used) on vertical two-phase local and mean heat-transfer coefficients, pressure drops and flow patterns. For this purpose, he performed experiments in a vertical, electrically heated tube by using three different gas-water mixtures; the gases used were air, helium and Freon-12 which allowed gas density changes by a factor of approximately 52. Results of measurements of the heat transfer coefficients, frictional pressure drops and flow patterns were presented along with the photographs of flow patterns. The author correlated his local heat transfer data with the modified theory of Spalding (1964) in the manner proposed by Vijay (1978). The author also conducted a flow-visualization study in order to confirm the existence of downflow of liquid film at the wall in bubble flow where local heat-transfer coefficients were observed to increase with increasing distance along the test section. The integrated mean heat-transfer coefficients were obtained from the measured local values of h_{TP} along the test section. The author also developed a simple correlation to predict \bar{h}_{TP} , which was based on a single-phase liquid flow model having a Reynolds number based on the actual mean velocity of the liquid in the two-phase flow.

Rezkallah and Sims (1987) tested eleven existing vertical two-phase heat transfer coefficient correlations against thirteen liquid-gas combinations taken by different authors. The data set covered different liquid and gas properties, pipe sizes, and flow patterns. The authors tried to keep the tested correlations' range of applicabilities suggested by the original authors. The results of the comparisons showed that most of the tested correlations gave reasonably good agreement with the water-air data.

However, glycerin and glycerin-water-air solutions where their Prandtl numbers are relatively quite high compared to that of water gave large deviations. Based on the comparisons the authors suggested two correlations for vertical laminar and turbulent flow heat transfer coefficients. However, their suggested correlation for the two-phase laminar flow has the same non-dimensional parameters as the correlation of Dorresteyn (1970) which utilized the so called "Liquid Acceleration Model". In this model it was implied that the effect of the gas phase was to accelerate the liquid phase, while the heat transfer coefficient was predicted using a conventional single-phase correlation with liquid properties and some adjusted superficial liquid velocity.

1.3.4 Simplified Numerical/Analytical Approach

Among the variety of flow regimes that can exist during gas-liquid flow, some of the flows are inherently unsteady processes with large variations in local mass flow rates and phase distribution with time at any cross section. Thus, large oscillations in local heat flux or heat transfer coefficients and oscillations of temperature of the wall can be expected. As a result some researchers have focused on the prediction of time varying unsteady state temperature and heat flux or heat transfer coefficients. In this approach some of them used the von Karman analogy, simplified two parallel plate system, or large

Taylor bubbles with a free falling film. When this time varying behavior was of concern to the designer, it was necessary to solve the complex set of equations for flow and heat transfer. However, in most cases of interest to the designer the average heat transfer coefficient is adequate. Thus some of the researchers tried to provide the average heat transfer coefficient equation in addition to the time varying temperature and heat transfer equations.

Davis et al. (1975) applied the von Karman analogy between heat transfer and momentum transfer in turbulent fluids to heat transfer through wavy liquid films in horizontal, stratified, gas-liquid flow. The authors considered relatively simple parallel-flat-plate system, and they assumed that the shear stress and the heat flux were essentially independent of the distance from the heat surface and might be taken to be their values at the wall. Also, they assumed that the liquid film was sufficiently thin and/or the pressure drop was sufficiently small. Thus, they used the same shear stress between the wall and the interface of liquid and gas. For wavy film systems, they assumed that $Pr_t = 1$. Nusselt numbers predicted from the von Karman analogy were compared and shown to be in good agreement with experimental data of Frisk and Davis (1972) for air-water flows involving three-dimensional wavy films and large amplitude roll waves.

Niu (1976) developed a numerical model for heat transfer during gas-liquid slug flow in horizontal tubes. The model was capable of calculating the time and position dependent temperatures of the fluids, the wall, as well as the heat flux providing the local heat transfer coefficients. Shaharabany (1976) and Shaharabany et al. (1978) designed and constructed an experimental system for the measurement of time varying temperature, heat flux and heat transfer coefficient during two-phase slug flow, and compared the

temperature and heat flux fluctuations with Niu (1976). Time varying temperatures of the inner and outer pipe walls were measured and used as time varying boundary conditions for the solution of the conduction equation in the wall of the pipe.

The conduction equation was solved numerically using finite difference techniques. Axial conduction was neglected and symmetry assumed with respect to the vertical pipe. Data covered the range of slug flow conditions for air-water in a horizontal pipe under conditions of uniform heat flux. Based on the Hubbard and Dukler (1975) hydrodynamic model, they evaluated heat transfer coefficients in the liquid slug at top, bottom, nose and body positions. Data showed that the heat transfer in the nose of the slug was higher than that in the slug body. Analysis of the data also showed that the heat transfer coefficients to the gas zone and to the liquid film zone were predictable from Colburn's (1933) correlation. However, slug heat transfer coefficients were not in agreement with the usual Colburn type correlations and varied around the slug periphery.

Dukler and Shaharabany (1977) in a design report suggested a method for calculating the average heat transfer coefficient to be expected during slug flow without the use of a complex computer program. This report presented design equations to calculate the average heat transfer coefficient in the liquid slug, the liquid film, and the gas phase. An equation was also presented to estimate the magnitude of wall temperature fluctuation in uniform flux heat transfer (such as in direct field heaters). Heat transfer coefficient predictions from those suggested equations were compared with the experimental data of Shaharabany (1976) and shown to be in good agreement.

Shoham et al. (1982) measured heat transfer characteristics for two-phase gas-liquid slug flow in a horizontal pipe. The time variation of temperature, heat transfer

coefficients, and heat flux were reported for the different zones of slug flow: the mixing region at the nose, the body of the slug, the liquid film, and the gas bubble behind the slug. Substantial differences in heat transfer coefficient existed between the bottom and the top of the slug. The results showed that the heat transfer coefficients in the liquid film varied as the liquid decelerated with distance behind the slug. The Colburn correlation was used to calculate values for comparison. A marked difference between the heat transfer coefficients at the top and bottom were observed, both at the nose and in the body of the slug. The disagreement in the region immediately behind the slug resulted from the fact that, at the bottom of the pipe, the coefficient at the end of the slug was higher than the predicted value. When the film zones were long enough, these differences disappeared. The theory based on laminar plug flow between parallel plates, which were held at constant but differing temperatures, was developed in order to support the experimental results. The resulting theory showed that the predicted trend was in accord with the experimental results.

Barnea and Yacoub (1983) developed a mathematical model with an analytical solution based on the method of slug characteristic lines (the slug trajectory lines) for the unsteady heat transfer process in vertical gas-liquid slug flow. The authors presented a solution for the temperature of gas and liquid as a function of time and axial location and the wall temperature fluctuations, as well as the time averaged heat transfer coefficients using the following assumptions: the gas was located in large Taylor bubbles; the liquid film adjacent to the gas bubble behaved as a free-falling film; and the pipe was heated in a region where fully developed slug flow existed. However, in order to evaluate the time

averaged heat transfer coefficient, information about time needed for a liquid particle to move from the bubble front to its tail were required.

1.3.5 Two-Phase Heat Transfer Experimental Data

Numerous researchers experimentally investigated the two-phase heat transfer for vertical and horizontal tubes and different flow patterns and fluids. However, several of them did not report their experimental data in detail. The seventeen (17) resources alphabetically listed in this section provide two-phase flow heat transfer experimental data for vertical and horizontal tubes and different flow patterns and fluids. The experimental data also cover a wide range of flow parameters (e.g., Reynolds number, Prandtl number, viscosity ratios, and void fraction) and two different boundary heating conditions (uniform heat flux and wall temperature). A summary of the resources with experimental data showing the type of fluid used, the type of heating, and the range of some key experimental parameters such as the Reynolds and Prandtl numbers, the ratio of superficial gas and liquid velocities, the type of article (paper or thesis), and pipe orientation (horizontal or vertical) is provided in Table 1.5.

Table 1.5 Resources with Experimental Data

Investigator(s)	Fluid	Type of Heating	Re _L	Pr _L	$\frac{V_{SG}}{V_{SL}}$	P/T	H/V
Aggour (1978)	Air/Water	Elect.	63.3-14.9x10 ⁴	0.709	0.022-305.8	T	V
	Helium/Water	Heated	13.95-2.3x10 ⁴	0.691	0.042-470		
	Freon/Water		1894-20.9x10 ⁴	0.769	0.035-114		
Chu & Jones (1980)	Air/Water	Elect.	1.6x10 ⁴ -		0.12-4.64	P	V
		Heated	11.2 x10 ⁴				
Davis et al. (1979)	Air/Water	Elect.	6210-2.0x10 ⁴			P	H
		Heated					

Table 1.5 Resources with Experimental Data – Cont.

Investigator(s)	Fluid	Type of Heating	Re_L	Pr_L	$\frac{V_{SG}}{V_{SL}}$	P/T	H/V
Dusseau (1968)	Air/Water	Steam Heated	1.4×10^4 - 4.9×10^4	2.5-6	2.2-17	T	V
Fried (1954)	Air/Water	Steam Heated	1.69×10^4 - -25.3×10^4	2-4	0.29-85	P	H
Frisk & Davis (1972)	Air/Water	Elect. Heated	104-248			P	H
Johnson (1955)	Oil/Air	Steam Heated	321-2230		0.46-127	P	H
Johnson & Abou-Sabe (1952)	Air/Water	Steam Heated	1.25×10^4 - -11.54×10^4	3-7	0.34-108	P	H
King (1952)	Air/Water	Steam Heated	2.25×10^4 - 11.9×10^4	~ 3.4	0.48-51.2	T	H
Kudirka (1964)	Air/Water	Elect. Heated	5.5×10^4 - 49.5×10^4		0.16-75	P	V
Pletcher (1966)	Air/Water	Elect. Heated				T	H
Rezkallah (1987)	Water/ Glycerine+Silicone liquid	Elect. Heated	$1.8-1.3 \times 10^5$	4.2-7000	0.01-7030	T	V
Shaharabanny et al. (1978)	Air/Water	Elect. Heated	11.3×10^4 - -33.7×10^4	4.52-6.17	$\dot{m}_G/\dot{m} =$ 0.0025-0.02	P	H
Shoham et al. (1982)	Air/Water	Elect. Heated		2.23-5.42	$\dot{m}_G/\dot{m} =$ 0.15-2.4	P	H
Vijay (1978)	Air/Water Glycerin/Air Glycerin+Air/Water	Elect. Heated	$250-12.6 \times 10^4$ 0.8-21.0 8.0-4500	5-8.3 5800-7125 180-238	0.03-6700 0.05-330 0.01-6700	T	V
Zaidi (1981)	Air/Water Surfactant Sol./Air	Elect. Heated	710- 15.3×10^4 $818-81.5 \times 10^4$	5.37-6.56 5.17-6.65	0.008-2033 0.02-2017	T	V

where T = Thesis, P = Paper, H = Horizontal, and V = Vertical

Aggour (1978) studied forced convective, co-current, two-phase, two-component (gas-water) flow in the thermal entry section of a vertical tube. Three gases (air, helium, and Freon-12) were used to investigate the effect of gas density on the local and mean heat transfer coefficients, frictional pressure drop and flow patterns.

Chu and Jones (1980) conducted experimental study to determine the two-phase heat transfer coefficient in an air-water, non-boiling vertical system. Correlations based on the Sieder-Tate (1936) type of equation were established to collapse the experimentally determined two-phase heat transfer coefficient utilizing a two-phase Reynolds number based on a liquid phase Reynolds number corrected for liquid holdup.

Davis et al. (1979) presented a method for predicting local Nusselt number for heat transfer to a stratified horizontal gas-liquid flow for turbulent liquid/turbulent gas conditions. A mathematical model based on the analogy between momentum transfer and heat transfer was developed and tested using experimental data taken for air/water flow.

Dusseau (1968) determined overall heat transfer coefficients for a vertical steam condenser using an air-water froth as the coolant and evaluated the applicability of such a coolant for practical use. The total heat transferred was determined by measuring the temperature and humidities of the inlet and outlet streams. More heat was transferred at high water inlet temperatures than at low inlet temperatures.

Pressure drop and heat transfer for an air-water mixture flowing in a horizontal 0.737-in. I.D. pipe were investigated by Fried (1954) at water rates of 2 to 26 gal/min (0.0076 m³/min to 0.098 m³/min) and air flow rates of 2 to 45 SCFM (0.057 m³/min to 1.274 m³/min), where the flow of both phases was always turbulent. Heat transfer coefficients were computed by use of logarithmic and integrated mean temperature

differences; and the latter gave the better correlation.

An experimental investigation of heat transfer from a flat plate to horizontal co-current air-water flow was carried out by Frisk and Davis (1972) to assess the effects of the different flow regimes on the effectiveness of heat transfer. Three-dimensional waves and roll waves were shown to increase the Nusselt number (compared with smooth films) by more than 100 percent. By using a surface-active agent to stabilize the flow, a direct comparison between wavy flow heat transfer and smooth flow heat transfer was obtained.

Johnson (1955) measured heat transfer and static pressure drop for two-phase, two-component flow of oil and air for flow in a steam-heated horizontal extra-heavy copper pipe. Correlations were presented and used in a comparison of the oil-air and water-air results for heat transfer and nonisothermal pressure drop in the same test system.

Johnson and Abou-Sabe (1952) measured the static pressure drop and heat transfer for two-phase, two-component flow of air and water for flow in horizontal brass tubing. Correlations were presented from which prediction of pressure drop and heat transfer might be made under restricted flow conditions.

King (1952) investigated the heat transfer and pressure drop characteristics for two-phase, two-component, non-isothermal flow of an air-water mixture in a horizontal 0.737 in. I.D. copper pipe. After correction to allow for the change of momentum of the fluids, the two-phase non-isothermal pressure drop was correlated by means of Martinelli's modulus X . A better correlation resulted when the ratio of the two-phase heat transfer coefficient to the single-phase liquid coefficient divided by the ratio of the two-phase pressure drop to the single-phase liquid pressure drop was plotted against X .

Kudirka (1964) studied hydrodynamic aspects of two-phase heat transfer in a vertical forced-circulation system for the low-quality range. The role and influence of nucleation and convective mechanisms in enhancing heat transfer, and the nature of the nucleation mechanisms, including the influence of flow pattern, mass velocity, void fraction, and quality on the rate and nature of heat transfer were investigated.

Novosad (1955) studied the heat transfer between the wall of a vertical tube and a liquid within the tube, when a gas was simultaneously bubbled through the liquid. Correlation of the experimental heat transfer coefficients was achieved by using the holdup (ratio of gas volume to total volume of gas-liquid mixture) in calculating the Reynolds number.

Pletcher (1966) experimentally investigated the heat transfer in horizontal annular two-phase two-component flow. Emphasis was placed on obtaining an understanding of the local rather than overall coefficients. A graphical correlation of the heat transfer results was obtained.

Rezkallah (1987) experimentally studied forced-convective heat transfer and hydro-dynamic aspects of co-current, two-phase, two-component flow in a vertical tube with essentially no evaporation. The effect of reducing the surface tension on the heat transfer coefficients, both local and length mean, the frictional pressure drop, and the flow pattern were investigated. The behavior and shape of the local heat transfer coefficients along the test section length remained unchanged in most cases with trends that varied according to the combination of the liquid and gas flow rates.

An experimental system was designed and constructed by Shaharabany (1976) for the measurement of time varying temperature, heat flux and heat transfer coefficient

during two-phase slug flow. Data were taken covering the full range of slug flow conditions for air-water in a horizontal pipe under conditions of uniform heat flux. Data showed that the heat transfer in the nose of the slug was higher than that in the slug body. Data analysis showed that the heat transfer coefficients to the gas zone and to the liquid film zone were predictable from Colburn's (1933) correlation. However, slug heat transfer coefficients were not in agreement with the usual correlations and vary around the slug periphery.

Time varying temperatures, heat flux and heat transfer coefficients were measured by Shaharabany et al. (1978) during slug flow in a horizontal pipe. The heat transfer coefficients in the liquid slugs were extremely large with the peak value occurring in the mixing zone at the front of the slug. Furthermore, substantial peripheral variations in heat transfer coefficients existed.

Heat transfer characteristics for two-phase gas-liquid slug flow in a horizontal pipe were measured by Shoham et al. (1982). The time variation of temperature, heat transfer coefficients, and heat flux were reported for the different zones of slug flow: the mixing region at the nose, the body of the slug, the liquid film, and the gas bubble behind the slug. Substantial differences in heat transfer coefficients existed between the bottom and the top of the slug. A qualitative theory was presented which explained this behavior.

Vijay (1978) used three liquids (water, glycerin, water and glycerin mixture) to study the influence of liquid viscosity and Prandtl number on the local heat transfer coefficients in vertical two-phase two-component flow. The type of flow pattern was found to depend on the liquid and air flow rates and the viscosity of the liquid. A theory was developed, by modifying the classical one-dimensional single-phase flow Graetz

problem, to explain the observed behavior of the local heat transfer coefficient as a function of the distance in the bubble and bubble-slug flow regimes.

An experimental investigation was made by Zaidi (1981) to determine the effect of reducing the surface tension on flow pattern frictional pressure drop and local and mean heat transfer coefficients in two-phase two-component (gas-liquid) upward flow. Local heat transfer coefficients were correlated by a modified form of the single-phase heat transfer theory of Spalding (1964), and mean heat transfer data were tested against some of the well-known existing correlations.

Among the above experimental two-phase heat transfer studies, seven (7) studies were theses and they reported two-phase heat transfer data with their limited experimental parameter ranges. However, only Aggour (1978), King (1952), Pletcher (1966), Rezkallah (1987), Vijay (1978), and Zaidi (1981) completely reported the two-phase heat transfer data with their experimental parameters such as flow pattern, mass flow rates for liquid and gas, superficial velocities for liquid and gas, pressure drop across the test section, bulk temperature, void fraction, and wall temperature or the ratio of viscosity at the wall temperature and at the bulk temperature in the test section.

The experimental studies of Aggour, Rezkallah, Vijay and Zaidi were in vertical tubes with comprehensive flow patterns covering bubbly, slug, churn, froth, annular, mist, and their transition flows (e.g., bubble-slug, bubble-froth, froth-annular, slug-annular, froth-annular, slug-churn, churn-annular, or annular-mist flows). However, the experimental studies of King and Pletcher were in horizontal tubes with limited flow patterns. The study of King (1952) covered only horizontal slug flow and the study of Pletcher (1966) covered only horizontal annular flow pattern. Thus, comprehensive

experimental studies in horizontal tubes covering wide range of flow patterns is lacking in the literature. This type of data could aid in development of accurate two-phase flow heat transfer correlations in horizontal tubes.

In the next section, those correlations introduced in Sections 1.3.1 through 1.3.3 will be examined for their general validity. In order to access their general validity, they will be compared against an extensive set of two-phase heat transfer experimental data available from the literature (Table 1.5), for vertical and horizontal tubes and different flow patterns and fluids. Furthermore, the objectives of this study will be introduced.

1.4 Preliminary Comparisons

Numerous heat transfer correlations and experimental data for forced convective heat transfer during gas-liquid two-phase flow in vertical and horizontal pipes have been published over the past 40 years and carefully reviewed in Section 1.3. In this section, in order to access the general validity of those available two-phase heat transfer correlations, they are compared against an extensive set of two-phase flow heat transfer experimental data available from the literature, for vertical and horizontal tubes and different flow patterns and fluids. Based on their physical merits and their comparison results, this section identifies and recommends the best two-phase heat transfer correlations. Also, from the comparison results, the shortcomings in the previous works are identified. Finally, at the end of this section, the objectives of this study are introduced. More detailed information about the preliminary comparisons described in the next section can be found in Kim et al. (1997).

1.4.1 Introduction of Preliminary Comparisons

In Section 1.3, a comprehensive literature search was carried out and a total of 20 two-phase heat transfer correlations were identified, and their ranges of applicability as proposed by the original authors were documented through Tables 1.2 to 1.4. In most cases, the identified heat transfer correlations were derived empirically and were based on a small set of experimental data with a limited range of variables and liquid-gas combinations. In order to access the general validity of those correlations, they were compared against an extensive set of two-phase flow heat transfer experimental data discussed in Section 1.3.5 (see Table 1.5) for vertical and horizontal tubes and different flow patterns and fluids. A total of 427 data points from four available experimental studies (King, 1952; Pleatcher, 1966; Rezkallah, 1987; and Vijay, 1978) were used for these comparisons, since those available studies completely reported two-phase heat transfer data with their limited experimental parameters such as flow pattern, mass flow rates for liquid and gas, superficial velocities for liquid and gas, pressure drop across the test section, bulk temperature, void fraction, and wall temperature or the ratio of viscosity at the wall and at the bulk in the test section.

Table 1.6 shows twenty of the identified correlations that were tested in this preliminary test. Also, the limitations of the twenty correlations used in the comparisons as proposed by the original authors are tabulated in Table 1.7. The ranges of the experimental data used to access the general validity of the correlations listed in Table 1.6 are provided in Table 1.8.

A summary of the results obtained by comparing the twenty identified two-phase flow heat transfer correlations with the 139 water-air experimental data of Vijay (1978),

Table 1.6 Heat Transfer Correlations Chosen for the Preliminary Comparisons

Source	Heat Transfer Correlations	Source	Heat Transfer Correlations
Aggour (1978)	$h_{TP} / h_L = (1-\alpha)^{-1/3}$ Laminar (L)	Knott et al. (1959)	$\frac{h_{TP}}{h_L} = \left(1 + \frac{V_{SG}}{V_{SL}}\right)^{1/3}$ where h_L is from Sider & Tate (1936)
	$Nu_L = 1.615 (Re_{SL} Pr_L D/L)^{1/3} (\mu_B / \mu_W)^{0.14}$		
Chu & Jones (1980)	$h_{TP} / h_L = (1-\alpha)^{-0.83}$ Turbulent (T)	Kudirka et al. (1965)	$Nu_{TP} = 125 \left(\frac{V_{SG}}{V_{SL}}\right)^{1/8} \left(\frac{\mu_G}{\mu_L}\right)^{0.6} (Re_{SL})^{1/4} (Pr_L)^{1/3} \left(\frac{\mu_B}{\mu_W}\right)^{0.14}$
	$Nu_L = 0.0155 Re_{SL}^{0.83} Pr_L^{0.5} (\mu_B / \mu_W)^{0.33}$		
Davis & David (1964)	$Nu_{TP} = 0.060 \left(\frac{\rho_L}{\rho_G}\right)^{0.28} \left(\frac{DG_{tx}}{\mu_L}\right)^{0.87} Pr_L^{0.4}$	Martin & Sims (1971)	$\frac{h_{TP}}{h_L} = 1 + 0.64 \sqrt{\frac{V_{SG}}{V_{SL}}}$ where h_L is from Sider & Tate (1936)
Dorresteyn (1970)	$h_{TP} / h_L = (1-\alpha)^{-1/3}$ (L)	Oliver & Wright (1964)	$Nu_{TP} = Nu_L \left(\frac{1.2}{R_L^{0.36}} - \frac{0.2}{R_L}\right)$ $Nu_L = 1.615 \left[\frac{(Q_G + Q_L)\rho D}{A\mu} Pr_L D/L\right]^{1/3} (\mu_B / \mu_W)^{0.1}$
	$h_{TP} / h_L = (1-\alpha)^{-0.8}$ (T)		
Dusseau (1968)	$Nu_L = 0.0123 Re_{SL}^{0.9} Pr_L^{0.33} (\mu_B / \mu_W)^{0.14}$	Ravipudi & Godbold (1978)	$Nu_{TP} = 0.56 \left(\frac{V_{SG}}{V_{SL}}\right)^{0.3} \left(\frac{\mu_G}{\mu_L}\right)^{0.2} (Re_{SL})^{0.6} (Pr_L)^{1/3} \left(\frac{\mu_B}{\mu_W}\right)^{0.14}$
	$Nu_{TP} = 0.029 (Re_{TP})^{0.87} (Pr_L)^{0.4}$		
Elamvaluthi & Srinivas (1984)	$Nu_{TP} = 0.5 \left(\frac{\mu_G}{\mu_L}\right)^{1/4} (Re_{TP})^{0.7} (Pr_L)^{1/3} \left(\frac{\mu_B}{\mu_W}\right)^{0.14}$	Rezkallah & Sims (1987)	$h_{TP} / h_L = (1-\alpha)^{-0.9}$ where h_L is from Sider & Tate (1936)
Groothuis & Hendaal (1959)	$Nu_{TP} = 0.029 (Re_{TP})^{0.87} (Pr_L)^{1/3} (\mu_B / \mu_W)^{0.14}$ (for water-air)	Serizawa et al. (1975)	$\frac{h_{TP}}{h_L} = 1 + 462 X_{TT}^{-1.27}$ where h_L is from Sider & Tate (1936)
	$Nu_{TP} = 2.6 (Re_{TP})^{0.39} (Pr_L)^{1/3} (\mu_B / \mu_W)^{0.14}$ (for gas-oil-air)		
Hughmark (1965)	$Nu_{TP} = 1.75 (R_L)^{-1/2} \left(\frac{\dot{m}_L c_L}{R_L k_L L}\right)^{1/3} \left(\frac{\mu_B}{\mu_W}\right)^{0.14}$	Shah (1981)	$\frac{h_{TP}}{h_L} = \left(1 + \frac{V_{SG}}{V_{SL}}\right)^{1/4}$ $Nu_L = 1.86 (Re_{SL} Pr_L D/L)^{1/3} (\mu_B / \mu_W)^{0.14}$ (L) $Nu_L = 0.023 Re_{SL}^{0.8} Pr_L^{0.4} (\mu_B / \mu_W)^{0.14}$ (T)
Khoze et al. (1976)	$Nu_{TP} = 0.26 Re_{SG}^{0.2} Re_{SL}^{0.55} Pr_L^{0.4}$	Ueda & Hanaoka (1967)	$Nu_{TP} = 0.075 (Re_M)^{0.6} \frac{Pr_L}{1 + 0.035(Pr_L - 1)}$
King (1952)	$\frac{h_{TP}}{h_L} = \frac{R_L^{-0.52}}{1 + 0.025 Re_{SG}^{0.5}} \left[\left(\frac{\Delta P}{\Delta L}\right)_{TP} / \left(\frac{\Delta P}{\Delta L}\right)_L\right]^{0.32}$ $Nu_L = 0.023 Re_{SL}^{0.8} Pr_L^{0.4}$	Vijay et al. (1982)	$h_{TP} / h_L = (\Delta P_{TP} / \Delta P_L)^{0.451}$ $Nu_L = 1.615 (Re_{SL} Pr_L D/L)^{1/3} (\mu_B / \mu_W)^{0.14}$ (L) $Nu_L = 0.0155 Re_{SL}^{0.83} Pr_L^{0.5} (\mu_B / \mu_W)^{0.33}$ (T)
		Sieder & Tate (1936)	$Nu_L = 1.86 (Re_{SL} Pr_L D/L)^{1/3} (\mu_B / \mu_W)^{0.14}$ (L) $Nu_L = 0.027 Re_{SL}^{0.8} Pr_L^{0.33} (\mu_B / \mu_W)^{0.14}$ (T)

Note: α and R_L are taken from the original experimental data for this study. $Re_{SL} < 2000$ implies laminar flow, otherwise turbulent. For Shah (1980), replace 2000 by 170. With regard to the eqs. given for Shah (1980) above, the laminar two-phase correlation was used along with the appropriate single phase correlation, since Shah recommended a graphical turbulent two-phase correlation.

Table 1.7 Limitations of the Heat Transfer Correlations Used in the Preliminary Comparisons (See Nomenclature for Abbreviations)

Source	Fluids	L/D	Orient.	\dot{m}_G / \dot{m}_L	V_{SG}/V_{SL}	Re_{SG}	Re_{SL}	Pr_L	Flow Pattern(s)
Aggour (1978)	A-W, Helium-W, Freon12-W	52.1	V	7.5×10^{-3} - 5.72×10^{-2}	0.02-470	13.95- 2.09×10^5		5.42-6.36	B, S, A, B-S, B-F, S-A, A-M
Chu & Jones (1980)	W-A	34	V		0.12-4.64	540-2700	16000-112000		B, S, F-A
Davis & David (1964)	Gas-Liquid		H & V						A, M-A
Dorrestijn (1970)	A-Oil	16	V		0.004-4500		300-66000		B, S, A
Dusseau (1968)	A-W	67	V	45-350		$0-4.29 \times 10^4$	1.4×10^4 - 4.9×10^4		F
Elamvaluthi & Srinivas (1984)	A-W A-Glycerin	86	V		0.3-2.5 0.6-4.6		300-14300		B, S
Groothuis & Hendaal (1965)	A-W Gas-Oil-A	14.3	V	244-977 269-513	1-250 0.6-80		>5000 1400-3500		S
Hughmark (1965)	Gas-Liquid		H						S
Khoze et al. (1976)	A-W, A-Poly methylsiloxane, A-Diphenyloxide	60-80	V			4000-37000	3.5-210	4.1-90	A
King (1952)	A-W	252	H		1.21-6.94	1570- 8.28×10^4	22500- 11.9×10^4		S
Knott et al. (1959)	Petroleum oil-Nitrogen gas	118.6	V	1.57×10^{-3} - 1.19	0.1-40	6.7-162	126-3920		B
Kudirka et al. (1965)	A-W, A-Ethylene glycol	17.6	V	1.92×10^{-4} - 0.1427 0-0.11	0.16-75 0.25-67		5.5×10^4 - 49.5×10^4 380-1700	140 @ 37.8°C	B, S, F
Martin & Sims (1971)	A-W	17	H		0.08-276				B, S, A
Oliver & Wright (1964)	A-85% Glycol, A-1.5% SCMC, A-0.5% Polyox		H				500-1800		S
Ravipudi & Godbold (1978)	A-W, A-Toluene, A-Benzene, A-Methanol		V		1-90	3562-82532	8554-89626		F
Rezkallah & Sims (1987)	A, W, Oil, etc.; 13 Liquid-Gas combinations	52.1	V		0.01-7030		$1.8-1.3 \times 10^5$	4.2-7000	B, S, C, A, F, B-S, B-F, S-C, S-A, C-A, F-A
Serizawa et al. (1975)	A-W	35	V						B
Shah (1980)	A, W, Oil, Nitrogen, Glycol, etc.; 10 combinations		H & V		0.004-4500		7-253000		B, S, F, F-A, M
Ueda & Hanaoka (1967)	A-Liquid	67	V	9.4×10^{-4} - 0.059	4-50			4-160	S, A
Vijay et al. (1982)	A-W, A-Glycerin, Helium-W, Freon12-W	52.1	V		0.005-7670		1.8-130000	5.5-7000	B, S, F, A, M, B-F, S-A, F-A, A-M

Table 1.8 Ranges of the Experimental Data Used in the Preliminary Comparisons

Water-Air Vertical Data (139 Points) of Vijay (1978)	$16.71 \leq \dot{m}_L \text{ (lbm/hr)} \leq 8996$ $0.058 \leq \dot{m}_G \text{ (lbm/hr)} \leq 216.82$ $0.007 \leq X_{TT} \leq 433.04$ $0.061 \leq \Delta P_{TP} \text{ (psi)} \leq 17.048$ $5.503 \leq Pr_L \leq 6.982$ $101.5 \leq h_{TP} \text{ (Btu/hr-ft}^2\text{-}^\circ\text{F)} \leq 7042.3$	$0.06 \leq V_{SL} \text{ (ft/sec)} \leq 34.80$ $0.164 \leq V_{SG} \text{ (ft/sec)} \leq 460.202$ $59.64 \leq T_{MIX} \text{ (}^\circ\text{F)} \leq 83.94$ $0.007 \leq \Delta P_{TPF} \text{ (psi)} \leq 16.74$ $0.708 \leq Pr_G \leq 0.710$ $0.813 \leq \mu_w/\mu_B \leq 0.933$	$231.83 \leq Re_{SL} \leq 126630$ $43.42 \leq Re_{SG} \leq 163020$ $14.62 \leq P_{MIX} \text{ (psi)} \leq 74.44$ $0.033 \leq \alpha \leq 0.997$ $11.03 \leq Nu_{TP} \leq 776.12$ $L/D = 52.1, D = 0.46 \text{ in.}$
Glycerin-Air Vertical Data (57 Points) of Vijay (1978)	$100.5 \leq \dot{m}_L \text{ (lbm/hr)} \leq 1242.5$ $0.085 \leq \dot{m}_G \text{ (lbm/hr)} \leq 99.302$ $0.15 \leq X_{TT} \leq 407.905$ $1.317 \leq \Delta P_{TP} \text{ (psi)} \leq 20.022$ $6307.04 \leq Pr_L \leq 6962.605$ $54.84 \leq h_{TP} \text{ (Btu/hr-ft}^2\text{-}^\circ\text{F)} \leq 159.91$	$0.31 \leq V_{SL} \text{ (ft/sec)} \leq 3.80$ $0.217 \leq V_{SG} \text{ (ft/sec)} \leq 117.303$ $80.40 \leq T_{MIX} \text{ (}^\circ\text{F)} \leq 82.59$ $1.07 \leq \Delta P_{TPF} \text{ (psi)} \leq 19.771$ $0.708 \leq Pr_G \leq 0.709$ $0.513 \leq \mu_w/\mu_B \leq 0.610$	$1.77 \leq Re_{SL} \leq 21.16$ $63.22 \leq Re_{SG} \leq 73698$ $17.08 \leq P_{MIX} \text{ (psi)} \leq 62.47$ $0.0521 \leq \alpha \leq 0.9648$ $12.78 \leq Nu_{TP} \leq 37.26$ $L/D = 52.1, D = 0.46 \text{ in.}$
Silicone-Air Vertical Data (162 points) of Rezkallah (1986)	$17.3 \leq \dot{m}_L \text{ (lbm/hr)} \leq 196$ $0.07 \leq \dot{m}_G \text{ (lbm/hr)} \leq 157.26$ $72.46 \leq T_w \text{ (}^\circ\text{F)} \leq 113.90$ $0.037 \leq \Delta P_{TP} \text{ (psi)} \leq 9.767$ $61.0 \leq Pr_L \leq 76.5$ $29.9 \leq h_{TP} \text{ (Btu/hr-ft}^2\text{-}^\circ\text{F)} \leq 683.0$	$0.072 \leq V_{SL} \text{ (ft/sec)} \leq 30.20$ $0.17 \leq V_{SG} \text{ (ft/sec)} \leq 363.63$ $66.09 \leq T_B \text{ (}^\circ\text{F)} \leq 89.0$ $0.094 \leq \Delta P_{TPF} \text{ (psi)} \leq 9.074$ $0.079 \leq Pr_G \leq 0.710$ $L/D = 52.1, D = 0.46 \text{ in.}$	$47.0 \leq Re_{SL} \leq 20930$ $52.1 \leq Re_{SG} \leq 118160$ $13.9 \leq P_{MIX} \text{ (psi)} \leq 45.3$ $0.011 \leq \alpha \leq 0.996$ $17.3 \leq Nu_{TP} \leq 386.8$
Water-Air Horizontal Data (48 points) of Pletcher (1966)	$0.069 \leq \dot{m}_L \text{ (lbm/sec)} \leq 0.3876$ $0.22 \leq \Delta P_{M/L} \text{ (lbf/ft}^3\text{)} \leq 26.35$ $7.23 \leq \phi_1 \leq 68.0$ $7372 \leq q'' \text{ (Btu/hr-ft}^2\text{)} \leq 11077$	$0.03 \leq \dot{m}_G \text{ (lbm/sec)} \leq 0.2568$ $0.021 \leq X_{TT} \leq 0.490$ $73.6 \leq T_w \text{ (}^\circ\text{F)} \leq 107.1$ $433 \leq h_{TP} \text{ (Btu/hr-ft}^2\text{-}^\circ\text{F)} \leq 1043.8$	$7.84 \leq \Delta P/L \text{ (lbf/ft}^3\text{)} \leq 137.5$ $1.45 \leq \phi_g \leq 3.54$ $64.9 \leq T_{MIX} \text{ (}^\circ\text{F)} \leq 99.4$ $L/D = 60.0, D = 1.0 \text{ in.}$
Water-Air Horizontal Data (21 points) of King (1952)	$1375 \leq \dot{m}_L \text{ (lbm/hr)} \leq 6410$ $1570 \leq Re_{SG} \leq 84200$ $136.8 \leq T_{MIX} \text{ (}^\circ\text{F)} \leq 144.85$ $147.9 \leq \Delta P_{TP} \text{ (psf)} \leq 3226$ $1.35 \leq h_{TP} / h_L \leq 3.34$	$0.82 \leq \dot{m}_G \text{ (SCFM)} \leq 43.7$ $0.41 \leq X_{TT} \leq 29.10$ $184.3 \leq T_w \text{ (}^\circ\text{F)} \leq 211.3$ $1462 \leq h_{TP} \text{ (Btu/hr-ft}^2\text{-}^\circ\text{F)} \leq 4415$ $1.35 \leq \phi_1 \leq 8.20$	$22500 \leq Re_{SL} \leq 119000$ $0.117 \leq R_L \leq 0.746$ $15.8 \leq P_{MIX} \text{ (psi)} \leq 55.0$ $1.08 \leq V_{SG}/V_{SL} \leq 6.94$ $L/D = 252, D = 0.737 \text{ in.}$

57 glycerin-air experimental data of Vijay (1978), 162 silicone-air experimental data of Rezkallah (1986), 48 water-air experimental data of Pletcher (1966), and 21 water-air experimental data of King (1952) are given in Tables 1.9 to 1.12, respectively. These tables give the total number of experimental data points used from each experimental study, the total number of data points for each flow pattern, the number of data points in each flow pattern that were predicted to within $\pm 30\%$ by the individual heat transfer correlations, and the percent overall mean and r.m.s. deviations for the predictions of

each correlation. Note that the magnitudes of mean and r.m.s. deviations in these tables range from 0.08% to 314,035% indicating a wide range of agreement/disagreement of the correlation with the experimental data.

The flow patterns for the experimental data were based on the procedures suggested by Govier and Aziz (1973), Griffith and Wallis (1961), Hewitt and Hall-Taylor (1970), Taitel et al. (1980), Taitel and Dukler (1976), and visual observation as appropriate. For each flow pattern, the tables also highlight the number of data points predicted by the correlation(s) that best satisfied the $\pm 30\%$ criterion.

1.4.2 Water-Air Data of Vijay (1978)

The results of comparisons shown in Table 1.9 indicate that, for bubbly, froth, annular, bubbly-froth, and froth-annular flows, several of the heat transfer correlations did a very good job of predicting the experimental water-air data of Vijay (1978) in a vertical tube. However, for slug, slug-annular, and annular-mist flows, only one correlation for each flow pattern showed good predictions. Considering the performance of the correlations for all the flow patterns and keeping in mind the values of the overall mean and r.m.s. deviations, three heat transfer correlations are recommended for this set of experimental data. These are the correlation of Knott et al. (1959) for bubbly, froth, bubbly-froth, froth-annular, and annular-mist flows; the correlation of Ravipudi and Godbold (1978) for annular, slug-annular, and froth-annular flows; and the correlation of Aggour (1978) for bubbly and slug flows. Figures 1.6 to 1.8 show how well the recommended correlations for each flow pattern performed with respect to the water-air experimental data of Vijay (1978).

Table 1.9 Comparison of Water-Air Experimental Data (139 Data Points) of Vijay (1978) with the Suggested Correlations (See Nomenclature for Abbreviations)

Source	Mean Dev. (%)	r.m.s. Dev. (%)	Data Points within $\pm 30\%$ for Each Flow Pattern (Pattern / Total No. of Data Points)							
			B (25)	S (25)	F (25)	A (25)	B-F (7)	S-A (10)	F-A (4)	A-M (18)
Aggour (1978)	-14.28	56.27	25	25	2	14	4	4	1	
Chu & Jones (1980)	-44.43	97.11	23	17	23	20	7	5	4	3
Davis & David (1964)	-155.91	541.35			3	8		3		
Dorrestejn (1970)	-30.85	67.36	4	20		11		2		
Dusseau (1968)	85.25	85.64								
Elamvaluthi & Srinivas (1984)	-218.73	402.73						2		
Groothuis & Hendal (1959)	-221.14	451.19		7		11		6		
Khoze et al. (1976)	-155.48	172.42						3		1
Knott et al. (1959)	3.76	33.95	25	20	25	19	7	3	4	11
Kudirka et al. (1965)	-71.82	240.25	4	6	6	18	2	2	4	3
Martin & Sims (1971)	-42.69	89.23	25	22	18	18	6	5	4	2
Oliver & Wright (1964)	5701.	25791.								
Ravipudi & Godbold (1978)	-14.66	86.60		21	16	21	4	7	4	3
Rezkallah & Sims (1987)	-35.36	80.03	25	22	17	14	7	5	4	4
Serizawa et al. (1975)	-81034.	299137.	2							
Shah (1981)	24.86	31.51	25	15	25	3	7	3	4	6
Ueda & Hanaoka (1967)	-135.90	352.79	20	14	25	20	7	2	4	1
Vijay et al. (1982)	46.26	58.59	21	2	23		6			

Note: Blanks indicate the correlation did not satisfy the $\pm 30\%$ criterion.

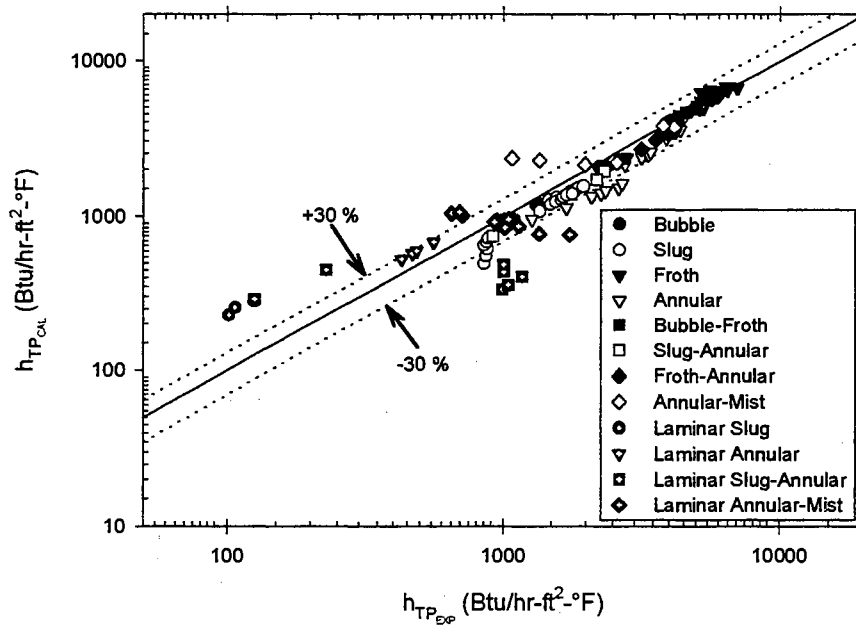


Figure 1.6 Comparison of Knott et al. (1959) Correlation with Vijay's (1978) Water-Air Experimental Data

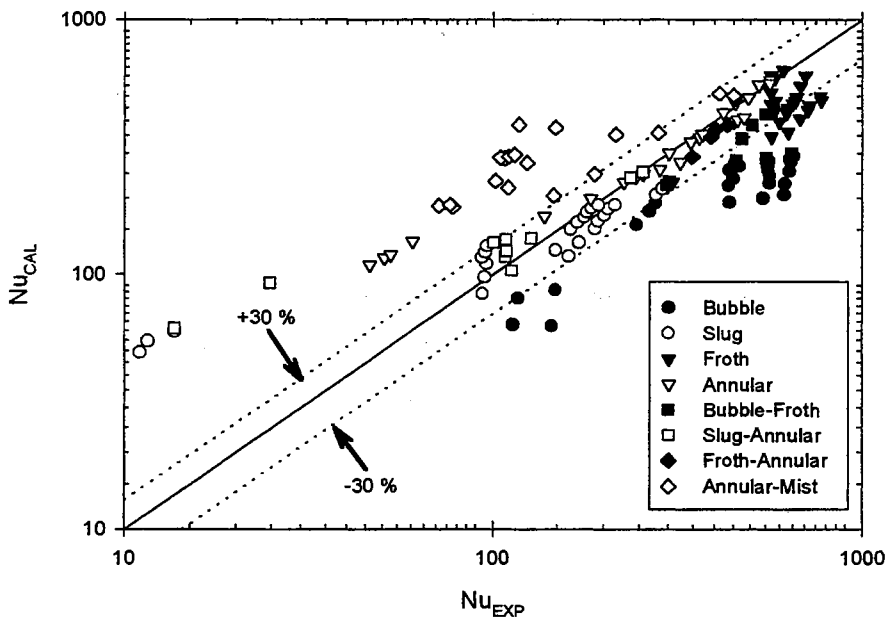


Figure 1.7 Comparison of Ravipudi & Godbold (1978) Correlation with Vijay's (1978) Water-Air Experimental Data

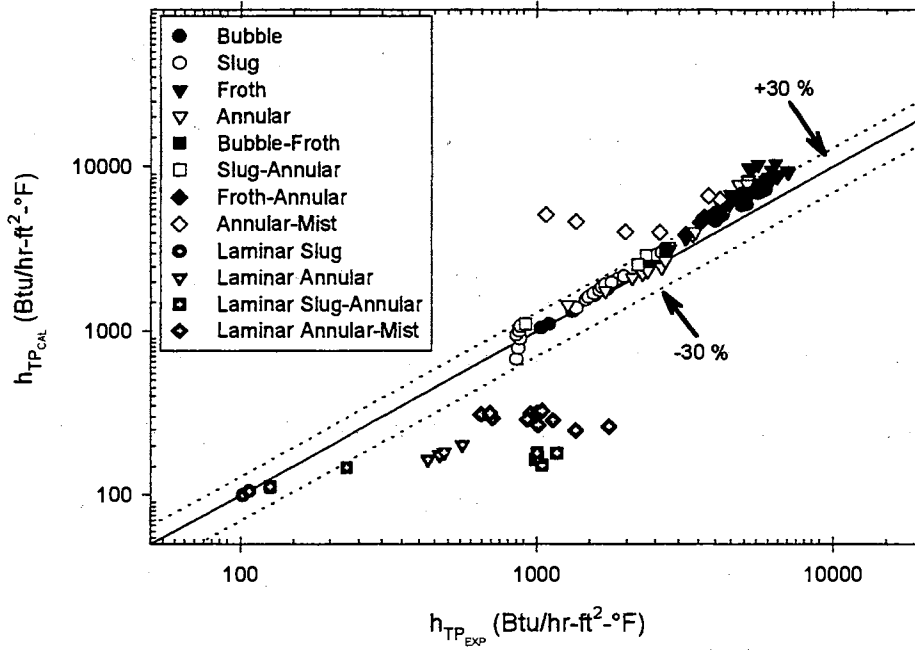


Figure 1.8 Comparison of Aggour (1978) Correlation with Vijay's (1978) Water-Air Experimental Data

1.4.3 Glycerin-Air Data of Vijay (1978)

From the comparison results shown in Table 1.10, it can be seen that only a few of the tested heat transfer correlations were capable of predicting with good accuracy the glycerin-air experimental data of Vijay (1978) in a vertical tube. Considering the overall performance of the correlations for all the flow patterns, only the correlation of Aggour (1978) is recommended for this set of experimental data. The performance of Aggour's (1978) correlation in different flow patterns (bubbly, slug, froth, annular, bubbly-slug, and slug-annular) with respect to the glycerin-air experimental data of Vijay (1978) is shown in Fig. 1.9

1.4.4 Silicone-Air Data of Rezkallah (1986)

For the silicone-air experimental data of Rezkallah (1986) in a vertical tube, a few of the correlations predicted the experimental data reasonably well (see Table 1.11). Again, considering the overall performance of the correlations for all the flow patterns and the values of the mean and r.m.s. deviations, only three of the tested heat transfer correlations are recommended. These are the correlation of Rezkallah and Sims (1987) for bubbly, slug, churn, bubbly-slug, bubbly-froth, slug-churn, and churn-annular flows; the correlation of Ravipudi and Godbold (1978) for churn, annular, bubbly-slug, slug-churn, churn-annular, and froth-annular flows; and the correlation of Shah (1981) for bubbly, froth, bubbly-froth, froth-annular, and annular-mist flows. Figures 1.10, 1.11 and 1.12 show the comparison between the predictions of the three recommended correlations and the silicone-air experimental data of Rezkallah (1986).

Table 1.10 Comparison of Glycerin-Air Experimental Data (57 Data Points) of Vijay (1978) with the Suggested Correlations (See Nomenclature for Abbreviations)

Source	Mean Dev. (%)	r.m.s. Dev. (%)	Data Points within $\pm 30\%$ for Each Flow Pattern (Pattern / Total No. of Data Points)					
			B (4)	S (19)	F (17)	A (8)	B-S (4)	S-A (5)
Aggour (1978)	-13.82	18.44	4	17	15	8	4	4
Chu & Jones (1980)	-99.03	102.81		2				
Davis & David (1964)	-149.87	285.90		2	4			
Dorresteyjn (1970)	88.51	88.69						
Dusseau (1968)	97.04	97.06						
Elamvaluthi & Srinivas (1984)	-1410.	1844.	1	1				
Groothuis & Hendal (1959)	-6301.	8960.						
Hughmark (1965)	-624.18	675.32						
Khoze et al. (1976)	-514.71	567.68						
Knott et al. (1959)	-85.93	96.64	3	2			2	
Kudirka et al. (1965)	61.62	61.86						
Martin & Sims (1971)	-164.31	185.58						
Oliver & Wright (1964)	5994.	18350.						
Ravipudi & Godbold (1978)	66.18	66.69						
Rezkallah & Sims (1987)	-51.49	54.86	1	1		6		
Serizawa et al. (1975)	-17574.	35334.						
Shah (1981)	-50.12	54.00	4	4			3	
Ueda & Hanaoka (1967)	-68.43	140.38		17	2		4	
Vijay et al. (1982)	26.58	33.12	4	17	9		4	

Note: Blanks indicate the correlation did not satisfy the $\pm 30\%$ criterion.

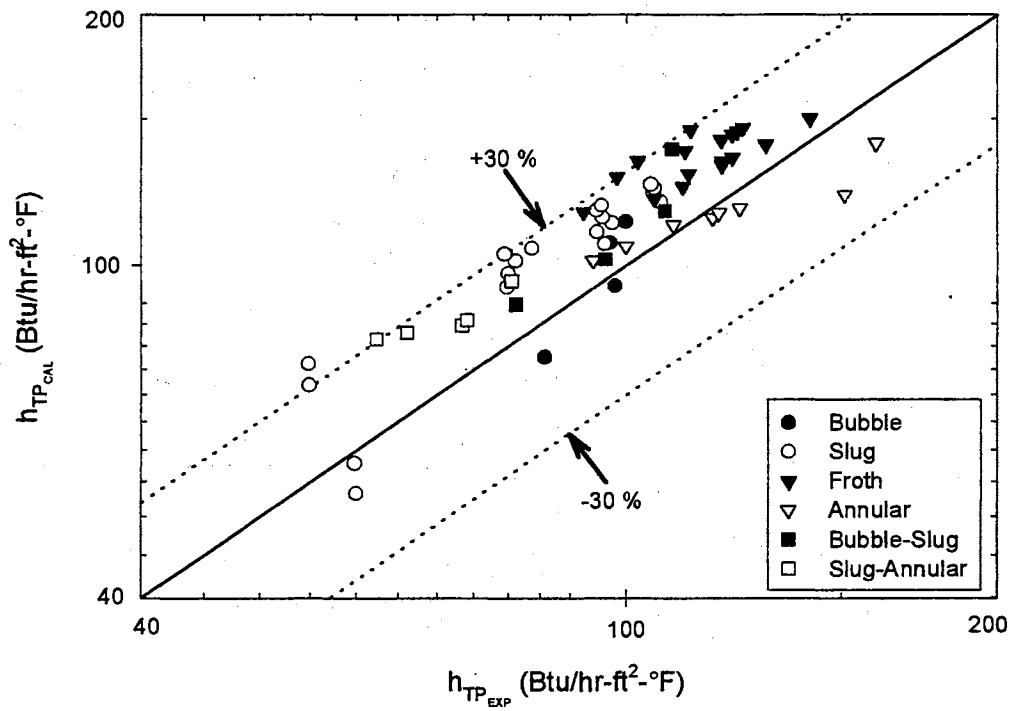


Figure 1.9 Comparison of Aggour (1978) Correlation with Vijay's (1978) Glycerin-Air Experimental Data

Table 1.11 Comparison of Silicone-Air Experimental Data (162 Data Points) of Rezkallah (1986) with the Suggested Correlations (See Nomenclature for Abbreviations)

Source	Mean Dev. (%)	r.m.s. Dev. (%)	Data Points within $\pm 30\%$ for Each Flow Pattern (Pattern / Total No. of Data Points)											
			B (26)	S (13)	C (11)	A (25)	F (18)	B-S (7)	B-F (10)	S-C (13)	C-A (12)	F-A (6)	A-M (21)	
Aggour (1978)	-5.57	74.95		3	2	4					1	1		10
Chu & Jones (1980)	-128.74	193.70	13	3			10			5				
Davis & David (1964)	-127.63	435.79		1	1	7					3	5	3	
Dorresteyn (1970)	20.42	59.91	24				2	2	8	1				4
Dusseau (1968)	86.69	87.22												
Elamvaluthi & Srinivas (1984)	-426.83	841.52		7				1	1	2				
Groothuis & Hendal (1959)	-623.48	1326.	1	5	2			4		5				
Hughmark (1965)	-126.83	364.56	4	7	7	6		5		9	7			
Khoze et al. (1976)	-295.28	366.85		2										
Knott et al. (1959)	-4.09	57.41	22	3	1	11	18	3	10	3	3	6	2	
Kudirka et al. (1965)	-65.83	130.59	4			5	8	2	5	1	1	6		
Martin & Sims (1971)	-63.47	149.26	21	3	3	9	11	2	10	3	9			
Oliver & Wright (1964)	12702	46885.	5	3	1			5		7				
Ravipudi & Godbold (1978)	-12.06	85.25	5	4	9	15	10	7	1	12	11	6	1	
Rezkallah & Sims (1987)	-20.02	52.55	26	8	9	14	10	6	10	12	10		6	
Serizawa et al. (1975)	-91540.	295080.	14											
Shah (1981)	9.28	42.96	25	3	1	11	18	3	10	6	4	6	10	
Ueda & Hanaoka (1967)	-528.50	984.09												
Vijay et al. (1982)	41.38	67.08	10			4	14	3	7	1	1	6		

Note: Blanks indicate the correlation did not satisfy the $\pm 30\%$ criterion.

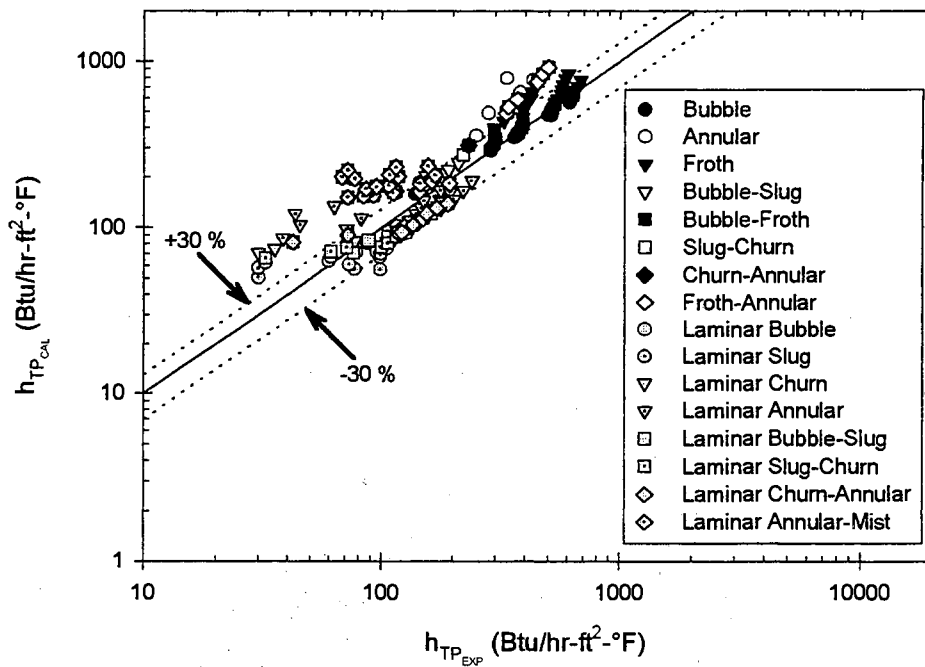


Figure 1.10 Comparison of Rezkallah & Sims (1987) Correlation with Rezkallah's (1986) Silicone-Air Experimental Data

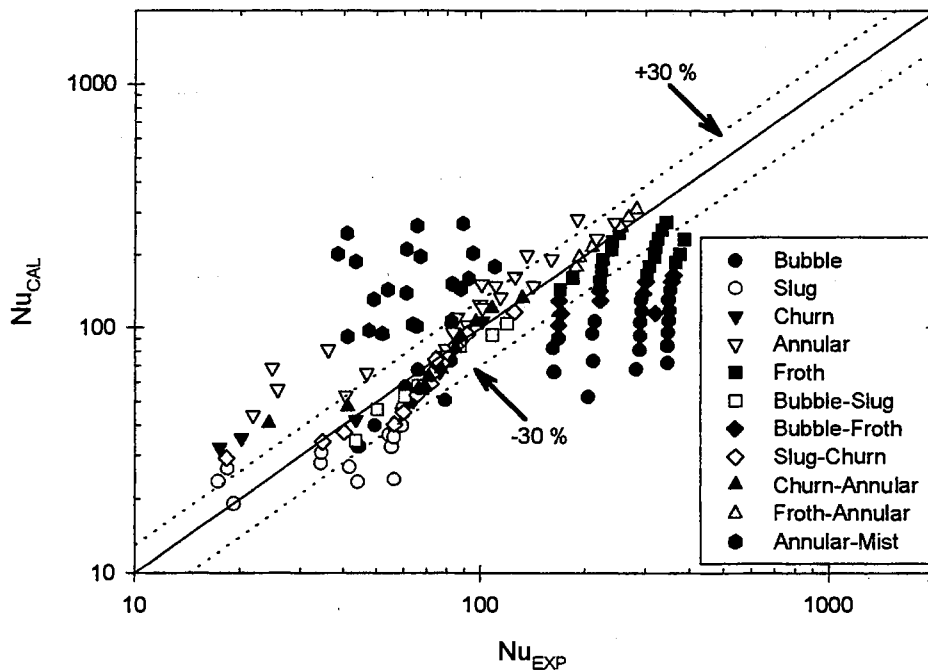


Figure 1.11 Comparison of Ravipudi & Godbold (1978) Correlation with Rezkallah's (1986) Silicone-Air Experimental Data

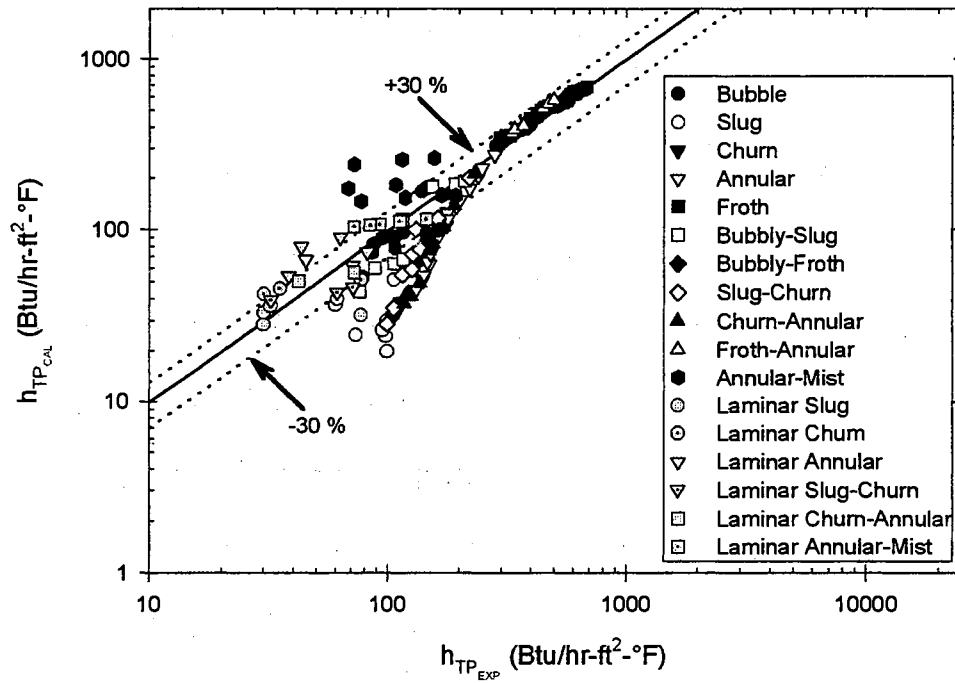


Figure 1.12 Comparison of Shah (1981) Correlation with Rezkallah's (1986) Silicone-Air Experimental Data

1.4.5 Water-Air Data of Pletcher (1966) and King (1952)

Table 1.12 shows the results of comparison for the 48 annular flow water-air experimental data of Pletcher (1966) and 21 slug flow water-air experimental data of King (1952) in horizontal tubes with the identified heat transfer correlations. For the annular flow data, only the correlation of Shah (1981) performed well. Figure 1.13 compares the performance of this correlation with the experimental data of Pletcher (1966). Also shown in Table 1.12 are the results of comparison between the heat transfer correlations and the slug flow experimental data of King (1952). The experimental data of King (1952) were predicted very well with five of the identified heat transfer correlations. Figure 1.14 shows how well the correlations of Chu and Jones (1980), King (1952), Kudrika et al. (1965), Martin and Sims (1971), and Ravipudi and Godbold (1978) predicted the slug flow data of King (1952).

1.4.6 Summary and Conclusions of the Preliminary Comparisons

The preliminary comparison study showed the ability of 20 two-phase heat transfer correlations to predict five sets of experimental data that were available in the open literature. Three of these experimental data sets were for the flow of air-water (Vijay, 1978), air-glycerin (Vijay, 1978), and air-silicone (Rezkallah, 1986) in various flow patterns within vertical pipes. The other two data sets were for the flow of air-water in slug (King, 1952) and annular (Pletcher, 1966) flow patterns within horizontal pipes.

The comparisons show the following recommendations, and the recommendations are summarized in Table 1.13 with regard to the main flow patterns. For air-water flow within vertical pipes, the comparisons recommend use of the Knott et al. (1959) correlation for bubbly, froth, bubbly-froth, froth-annular, and annular-mist flow patterns;

Table 1.12 Comparison of 48 Water-Air Experimental Data Points of Pletcher (1966) and 21 Water-Air Experimental Data Points of King (1952) with the Suggested Correlations (See Nomenclature for Abbreviations)

Source	Annular Flow (Pletcher, 1966)			Slug Flow (King, 1952)		
	Mean Dev. (%)	r.m.s. Dev. (%)	No. of $\pm 30\%$ Data Points	Mean Dev. (%)	r.m.s. Dev. (%)	No. of $\pm 30\%$ Data Points
Aggour (1978)	-233.85	314.86		-57.46	66.21	3
Chu & Jones (1980)	insufficient exp. information provided			0.08	16.33	20
Davis & David (1964)	99.93	99.93		-2166.	3448.	
Dorresteiin (1970)	-232.01	297.41	5	-45.74	54.06	6
Dusseau (1968)	99.97	99.97		68.63	69.03	
Elamvaluthi & Srinivas (1984)	-402.71	434.73		-89.46	95.87	
Groothuis & Hendaal (1959)	-480.49	538.78		-65.33	77.95	5
Hughmark (1965)	insufficient exp. information provided			56.06	59.25	2
Khoze et al. (1959)	-122.58	141.38	6	-121.91	127.86	
King (1952)	insufficient exp. information provided			4.77	12.14	21
Knott et al. (1959)	-80.79	101.76	6	21.44	26.03	12
Kudirka et al. (1965)	-52.30	59.92	11	-4.30	27.61	18
Martin & Sims (1971)	-246.76	278.68		8.79	18.90	19
Oliver & Wright (1964)	-616.92	1201.	6	91.82	91.85	
Ravipudi & Godbold (1978)	-193.51	212.15		15.72	18.39	19
Rezkallah & Sims (1987)	-333.49	405.60		-46.47	57.37	7
Serizawa et al. (1975)	-256486.	314035.		-8791.	13529.	
Shah (1981)	-13.92	31.98	33	37.42	39.65	7
Ueda & Hanaoka (1967)	-186.16	198.71		-34.09	163.50	9
Vijay et al. (1982)	4.34	37.11	26	-44.	53.21	7

Note: Blanks indicate the correlation did not satisfy the $\pm 30\%$ criterion.

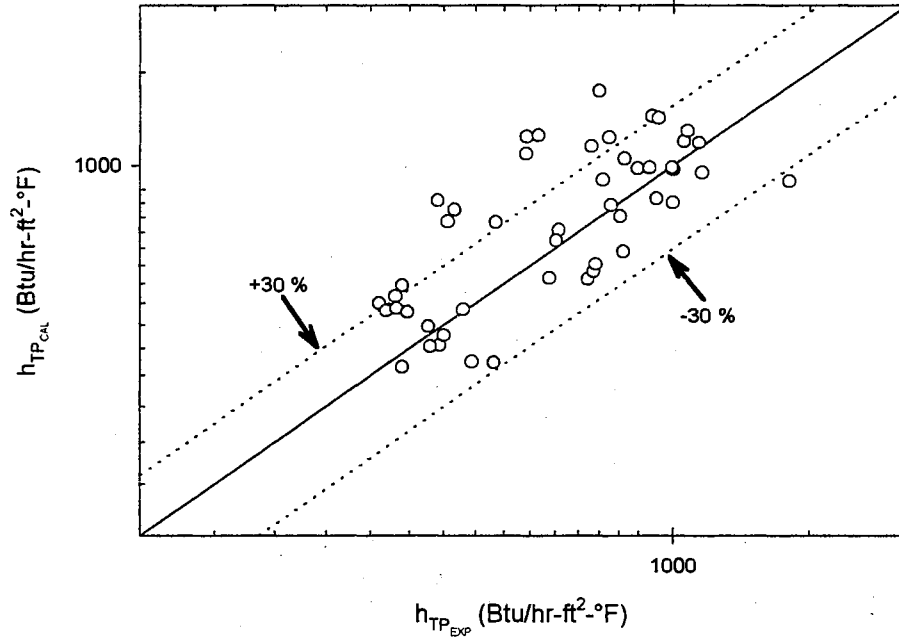


Figure 1.13 Comparison of Shah (1981) Correlation with Pletcher's (1966) Water-Air Experimental Data

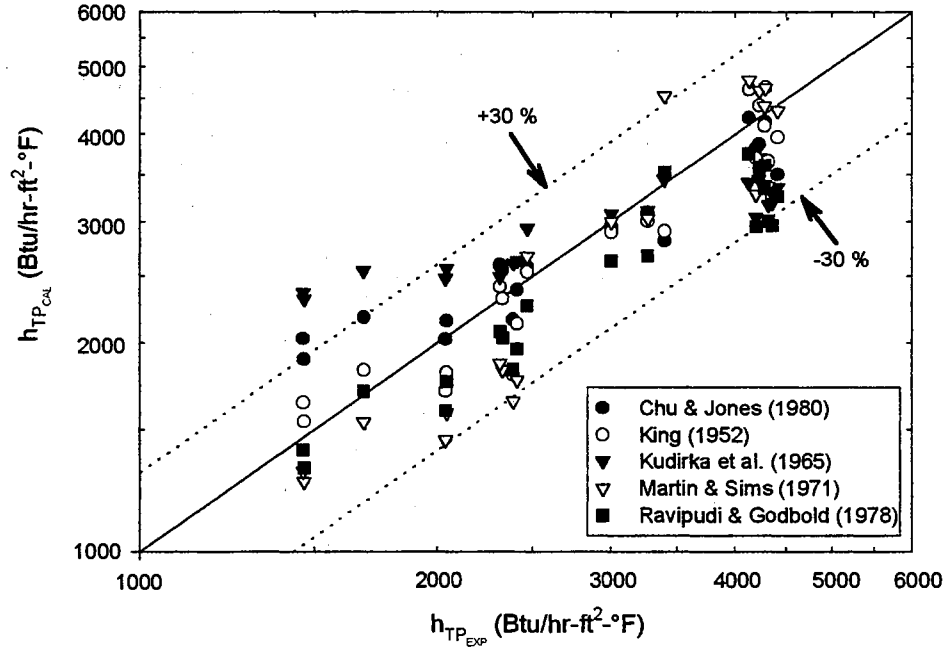


Figure 1.14 Comparison of Correlations of Chu & Jones (1980), King (1952), Kudirka et al. (1965), Martin & Sims (1971), and Ravipudi & Godbold (1978) with King's (1952) Water-Air Experimental Data

Table 1.13 Recommended Correlations from the Preliminary Comparisons with Regard to Pipe Orientation, Fluids, and Flow Patterns

Source	Correlation	Vertical Experimental Pipe														Horizontal	
		Water-Air				Glycerin-Air				Silicone-Air						W-A	
		B	S	F	A	B	S	F	A	B	S	C	A	F	A	S	
Aggour (1978)	$h_{TP} / h_L = (1-\alpha)^{-1/3}$ Laminar (L) $Nu_L = 1.615 (Re_{SL} Pr_L D / L)^{1/3} (\mu_B / \mu_W)^{0.14}$ (L) $h_{TP} / h_L = (1-\alpha)^{-0.83}$ Turbulent (T) $Nu_L = 0.0155 Re_{SL}^{0.83} Pr_L^{0.5} (\mu_B / \mu_W)^{0.33}$ (T)	✓	✓			✓	✓	✓	✓								
Chu & Jones (1980)	$Nu_{TP} = 0.43 (Re_{TP})^{0.55} (Pr_L)^{1/3} \left(\frac{\mu_B}{\mu_W}\right)^{0.14} \left(\frac{Pa}{P}\right)^{0.17}$				✓											✓	
King (1952)	$\frac{h_{TP}}{h_L} = \frac{R_L^{-0.52}}{1 + 0.025 Re_{SG}^{0.5}} \left[\left(\frac{\Delta P}{\Delta L}\right)_{TP} / \left(\frac{\Delta P}{\Delta L}\right)_L \right]^{0.32}$	insufficient experimental information provided														✓	
Knott et al. (1959)	$\frac{h_{TP}}{h_L} = \left(1 + \frac{V_{SG}}{V_{SL}}\right)^{1/3}$ where h_L is from Sider & Tate (1936)	✓		✓											✓		
Kudirka et al. (1965)	$Nu_{TP} = 125 \left(\frac{V_{SG}}{V_{SL}}\right)^{1/8} \left(\frac{\mu_G}{\mu_L}\right)^{0.6} (Re_{SL})^{1/4} (Pr_L)^{1/3} \left(\frac{\mu_B}{\mu_W}\right)^{0.14}$															✓	
Martin & Sims (1971)	$\frac{h_{TP}}{h_L} = 1 + 0.64 \sqrt{\frac{V_{SG}}{V_{SL}}}$ where h_L is from Sider & Tate (1936)	✓														✓	
Ravipudi & Godbold (1978)	$Nu_{TP} = 0.56 \left(\frac{V_{SG}}{V_{SL}}\right)^{0.3} \left(\frac{\mu_G}{\mu_L}\right)^{0.2} (Re_{SL})^{0.6} (Pr_L)^{1/3} \left(\frac{\mu_B}{\mu_W}\right)^{0.14}$				✓							✓	✓			✓	
Rezkallah & Sims (1987)	$h_{TP} / h_L = (1-\alpha)^{-0.9}$ where h_L is from Sider & Tate (1936)	✓								✓	✓	✓					
Shah (1981)	$\frac{h_{TP}}{h_L} = \left(1 + \frac{V_{SG}}{V_{SL}}\right)^{1/4}$ $Nu_L = 1.86 (Re_{SL} Pr_L D / L)^{1/3} (\mu_B / \mu_W)^{0.14}$ (L) $Nu_L = 0.023 Re_{SL}^{0.8} Pr_L^{0.4} (\mu_B / \mu_W)^{0.14}$ (T)	✓		✓		✓				✓				✓	✓		

use of the Ravipudi and Godbold (1978) correlation for annular, slug-annular, and froth-annular flow patterns; and use of the Aggour (1978) correlation for bubbly and slug flow patterns. For air-glycerin flow within vertical pipes, the comparisons recommend use of the Aggour (1978) correlation for bubbly, slug, froth, annular, bubbly-slug, and slug-annular flow patterns. For air-silicone flow within vertical pipes, the comparisons recommend use of the Rezkallah and Sims (1987) correlation for bubbly, slug, churn, bubbly-slug, bubbly-froth, slug-churn, and churn-annular flow patterns; use of the Ravipudi and Godbold (1978) correlation for churn, annular, bubbly-slug, slug-churn, churn-annular, and froth-annular; and use of the Shah (1981) correlation for bubbly, froth, bubbly-froth, froth-annular, and annular-mist flow patterns. With regard to air-water flow in horizontal pipes, the comparisons recommend use of the Shah (1981) correlation for annular and use of the Kudrika et al. (1965) correlation for slug flow patterns.

The above recommended correlations all have the following important parameters in common: Re_{SL} , Pr_L , μ_B/μ_W and either void fraction (α), superficial velocity ratio of gas and liquid (V_{SG}/V_{SL}), or viscosity ratio of gas and liquid (μ_G/μ_L).

For air-water and glycerin-air flows within vertical pipes, the correlation of Aggour (1978) is recommended for bubbly and slug flow patterns. However, for silicone-air flow, use of the Aggour (1978) correlation is not recommended for the same flow patterns even though the flow is within a vertical pipe. For air-water and silicone-air flows within vertical pipes, the correlation of Rezkallah & Sims (1987) is recommended for bubbly flow pattern. However, for glycerin-air flow, use of the Rezkallah & Sims (1987) correlation is not recommended for the same flow pattern even though the flow is

within a vertical pipe. Those correlations can be classified as the explicit void fraction type correlations having the parameter of void fraction (α) for two-phase heat transfer as can be seen from Section 1.3.3. Since those correlations are not capable of predicting the two-phase heat transfer for all fluid combinations in vertical pipes, there appears to be at least one parameter [ratio], which is related to fluid combinations, that is missing from those correlations.

For air-water flow within a horizontal pipe, the correlation of Kudirka et al. (1965) is recommended for slug flow pattern. However, use of the same correlation is not recommended for the same flow pattern within a vertical pipe even though the same two-phase fluid (air-water) is used. For air-water flow, the correlation of Ravipudi & Godbold (1978) is recommended for a vertical annular flow pattern. However, the same correlation is not recommended for the same flow pattern within a horizontal pipe. Also, the correlation of Ravipudi & Godbold is not recommended for vertical air-water slug flow pattern but recommended for horizontal air-water slug flow pattern. Those correlations can be classified as the extended Sieder-Tate type correlation having the parameters of superficial velocity ratio of gas and liquid (V_{SG}/V_{SL}) and viscosity ratio of gas and liquid (μ_G/μ_L) for two-phase heat transfer as can be seen from Section 1.3.1. Since those correlations are not capable of predicting the two-phase heat transfer for vertical and horizontal pipes with the same fluid combinations, there appears to be at least one parameter [ratio], which is related to pipe orientation, that is missing from those correlations.

The correlation of Shah (1981) is recommended for water-air, glycerin-air, or silicone-air bubbly flow pattern within a vertical pipe, and also recommended for air-

water and silicone-air froth flow pattern within a vertical pipe. This correlation can be classified as the extended Sieder-Tate type correlation having the parameter of $(1+V_{SG}/V_{SL})$ for two-phase heat transfer, and the correlation's derivation was based on the separated flow model concept as can be seen from Section 1.3.1. This separated flow model analysis may be helpful to find a parameter [ratio] which is related to fluid combinations for bubbly and froth flow patterns within a vertical pipe.

1.5 Shortcomings of the Previous Work

From the previous section, the general validities of the several two-phase heat transfer correlations were compared against the large sets of available experimental data. However, since there is no single correlation capable of predicting the two-phase heat transfer for all fluid combinations in vertical pipes, there appears to be at least one parameter [ratio], which is related to fluid combination, that is missing from the previous works. Also, since, for the horizontal data available, the recommended correlations differ from those of vertical pipes, there must also be at least one additional parameter [ratio], related to pipe orientation, that is missing from the previous work. In addition to these shortcomings in the previous work, the available two-phase heat transfer studies lack the following in-depth studies:

- No systematic parametric study has been performed on the numerous two-phase flow forced convective heat transfer correlations in vertical and horizontal pipes that have been published in the literature for the past 40 years. The two-phase heat transfer correlations all have the following important parameters in common: Re_{SL} , Pr_L , μ_B/μ_W

and either void fraction (α), superficial velocity ratio of gas and liquid (V_{SG}/V_{SL}), or viscosity ratio of gas and liquid (μ_G/μ_L). However, no investigation has been performed to identify the effects of those important parameters on the two-phase heat transfer.

- Comprehensive experimental data sets in horizontal tubes covering a wide range of flow patterns are lacking in the current literature as can be seen from Section 1.3.5. When a gas-liquid mixture flows in a pipe, a variety of flow patterns may occur, depending primarily on flow rates, the physical properties of the fluids, and the pipe inclination angle. The variety of flow patterns reflects the different ways that the gas and liquid phases are distributed in a pipe, and as the spatial distribution of each changes from one flow pattern to another, the heat transfer mechanism can be different according to the different flow patterns. In order to develop a correlation(s) which is robust enough to span all or most of the fluid combinations, pipe orientations, and flow patterns, additional experimental data sets which are not in the currently available experimental literature are required. Table 1.14 shows the sources of the available experimental data in the open literature which reported complete information on two-phase heat transfer data along with the fluid combinations used, flow patterns observed, and the number of data points taken. A total of 1128 data points are available for vertical tubes with comprehensive flow patterns covering bubbly, slug, churn, froth, annular, mist, and their transition flows and different fluid combinations. However, only 69 data points are available for horizontal tubes with very limited flow patterns covering slug and annular flows and fluid combination (air-water only). Thus, comprehensive experimental studies in horizontal tubes covering

Table 1.14 Available Experimental Data Points (See Nomenclature for Flow Pattern Abbreviations)

Source	Vertical Experimental Tube			Horizontal Experimental Tube		
	Fluids	Flow Pattern	Data Points	Fluids	Flow Pattern	Data Points
Aggour (1978)	Air/Water	B, S, F, A, B-F	109			
	Helium/Water	B, S, F, A, B-S, B-F, S-A, A-M	53			
	Freon/Water	B, S, F, A, B-S, B-F, S-A	44			
King (1952)				Air/Water	S	21
Pletcher (1966)				Air/Water	A	48
Rezkallah (1986)	Air/Water	B, S, C, A, F, B-S, B-F, S-C, S-F, C-A, F-A, A-M	64			
	Air/Glycerin +Water	B, S, C, A, F, B-S, B-F, S-C, S-F, C-A, F-A, A-M	124			
	Air/Silicone	B, S, C, A, F, B-S, B-F, S-C, C-A, F-A, A-M	190			
Vijay (1978)	Air/Water	B, S, F, A, B-F, S-A, F-A, A-M	181			
	Air/Glycerin	B, S, F, A, B-S, S-A	57			
	Air/Glycerin +Water	B, S, F, A, B-S, S-A	94			
Zaidi (1981)	Air/Water	B, S, C, A, F, B-S, B-F, S-A, S-F, C-A, A-F, A-M	118			
	Air/Glycerin +Water	B, S, C, A, F, B-S, B-F, S-F, C-A, A-F, A-M	94			

wide range of flow patterns and fluid combinations are needed.

1.6 Objectives

The main purpose of this study is the development of a two-phase heat transfer correlation(s) which is robust enough to span all or most of the fluid combinations, pipe orientations, and flow patterns. In order to achieve this goal successfully, the following specific tasks were accomplished:

1. A literature search for the two-phase heat transfer coefficient correlations and the two-phase flow experimental data for horizontal/vertical tubes was conducted to aid in the development/identification of the best two-phase heat transfer correlation(s). In addition, in order to understand the importance of the parameters in the identified existing two-phase heat transfer correlations such as Re_{SL} , Pr_L , μ_B/μ_W and either void fraction (α), superficial velocity ratio of gas and liquid (V_{SG}/V_{SL}), or viscosity ratio of gas and liquid (μ_G/μ_L), the general validity of the performance of the selected correlations was tested against the recommended particular range of the parameters suggested by the original authors. Based on the tabulated and graphical results of the comparisons with and without considering author-specified ranges of applicability, appropriate correlations for different flow patterns and tube orientations were recommended.
2. The exponents of the key parameters that commonly appeared in the recommended correlations from the results of the above task were varied to investigate the role of those parameters in two-phase heat transfer. Based on the tabulated and graphical

results of the comparisons between the predictions of the modified heat transfer correlations and the available experimental data, appropriate correlations for different flow patterns, pipe orientations, and gas-liquid combinations were recommended.

3. Since there was no single correlation capable of predicting heat transfer rate with good accuracy for all fluid combinations and flow patterns in vertical pipes based on the results of tasks 1 and 2, a new correlation was developed based on the physical mechanism of the two-phase heat transfer along with the knowledge obtained from the completion of the tasks 1 and 2.
4. In order to aid in the development of a robust two-phase heat transfer correlation, comprehensive experimental data sets in horizontal tubes covering several different flow patterns and fluid combinations are necessary. For this purpose, an experimental setup for two-phase heat transfer measurements in a horizontal pipe was constructed and air-water two-phase heat transfer data was obtained.
5. The robust heat transfer correlation developed for turbulent flow for different flow patterns and fluid combinations in vertical pipes was applied to the air-water heat transfer experimental data obtained from this study.

Throughout this chapter, the background of this study, general flow patterns in vertical and horizontal pipes, literature survey, preliminary comparisons, shortcomings of previous works, and the objectives of this study were introduced. In the next chapter, development of the robust two-phase heat transfer correlation for several fluid combinations and different flow patterns in vertical pipes will be introduced.

CHAPTER II

DEVELOPMENT OF A GENERAL TWO-PHASE HEAT TRANSFER CORRELATION FOR VERTICAL PIPES

In order to develop a general two-phase heat transfer correlation which is robust enough to span all or most of the fluid combinations and flow patterns in vertical pipes, a systematic approach must be used. To achieve this goal successfully, the following three tasks were completed using extensive sets of experimental data available from the literature (see Table 1.14):

1. The general validity of the performance of the previously identified correlations (see Table 1.6) was tested against the recommended particular range of the parameters suggested by the original authors.
2. In order to improve the applicability of the previously recommended correlations to different flow patterns and fluid combinations, each exponent of the key parameters that appeared in the previously recommended correlations was varied to investigate how critical that parameter is, and also to find out whether or not a changed exponent value can yield improved fits of the correlation to the experimental data.
3. With the outcome of the tasks 1 and 2 described above, a new improved two-phase heat transfer correlation was developed, and the performance of the correlation was compared against previously recommended correlations.

Each of the three tasks mentioned above was successfully completed and the results were published in the open literature [see Kim et al. (1999a, 1999b, 1999c)]. In the following sections, a summary of each work will be presented.

2.1 Comparison of 20 Two-Phase Heat Transfer Correlations with Seven Sets of Experimental Data, Including Flow Pattern and Tube Inclination Effects

In this study, the validity of twenty heat transfer correlations obtained from a comprehensive literature review were assessed. These correlations were tested against seven extensive sets of two-phase flow experimental data available from the literature, for vertical and horizontal tubes and different flow patterns and fluids. A total of 524 data points from five available experimental studies were used for these comparisons. Based on the tabulated and graphical results of the comparisons with and without considering author-specified ranges of applicability, appropriate correlations for different flow patterns and tube orientations were recommended. This was the subject of the paper published by Kim et al. (1999a).

2.1.1 Introduction

Numerous heat transfer correlations and experimental data for forced convective heat transfer during gas-liquid two-phase flow in vertical and horizontal pipes have been published over the past 40 years. In this study, a comprehensive literature search was carried out and a total of 38 two-phase flow heat transfer correlations [see references 1 to 39 of Kim et al. (1999a)] were identified. The validity of these correlations and their ranges of applicability have been documented by the original authors (Kim et al., 1999a). In most cases, the identified heat transfer correlations were derived empirically and were

based on a small set of experimental data with a limited range of variables and liquid-gas combinations. In order to assess the validity of those correlations, they were compared against seven extensive sets of two-phase flow heat transfer experimental data available from the literature, for vertical and horizontal tubes and different flow patterns and fluids. A total of 524 data points from five available experimental studies [see references 1, 10, 40, 41, 42 of Kim et al. (1999a)] were used for these comparisons. The experimental data included five different liquid-gas combinations (water-air, glycerin-air, silicone-air, water-helium, water-freon 12), and covered a wide range of variables, including liquid and gas flow rates and properties, flow patterns, pipe sizes, and pipe inclination.

Table 1.6 shows twenty of the 38 heat transfer correlations that were identified and tested in this study. The rest of the two-phase flow heat transfer correlations [see references 22 to 39 of Kim et al. (1999a)] were not tested since the required information for the correlations was not available through the identified experimental studies. The limitations of the twenty correlations used in this study as proposed by the original authors are tabulated in Table 1.7. This table lists the ranges of the five dimensionless parameters \dot{m}_G/\dot{m}_L , V_{SG}/V_{SL} , Re_{SG} , Re_{SL} , and Pr_L that were mainly used in the development of these correlations. Among the listed parameters only V_{SG}/V_{SL} and Re_{SL} have been most consistently supplied. For this reason, only these two parameters were chosen to check the validity of the identified heat transfer correlations with the seven sets of experimental data. The ranges of the seven sets of experimental data used to assess the validity of the correlations listed in Table 1.6 are provided in Table 2.1. It should be

Table 2.1 Ranges of the Experimental Data Used in this Study

Water-Air Vertical Data (139 Points) of Vijay (1978)	$16.71 \leq \dot{m}_L \text{ (lbm/hr)} \leq 8996$ $0.058 \leq \dot{m}_G \text{ (lbm/hr)} \leq 216.82$ $0.007 \leq X_{TT} \leq 433.04$ $0.061 \leq \Delta P_{TP} \text{ (psi)} \leq 17.048$ $5.503 \leq Pr_L \leq 6.982$ $101.5 \leq h_{TP} \text{ (Btu/hr-ft}^2\text{-}^\circ\text{F)} \leq 7042.3$	$0.06 \leq V_{SL} \text{ (ft/sec)} \leq 34.80$ $0.164 \leq V_{SG} \text{ (ft/sec)} \leq 460.202$ $59.64 \leq T_{MIX} \text{ (}^\circ\text{F)} \leq 83.94$ $0.007 \leq \Delta P_{TPF} \text{ (psi)} \leq 16.74$ $0.708 \leq Pr_G \leq 0.710$ $0.813 \leq \mu_w/\mu_B \leq 0.933$	$231.83 \leq Re_{SL} \leq 126630$ $43.42 \leq Re_{SG} \leq 163020$ $14.62 \leq P_{MIX} \text{ (psi)} \leq 74.44$ $0.033 \leq \alpha \leq 0.997$ $11.03 \leq Nu_{TP} \leq 776.12$ $L/D = 52.1, D = 0.46 \text{ in.}$
Glycerin-Air Vertical Data (57 Points) of Vijay (1978)	$100.5 \leq \dot{m}_L \text{ (lbm/hr)} \leq 1242.5$ $0.085 \leq \dot{m}_G \text{ (lbm/hr)} \leq 99.302$ $0.15 \leq X_{TT} \leq 407.905$ $1.317 \leq \Delta P_{TP} \text{ (psi)} \leq 20.022$ $6307.04 \leq Pr_L \leq 6962.605$ $54.84 \leq h_{TP} \text{ (Btu/hr-ft}^2\text{-}^\circ\text{F)} \leq 159.91$	$0.31 \leq V_{SL} \text{ (ft/sec)} \leq 3.80$ $0.217 \leq V_{SG} \text{ (ft/sec)} \leq 117.303$ $80.40 \leq T_{MIX} \text{ (}^\circ\text{F)} \leq 82.59$ $1.07 \leq \Delta P_{TPF} \text{ (psi)} \leq 19.771$ $0.708 \leq Pr_G \leq 0.709$ $0.513 \leq \mu_w/\mu_B \leq 0.610$	$1.77 \leq Re_{SL} \leq 21.16$ $63.22 \leq Re_{SG} \leq 73698$ $17.08 \leq P_{MIX} \text{ (psi)} \leq 62.47$ $0.0521 \leq \alpha \leq 0.9648$ $12.78 \leq Nu_{TP} \leq 37.26$ $L/D = 52.1, D = 0.46 \text{ in.}$
Silicone-Air Vertical Data (162 points) of Rezkallah (1987)	$17.3 \leq \dot{m}_L \text{ (lbm/hr)} \leq 196$ $0.07 \leq \dot{m}_G \text{ (lbm/hr)} \leq 157.26$ $72.46 \leq T_w \text{ (}^\circ\text{F)} \leq 113.90$ $0.037 \leq \Delta P_{TP} \text{ (psi)} \leq 9.767$ $61.0 \leq Pr_L \leq 76.5$ $29.9 \leq h_{TP} \text{ (Btu/hr-ft}^2\text{-}^\circ\text{F)} \leq 683.0$	$0.072 \leq V_{SL} \text{ (ft/sec)} \leq 30.20$ $0.17 \leq V_{SG} \text{ (ft/sec)} \leq 363.63$ $66.09 \leq T_B \text{ (}^\circ\text{F)} \leq 89.0$ $0.094 \leq \Delta P_{TPF} \text{ (psi)} \leq 9.074$ $0.079 \leq Pr_G \leq 0.710$	$47.0 \leq Re_{SL} \leq 20930$ $52.1 \leq Re_{SG} \leq 118160$ $13.9 \leq P_{MIX} \text{ (psi)} \leq 45.3$ $0.011 \leq \alpha \leq 0.996$ $17.3 \leq Nu_{TP} \leq 386.8$ $L/D = 52.1, D = 0.46 \text{ in.}$
Water-Helium Vertical Data (53 Points) of Aggour (1978)	$267 \leq \dot{m}_L \text{ (lbm/hr)} \leq 8996$ $0.020 \leq \dot{m}_G \text{ (lbm/hr)} \leq 33.7$ $0.16 \leq X_{TT} \leq 769.6$ $0.3 \leq \Delta P_{TP} \text{ (psi)} \leq 13.2$ $5.78 \leq Pr_L \leq 7.04$ $794 \leq h_{TP} \text{ (Btu/hr-ft}^2\text{-}^\circ\text{F)} \leq 6061$	$1.03 \leq V_{SL} \text{ (ft/sec)} \leq 34.70$ $0.423 \leq V_{SG} \text{ (ft/sec)} \leq 483.6$ $67.4 \leq T_{MIX} \text{ (}^\circ\text{F)} \leq 82.0$ $0.01 \leq \Delta P_{TPF} \text{ (psi)} \leq 12.5$ $0.6908 \leq Pr_G \leq 0.691$ $83.9 \leq T_w \text{ (}^\circ\text{F)} \leq 95.7$	$3841 \leq Re_{SL} \leq 125840$ $14.0 \leq Re_{SG} \leq 23159$ $15.5 \leq P_{MIX} \text{ (psi)} \leq 53.3$ $0.038 \leq \alpha \leq 0.958$ $86.6 \leq Nu_{TP} \leq 668.2$ $L/D = 52.1, D = 0.46 \text{ in}$
Water-Freon 12 Vertical Data (44 Points) of Aggour (1978)	$267 \leq \dot{m}_L \text{ (lbm/hr)} \leq 3598$ $0.84 \leq \dot{m}_G \text{ (lbm/hr)} \leq 206.59$ $0.16 \leq X_{TT} \leq 226.5$ $0.04 \leq \Delta P_{TP} \text{ (psi)} \leq 4.92$ $5.63 \leq Pr_L \leq 6.29$ $800 \leq h_{TP} \text{ (Btu/hr-ft}^2\text{-}^\circ\text{F)} \leq 4344$	$1.03 \leq V_{SL} \text{ (ft/sec)} \leq 13.89$ $0.51 \leq V_{SG} \text{ (ft/sec)} \leq 117.7$ $75.26 \leq T_{MIX} \text{ (}^\circ\text{F)} \leq 83.89$ $0.02 \leq \Delta P_{TPF} \text{ (psi)} \leq 4.48$ $0.769 \leq Pr_G \leq 0.77$ $90.36 \leq T_w \text{ (}^\circ\text{F)} \leq 94.89$	$4190 \leq Re_{SL} \leq 51556$ $859.5 \leq Re_{SG} \leq 209430$ $15.8 \leq P_{MIX} \text{ (psi)} \leq 27.8$ $0.035 \leq \alpha \leq 0.934$ $87.1 \leq Nu_{TP} \leq 472.4$ $L/D = 52.1, D = 0.46 \text{ in}$
Water-Air Horizontal Data (48 points) of Pletcher (1966)	$0.069 \leq \dot{m}_L \text{ (lbm/sec)} \leq 0.3876$ $0.22 \leq \Delta P_M/L \text{ (lbf/ft}^3\text{)} \leq 26.35$ $7.23 \leq \phi_1 \leq 68.0$ $7372 \leq q'' \text{ (Btu/hr-ft}^2\text{)} \leq 11077$	$0.03 \leq \dot{m}_G \text{ (lbm/sec)} \leq 0.2568$ $0.021 \leq X_{TT} \leq 0.490$ $73.6 \leq T_w \text{ (}^\circ\text{F)} \leq 107.1$ $433 \leq h_{TP} \text{ (Btu/hr-ft}^2\text{-}^\circ\text{F)} \leq 1043.8$	$7.84 \leq \Delta P/L \text{ (lbf/ft}^3\text{)} \leq 137.5, 1.45 \leq \phi_g \leq 3.54$ $64.9 \leq T_{MIX} \text{ (}^\circ\text{F)} \leq 99.4$ $L/D = 60.0, D = 1.0 \text{ in.}$
Water-Air Horizontal Data (21 points) of King (1952)	$1375 \leq \dot{m}_L \text{ (lbm/hr)} \leq 6410$ $1570 \leq Re_{SG} \leq 84200$ $136.8 \leq T_{MIX} \text{ (}^\circ\text{F)} \leq 144.85$ $1.027 \leq \Delta P_{TP} \text{ (psi)} \leq 22.403$ $1.35 \leq h_{TP} / h_L \leq 3.34$	$0.82 \leq \dot{m}_G \text{ (SCFM)} \leq 43.7$ $0.41 \leq X_{TT} \leq 29.10$ $184.3 \leq T_w \text{ (}^\circ\text{F)} \leq 211.3$ $1462 \leq h_{TP} \text{ (Btu/hr-ft}^2\text{-}^\circ\text{F)} \leq 4415, 1.35 \leq \phi_1 \leq 8.20$	$22500 \leq Re_{SL} \leq 119000$ $0.117 \leq R_L \leq 0.746$ $15.8 \leq P_{MIX} \text{ (psi)} \leq 55.0$ $0.33 \leq V_{SG}/V_{SL} \leq 7.65$ $L/D = 252, D = 0.737 \text{ in.}$

noted that for consistency, the validity of the identified heat transfer correlations were based on the comparison between the predicted and experimental two-phase heat transfer coefficients meeting the $\pm 30\%$ criterion. For this reason, all of the Nu_{TP} correlations in Table 1.6 were converted to h_{TP} correlations using the following simple two-phase mixture thermal conductivity relation: $k_{TP} = xk_G + (1 - x)k_L$.

The flow pattern identification for the experimental data was based on the procedures suggested by Govier and Aziz (1973), Griffith and Wallis (1961), Hewitt and Hall-Taylor (1970), Taitel et al. (1980), Taitel and Dukler (1976), and visual observation as appropriate.

2.1.2 Results from Comparison with Correlation Limitations

Table 2.2 gives a summary of the results obtained by comparing the twenty identified two-phase flow heat transfer correlations with the 139 water-air experimental data of Vijay (1978). Since some of the identified heat transfer correlations did not provide ranges for Re_{SL} or V_{SG}/V_{SL} , those correlations were not listed in the comparison tables. This table shows the total number of experimental data points for each flow pattern, the ratio of the number of data points in each flow pattern that were predicted to within $\pm 30\%$ by the individual heat transfer correlations to the total number of data points that fell within the restrictions for Re_{SL} or V_{SG}/V_{SL} that accompanied the correlations, and the percent overall mean and r.m.s. deviations of the predictions from the data for each correlation. For each flow pattern, the table also highlights the number of data points predicted by the correlation(s) that best satisfied the $\pm 30\%$ two-phase heat transfer coefficient criterion.

From the comparison results shown in Table 2.2, several water-air data points of

Table 2.2 Comparison of Water-Air Experimental Data (139 Data Points) of Vijay (1978) with the Studied Correlations (See Nomenclature for Abbreviations)

Source	Mean Dev. (%)	r.m.s. Dev. (%)	Data Points within $\pm 30\%$ / Data Points for Each Flow Pattern within Re_{SL} Range of Correlation							
			B (25)	S (25)	F (25)	A (25)	B-F (7)	S-A (10)	F-A (4)	A-M (18)
Chu & Jones (1980)	6.17	15.49	17/17	9/9	19/19	7/7	6/6	1/1	4/4	
Dorresteiijn (1970)	-17.19	61.33	7/7	20/22	1/2	11/21	0/1	2/8	0/4	0/15
Dusseau (1968)	99.29	99.29	0/5	0/9	0/2	0/10	0/1	0/1	0/4	0/1
Elamvaluthi & Srinivas (1984)	-123.76	183.21	0/2	0/13		1/14		2/7		0/15
Groothuis & Hendal (1959)	-103.78	116.24	0/25	1/16	0/25	4/14	0/7	1/2	0/4	0/2
Khoze et al. (1976)										
Knott et al. (1959)	-19.65	68.50	0/3			4/4		0/7		7/13
Kudirka et al. (1965)	-1.47	47.53	4/25	6/22	6/25	18/21	2/7	2/8	4/4	12/15
Oliver & Wright (1964)	3798.2	4673.2						0/5		0/9
Ravipudi & Godbold (1978)	18.02	23.61	0/13	16/16	10/10	14/14	4/5	2/2	4/4	2/2
Rezkallah & Sims (1987)	-35.33	79.99	25/25	22/25	17/25	14/25	7/7	5/10	4/4	4/18
Shah (1980)										

Note: Correlations not listed in the table did not provide an Re_{SL} range. Blanks indicate no data points fell within the Re_{SL} range of the correlation.

Source	Mean Dev. (%)	r.m.s. Dev. (%)	Data Points within $\pm 30\%$ / Data Points for Each Flow Pattern within V_{SG}/V_{SL} Range of Correlation							
			B (25)	S (25)	F (25)	A (25)	B-F (7)	S-A (10)	F-A (4)	A-M (18)
Aggour (1978)	-25.33	54.75	25/25	25/25	2/25	14/21	4/7	4/9	1/4	0/6
Chu & Jones (1980)	2.19	19.09	10/11	17/19	23/25	1/1	6/6	1/1	4/4	
Dorresteiijn [4]	-28.79	63.33	7/25	20/25	1/25	11/25	0/7	2/10	0/4	0/15
Elamvaluthi & Srinivas (1984)	-86.62	90.44	0/2	0/18	0/24	0/1	0/4	0/1	0/4	
Groothuis & Hendal (1959)	-74.82	106.50		7/17	0/11	11/21	0/1	6/8	0/4	0/4
Knott et al. (1959)	7.29	12.91	15/15	16/18	24/24		7/7	1/1	3/3	
Kudirka et al. (1965)	-16.60	137.92	3/6	6/23	6/25	17/20	2/6	2/4	4/4	2/2
Ravipudi & Godbold (1978)	-0.91	43.40		13/15	11/11	20/20	1/1	4/5	4/4	2/2
Rezkallah & Sims (1987)	-34.73	80.04	25/25	22/25	17/25	14/25	7/7	5/10	4/4	4/16
Shah (1981)	24.27	30.91	25/25	15/25	25/25	3/25	7/7	3/10	4/4	6/15
Ueda & Hanaoka (1967)	-13.99	23.37		1/4	1/1	14/15		1/3	1/1	

Note: Correlations not listed in the table did not provide a V_{SG}/V_{SL} range. Blanks indicate no data points fell within the V_{SG}/V_{SL} range of the correlation.

Vijay (1978) were within the accompanying Re_{SL} and V_{SG}/V_{SL} parameter ranges of the heat transfer correlations. Considering the author-specified ranges of Re_{SL} and V_{SG}/V_{SL} along with the overall performance for all flow patterns and mean and r.m.s. deviations, the correlation of Chu and Jones (1980) is recommended for all the flow patterns except the annular-mist flow pattern. Also, the correlation of Ravipudi and Godbold (1978) is recommended for all of the flow patterns except for the bubbly flow pattern. The performances of Chu and Jones' (1980) and Ravipudi and Godbold's (1978) correlations in different flow patterns with respect to the parameters of Re_{SL} and V_{SG}/V_{SL} plotted on the horizontal axis and the dimensionless value of $h_{TP_{CAL}}/h_{TP_{EXP}}$ plotted on the vertical axis are given in Figures 2.1 and 2.2, respectively. For bubbly and slug flow patterns, the correlation of Aggour (1978) is recommended, based on the comparison results with and without (see Table 2.3) the restriction of V_{SG}/V_{SL} accompanying the correlation, even though there was no author-specified Re_{SL} restrictions.

Further details of the comparison results of several heat transfer correlations with different fluid combinations (air-glycerin data of Vijay, 1978; air-silicone data of Rezkallah, 1987; water-helium data of Aggour, 1978; water-freon 12 data of Aggour 1978; air-water in slug flow data of King, 1952; and annular flow data of Pletcher, 1966) can be found in Kim et al. (1999a).

2.1.3 Results from Comparison without Correlation Limitations

In this section the author-proposed restrictions on V_{SG}/V_{SL} and Re_{SL} were not imposed on the identified heat transfer correlations. However, the heat transfer correlations were compared with the same seven sets of experimental data used in the previous section's comparisons. A summary of the results obtained by comparing the

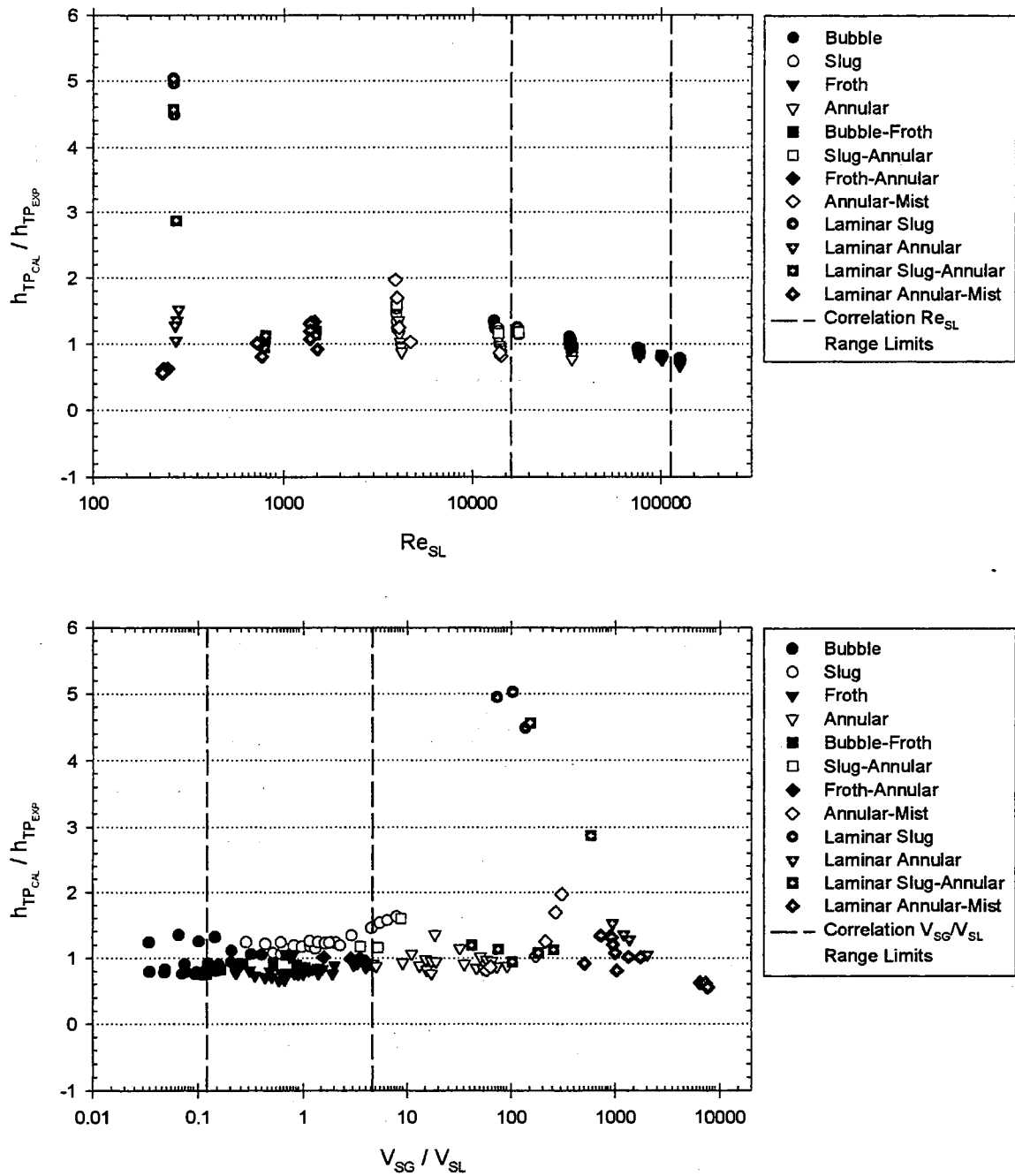


Figure 2.1 Comparison of Chu & Jones (1980) Correlation with Vijay's (1978) Water-Air Experimental Data

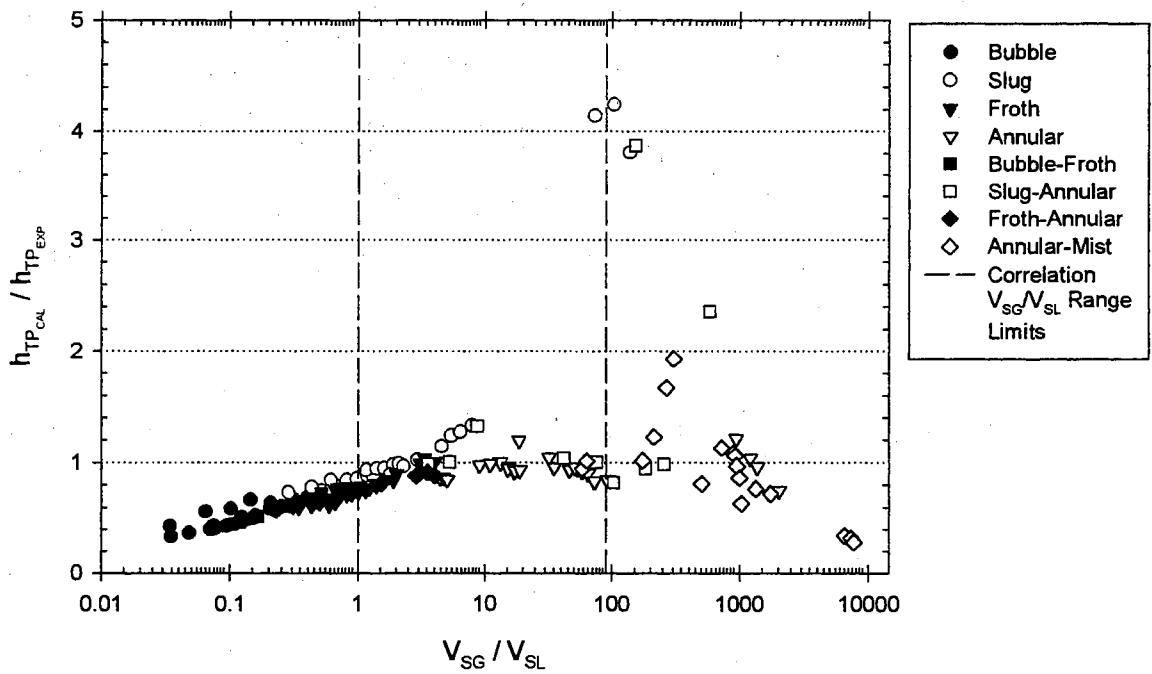
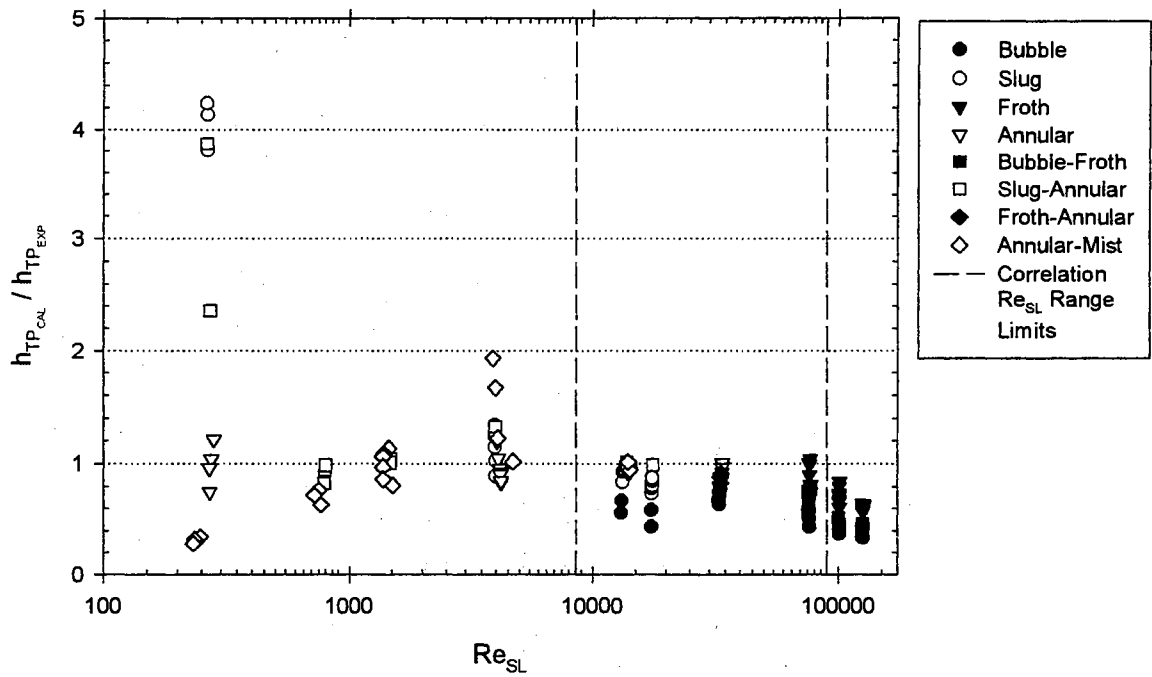


Figure 2.2 Comparison of Ravipudi & Godbold (1978) Correlation with Vijay's (1978) Water-Air Experimental Data

Table 2.3 Comparison of Water-Air Experimental Data (139 Data Points) of Vijay (1978) with the Studied Correlations (See Nomenclature for Abbreviations)

Source	Mean	r.m.s.	Data Points within $\pm 30\%$ for Each Flow Pattern (Pattern / Total No. of Data Points)									
			Dev. (%)	Dev. (%)	B (25)	S (25)	F (25)	A (25)	B-F (7)	S-A (10)	F-A (4)	A-M (18)
Aggour (1978)	-14.28	56.27										
Chu & Jones (1980)	-13.11	69.98	23	17	23	22	7	7	4	10		
Davis & David (1964)	-88.64	90.04									1	
Dorresteyn (1970)	-26.62	63.53	7	20	1	11		2				
Dusseau (1968)	99.31	99.31										
Elamvaluthi & Srinivas (1984)	-121.93	157.26				1		2				
Groothuis & Hendal (1959)	-116.88	162.25		7		11		7				
Khoze et al. (1976)	-133.21	159.97				4		4		6		
Knott et al. (1959)	3.76	33.95	25	20	25	19	7	3	4	11		
Kudirka et al. (1965)	-37.46	196.65	4	6	6	18	2	2	4	4		
Martin & Sims (1971)	-42.69	89.23	25	22	18	18	6	5	4	2		
Oliver & Wright (1964)	1500.	4349.										
Ravipudi & Godbold (1978)	8.44	61.16		21	16	25	4	7	4	12		
Rezkallah & Sims (1987)	-35.36	80.03	25	22	17	14	7	5	4	4		
Serizawa et al. (1975)	-3459.	13064.	25	18	14		7		1			
Shah (1981)	24.86	31.51	25	15	25	3	7	3	4	6		
Ueda & Hanaoka (1967)	-33.85	105.29	25	19	25	20	7	2	4	2		
Vijay et al. (1982)	46.26	58.59	21	2	23		6					

Note: Blanks indicate the correlation did not satisfy the $\pm 30\%$ criterion.

twenty identified two-phase flow heat transfer correlations with the 139 water-air experimental data of Vijay (1978) is given in Table 2.3. For this comparison, the limitations of the correlations proposed by the original authors were ignored in order to access the general validity of the correlations. The difference between this table and the previous table of comparison results (Table 2.2) is that only the experimental data points that fell within the ranges of Re_{SL} and V_{SG}/V_{SL} suggested by the original authors of the correlations were used. Tables 2.3 gives the total number of experimental data points

used from each experimental study, the total number of data points for each flow pattern, the number of data points in each flow pattern that were predicted to within $\pm 30\%$ by the individual heat transfer correlations, and the percent overall mean and r.m.s. deviations for the predictions of each correlation. The percent mean and r.m.s. deviations were calculated using the difference of the heat transfer coefficients between the experimental value and predicted value divided by the experimental value. Note that the magnitudes of mean and r.m.s. deviations in these comparisons including other fluid combinations [see Tables 9 to 15 of Kim et al. (1999a)] range from 0.08% to 13,064% indicating a wide range of agreement/disagreement of the correlation with the experimental data. For each flow pattern, the table also highlights the number of data points predicted by the correlation(s) that best satisfied the $\pm 30\%$ criterion. Further details on these comparisons may be found in Kim et al. (1999a).

The results shown in Table 2.3 indicate that, for bubbly, froth, annular, bubbly-froth, and froth-annular flow patterns, several of the heat transfer correlations did a very good job of predicting the experimental water-air data of Vijay (1978) in a vertical tube. However, for slug, slug-annular, and annular-mist flows, only one correlation for each flow pattern showed good predictions. Considering the performance of the correlations for all flow patterns and keeping in mind the values of the overall mean and r.m.s. deviations, four heat transfer correlations are recommended for this set of experimental data. These are the correlation of Knott et al. (1959) for bubbly, froth, bubbly-froth, and froth-annular flow patterns; the correlation of Ravipudi and Godbold (1978) for annular, slug-annular, froth-annular, and annular-mist flow patterns; the correlation of Chu and Jones (1980) for annular, bubbly-froth, slug-annular, and froth-annular flow patterns; and

the correlation of Aggour (1978) for bubbly and slug flow patterns. Figure 2.3 shows how well the recommended correlation of Knott et al. (1959) performed with respect to the

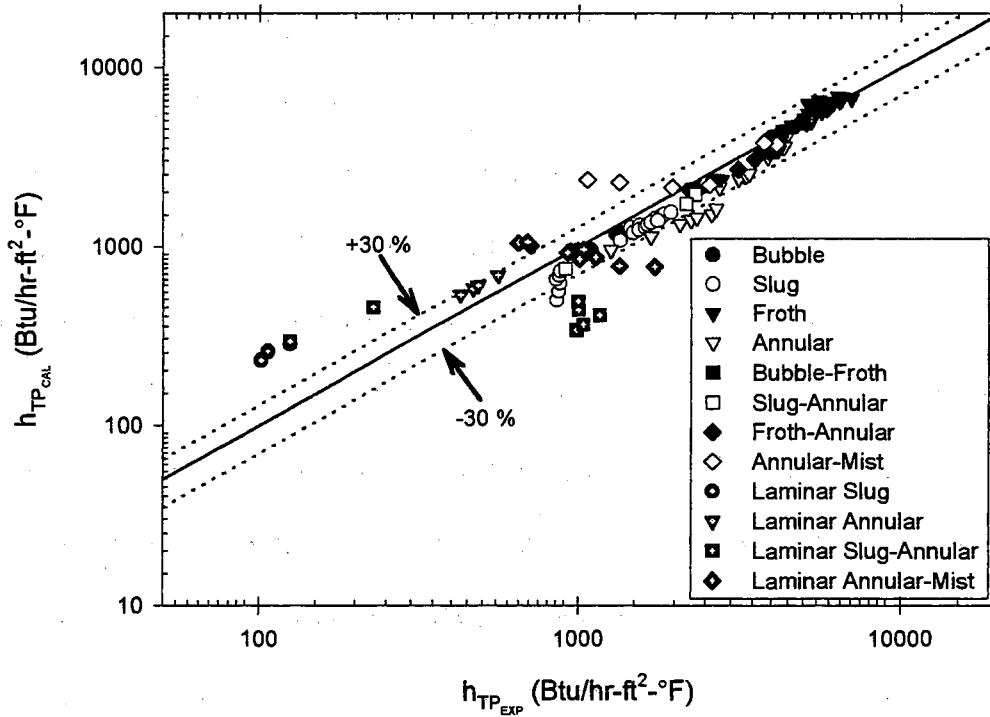


Figure 2.3 Comparison of Knott et al. (1959) Correlation with Vijay's (1978) Water-Air Experimental Data

water-air experimental data of Vijay (1978). Further details of the comparison results of several heat transfer correlations with different fluid combinations (air-glycerin data of Vijay, 1978; air-silicone data of Rezkallah, 1987; water-helium data of Aggour, 1978; water-freon 12 data of Aggour, 1978; air-water in slug flow data of King, 1952; and annular flow data of Pletcher, 1966) can be found in Kim et al. (1999a).

2.1.4 Summary and Conclusions

We have studied the ability of 20 two-phase heat transfer correlations to predict seven sets of experimental data that are available in the open literature. Five of these experimental data sets are concerned with flow patterns in vertical pipes: the air-water data of Vijay (1978), the air-glycerin data of Vijay (1978), the air-silicone data of Rezkallah (1987), the water-helium data of Aggour (1978), and the water-freon 12 data of Aggour (1978). The other two data sets are for patterns within horizontal pipes: the air-water slug flow data of King (1952) and annular flow data of Pletcher (1966).

In order to assess the validity of the two-phase heat transfer correlations, predictions of the identified 20 heat transfer correlations were compared with the seven sets of experimental data with or without considering the restrictions of Re_{SL} and V_{SG}/V_{SL} accompanying the correlations. The comparison results between those heat transfer correlations and the seven sets of experimental data are summarized in Table 2.4 for major flow patterns and Table 2.5 for transitional flow patterns. There were no remarkable differences for the recommendations of the heat transfer correlations based on the results along with or without the restrictions of Re_{SL} and V_{SG}/V_{SL} , except for the correlations of Chu and Jones (1980) and Ravipudi and Godbold (1978), for the water-air experimental data of Vijay (1978).

Based on the results without the authors' restrictions, the correlation of Chu and Jones (1980) was recommended for only annular, bubbly-froth, slug-annular, and froth-annular flow patterns, and the correlation of Ravipudi and Godbold (1978) was recommended for only annular, slug-annular, and froth-annular flow patterns of the vertical tube water-air experimental data. However, considering the Re_{SL} and V_{SG}/V_{SL}

Table 2.4 Recommended Correlations from the General Comparisons with Regard to Pipe Orientation, Fluids, and Major Flow Patterns (See Nomenclature for Abbreviations)

Correlations with Restrictions on Re_{SL} and V_{SG}/V_{SL}	Vertical Experimental Pipe																Horizontal						
	Water-Air				Glycerin-Air				Silicone-Air				Water-Helium				Water-Freon 12				Water-Air		
	B	S	F	A	B	S	F	A	B	S	C	A	F	B	S	F	A	B	S	F	A	A	S
Aggour (1978)	-V	-V			-V	-V	-V	-V										-V	-V	-V	-V		
Chu & Jones (1980)	RV	RV	RV	RV					R				R	RV	V	RV		R		RV			RV
Knott et al. (1959)	V	V	V	R									V	V	V	V		V		V			
Kudirka et al. (1965)				RV														V					RV
Ravipudi & Godbold (1978)		RV	RV	RV							V	RV	V		R	RV			V		RV		RV
Rezkallah & Sims (1987)	RV	RV							RV	RV	RV			RV				RV	RV	RV	RV		
Shah (1981)	V		V		RV				V				V	V		V		V		V		V	
Correlations with No Restrictions	Water-Air				Glycerin-Air				Silicone-Air				Water-Helium				Water-Freon 12				Water-Air		
Aggour (1978)	N	N			N	N	N	N										N	N	N	N		
Chu & Jones (1980)				N										N		N				N			N
Knott et al. (1959)	N		N										N	N	N	N	N	N		N			
Kudirka et al. (1965)																							N
Martin & Sims (1971)	N													N				N	N	N	N		N
Ravipudi & Godbold (1978)				N							N	N							N				N
Rezkallah & Sims (1987)	N								N	N	N			N				N	N	N	N		
Shah (1981)	N		N		N				N				N	N		N		N		N		N	
Correlation Recommendations Based on Comparisons Above	Water-Air				Glycerin-Air				Silicone-Air				Water-Helium				Water-Freon 12				Water-Air		
Aggour (1978)	√	√			√	√	√	√										√	√	√	√		
Chu & Jones (1980)				√										√		√				√			√
Knott et al. (1959)			√										√	√	√	√		√		√			
Kudirka et al. (1965)																							√
Martin & Sims (1971)	√													√				√	√	√	√		√
Ravipudi & Godbold (1978)				√							√	√							√				√
Rezkallah & Sims (1987)	√								√	√	√			√				√	√	√	√		
Shah (1981)	√		√		√				√				√	√		√		√		√		√	

Note: R = Recommended correlation with the range of Re_{SL} . V = Recommended correlation with the range of V_{SG}/V_{SL} . N = Recommended correlation with no restrictions. √ = Recommended correlation with and without restrictions. - = Correlation that did not provide ranges for either Re_{SL} or V_{SG}/V_{SL} . Correlation of Martin & Sims (1971) did not provide ranges for Re_{SL} and V_{SG}/V_{SL} .

Table 2.5 Recommended Correlations from the General Comparisons with Regard to Experimental Fluids and Transition Flow Patterns (See Nomenclature for Abbreviations)

Correlations with Restrictions on Re_{SL} and V_{SG}/V_{SL}	Vertical Experimental Pipe																			
	Water-Air				Glycerin-Air		Silicone-Air						Water-Helium				Water-Freon 12			
	B-F	S-A	F-A	A-M	B-S	S-A	B-S	B-F	S-C	C-A	F-A	A-M	B-S	B-F	S-A	A-M	B-S	B-F	S-A	S-A
Aggour (1978)					-V	-V														-V
Chu & Jones (1980)	RV	RV	RV					R					V				V			
Knott et al. (1959)	V							V			V									
Kudirka et al. (1965)			RV	R				V			RV						RV			
Ravipudi & Godbold (1978)	RV	RV	RV	RV			V		V	V	RV		R		R					V
Rezkallah & Sims (1987)	RV		RV				RV	RV	RV	RV			RV							RV
Shah (1981)	V		V					V			V	R				V				
Correlations with No Restrictions	Water-Air				Glycerin-Air		Silicone-Air						Water-Helium				Water-Freon 12			
Aggour (1978)					N	N						N	N							N
Chu & Jones (1980)	N	N	N										N				N			
Knott et al. (1959)	N		N					N			N				N					
Kudirka et al. (1965)			N								N						N			
Martin & Sims (1971)			N										N							N
Ravipudi & Godbold (1978)		N	N	N			N		N	N	N		N							N
Rezkallah & Sims (1987)	N		N				N	N	N	N			N							N
Shah (1981)	N		N		N			N			N	N				N				
Correlation Recommendations Based on Comparisons Above	Water-Air				Glycerin-Air		Silicone-Air						Water-Helium				Water-Freon 12			
Aggour (1978)					√	√														√
Chu & Jones (1980)	√	√	√										√				√			
Knott et al. (1959)	√							√			√									
Kudirka et al. (1965)			√								√						√			
Martin & Sims (1971)			√										√							√
Ravipudi & Godbold (1978)		√	√	√			√		√	√	√		√							√
Rezkallah & Sims (1987)	√		√				√	√	√	√			√							√
Shah (1981)	√		√					√			√					√				

Note: R = Recommended correlation with the range of Re_{SL} . V = Recommended correlation with the range of V_{SG}/V_{SL} . N = Recommended correlation with no restrictions. √ = Recommended correlation with and without restrictions. - = Correlation that did not provide ranges for either Re_{SL} or V_{SG}/V_{SL} . Correlation of Martin & Sims (1971) did not provide ranges for Re_{SL} and V_{SG}/V_{SL} .

restrictions, the correlation of Chu and Jones (1980) was recommended for all of the vertical tube water-air flow patterns including transitional flow patterns except the annular-mist flow pattern, and the correlation of Ravipudi and Godbold (1978) was recommended for slug, froth, and annular main flow patterns and all of the transitional flow patterns of the water-air experimental data of Vijay (1978).

With the data at hand, we make the following recommendations. For water-air flow within vertical pipes, we recommend use of the Knott et al. (1959) correlation for froth and bubbly-froth flow patterns; use of the Chu and Jones correlation for annular, bubbly-froth, slug-annular, and froth-annular flow patterns; use of the Ravipudi and Godbold (1978) correlation for annular, slug-annular, froth-annular, and annular-mist flow patterns; use of the Aggour (1978) correlation for bubbly and slug flow patterns; and use of the Rezkallah and Sims (1987) correlation for bubbly, bubbly-froth, and froth-annular flow patterns.

For glycerin-air flow within vertical pipes, we recommend use of the Aggour (1978) correlation for bubbly, slug, froth, annular, bubbly-slug, and slug-annular flow patterns.

For silicone-air flow within vertical pipes, we recommend use of the Rezkallah and Sims (1987) correlation for bubbly, slug, churn, bubbly-slug, bubbly-froth, slug-churn, and churn-annular flow patterns; use of the Ravipudi and Godbold (1978) correlation for churn, annular, bubbly-slug, slug-churn, churn-annular, and froth-annular flow patterns; and use of the Shah (1980) correlation for bubbly, froth, bubbly-froth, and froth-annular flow patterns.

For water-helium flow within vertical pipes, we recommend use of the Knott et al. (1959) correlation for bubbly, slug, and froth flow patterns; use of the Chu and Jones (1980) correlation for bubbly, froth, and bubbly-slug flow patterns; and use of the Shah (1980) correlation for bubbly, froth, and annular-mist flow patterns.

For water-freon 12 flow within vertical pipes, we recommend using one of the three correlations of Aggour (1978), Martin and Sims (1971), and Rezkallah and Sims (1987) for bubbly, slug, froth, annular, and slug-annular flow patterns. With regard to air-water flow in horizontal pipes, we recommend use of the Shah (1980) correlation for the annular flow pattern, and use of the Chu and Jones (1980), Kudirka et al. (1965), and Ravipudi and Godbold (1978) correlations for the slug flow pattern.

The above recommended correlations all have the following important parameters in common: Re_{SL} , Pr_L , μ_B/μ_w and either void fraction (α) or superficial velocity ratio (V_{SG}/V_{SL}). It appears that void fraction and superficial velocity ratio, although not directly related, may serve the same function in two-phase heat transfer correlations. However, since there is no single correlation capable of predicting the flow for all fluid combinations in vertical pipes, there appears to be at least one parameter [ratio], which is related to fluid combinations, that is missing from these correlations. In addition, since, for the horizontal data available, the recommended correlations differ from those of vertical pipes, there must also be at least one additional parameter [ratio], related to pipe orientation, that is missing from the correlations.

In order to improve the applicability of those recommended correlations to the available experimental data covering different flow patterns and fluid combinations, the exponent value on either one of the three key parameters (α , $1-V_{SG}/V_{SL}$, or V_{SG}/V_{SL})

which is typically added to most single-phase heat transfer correlations to account for two-phase effects has been parametrically varied and optimized such that the final results are much improved fits of the correlations to the open literature experimental data. This was the subject of the paper published by Kim et al. (1999b). In the next section, summary of this study will be described.

2.2 Development of Improved Two-Phase Two-Component Pipe Flow Heat Transfer Correlations from Existing Correlations and Published Data

In this study, six two-phase nonboiling heat transfer correlations obtained from the recommendations of our previous work were assessed. These correlations were modified using seven extensive sets of two-phase flow experimental data available from the literature, for vertical and horizontal tubes and different flow patterns and fluids. A total of 524 data points from five available experimental studies (which included the seven sets of data) were used for improvement of the six identified correlations. Based on the tabulated and graphical results of the comparisons between the predictions of the modified heat transfer correlations and the available experimental data, appropriate improved correlations for different flow patterns, tube orientations, and liquid-gas combinations were recommended.

2.2.1 Introduction

Tables 2.4 and 2.5 show the recommended two-phase heat transfer correlations based on the results of the general validity test performed by Kim et al. (1999a). These correlations have some of the following important parameters in common: Re_{SL} , Pr_L , μ_B/μ_W and either void fraction (α) or superficial velocity ratio (V_{SG}/V_{SL} or $1 + V_{SG}/V_{SL}$).

Since there is no single correlation capable of predicting heat transfer rate for all fluid combinations in vertical pipes, there appears to be at least one parameter [ratio], which is related to fluid combinations, that is missing from these correlations. In addition, since, for the horizontal data available, the recommended correlations differ from those of vertical pipes, there must also be at least one additional parameter [ratio], related to pipe orientation, that is missing from the correlations. In order to improve the applicability of these correlations to different flow patterns, liquid combinations, and pipe orientation, six of the recommended correlations in Tables 2.4 and 2.5 that showed the best overall performance were chosen for further study. The six selected correlations (Aggour, 1978; Knott et al., 1959; Kudirka et al., 1965; Ravipudi & Godbold, 1978; Rezkallah & Sims, 1987; and Shah, 1980) represent the three groups of two-phase heat transfer correlations discussed in Section 1.3.

The exponents of the key parameters that appear in these six two-phase heat transfer correlations were varied in order to get the best agreement between these correlations and an extensive set of experimental data available from the literature. The key parameters that were studied included $(1-\alpha)$, $(1+V_{SG}/V_{SL})$, and (V_{SG}/V_{SL}) . Seven sets of experimental data (a total of 524 data points) from five available experimental studies (Aggour, 1978; King, 1952; Pletcher, 1966; Rezkallah, 1987; and Vijay, 1978) were used in this study. The experimental data included five different liquid-gas combinations (water-air, glycerin-air, silicone-air, water-helium, water-freon 12), and covered a wide range of variables, including liquid and gas flow rates and properties, flow patterns, pipe sizes, and pipe orientation. The ranges of these seven sets of experimental data are provided in Table 2.1.

2.2.2 Results and Discussion

Table 2.6 gives a summary of the optimal values for the exponent (n) of the key parameter in each of the six selected two-phase heat transfer correlations. These values were obtained by varying the exponents of the key parameters in the correlations in order to get the best agreement (based on mean and r.m.s. deviations) between the correlations and the experimental data. The two-phase heat transfer experimental data used for this purpose were the 139 water-air experimental data points of Vijay (1978) in a vertical pipe, 57 glycerin-air experimental data points of Vijay (1978) in a vertical pipe, 162 silicone-air experimental data points of Rezkallah (1987) in a vertical pipe, 53 water-helium experimental data points of Aggour (1978) in a vertical pipe, 44 water-freon 12 experimental data points of Aggour (1978) in a vertical pipe, 48 water-air experimental data points of Pletcher (1966) in a horizontal pipe, and the 21 water-air experimental data points of King (1952) in a horizontal pipe. Table 2.6, aside from the optimal n values for each flow pattern, gives the percent overall mean, r.m.s., and range of deviations of the predictions from the data for each experimental data set based on the optimal and original n values. For the seven sets of different experimental fluid combinations and pipe orientation, this table also highlights the optimal n values of certain correlations that best predicted the experimental data.

The results of predictions for the water-air experimental data of Vijay (1978) in a vertical pipe shown in Table 2.6 indicate that the correlations of Aggour (1978), Rezkallah and Sims (1987), and Shah (1981) did a good job with different exponent (n) values for each flow pattern. The mean and r.m.s. deviations of the predictions for the optimal n values for these correlations are much lower than those based on the original n

Table 2.6 Different Values for the Exponent of the Key Parameters of Six Two-Phase Heat Transfer Correlations [1, 11, 12, 15, 16, and 18] [See Nomenclature for Abbreviations and Kim et al. (1999b) for Reference Numbers]

Aggour [1] Correlation with the Optimal n Values for Each Flow Pattern, $h_{TP} = \text{fctn}(Re_{SL}, Pr_L, \dots)(1-\alpha)^n$							
Flow Pattern	Vijay [40] W-A	Vijay [40] G-A	Rezkallah [41] S-A	Aggour [1] W-H	Aggour [1] W-F12	Pletcher [42] W-A	King [10] W-A
Bubbly	0.595	-0.240	5.303	-0.174	-0.741		
Slug	-0.60	-0.111	-0.733	-0.603	-0.849		-0.442
Froth	-0.172	-0.242	-0.641	-0.339	-0.414		
Annular	-0.645	-0.351	-0.366	-0.608	-0.859	-0.851	
Churn			-0.673				
Bubbly-Slug		-0.095	0.077	-0.874	-1.144		
Bubbly-Froth	-0.090		1.872	0.70	0.70		
Slug-Annular	-0.683	-0.235		0.773	-0.787		
Slug-Churn			-0.551				
Froth-Annular	-0.542		0.211				
Annular-Mist	-0.530		-0.428	-0.413			
Churn-Annular			-0.663				
Mean Dev. (%)	1.50	-0.49	-5.57	-0.85	1.03	28.62	4.70
rms Dev. (%)	29.49	6.27	66.98	17.29	8.22	52.48	13.53
Dev. Range (%)	-126.0 & 70.8	-18.2 & 19.4	-226.8 & 74.8	-27.7 & 47.7	-15.7 & 13.5	-125.0 & 77.3	-36.1 & 33.3
Aggour [1] Correlation with the Original n Values for All Flow Patterns, $n = -1/3$ (Laminar) and -0.83 (Turbulent)							
Mean Dev. (%)	-14.28	-13.82	-5.57	-45.20	-1.04	-233.85	-57.46
rms Dev. (%)	56.27	18.44	74.95	72.51	14.35	316.86	66.21
Dev. Range (%)	-380.5 & 85.4	-39.0 & 19.3	-226.8 & 74.8	-369.3 & 12.8	-28.6 & 36.8	-770.8 & 71.4	-138.2 & -14.6

Rezkallah & Sims [16] Correlation with the Optimal n Values for Each Flow Pattern, $h_{TP} = \text{fctn}(Re_{SL}, Pr_L, \dots)(1-\alpha)^n$							
Flow Pattern	Vijay [40] W-A	Vijay [40] G-A	Rezkallah [41] S-A	Aggour [1] W-H	Aggour [1] W-F12	Pletcher [42] W-A	King [10] W-A
Bubbly	-0.571	0.467	-1.282	-0.953	-1.243		
Slug	-0.623	0.059	-0.664	-0.653	-0.90		-0.473
Froth	-0.411	-0.151	-0.374	-0.502	-0.637		
Annular	-0.664	-0.30	-0.480	-0.637	-0.880	-0.401	
Churn			-0.628				
Bubbly-Slug		0.133	-0.898	-0.996	-1.280		
Bubbly-Froth	-0.463		-0.556	0.013	-1.50		
Slug-Annular	-0.661	-0.161		-0.660	-0.825		
Slug-Churn			-0.548				
Froth-Annular	-0.664		-0.318				
Annular-Mist	-0.519		-0.393	-0.431			
Churn-Annular			-0.662				
Mean Dev. (%)	1.36	-1.15	6.73	0.34	1.74	9.14	4.59
rms Dev. (%)	33.69	10.51	37.68	11.72	7.55	30.99	16.39
Dev. Range (%)	-145.4 & 67.6	-24.9 & 19.0	-147.5 & 59.6	-27.1 & 34.6	-20.6 & 20.0	-56.5 & 57.4	-34.7 & 31.9
Rezkallah & Sims [16] Correlation with the Original n Value for All Flow Patterns, $n = -0.9$							
Mean Dev. (%)	-35.36	-51.49	-20.02	-47.53	-0.12	-333.49	-46.47
rms Dev. (%)	80.03	54.86	52.55	87.39	11.90	405.60	57.37
Dev. Range (%)	-473.0 & 37.5	-82.9 & 2.46	-204.1 & 42.9	-457.6 & 16.6	-27.3 & 35.9	-996.1 & -43.5	-120.9 & 3.6

Table 2.6 (Cont'd.) Different Values for the Exponent of the Key Parameters of Six Two-Phase Heat Transfer Correlations [1, 11, 12, 15, 16, and 18] [See Nomenclature for Abbreviations and Kim et al. (1999b) for Reference Numbers]

Knott et al. [11] Correlation with the Optimal n Values for Each Flow Pattern, $h_{TP} = \text{fcn}(Re_{SL}, Pr_L, \dots)(1 + V_{SG}/V_{SL})^n$							
Flow Pattern	Vijay [40] W-A	Vijay [40] G-A	Rezkallah [41] S-A	Aggour [1] W-H	Aggour [1] W-F12	Pletcher [42] W-A	King [10] W-A
Bubbly	0.529	-0.402	1.273	0.829	1.082		
Slug	0.334	-0.034	0.368	0.381	0.560		0.521
Froth	0.288	0.088	0.325	0.323	0.486		
Annular	0.374	0.162	0.280	0.337	0.505	0.477	
Churn			0.336				
Bubbly-Slug		-0.092	0.815	0.727	0.993		
Bubbly-Froth	0.371		0.591	0.650	1.370		
Slug-Annular	0.358	0.088		0.364	0.50		
Slug-Churn			0.382				
Froth-Annular	0.435		0.237				
Annular-Mist	0.308		0.233	0.222			
Churn-Annular			0.367				
Mean Dev. (%)	2.21	-1.56	7.22	0.20	2.29	23.40	1.74
rms Dev. (%)	20.35	8.59	26.77	10.80	7.99	48.70	11.76
Dev. Range (%)	-161.4 & 62.6	-23.0 & 17.3	-130.6 & 65.4	-26.9 & 30.0	-20.9 & 23.5	-125.0 & 77.3	-38.3 & 22.0
Knott et al. [11] Correlation with the Original n Value for All Flow Patterns, n = 1/3							
Mean Dev. (%)	3.76	-85.93	-4.09	0.74	27.20	-80.79	21.44
rms Dev. (%)	33.95	96.64	57.41	27.07	30.85	101.76	26.03
Dev. Range (%)	-139.5 & 65.8	-163.9 & -5.7	-235.7 & 67.0	-150.1 & 33.2	6.4 & 55.9	-231.0 & 10.3	-15.8 & 40.8

Shah [18] Correlation with the Optimal n Values for Each Flow Pattern, $h_{TP} = \text{fcn}(Re_{SL}, Pr_L, \dots)(1 + V_{SG}/V_{SL})^n$							
Flow Pattern	Vijay [40] W-A	Vijay [40] G-A	Rezkallah [41] S-A	Aggour [1] W-H	Aggour [1] W-F12	Pletcher [42] W-A	King [10] W-A
Bubbly	0.703	-0.402	0.094	0.952	1.216		
Slug	0.399	-0.034	0.365	0.395	0.625		0.589
Froth	0.314	0.088	0.968	0.346	0.531		
Annular	0.398	0.162	0.265	0.346	0.515	0.218	
Churn			0.330				
Bubbly-Slug		-0.092	0.517	0.765	1.041		
Bubbly-Froth	0.422		-0.116	0.70	1.60		
Slug-Annular	0.402	0.088		0.375	0.517		
Slug-Churn			0.367				
Froth-Annular	0.454		0.126				
Annular-Mist	0.303		0.178	0.227			
Churn-Annular			0.361				
Mean Dev. (%)	1.26	-1.56	6.91	0.67	2.75	4.89	1.93
rms Dev. (%)	28.91	10.38	39.10	10.85	8.69	24.14	13.95
Dev. Range (%)	-129.2 & 46.0	-23.0 & 17.3	-152.0 & 76.2	-27.3 & 29.7	-22.5 & 24.3	-47.2 & 44.2	-35.7 & 22.0
Shah [18] Correlation with the Original n Value for All Flow Patterns, n = 1/3							
Mean Dev. (%)	24.86	-50.12	9.28	20.88	37.89	-13.92	37.42
rms Dev. (%)	31.51	54.0	42.96	26.70	41.65	31.98	39.65
Dev. Range (%)	-29.4 & 72.8	-86.7 & -1.3	-235.9 & 80.0	-42.1 & 56.3	14.1 & 70.6	-76.4 & 33.8	6.2 & 54.6

Table 2.6 (Cont'd.) Different Values for the Exponent of the Key Parameters of Six Two-Phase Heat Transfer Correlations [1, 11, 12, 15, 16, and 18] [See Nomenclature for Abbreviations and Kim et al. (1999b) for Reference Numbers]

Kudirka et al. [12] Correlation with the Optimal n Values for Each Flow Pattern, $Nu_{TP} = fctn(Re_{SL}, Pr_L, \dots)(V_{SG}/V_{SL})^n$							
Flow Pattern	Vijay [40] W-A	Vijay [40] G-A	Rezkallah [41] S-A	Aggour [1] W-H	Aggour [1] W-F12	Pletcher [42] W-A	King [10] W-A
Bubbly	-0.045	-0.399	-0.060	-0.015	-0.063		
Slug	-0.246	0.527	-0.198	-0.222	-0.380		0.083
Froth	-0.184	0.437	-0.305	-0.098	-0.208		
Annular	0.032	0.335	-0.017	0.053	0.218	-0.024	
Churn			-0.109				
Bubbly-Slug		1.131	0.021	-0.730	-0.018		
Bubbly-Froth	-0.195		-0.160	-2.620	-0.174		
Slug-Annular	-0.144	0.343		-0.039	-0.016		
Slug-Churn			-0.162				
Froth-Annular	0.247		0.298				
Annular-Mist	-0.006		-0.054	-0.037			
Churn-Annular			-0.041				
Mean Dev. (%)	-4.62	21.63	-5.30	2.70	3.82	-0.12	-2.56
rms Dev. (%)	52.27	37.12	39.68	30.72	24.37	18.50	26.63
Dev. Range (%)	-227.9 & 53.4	-51.4 & 87.0	-158.1 & 60.7	-130.2 & 46.9	-60.7 & 49.9	-48.9 & 48.4	-59.7 & 28.6
Kudirka et al. [12] Correlation with the Original n Value for All Flow Patterns, n = 1/8							
Mean Dev. (%)	-71.82	61.62	-65.83	-39.18	10.76	-52.30	-4.30
rms Dev. (%)	240.25	61.86	130.59	80.45	40.39	59.92	27.61
Dev. Range (%)	-1330.6 & 55.3	45.1 & 72.2	-423.9 & 64.5	-236.8 & 48.9	-80.1 & 51.5	-157.6 & 8.5	-61.9 & 27.5
Ravipudi & Godbold [15] Correlation with the Optimal n Values for Each Flow Pattern, $Nu_{TP} = fctn(Re_{SL}, Pr_L, \dots)(V_{SG}/V_{SL})^n$							
Flow Pattern	Vijay [40] W-A	Vijay [40] G-A	Rezkallah [41] S-A	Aggour [1] W-H	Aggour [1] W-F12	Pletcher [42] W-A	King [10] W-A
Bubbly	-0.032	-0.425	-0.024	-0.002	-0.045		
Slug	0.070	0.897	0.344	0.164	0.309		0.463
Froth	-0.001	0.570	-0.135	0.061	-0.103		
Annular	0.268	0.515	0.224	0.224	0.395	0.123	
Churn			0.282				
Bubbly-Slug		-1.190	0.299	0.519	-0.149		
Bubbly-Froth	-0.072		-0.075	-2.751	-0.088		
Slug-Annular	0.20	0.599		0.205	0.312		
Slug-Churn			0.312				
Froth-Annular	0.393		0.236				
Annular-Mist	0.184		0.099	0.119			
Churn-Annular			0.290				
Mean Dev. (%)	4.04	24.40	3.66	5.85	8.42	2.05	3.16
rms Dev. (%)	29.77	40.92	29.50	15.73	17.48	19.23	13.36
Dev. Range (%)	-171.5 & 42.0	-48.9 & 89.8	-143.5 & 74.9	-35.3 & 31.1	-17.3 & 41.7	-40.4 & 44.7	-22.8 & 24.3
Ravipudi & Godbold [15] Correlation with the Original n Value for All Flow Patterns, n = 0.3							
Mean Dev. (%)	-14.66	66.18	-12.06	-10.69	28.72	-193.51	15.72
rms Dev. (%)	86.60	66.69	85.25	58.86	33.61	212.15	18.39
Dev. Range (%)	-371.0 & 66.5	53.7 & 87.5	-501.8 & 79.2	-275.0 & 61.8	-9.5 & 67.5	-379.1 & -45.3	-3.7 & 32.1

value(s). Considering the performance of the correlations for all of the flow patterns and keeping in mind the values of the overall mean and r.m.s. deviations, the heat transfer correlation of Shah (1981) with the different exponent (n) values for the parameter $(1+V_{SG}/V_{SL})$ is recommended for the water-air experimental data of Vijay (1978).

As shown in Table 2.6, for the glycerin-air experimental data of Vijay (1978) in a vertical pipe, the correlations of Aggour (1978), Rezkallah and Sims (1987), Knott et al. (1959), and Shah (1981) were capable of predicting the experimental data with good accuracy. Considering the overall performance of the correlations for all flow patterns, the correlation of Aggour (1978) with different exponent (n) values for the parameter $(1-\alpha)$ is recommended for this set of experimental data with extremely high liquid Prandtl number (6300 ~ 7000).

For the silicone-air experimental data of Rezkallah (1987) in a vertical pipe, the correlations of Ravipudi and Godbold (1978) and Knott et al. (1959) predicted the experimental data reasonably well with good r.m.s. deviation. The r.m.s. and max. deviations based on the different values of exponent n are much improved compared to those based on the original n value. Again, considering the overall performance of the correlations for all flow patterns, the correlation of Knott et al. (1959) with the exponent (n) values for the parameter $(1+V_{SG}/V_{SL})$ is recommended for this experimental data set with moderately high liquid Prandtl number (61 ~ 77).

The results of predictions for the water-helium experimental data of Aggour (1978) in a vertical pipe with the different exponent (n) values are also given in Table 2.6. The correlations of Rezkallah and Sims (1987), Knott et al. (1959), and Shah (1981) predicted the experimental data very accurately with good mean, r.m.s. and max.

deviations. The magnitudes of the mean, r.m.s. and max. deviations for the optimal n values are much smaller than those calculated from the original n values. Among the three correlations, the correlation of Knott et al. (1959) with the different exponent (n) values for the parameter $(1+V_{SG}/V_{SL})$ is recommended for the water-helium experimental data of Aggour (1978) in which the gas density change from air to helium is approximately a factor of 10.

Most of the six two-phase heat transfer correlations shown in Table 2.6 predicted the water-freon 12 experimental data of Aggour (1978) in a vertical pipe very accurately with good mean and r.m.s. deviations. The magnitudes of the r.m.s. deviations with the optimal n values were about two times better than those with the original n values. Among the six correlations, the correlation of Aggour (1978) with the different exponent (n) values for the parameter $(1-\alpha)$ is recommended for this experimental data set.

The water-air experimental data of Pletcher (1966) in a horizontal pipe with annular flow were accurately predicted by the correlations of Kudirka et al. (1965) and Ravipudi and Godbold (1978). Between these two correlations which belong to the same heat transfer correlation group and were developed based on the dimensional analysis concept, the correlation of Kudirka et al. (1965) with $n = -0.024$ for the exponent of (V_{SG}/V_{SL}) is recommended for this set of experimental data.

Table 2.6 also shows the results of the predictions for the water-air slug flow experimental data of King (1952) in a horizontal pipe. The correlations of Knott et al. (1959) and Shah (1981) accurately predicted the horizontal slug flow water-air experimental data. Between these two correlations which were based on the separated

flow model concept, the correlation of Knott et al. (1959) with the exponent (n) value of 0.521 for the parameter $(1+V_{SG}/V_{SL})$ is recommended for this set of experimental data.

Table 2.7 summarizes this study's recommended modified two-phase heat transfer correlations for five fluid combinations (W-A, G-A, S-A, W-H, W-F12) and four major flow patterns (bubbly, slug, froth, annular) in a vertical pipe. In this table, the optimal values of n listed in Table 2.6 for the four major flow patterns have been rounded off to two significant digits without significant loss of accuracy. For comparison purposes, the table also provides the original and the optimal n values for each correlation. Referring to Table 2.7, it is interesting to observe that generally for three of the four major flow patterns: slug, froth, and annular, the reported exponent n values for a given fluid combination show a weaker dependence on flow pattern than for fluid combination. It should also be mentioned that Table 2.7 does not provide information on horizontal pipe flows and the transitional vertical pipe flows. For horizontal pipe flows, we have information on only two flow patterns (slug and annular); and for transitional flows, there is an insufficient number of data points in each transitional flow pattern to plot and determine appropriate n values.

Table 2.8 shows the results of our attempt to unify the exponent n values provided in Table 2.7 for each fluid combination and different flow patterns. The mean and r.m.s. deviations reported in Table 2.8 for the simplified exponent n values show only a slight increase over those given in Table 2.7 for the modified exponent n values. As can be seen from the results of Table 2.8, the flow pattern dependency of the two-phase heat transfer correlations for a vertical pipe can be overcome by using an appropriate key parameter in the heat transfer correlation with an optimal exponent n value. For prediction of water-

Table 2.7 Recommended Modified Two-Phase Heat Transfer Correlations for Five Fluid Combinations and Four Major Flow Patterns in a Vertical Pipe [See Nomenclature for Abbreviations and Kim et al. (1999b) for Reference Numbers]

Recommended Exponent Values for Parameters [Shown in Table 2.6] of the Two-Phase Heat Transfer Correlations					
Correlation	Shah [18]	Aggour [1]	Knott et al. [11]	Knott et al. [11]	Aggour [1]
Flow Pattern	Vijay [40] W-A	Vijay [40] G-A	Rezkallah [41] S-A	Aggour [1] W-H	Aggour [1] W-F12
Bubbly	0.70	-0.24	1.27	0.83	-0.74
Slug	0.40	-0.11	0.37	0.38	-0.85
Froth	0.31	-0.24	0.33	0.32	-0.41
Annular	0.40	-0.35	0.28	0.34	-0.86
Mean Dev. (%)	1.66	-0.61	6.80	-0.03	0.65
rms Dev. (%)	25.19	8.49	35.07	10.23	7.83
Dev. Range (%)	-128.4 & 39.6	-18.4 & 19.4	-130.6 & 65.4	-17.7 & 30.0	-15.7 & 20.4
Original n Value Results for Each Correlation Taken from Table 2.6					
Mean Dev. (%)	24.86	-13.82	-4.09	0.74	-1.04
rms Dev. (%)	31.51	18.44	57.41	27.07	14.35
Dev. Range (%)	-29.4 & 72.8	-39.0 & 19.3	-235.7 & 67.0	-150.1 & 33.2	-28.6 & 36.8
Optimal n Value Results for Each Correlation Taken from Table 2.6					
Mean Dev. (%)	1.26	-0.49	7.22	0.20	1.03
rms Dev. (%)	28.91	6.27	26.77	10.80	8.22
Dev. Range (%)	-129.2 & 46.0	-18.2 & 19.4	-130.6 & 65.4	-26.9 & 30.0	-15.7 & 13.5

Table 2.8 Recommended Simplified Two-Phase Heat Transfer Correlations for Five Fluid Combinations and Four Major Flow Patterns in a Vertical Pipe [See Nomenclature for Abbreviations and Kim et al. (1999b) for Reference Numbers]

Recommended Simplified Exponent Values for Parameters [Shown in Table 2.6] of the Two-Phase Heat Transfer Correlations					
Correlation	Shah [18]	Aggour [1]	Knott et al. [11]	Knott et al. [11]	Aggour [1]
Flow Pattern	Vijay [40] W-A	Vijay [40] G-A	Rezkallah [41] S-A	Aggour [1] W-H	Aggour [1] W-F12
Bubbly	0.39	-0.28	0.29	0.34	-0.82
Slug					
Froth					
Annular					
Mean Dev. (%)	2.56	-5.14	12.11	3.21	-1.69
rms Dev. (%)	23.92	14.87	36.59	12.31	14.23
Dev. Range (%)	-117.6 & 40.2	-27.8 & 31.7	-142.6 & 69.1	-20.2 & 32.1	-27.9 & 23.1

air, silicone-air, and water-helium two-phase heat transfer, the parameter $(1+V_{SG}/V_{SL})$ and an appropriate exponent n should be used in the heat transfer correlations. Similarly, for prediction of glycerin-air and water-freon 12 two-phase heat transfer, the parameter $(1-\alpha)$ and an appropriate exponent n value should be used in the heat transfer correlations.

Figure 2.4 compares the performance of Knott et al. (1959) original and modified two-phase heat transfer correlations with Aggour (1978) water-helium experimental data in a vertical pipe. This figure shows the results of predictions from the correlations with the original n values (see Table 2.6), optimal n values (see Table 2.6), and the simplified n values (see Table 2.8).

Table 2.9 shows the results of our attempts to overcome the fluid combination dependency of the two-phase heat transfer correlations for a vertical pipe. For this purpose, we combined the experimental data for each of the four major flow patterns (bubbly, slug, froth, annular) and the five different fluid combinations (W-A, G-A, S-A, W-H, W-F12). With this combined data, we obtained the optimal value of the exponent n for the key parameters in the six recommended correlations by Kim et al. (1999a). Comparing the overall performance (by mean and r.m.s. deviations) of the predictions for each flow pattern for all five fluid combinations, the correlation of Aggour (1978) with $n = -0.6$ for the parameter $(1-\alpha)$ is recommended for slug flow, the correlation of Rezkallah and Sims (1987) with $n = -0.43$ for the parameter $(1-\alpha)$ is recommended for froth flow, the correlation of Shah (1981) with $n = 0.8$ for the parameter $(1+V_{SG}/V_{SL})$ is recommended for bubbly flow, and the correlation of Ravipudi and Godbold (1978) with $n = 0.26$ for the parameter (V_{SG}/V_{SL}) is recommended for annular flow. Figure 2.5 shows

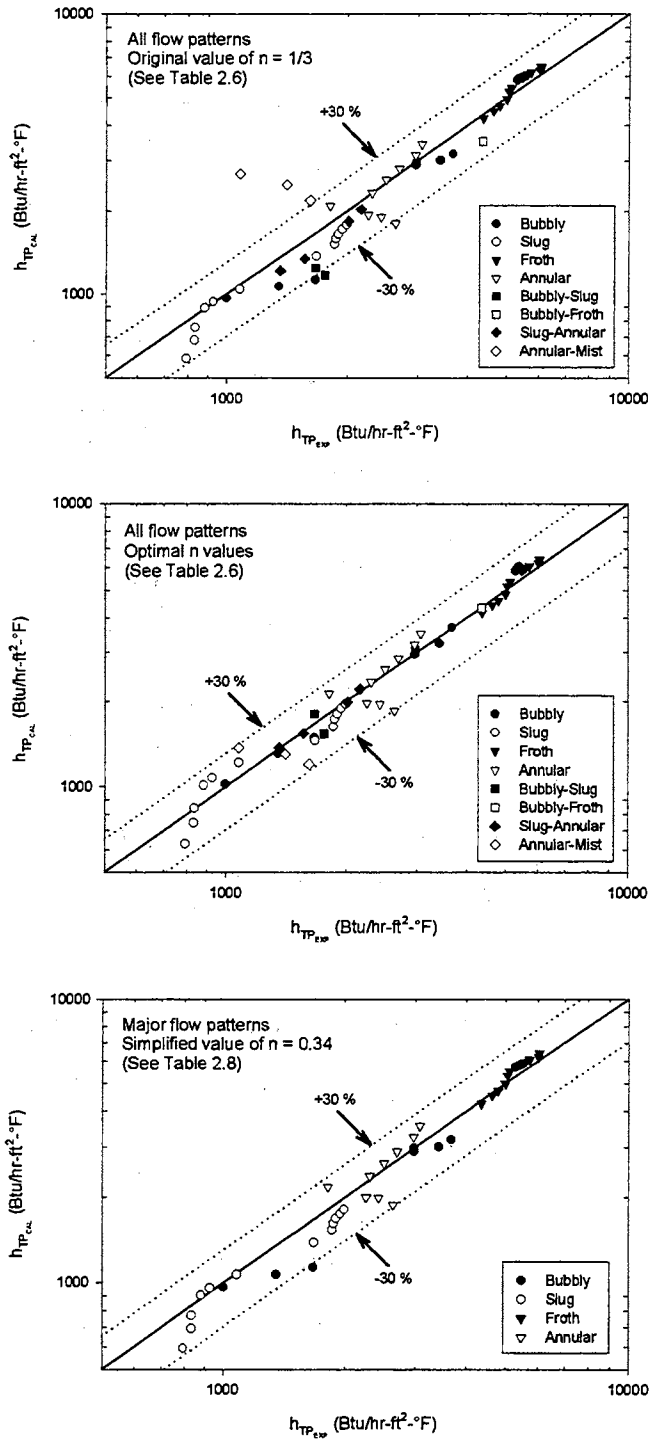


Figure 2.4 Comparison of Knott et al. (1959) Original and Modified Correlations with Aggour [1] Water-Helium Experimental Data in a Vertical Pipe (See Tables 2.6 and 2.8)

Table 2.9 Simplified Two-Phase Heat Transfer Correlations, with Recommendations, Predicting all Five Fluid Combinations for Each of the Four Major Flow Patterns in a Vertical Pipe [See Nomenclature for Abbreviations and Kim et al. (1999b) for Reference Numbers]

Aggour [1] Correlation with Different n Values for Flow Patterns, $h_{TP} = \text{fctn}(Re_L, Pr_L, \dots)(1-\alpha)^n$								
Flow Pattern (Data Pts.)	Vijay [40] W-A	Vijay [40] G-A	Rezkallah [41] S-A	Aggour [1] W-H	Aggour [1] W-F12	Mean Dev. (%)	rms Dev. (%)	Dev. Range (%)
Bubbly (71)			0.47			-7.62	10.63	-59.7 & 76.9
Slug (74)			-0.60			-4.72	36.72	-90.2 & 67.0
Froth (82)			-0.21			-10.07	25.04	-60.5 & 20.5
Annular (81)			-0.63			-16.72	68.88	-278.0 & 50.8
Rezkallah & Sims [16] Correlation with Different n Values for Flow Patterns, $h_{TP} = \text{fctn}(Re_L, Pr_L, \dots)(1-\alpha)^n$								
Bubbly			-0.76			2.07	13.83	-43.3 & 42.5
Slug			-0.62			-12.15	24.08	-129.7 & 61.3
Froth			-0.43			-10.42	26.46	-68.2 & 15.4
Annular			-0.65			-21.94	82.63	-357.4 & 49.8
Knott et al. [11] Correlation with Different n Values for Flow Patterns, $h_{TP} = \text{fctn}(Re_L, Pr_L, \dots)(1 + V_{SG}/V_{SL})^n$								
Bubbly			0.70			2.30	13.72	-44.1 & 43.9
Slug			0.35			-6.71	50.01	-161.0 & 66.2
Froth			0.27			-10.89	33.13	-79.6 & 18.5
Annular			-0.36			-20.02	79.52	-297.4 & 51.3
Shah [18] Correlation with Different n Values for Flow Patterns, $h_{TP} = \text{fctn}(Re_L, Pr_L, \dots)(1 + V_{SG}/V_{SL})^n$								
Bubbly			0.80			-4.48	12.99	-47.7 & 17.0
Slug			0.39			-8.52	50.09	-130.5 & 75.4
Froth			0.29			-14.71	37.0	-90.6 & 20.0
Annular			0.37			-24.58	85.63	-320.0 & 51.2
Kudirka et al. [12] Correlation with Different n Values for Flow Patterns, $Nu_{TP} = \text{fctn}(Re_L, Pr_L, \dots)(V_{SG}/V_{SL})^n$								
Bubbly			-0.04			-10.21	52.88	-156.6 & 65.0
Slug			-0.24			-1.14	55.52	-194.0 & 77.5
Froth			-0.15			38.77	46.69	-14.7 & 89.2
Annular			0.04			5.46	57.87	-190.3 & 83.6
Ravipudi & Godbold [15] Correlation with Different n Values for Flow Patterns, $Nu_{TP} = \text{fctn}(Re_L, Pr_L, \dots)(V_{SG}/V_{SL})^n$								
Bubbly			-0.02			1.21	21.13	-45.4 & 78.8
Slug			0.15			25.69	49.22	-135.6 & 86.9
Froth			-0.01			33.06	41.91	-3.9 & 87.8
Annular			0.26			5.25	38.82	-113.7 & 77.1

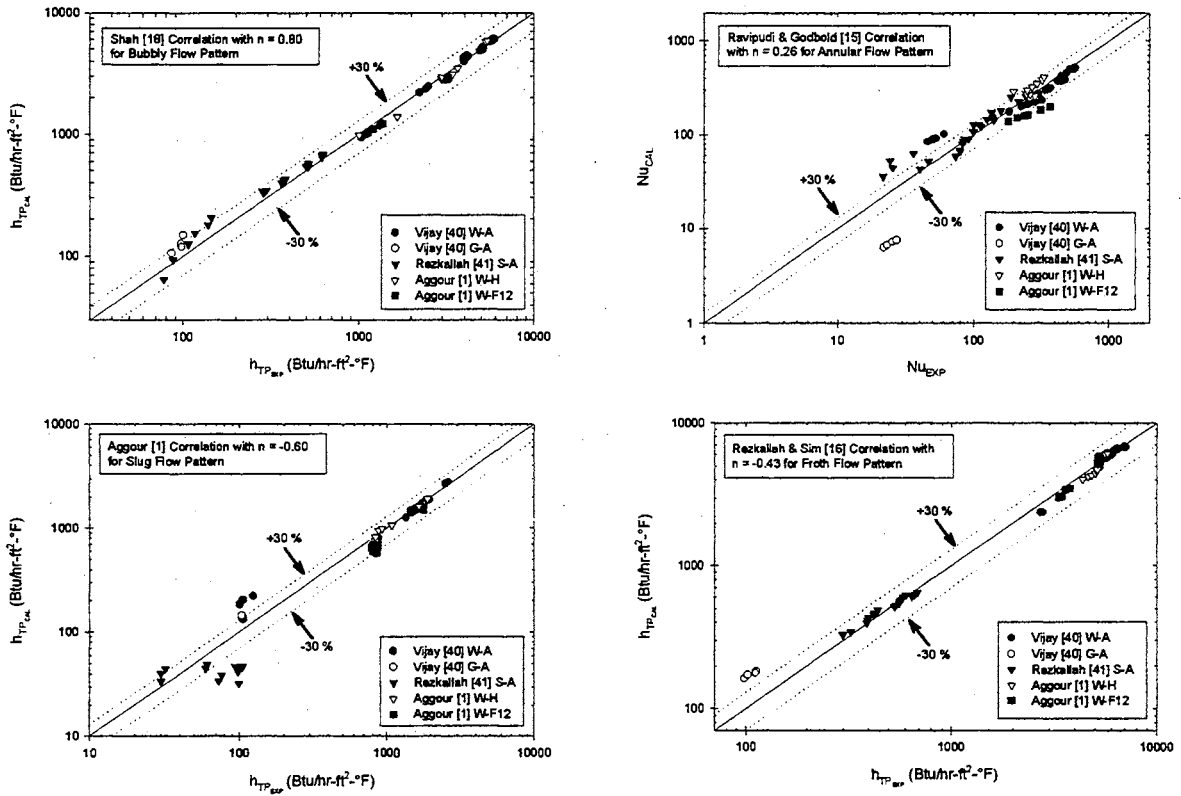


Figure 2.5 Comparison of the Modified Shah (1981), Aggour (1978), Rezkallah & Sims (1987), and Ravipudi & Godbold (1978) Correlations with the Experimental Data of Four Major Flow Patterns in a Vertical Pipe [see Kim et al. (1999b) for Reference Numbers]

how well these four recommended heat transfer correlations predict the vertical pipe two-phase heat transfer data for each flow pattern and all five fluid combinations. As can be seen from the figure, the correlations with the recommended n values do a very good job of predicting the majority of the heat transfer data with a $\pm 30\%$ deviation. The experimental data that completely fell outside of the $\pm 30\%$ band were the glycerin-air froth flow data of Vijay (1978) using Rezkallah and Sims' (1987) correlation, the water-air slug flow data of Vijay (1978) using Aggour's (1978) correlation, and the water-air annular flow data of Vijay (1978) using Ravipudi and Godbold's (1978) correlation. To further improve the predictive capabilities of the recommended correlations in predicting the two-phase heat transfer coefficient in each flow pattern regardless of the fluid combination, there appears to be at least one additional parameter [ratio], which is related to the effects of different fluid combinations on two-phase heat transfer, that must be added to the recommended correlations.

2.2.3 Summary and Conclusions

We have modified the ability of the six two-phase heat transfer correlations recommended by Kim et al. (1999a) to predict seven sets of experimental data that are available in the open literature. Five of these experimental data sets are for various flow patterns of water-air (1978), glycerin-air (1978), silicone-air (1987), water-helium (1978), and water-freon 12 (1978) in vertical pipes. The other two data sets are from the flow of water-air for slug (1952) and annular (1966) flow patterns in horizontal pipes.

Based on the improvements of the predictability of the two-phase heat transfer correlations shown in Table 2.6, we make the following recommendations: for glycerin-air and water-freon 12 flows within vertical pipes, we recommend use of the Aggour

(1978) correlation along with the optimal n values listed in Table 2.6 for the different fluid combinations; use of the Knott et al. (1959) correlation with the optimal n values listed in Table 2.6 for silicone-air and water-helium flows within vertical pipes and water-air slug flow within horizontal pipes; use of the Shah (1981) correlation along with the optimal n values listed in Table 2.6 for water-air flow within vertical pipes; and use of the Kudirka et al. (1965) correlation with the optimal n values for water-air annular flow within horizontal pipes.

Simplifying the modified exponent n values listed in Table 2.7 which depend on the four major flow patterns (bubbly, slug, froth, annular) in vertical pipes was successfully completed without significant loss of accuracy (see Table 2.8). The simplified exponent n values are 0.39 for the parameter $(1+V_{SG}/V_{SL})$ in the Shah (1981) correlation for predicting the water-air flow; -0.28 for the parameter $(1-\alpha)$ in the Aggour (1978) correlation for glycerin-air flow; 0.29 for the parameter $(1+V_{SG}/V_{SL})$ in the Knott et al. (1959) correlation for silicone-air flow; 0.34 for the parameter $(1+V_{SG}/V_{SL})$ in the Knott et al. (1959) correlation for water-helium flow; and -0.82 for the parameter $(1-\alpha)$ in correlation for water-freon 12 flow.

Attempts to simplify the exponent values in the six two-phase heat transfer correlations according to the major flow patterns regardless of the fluid combinations for predicting the five sets of two-phase heat transfer experimental data in vertical pipes were also made (see Table 2.9). Recommended exponent n values are 0.8 for the parameter $(1+V_{SG}/V_{SL})$ in the Shah (1981) correlation for bubbly flow; -0.6 for the parameter $(1-\alpha)$ in the Aggour (1978) correlation for slug flow; -0.43 for the parameter $(1-\alpha)$ in the Rezkallah and Sims (1987) correlation for froth flow; and 0.26 for the parameter

(V_{SG}/V_{SL}) in the Ravipudi and Godbold (1978) correlation for annular flow. To further improve the predictive capabilities of the recommended correlations in predicting the two-phase heat transfer coefficient in each flow pattern, there appears to be at least one additional parameter, related to the effects of different fluid combinations on two-phase heat transfer, that might be required.

In order to improve the applicability of the prediction of heat transfer rate in vertical turbulent two-phase flows regardless of fluid combination and flow pattern, this study developed a new general correlation, and compared the accuracy of this new correlation with that of the previously recommended correlations (see Kim et al., 1999c or Kim et al., 2000). Summary of the development and comparisons will be presented in the following section.

2.3 A General Heat Transfer Correlation for Turbulent Gas-Liquid Two-Phase Flow in Vertical Pipes

In this study, a general two-phase non-boiling heat transfer correlation for turbulent flow ($Re_{SL} > 4000$) in vertical tubes with different fluid flow patterns and fluid combinations was developed using experimental data available from the literature. A total of 255 data points from three available studies (which included the four sets of data) were used to determine the curve-fitted constants in the new improved general correlation. The performance of the general correlation was compared against two-phase correlations from the literature, which were developed for specific fluid combinations.

2.3.1 Introduction

Previously Kim et al. (1999a, 1999b) identified 20 two-phase flow heat transfer correlations from the published studies, and these correlations were compared against a large set of two-phase flow experimental data, for vertical and horizontal tubes and different fluid patterns and fluids. Table 2.10 presents Kim et al.'s (1999a) recommended turbulent ($Re_{SL} > 4000$) two-phase heat transfer correlations for four fluid combinations (water-air, silicone-air, water-helium, and water-freon 12) in vertical pipes. The parametric ranges of the 255 data points from three available experimental studies of Aggour (1978), Vijay (1978), and Rezkallah (1987) (which included the four sets of data) used in Table 2.10 are provided in Table 2.11.

From Table 2.10, it is recommended that for the water-air data of Vijay (1978), use the correlation of Shah (1981) for bubbly, slug, froth, bubbly-froth, and froth-annular flow patterns; for the silicone-air data of Rezkallah (1987), use the correlation of Rezkallah and Sims (1987) for bubbly and bubbly-froth patterns; for the water-helium data of Aggour (1978), use the correlation of Knott et al. (1959) for all of the flow patterns in Table 2.10 except the bubbly-slug and annular-mist flow patterns; and for the water-freon 12 data of Aggour (1978), use the correlation of Aggour (1978) for all of the flow patterns listed in Table 2.10. Comparing the performance of the predictions for water-air and silicone-air data with the water-helium and water-freon 12 data in Table 2.10, for water-air and silicone-air data, it was more difficult to find a good correlation from the available literature, which could be applicable to several different flow patterns in a gas-liquid fluid combination.

In order to improve the applicability of the prediction of heat transfer rate in

Table 2.10 Results of the Predictions for Available Experimental Data Using the Recommended Correlations by Kim et al. (1999a)

Experimental Study ($Re_{SL} > 4000$ Only)	Vijay (1978) Water-Air (105 Data Points)	Rezkallah (1987) Silicone-Air (56 Data Points)	Aggour (1978) Water-Helium (50 Data Points)	Aggour (1978) Water-Freon 12 (44 Data Points)
Used Correlation	Shah (1981)	Rezkallah & Sims (1987)	Knott et al. (1959)	Aggour (1978)
Flow Pattern	No. of Data Points within $\pm 30\%$ / Total No. of Data Points for Each Flow Pattern			
Bubbly	25 / 25	20 / 20	9 / 10	6 / 6
Slug	12 / 17		10 / 10	6 / 6
Froth	25 / 25	10 / 18	12 / 12	10 / 10
Annular	3 / 21	0 / 2	8 / 9	14 / 14
Bubbly-Slug			1 / 2	3 / 4
Bubbly-Froth	7 / 7	10 / 10	1 / 1	1 / 1
Slug-Annular	1 / 2		4 / 4	3 / 3
Froth-Annular	4 / 4	0 / 6		
Annular-Mist	0 / 4		0 / 2	
All Flow Patterns	77 / 105	40 / 56	45 / 50	43 / 44
Mean Dev. (%)	21.42	-17.98	3.85	-1.0
rms Dev. (%)	26.32	31.65	18.04	14.35
Dev. Range (%)	-1.20 & 61.47	-84.17 & 8.60	-75.97 & 33.35	-28.64 & 36.81

Note: Blanks indicate that there is no experimental data available for that flow pattern.

vertical turbulent two-phase flows regardless of fluid combination and flow pattern, this study developed a new general correlation, and compared the accuracy of this new correlation with that of the recommended fluid combination dependent correlations in Table 2.10.

2.3.2 Development of A New General Correlation

In order to improve the prediction of heat transfer rate in vertical turbulent two-phase flow, regardless of fluid combination and flow pattern, this study developed a new

Table 2.11 Ranges of the Experimental Data for Vertical Tubes Used in this Study

Water-Air Data (105 Points) of Vijay (1978)	$267.56 \leq \dot{m}_L \text{ (lbm/hr)} \leq 8996$ $0.058 \leq \dot{m}_G \text{ (lbm/hr)} \leq 206.43$ $0.152 \leq X_{IT} \leq 433.04$ $0.356 \leq \Delta P_{TP} \text{ (psi)} \leq 17.048$ $5.503 \leq Pr_L \leq 6.857$ $866.4 \leq h_{TP} \text{ (Btu/hr-ft}^2\text{-}^\circ\text{F)} \leq 7042.3$	$1.03 \leq V_{SL} \text{ (ft/sec)} \leq 34.80$ $0.164 \leq V_{SG} \text{ (ft/sec)} \leq 220.54$ $59.64 \leq T_{MIX} \text{ (}^\circ\text{F)} \leq 80.62$ $0.007 \leq \Delta P_{TPF} \text{ (psi)} \leq 16.74$ $0.709 \leq Pr_G \leq 0.710$ $0.813 \leq \mu_w/\mu_B \leq 0.905$	$4004.6 \leq Re_{SL} \leq 126630$ $43.42 \leq Re_{SG} \leq 153674$ $15.46 \leq P_{MIX} \text{ (psi)} \leq 74.44$ $0.033 \leq \alpha \leq 0.945$ $94.84 \leq Nu_{TP} \leq 776.12$ $L/D = 52.1, D = 0.46 \text{ in.}$
Silicone-Air Data (56 points) of Rezkallah (1987)	$3058 \leq \dot{m}_L \text{ (lbm/hr)} \leq 7196$ $0.07 \leq \dot{m}_G \text{ (lbm/hr)} \leq 55.94$ $72.46 \leq T_w \text{ (}^\circ\text{F)} \leq 94.2$ $2.165 \leq \Delta P_{TP} \text{ (psi)} \leq 9.767$ $64.6 \leq Pr_L \leq 71.1$ $286.0 \leq h_{TP} \text{ (Btu/hr-ft}^2\text{-}^\circ\text{F)} \leq 683.0$	$12.83 \leq V_{SL} \text{ (ft/sec)} \leq 30.20$ $0.17 \leq V_{SG} \text{ (ft/sec)} \leq 59.73$ $72.41 \leq T_B \text{ (}^\circ\text{F)} \leq 81.19$ $1.217 \leq \Delta P_{TPF} \text{ (psi)} \leq 9.074$ $0.079 \leq Pr_G \leq 0.710$	$8349 \leq Re_{SL} \leq 20930$ $52.1 \leq Re_{SG} \leq 41599$ $17.6 \leq P_{MIX} \text{ (psi)} \leq 45.3$ $0.011 \leq \alpha \leq 0.68$ $161.9 \leq Nu_{TP} \leq 386.8$ $L/D = 52.1, D = 0.46 \text{ in.}$
Water-Helium Data (50 Points) of Aggour (1978)	$267 \leq \dot{m}_L \text{ (lbm/hr)} \leq 8995$ $0.020 \leq \dot{m}_G \text{ (lbm/hr)} \leq 19.05$ $0.23 \leq X_{IT} \leq 769.6$ $0.3 \leq \Delta P_{TP} \text{ (psi)} \leq 13.2$ $5.78 \leq Pr_L \leq 7.04$ $794 \leq h_{TP} \text{ (Btu/hr-ft}^2\text{-}^\circ\text{F)} \leq 6061$	$1.03 \leq V_{SL} \text{ (ft/sec)} \leq 34.70$ $0.42 \leq V_{SG} \text{ (ft/sec)} \leq 355.6$ $67.4 \leq T_{MIX} \text{ (}^\circ\text{F)} \leq 82.0$ $0.01 \leq \Delta P_{TPF} \text{ (psi)} \leq 12.5$ $0.6908 \leq Pr_G \leq 0.691$ $83.9 \leq T_w \text{ (}^\circ\text{F)} \leq 95.7$	$4011 \leq Re_{SL} \leq 125835$ $14.0 \leq Re_{SG} \leq 13071$ $15.5 \leq P_{MIX} \text{ (psi)} \leq 53.3$ $0.038 \leq \alpha \leq 0.949$ $86.6 \leq Nu_{TP} \leq 668.2$ $L/D = 52.1, D = 0.46 \text{ in.}$
Water-Freon 12 Data (44 Points) of Aggour (1978)	$267 \leq \dot{m}_L \text{ (lbm/hr)} \leq 3598$ $0.84 \leq \dot{m}_G \text{ (lbm/hr)} \leq 206.59$ $0.16 \leq X_{IT} \leq 226.5$ $0.04 \leq \Delta P_{TP} \text{ (psi)} \leq 4.92$ $5.63 \leq Pr_L \leq 6.29$ $800 \leq h_{TP} \text{ (Btu/hr-ft}^2\text{-}^\circ\text{F)} \leq 4344$	$1.03 \leq V_{SL} \text{ (ft/sec)} \leq 13.89$ $0.51 \leq V_{SG} \text{ (ft/sec)} \leq 117.7$ $75.26 \leq T_{MIX} \text{ (}^\circ\text{F)} \leq 83.89$ $0.02 \leq \Delta P_{TPF} \text{ (psi)} \leq 4.48$ $0.769 \leq Pr_G \leq 0.77$ $90.36 \leq T_w \text{ (}^\circ\text{F)} \leq 94.89$	$4190 \leq Re_{SL} \leq 51556$ $859.5 \leq Re_{SG} \leq 209430$ $15.8 \leq P_{MIX} \text{ (psi)} \leq 27.8$ $0.035 \leq \alpha \leq 0.934$ $87.1 \leq Nu_{TP} \leq 472.4$ $L/D = 52.1, D = 0.46 \text{ in.}$

general correlation using the following definitions and assumptions. Some of the definitions and equations can be found from Section 1.1 will be repeated here for convenience.

The void fraction α is defined as the ratio of the gas-flow cross-sectional area A_G to the total cross-sectional area A ,

$$\alpha = \frac{A_G}{A} \quad (1.4)$$

where A must equal the sum of the cross-sectional areas (A_G and A_L) occupied by the two phases:

$$A = A_G + A_L \quad (1.5)$$

Many two-phase flow correlations are based on a variable called superficial velocity. The superficial velocity of a fluid phase is defined as the velocity which that phase would exhibit if it flowed through the total cross section of the pipe alone. The superficial gas velocity, V_{SG} , is then defined as:

$$V_{SG} = \frac{Gx}{\rho_G} = \frac{Q_G}{A} \quad (1.18)$$

where G is the total mass flux or mass velocity, x the gas-phase mass flow fraction, ρ_G the density of gas, and Q_G the volumetric flow rate of gas. The actual gas velocity, V_G can be calculated from

$$V_G = \frac{Q_G}{A_G} = \frac{\dot{m}_G}{\rho_G A_G} = \frac{\dot{m}x}{\rho_G \alpha A} \quad (1.19)$$

where \dot{m}_G is the gas mass flow rate, and \dot{m} is the total mass flow rate. Similarly, for the liquid, V_{SL} and V_L are defined as:

$$V_{SL} = \frac{G(1-x)}{\rho_L} = \frac{Q_L}{A} \quad (1.20)$$

$$V_L = \frac{Q_L}{A_L} = \frac{\dot{m}_L}{\rho_L A_L} = \frac{\dot{m}(1-x)}{\rho_L (1-\alpha)A} \quad (1.21)$$

where V_L is the actual liquid velocity, \dot{m}_L is the liquid mass flow rate, ρ_L is the density of liquid, and Q_L is the volumetric flow rate of liquid.

The total gas-liquid two-phase heat transfer is assumed to be the sum of the individual single-phase heat transfers of the gas and liquid, along with the appropriate corresponding cross-sectional areas in contact with each phase:

$$h_{TP} = (1-\alpha)h_L + \alpha h_G \quad (2.1)$$

There are several well-known single-phase heat transfer correlations in the literature. This study chose the Sieder and Tate (1936) equation as the fundamental single-phase heat transfer correlation because of its practical simplicity (see Table 1.6). Based upon the chosen single-phase correlation, the single-phase heat transfer coefficients in Equation (2.1), h_L and h_G , can be modeled as functions of Reynolds number, Prandtl number and the ratio of bulk to wall viscosities. Thus, Equation (2.1) can be expressed as:

$$h_{TP} = (1-\alpha) \text{fctn}(\text{Re}, \text{Pr}, \mu_B/\mu_W)_L + \alpha \text{fctn}(\text{Re}, \text{Pr}, \mu_B/\mu_W)_G \quad (2.2)$$

$$h_{TP} = (1-\alpha)h_L \left[1 + \frac{\alpha}{1-\alpha} \frac{\text{fctn}(\text{Re}, \text{Pr}, \mu_B/\mu_W)_G}{\text{fctn}(\text{Re}, \text{Pr}, \mu_B/\mu_W)_L} \right] \quad (2.3)$$

$$h_{TP} = (1-\alpha)h_L \left[1 + \frac{\alpha}{1-\alpha} \text{fctn} \left\{ \left(\frac{\text{Re}_G}{\text{Re}_L} \right), \left(\frac{\text{Pr}_G}{\text{Pr}_L} \right), \left(\frac{(\mu_B/\mu_W)_G}{(\mu_B/\mu_W)_L} \right) \right\} \right] \quad (2.4)$$

Substituting the definition of Reynolds number ($\text{Re} = \rho V D / \mu_B$) for the gas (Re_G) and liquid (Re_L) yields

$$\frac{h_{TP}}{(1-\alpha)h_L} = \left[1 + \frac{\alpha}{1-\alpha} \text{fctn} \left\{ \left(\frac{(\rho VD)_G (\mu_B)_L}{(\rho VD)_L (\mu_B)_G} \right), \left(\frac{Pr_G}{Pr_L} \right), \left(\frac{(\mu_B/\mu_w)_G}{(\mu_B/\mu_w)_L} \right) \right\} \right] \quad (2.5)$$

Rearranging yields

$$\frac{h_{TP}}{(1-\alpha)h_L} = \left[1 + \frac{\alpha}{1-\alpha} \text{fctn} \left\{ \left(\frac{\rho_G}{\rho_L} \right) \left(\frac{V_G}{V_L} \right) \left(\frac{D_G}{D_L} \right), \left(\frac{Pr_G}{Pr_L} \right), \left(\frac{(\mu_w)_L}{(\mu_w)_G} \right) \right\} \right] \quad (2.6)$$

Substituting Equations (1.4) and (1.5) for the ratio of gas to liquid diameters (D_G/D_L) in Equation (2.6), and based upon practical considerations assuming that the ratio of liquid to gas viscosities evaluated at the wall temperature $[(\mu_w)_L/(\mu_w)_G]$ is comparable to the ratio of those viscosities evaluated at the bulk temperature (μ_L/μ_G) , the above correlation would reduce to

$$\frac{h_{TP}}{(1-\alpha)h_L} = \left[1 + \frac{\alpha}{1-\alpha} \text{fctn} \left\{ \left(\frac{\rho_G}{\rho_L} \right) \left(\frac{V_G}{V_L} \right) \left(\frac{\sqrt{\alpha}}{\sqrt{1-\alpha}} \right), \left(\frac{Pr_G}{Pr_L} \right), \left(\frac{\mu_L}{\mu_G} \right) \right\} \right] \quad (2.7)$$

For use in further simplifying Equation (2.7), combine Equations (1.19) and (1.21) for V_G (gas velocity) and V_L (liquid velocity) in the following form:

$$K = \frac{V_G}{V_L} = \left(\frac{x}{1-x} \right) \left(\frac{1-\alpha}{\alpha} \right) \frac{\rho_L}{\rho_G} \quad (1.11)$$

where K is often referred to as the 'slip ratio', and is usually greater than unity, which means that V_G is usually greater than V_L . The relative velocity, $V_G - V_L$, is often referred to as the 'slip velocity'.

Substituting Equation (1.11) into Equation (2.7) yields

$$h_{TP} = (1-\alpha)h_L \left[1 + \text{fctn} \left\{ \left(\frac{x}{1-x} \right) \left(\frac{\alpha}{1-\alpha} \right), \left(\frac{Pr_G}{Pr_L} \right), \left(\frac{\mu_L}{\mu_G} \right) \right\} \right] \quad (2.8)$$

Assuming that two-phase heat transfer coefficient can be expressed using a power-law relationship on the parameters $[x/(1-x)]$, $[\alpha/(1-\alpha)]$, $[Pr_G/Pr_L]$, and $[\rho_L/\rho_G]$ that appear in Equation (2.8) [e.g. $fctn\{x/(1-x) = Const.\{x/(1-x)\}^m$], then Equation (2.8) can be expressed as:

$$h_{TP} = (1 - \alpha)h_L \left[1 + Const. \left(\frac{x}{1-x} \right)^m \left(\frac{\alpha}{1-\alpha} \right)^n \left(\frac{Pr_G}{Pr_L} \right)^p \left(\frac{\mu_L}{\mu_G} \right)^q \right] \quad (2.9)$$

In Equation (2.9), in order to evaluate the liquid single-phase heat transfer (h_L), the Sieder and Tate (1936) equation is used as mentioned earlier. For the Reynolds number involved in the single-phase heat transfer correlation, the following relationship is used to evaluate the in-situ Reynolds number (liquid phase) rather than the superficial Reynolds number (Re_{SL}) as commonly used in the correlations of Table 1.6:

$$Re_L = \left(\frac{\rho V D}{\mu_B} \right)_L = \frac{4\dot{m}_L}{\pi \sqrt{1-\alpha} \mu_L D} \quad (2.10)$$

It should be noted that any other well-known single-phase turbulent heat transfer correlation could have been used in place of the Sieder and Tate (1936) correlation. The difference resulting from the use of a different single-phase heat transfer correlation will be absorbed during the determination of the values of the leading coefficient and exponents on different parameters in Equation (2.9).

In order to determine the values of leading coefficient and the exponents in Equation (2.9), four sets of experimental data (a total of 255 data points) from three available experimental studies (Aggour, 1978, Rezkallah, 1987, Vijay, 1978) were used in this study. The ranges of these four sets of experimental data are provided in Table 2.11. The experimental data included four different liquid-gas combinations (water-air,

silicone-air, water-helium, water-freon 12), and covered wide range of variables, including liquid and gas flow rates, properties, and flow patterns. It should be also mentioned here that the selected experimental data were only for turbulent two-phase heat transfer data in which the superficial Reynolds numbers of liquid (Re_{SL}) were all greater than 4000.

2.3.3 Prediction Results and Discussion

A general correlation that can be used to predict turbulent two-phase gas-liquid non-boiling heat transfer rate for wide range of fluid combinations and several different flow patterns was obtained by curve-fitting Equation (2.9) to the 255 data points obtained from the literature (see Table 2.11). The best-fit correlation is

$$\frac{h_{TP}}{(1-\alpha)h_L} = \left[1 + 0.27 \left(\frac{x}{1-x} \right)^{-0.04} \left(\frac{\alpha}{1-\alpha} \right)^{1.21} \left(\frac{Pr_G}{Pr_L} \right)^{0.66} \left(\frac{\mu_G}{\mu_L} \right)^{-0.72} \right] \quad (2.11)$$

where $4000 < Re_{SL} < 1.26 \times 10^5$, $8.4 \times 10^{-6} < \left(\frac{x}{1-x} \right) < 0.77$, $0.01 < \left(\frac{\alpha}{1-\alpha} \right) < 18.61$,

$$1.18 \times 10^{-3} < \left(\frac{Pr_G}{Pr_L} \right) < 0.14, \text{ and } 3.64 \times 10^{-3} < \left(\frac{\mu_G}{\mu_L} \right) < 0.02.$$

In the development of the above curve-fitted correlation, the values of the void fraction (α) were directly taken from the original experimental data (Aggour, 1978, Rezkallah, 1987, Vijay, 1978). These α values were calculated by the original investigators based on the equation provided by Chisholm (1973) along with Equation (1.11). The equation suggested by Chisholm (1973) is

$$K = \left(\frac{\rho_L}{\rho_{MIX}} \right)^{1/2} \quad (2.12)$$

where

$$\frac{1}{\rho_{\text{MIX}}} = \frac{(1-x)}{\rho_L} + \frac{x}{\rho_G} \quad (2.13)$$

Then from Equation (1.11)

$$\frac{1}{\alpha} = 1 + K \left(\frac{1-x}{x} \right) \frac{\rho_G}{\rho_L} \quad (2.14)$$

Equation (2.11) gives a representation of the 255 experimental data points. Comparing Equation (2.11)'s predicted heat transfer coefficients to the experimentally determined values (see Table 2.12) yields a mean deviation of 2.54%, an rms deviation of 12.78%, and a deviation range of -64.71% to 39.55%. It should be noted that the exponent value on the parameter $[x/(1-x)]$ in Equation (2.11) has a very small magnitude (0.04) for the sets of experimental data used in this study. However, this term appears to play a very important role since elimination of $[x/(1-x)]$ yielded substantial under predictions, resulting in the best achievable mean deviation being 10.55% with a corresponding rms deviation of 15.6%. This caused about 89 % of the experimental data (224 data points) to be under predicted.

Figure 2.6 shows how well the general correlation predicted the four different sets of gas-liquid experimental data. About 83% of the data (212 data points) were predicted with less than $\pm 15\%$ deviation, and about 96% of the data (245 data points) were predicted with less than $\pm 30\%$ deviation. Table 2.12 also shows the results of the general correlation's predictions of the individual data sets. About 93% of the water-air data of Vijay (1978) (98 data points out of 105), 100% of the silicone-air data of Rezkallah (1987) (56 data points), 96% of the water-helium data of Aggour (1978) (48 data points out of 50), and 98% of the water-freon 12 data of Aggour (1978) (43 data points out of 44) were predicted with less than $\pm 30\%$ deviation. Comparing the performance of the

Table 2.12 Results of the Predictions for Available Two-Phase Heat Transfer Experimental Data Using the Recommended General Correlation (Equation 2.11)

General Form of the Two-Phase Heat Transfer Coefficient Correlation:									
$h_{TP} = (1 - \alpha)h_L \left[1 + C \left(\frac{x}{1-x} \right)^m \left(\frac{\alpha}{1-\alpha} \right)^n \left(\frac{Pr_G}{Pr_L} \right)^p \left(\frac{\mu_G}{\mu_L} \right)^q \right]$									
Fluids ($Re_{SL} > 4000$)	Value of C and Exponents (m, n, p, q)					Mean Dev. (%)	rms Dev. (%)	Number of Data within $\pm 30\%$	Range of Dev. (%)
	C	m	n	p	q				
All of the Data Points in Table 2.11 255 data points	0.27	-0.04	1.21	0.66	-0.72	2.54	12.78	245	-64.71 and 39.55
Water-air 105 data points Vijay (1978)						3.53	12.98	98	-34.97 and 39.55
Silicone-air 56 data points Rezkallah (1987)						5.25	7.77	56	-7.25 and 12.13
Water-helium 50 data points Aggour (1978)						-1.66	15.68	48	-64.71 and 32.19
Water-freon 12 44 data points Aggour (1978)						1.51	13.74	43	-24.51 and 32.96

Table 2.13 Summary of the Values of the Leading Coefficient (C) and Exponents (m, n, p, q) in the General Heat Transfer Coefficient Correlation (h_{TP}) and the Prediction Results

General Form of the Two-Phase Heat Transfer Coefficient Correlation:									
$h_{TP} = (1 - \alpha)h_L \left[1 + C \left(\frac{x}{1-x} \right)^m \left(\frac{\alpha}{1-\alpha} \right)^n \left(\frac{Pr_G}{Pr_L} \right)^p \left(\frac{\mu_G}{\mu_L} \right)^q \right]$									
Fluids ($Re_{SL} > 4000$)	Value of C and Exponents (m, n, p, q)					Mean Dev. (%)	rms Dev. (%)	Number of Data within $\pm 30\%$	Range of Dev. (%)
	C	m	n	p	q				
All of the Data Points in Table 2.11 255 data points	0.27	-0.04	1.21	0.66	-0.72	2.54	12.78	245	-64.71 and 39.55
Water-air 105 data points Vijay (1978)	16.69	-0.32	1.65	1.23	0.40	3.22	8.04	105	-18.25 and 27.0
Silicone-air 56 data points Rezkallah (1987)	2.19	0.40	0.21	0.87	-0.96	0.55	3.38	56	-5.37 and 10.34
Water-helium 50 data points Aggour (1978)	61.16	-0.29	1.58	0.24	1.47	3.03	12.24	49	-28.05 and 34.92
Water-freon 12 44 data points Aggour (1978)	599.9	-0.30	1.64	5.27	-0.85	1.67	11.56	44	-25.04 and 28.42

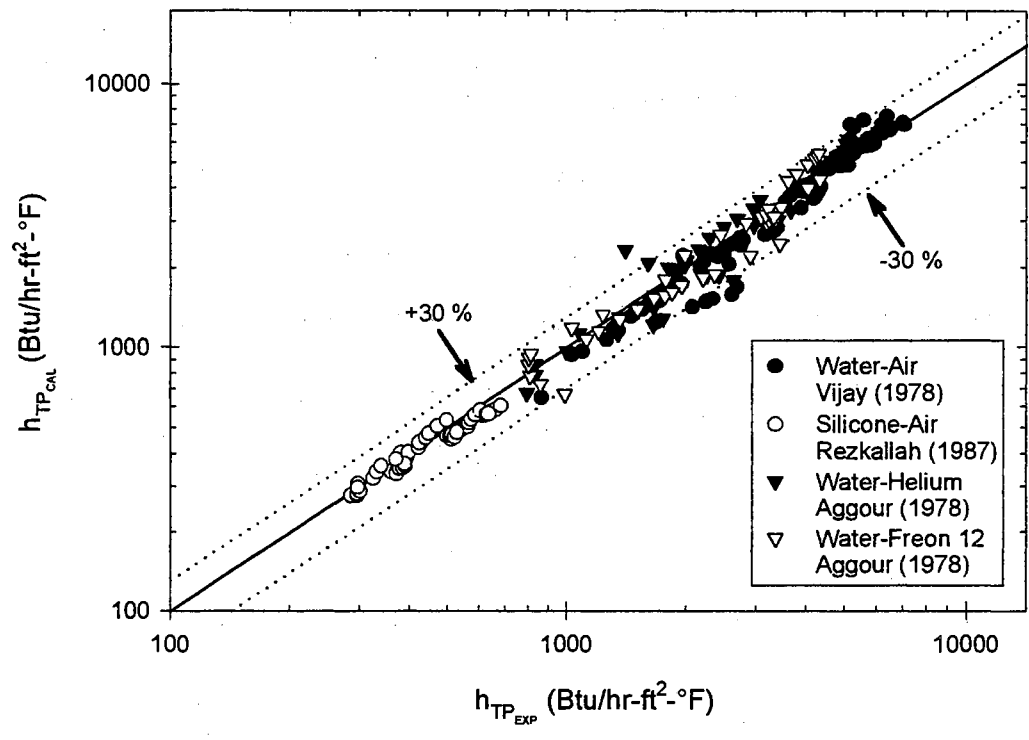


Figure 2.6 Comparison of the General Correlation (Equation 2.11) with All of the Two-Phase Heat Transfer Experimental Data (255 Data Points) in Table 2.11

developed general correlation, Equation (2.11), with those listed in Table 2.10 (Shah, 1981, Rezkallah and Sims, 1987, Knott et al., 1959, and Aggour, 1978) for the specific fluid combinations (water-air, silicone-air, water-helium, and water-freon 12), clearly shows that the general correlation is as good or better than the specific fluid dependent correlations in predicting the experimental data of Table 2.11. Specifically, for the water-air experimental data of Vijay (1978) and the silicone-air experimental data of Rezkallah (1987), the performance of the general correlation is significantly better than the fluid combination specific correlations of Shah (1981) for water-air and Rezkallah and Sims (1987) for silicone-air that were recommended by Kim et al. (1999a) in Table 2.10.

To further improve the capabilities of the general correlation in predicting the specific fluid combination experimental data, the general form of the correlation (Equation 2.9) was curve-fitted to each of the four different fluid combination experimental data sets. Table 2.13 gives a summary of the curve-fitted values of the leading coefficient (C) and the exponents (m, n, p, and q) in the general form of the heat transfer correlation (Equation 2.9), and the prediction results for each of the four fluid combinations in terms of % mean deviation, % rms deviation, % range of deviation, and the number of data points within $\pm 30\%$ deviation. For comparison purposes, the table also lists the values of the curve-fitted parameters (C, m, n, p, and q) for the general (fluid independent) correlation (Equation 2.11) and the prediction results.

As can be seen from Table 2.13, for the water-air data of Vijay (1978), the correlation predicts the heat transfer coefficient of the 105 experimental water-air data points with a mean deviation of 3.22%, an rms deviation of 8.04%, and a deviation range of -18.25% to 27.0% . About 94% of the data (99 data points out of 105) were predicted

with less than $\pm 15\%$ deviation. Comparing the performance of this correlation with that of Shah (1981) presented in Table 2.10 for the same data set (mean = 21.42%, rms = 26.32%, range = -1.2% and 61.47%), clearly shows the superb predictive capability of the fluid combination dependent general correlation developed in this study.

For the silicone-air experimental data of Rezkallah (1987), the correlation prediction results for the 56 experimental silicone-air data points had a mean deviation equal to 0.55%, an rms deviation equal to 3.38%, and a range of deviation from -5.37% to 10.34%. All of the data (56 data points) were predicted with less than $\pm 15\%$ deviation. In contrast, as shown in Table 2.10, the Rezkallah and Sims (1987) correlation predictions were generally poorer for the same experimental data set (mean = -17.98%, rms = 31.65%, and range = -84.17% to 8.6%). Again, the new correlation does an excellent job of predicting the experimental data.

For the water-helium experimental data of Aggour (1978), the correlation predicts the 50 data points with a mean deviation of 3.03%, an rms deviation of 12.24%, and a deviation range of -28.05% to 34.92%. About 86% of the data (43 data points out of 50) was predicted with less than $\pm 15\%$ deviation. Comparing the performance of this correlation with that of Knott et al. (1959) presented in Table 2.10 for the same data set (mean = 3.85%, rms = 18.04%, range = -75.97% to 33.35%), shows the improved predictive capability of this study's fluid combination dependent general correlation.

For the water-freon 12 experimental data of Aggour (1978), the correlation prediction results for the 44 experimental water-freon 12 data points had a mean deviation equal to 1.67%, an rms deviation equal to 11.56%, and a range of deviation from -25.04% to 28.42%. About 86% of the data (36 data points out of 44) were

predicted with less than $\pm 15\%$ deviation. As shown in Table 2.10, the same data set was predicted by the correlation of Aggour (1978) (mean = -1.0%, rms = 14.35%, and range = -28.64% to 36.81%). Again, the new fluid combination dependent general correlation predicts the experimental data with excellent accuracy.

The tabulated curve-fitted values, for the fluid combination dependent general correlations summarized in Table 2.13, give a representation of the effects of gas and liquid two-phase mixture on the two-phase heat transfer, and they can vary widely depending upon the properties of the gas and liquid. It is interesting to observe that the variation in the exponent values m and n for the parameters $[x/(1-x)]$ and $[\alpha/(1-\alpha)]$ was much smaller than the variation in the exponents of the other parameters in the correlation. From this, it can be concluded that the effects of these parameters on the two-phase heat transfer have a weaker dependency on the gas properties than the other parameters in the general correlation. Also, it can be observed from Table 2.13 that the magnitude of the leading coefficient (C) is considerably larger when helium or freon 12 is mixed with water in two-phase flow. Based on this observation, it appears that those parameters in the general correlation, representing mixing effects of gas-liquid on the two-phase heat transfer, may contribute more to the correlation if an inert or relatively inert type of gas is mixed with the liquid.

2.3.4 Summary and Conclusions

We have developed a new general semi-mechanistic heat transfer correlation (see Equation 2.11), which can be applied to turbulent gas-liquid two-phase flow in vertical pipes with different fluid flow patterns and fluid combinations. The general correlation gives a very good representation of the 255 experimental data points referred to in Table

2.11 for water-air (Vijay, 1978), silicone-air (Rezkallah, 1987), water-helium (Aggour, 1978), and water-freon 12 (Aggour, 1978) with a mean deviation of 2.54%, an rms deviation of 12.78%, and a deviation range of -64.71% to 39.55%. Additional improvements in the predictive capability of the general correlation can be obtained by using the fluid dependent curve-fitted values listed in Table 2.13 for the leading coefficient (C) and the exponents (m, n, p, and q) of Equation (2.9).

It was concluded from the observations of the variations in the exponent values on the parameters in the fluid combination dependent general correlations that the effects of the parameters $[x/(1-x)]$ and $[\alpha/(1-\alpha)]$ on two-phase heat transfer had a weaker dependency upon the gas properties than the other parameters in the general correlation. Also, it was observed that those parameters in the general correlation, representing mixing effects of gas-liquid on the two-phase heat transfer, may contribute more to the correlation if an inert or relatively inert type of gas (helium and freon 12) is mixed with the liquid (water).

For the future work, it is planned to continue this study by investigating the development of a correlation which is robust enough to span all or most of the fluid combinations, flow patterns, and pipe orientations (vertical and horizontal). This may require additional horizontal experimental data sets which are not in the current open literature. In order to aid in this two-phase heat transfer correlation development, a new horizontal experimental setup has been built. In the following chapter, details of this new horizontal two-phase flow experimental setup will be presented.

CHAPTER III

EXPERIMENTAL SETUP AND DATA REDUCTION

A schematic diagram of the experimental apparatus for the heat transfer and pressure drop measurements is shown in Figure 3.1. Presented in this chapter is a description of the experimental apparatus including the necessary instrumentation in detail. The design, construction, and instrumentation of the experimental setup explained in this chapter was a joint effort between the present author and two Master's degree students, Ryali (1999) and Kim (2000). Following the apparatus description is the explanation of the calibration process. At the end of this chapter, the data reduction techniques, computer programs assisting with the measurements of heat transfer and pressure drop, and experimental procedure are introduced. The uncertainty analysis of the overall experimental procedures using the method of Kline and McClintock (1953) showed that there was a maximum of 11.5% uncertainty for heat transfer coefficient calculations and the details are presented in Appendix A.

3.1 Description of the Experimental Setup and Equipments

This section will introduce the two-phase experimental setup and all the equipment which were used to perform pressure drop and heat transfer measurements for a variety of different flow patterns in a horizontal circular tube.

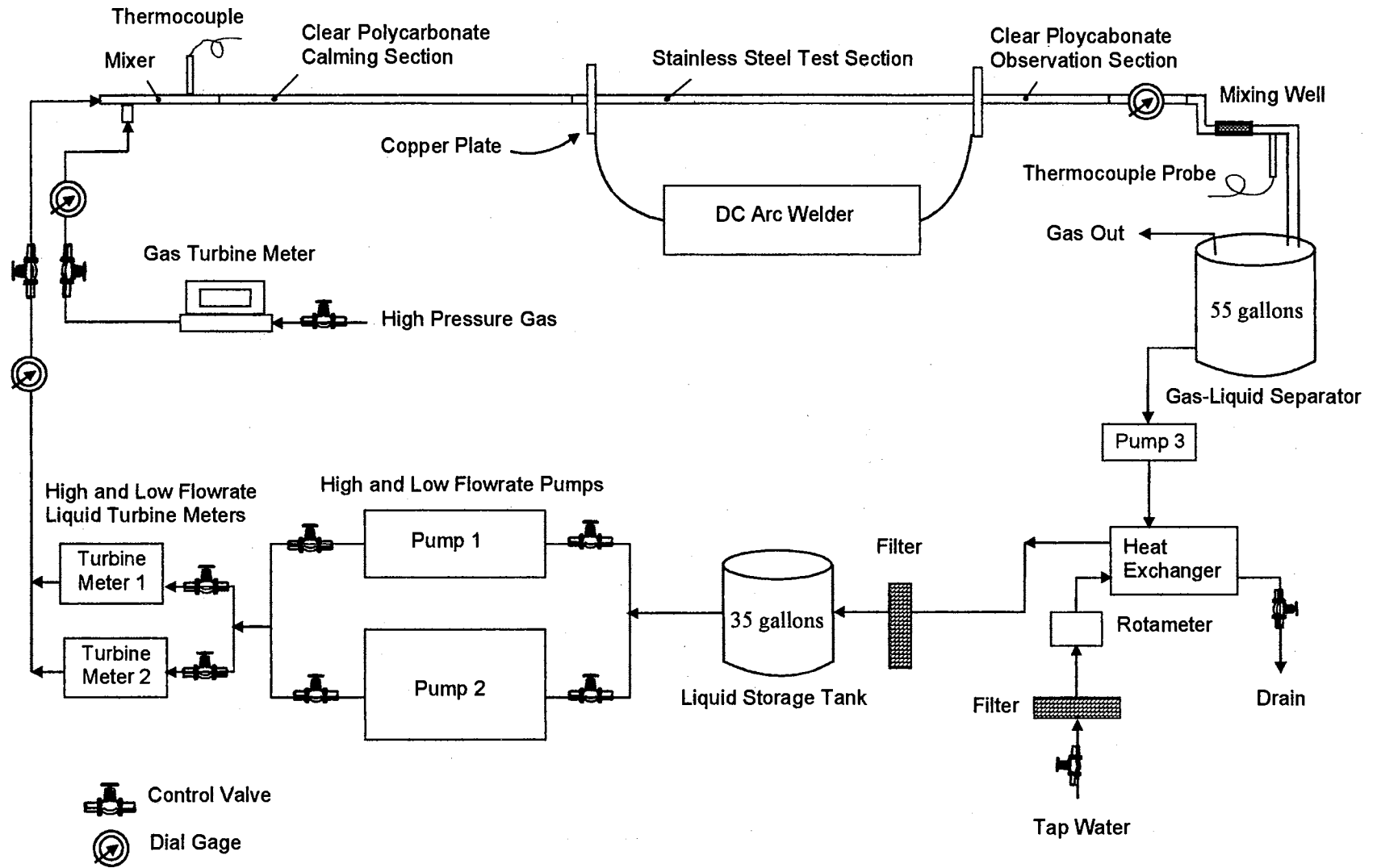


Figure 3.1 Schematic Diagram of the Experimental Setup

3.1.1 Test Section

The test section for the heat transfer and pressure drop measurements is a horizontal seamless 316 schedule 40 stainless steel circular pipe with an average inside diameter of 1.097 inches (2.79 cm) and an average outside diameter of 1.315 inches (3.34 cm). The length of the test section is 110 inches (2.79 m) providing a maximum length to diameter ratio (L/D) of 100. The stainless steel pipe was procured from Stillwater Steel and Supply, Stillwater, OK.

In order to apply uniform wall heat flux boundary condition to the test section, copper plates (5 inch x 7 inch x 0.25 inch) were silver soldered to the inlet and exit of the test section. Supporting copper material was bolted to the end plates such that bus bars (2 inch x 7 inch) could be dropped into position for attachment to welding cables for heat addition. These bus bars were then bolted to phenolic plates (5 inch x 7 inch x 0.5 inch). The phenolic plates were used to insulate the electrodes and to minimize heat loss beyond the electrode region (see Figure 3.2) and also worked as supports for the electrode plates.

Welding cables are attached to the copper plates and the heat source is a Lincolnweld SA-750. This welder is a three-phase motor generator set composed of an induction motor driving type electric welder and is used with variable voltage to produce a DC electric current through the test section. The rating of the machine is 750 amperes at 40 volts continuous duty giving maximum open circuit voltage of 86 volts. To ensure minimal vibrational effects from the welder, it is sitting on a 1.5 inch wooden board placed on several rubber damping pads.

In order to connect the stainless steel tube with the clear polycarbonate calming section tube, Nylon 101 was machined to be a threaded flange and bolted to the

polycarbonate tube's Acrylic flange (see Figure 3.2). The reason for using Nylon 101 is that it is an excellent high voltage insulator and has relatively high strength for ability to hold good thread.

For the heat transfer measurements, the entire length of the test section was surrounded with fiberglass pipe wrap insulation, followed by a thin polymer vapor seal to prevent moisture penetration.

3.1.2 Thermocouples

OMEGA TT-T-30 copper-constantan insulated T-type thermocouple wires were cemented with Omegabond 101 to the outside wall of the stainless steel test section. The length of each thermocouple wire is 12 inches (30.48 cm) plus 1.5 times the outside diameter of the tube. This length is long enough to eliminate thermocouple error due to lead wire heat conduction in the temperature gradient field (Yoo, 1974).

OMEGA EXPP-T-20-TWSH extension wires were used for relay to the data acquisition system. Thermocouples were placed on the outer surface of the tube wall at uniform intervals of 10 inches (25.4 cm) from the entrance to the exit of the test section (see Figure 3.3). There are 10 stations in the test section. All stations have four thermocouples, and they are labeled looking at the tail of the fluid flow with peripheral location number one being at the top of the tube, two being 90 degrees in the clockwise direction, three at the bottom of the tube, and four being 90 degrees from the bottom in clockwise sense.

All the thermocouples were monitored with a Cole-Parmer MAC-14 datalogger which has 96 channel capacity for the temperature measurement. The thermocouple readings were averaged over a user chosen length of time (typically 60 seconds) before

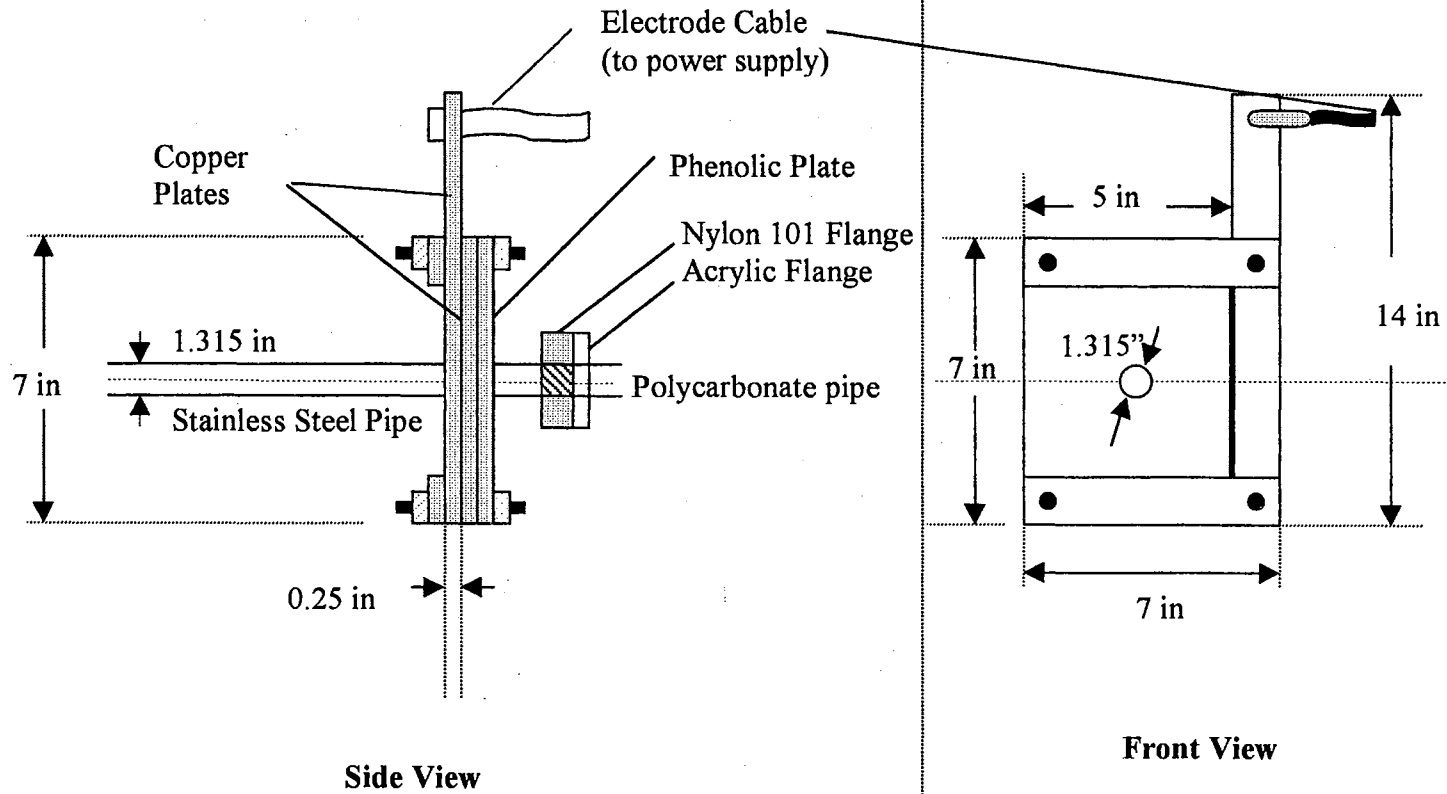


Figure 3.2 Copper Plate and Electrode Cables

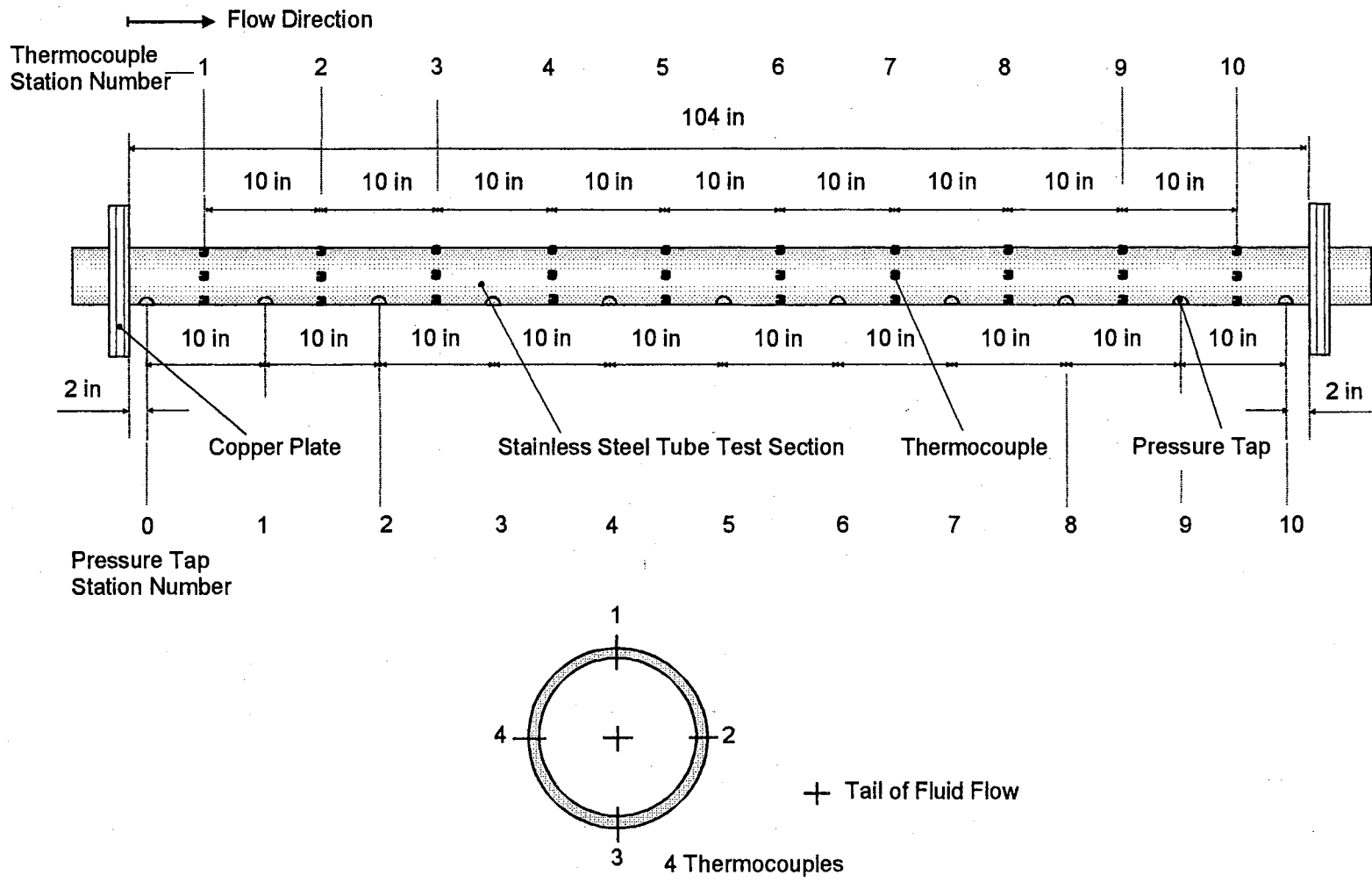


Figure 3.3 Thermocouple and Pressure Tap Locations Along the Test Section

the heat transfer measurements were actually recorded. The average system stabilization time period was from 30 to 60 minutes after the system attained steady-state. The inlet liquid and gas temperatures were measured by OMEGA TT-T-30 T-type thermocouple wires, and the exit bulk temperature was measured by an OMEGA TJ36-CPSS-14U-12 thermocouple probe inserted after the mixing well.

Thermocouple beads were attached to the outside of the stainless steel tube wall using Omegabond 101 epoxy adhesive having high thermal conductivity (0.6 Btu/hr-ft-°F), and very high electrical resistivity of 3.28×10^{15} ohm-ft. An initial drop of epoxy (approximately 0.04 inch in radius), was placed at each thermocouple location and allowed to cure for twenty four hours. Each thermocouple was then placed on the hardened Omegabond surface (preventing direct contact with the stainless steel tube surface and providing electrical insulation), held in place with a strip of electrical tape such that the bead and hardened surface were exposed, and then coated with another drop of Omegabond to ensure permanent positioning.

3.1.3 Pressure Taps and Pressure Transducers

Eleven holes of 0.068 inch (0.173 cm) diameter yielding the ratio of tube wall thickness to tap hole diameter of 1.6 were drilled at the bottom of the stainless circular tube in the test section to accommodate eleven pressure taps (see Figure 3.3). In drilling the pressure taps, it was ensured that the ratio of tube wall thickness to tap hole diameter was greater than 1.5 and less than 15 for the best pressure measurement results (Yoo, 1974). The hole spacing is 10 inches (25.4 cm) and is uniform through out the test section. The pressure taps are standard saddle type self-tapping valves with the tapping core

removed. Vinyl tubing (0.25 inch diameter) was used to connect the pressure taps to a scani-valve (W0601/1P-12T, Scanivalve Corp., Liberty Lake, Washington) which has 24 channel connectors with one reference channel connector for reading pressure difference between two locations. The first pressure tap from the inlet is used as the reference pressure channel.

Using the reference pressure tap (station number 0 in Figure 3.3), the test section system pressure was measured by an OMEGA PX242-060G pressure transducer. It has 0 to 60 psig operation range with minimum of two times full scale operable overpressure, $\pm 1.5\%$ full scale linearity, $\pm 0.25\%$ full scale hysteresis and repeatability, and -18 to 63°C compensated temperature range.

In order to acquire pressure drop measurements, Validyne model DP15 wet-wet differential pressure transducer with CD15 carrier demodulator was used. The DP15 is a general purpose differential pressure transducer that features field replaceable sensing diaphragms so that the full scale may be changes anywhere between 0.08 psid and 3200 psid. During the differential pressure drop measurements in this study, DP15 No. 20 diaphragm was used for the differential pressure ranges up to 5.5 inches of water. This pressure transducer is accurate to $\pm 0.25\%$ of full scale, including linearity, hysteresis and repeatability. It can also be over pressured by 200% of the full scale. The CD15 is a sine wave carrier demodulator designed to operate with variable reluctance transducers to provide a DC output signal for dynamic as well as steady state pressure measurements. The DP15 pressure transducer with the CD15 demodulator was connected to the computer through an A/D computer board model CIO-AD08 manufactured by Computer

Boards Inc. The CIO-AD08 A/D board features maximum 50 kHz sampling rate, 8 single ended input channels, 12-bit A/D resolution and 7 digital input/output bits.

It also should be mentioned here that three dial type pressure gages were installed into the test setup (refer to Figure 3.1) to monitor the operating pressures inside the experimental setup. A 100 psi pressure gage (model PGC-20L-100, OMEGA Engineering, Inc.) was installed after the liquid pumps and a 60 psi pressure gage (model PGC-20L-60, OMEGA Engineering, Inc) was installed after the test section. For the gas inlet line, a 200 psi pressure gage (model PGC-20L-200, OMEGA Engineering, Inc) was installed to monitor the inlet gas pressure.

3.1.4 Gas-Liquid Mixer and Calming Section

The two-phase gas and liquid mixer generated a desired flow pattern such as stratified, wavy, slug, bubbly, or annular flow by controlling each amount of the gas and the liquid in two-phase flow (see Figure 3.4). The mixer consisted of a perforated copper tube (0.24 in O.D.) inserted into the liquid stream by means of a tee and a compression fitting. The end of the copper tube was silver-soldered, and four 1/16 in (1.6 mm) holes, positioned at 90° intervals around the perimeter of the tube, were placed at eight axial locations, equally spaced, as shown in Figure 3.4. The two-phase flow leaving mixer entered the transparent calming section.

The calming section serves as a flow developing and turbulence reduction device. The calming section is a 1 inch (2.54 cm) I.D. and 1/8 inch (3.18 mm) thick clear polycarbonate tube which is 96 inches (2.44 m) in length ($L/D = 88$). The clear polycarbonate tube has high impact strength (Izod impact in the range of 12-16 ft-lbs/in),

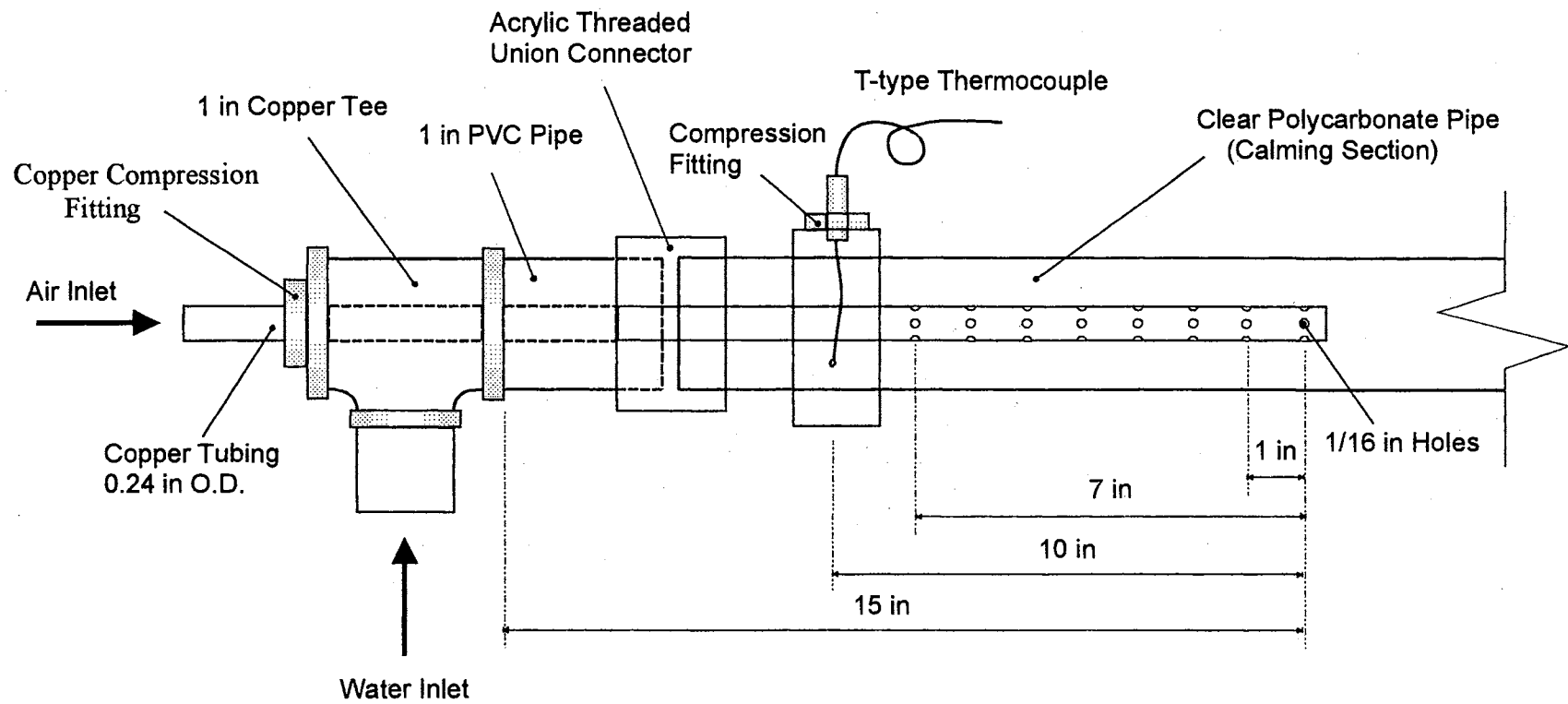


Figure 3.4 Schematic Diagram of the Gas-Liquid Mixer

and features good resistance to low temperatures down to -211°F and a high heat distortion temperature, $280^{\circ}\text{-}290^{\circ}\text{F}$ at 264 psi. Also, the clear section provides a good visual observation of the flow, which aids in recognizing the flow pattern. One end of the calming section was connected to the test section with an acrylic flange, which is clearly shown in Figure 3.5, the other end of the calming section was connected to the gas-liquid mixer (see Figure 3.6).

The acrylic flange was glued to the calming section with Weld-On3 cement procured from Cope Plastics, Inc., Oklahoma City, OK. This flange was 1/4 inch (0.64 cm) thick by 5 inches (12.7 cm) in diameter, with a 1.25 inch (3.175 cm) internal diameter hole carefully drilled so that the calming section was glued into it. After gluing the two, the resulting piece was left undistributed for at least 24 hours so that the glue could harden completely.

Eight quarter inch (0.635 cm) holes were drilled in the Nylon101 flange, so that it could be easily bolted to the acrylic flange, which was screwed to the test section. A small groove of 1/10 depth was cut in the Nylon101 flange, and an O-ring was placed in the groove (refer to Figure 3.5). The two flanges were bolted together very carefully so that the heated test section never touched the Polycarbonate tube. This was done so that the Polycarbonate tube wouldn't melt while applying heat to the test section.

The entire length of the calming section together with the test section described earlier was leveled for reducing the inclination effect on horizontal two-phase heat transfer and pressure drop measurements.

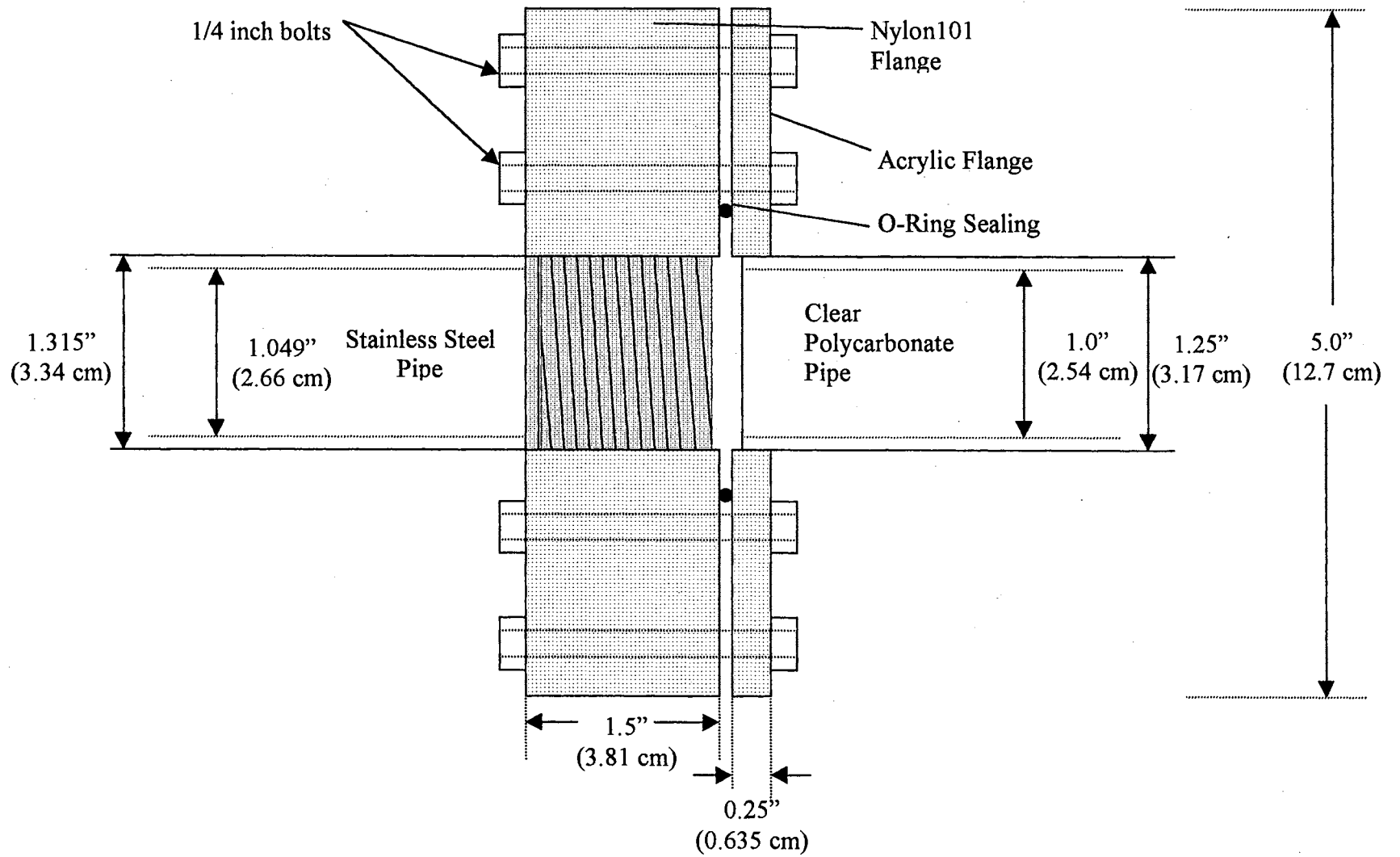


Figure 3.5 Flange Connection between Stainless Steel Pipe and Calming Section

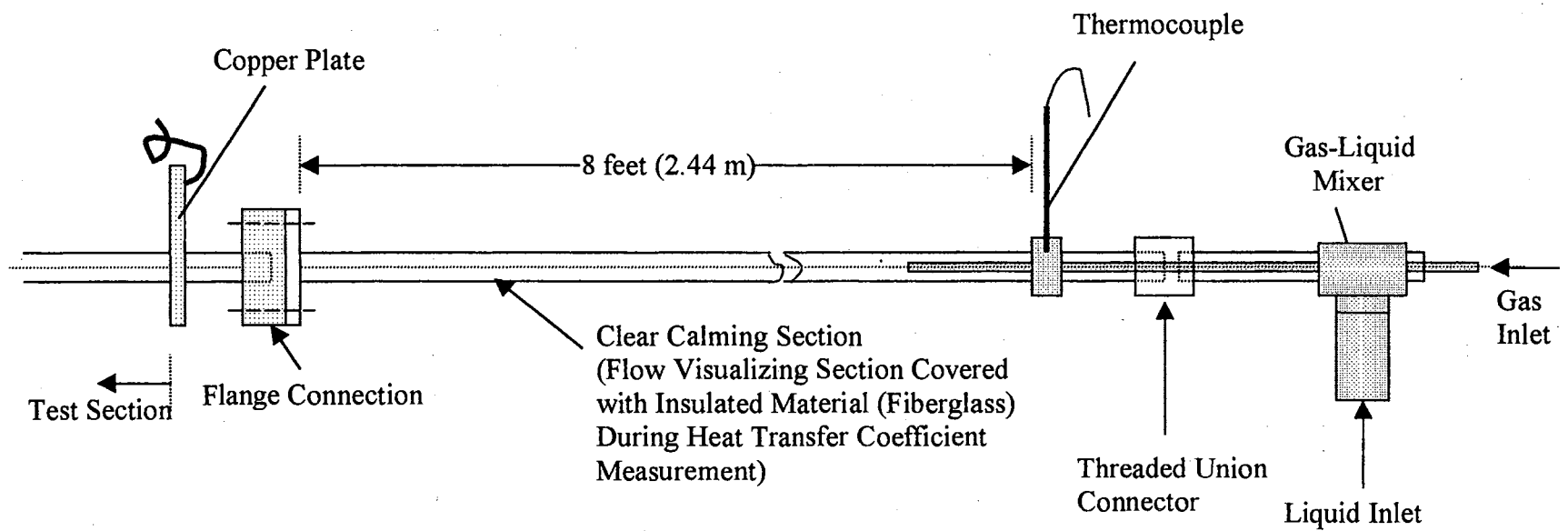


Figure 3.6 Mixer, Calming Section, and Flange Connection to Stainless Steel Test Section

3.1.5 Mixing Well

To ensure a uniform fluid bulk temperature at the exit of the test section, a mixing well was utilized. An alternating polypropylene baffle type OMEGA FMX7109-P static mixer for both gas and liquid phases was used. The static mixer has a diameter of 0.9 inch (2.30 cm) with 5.3 inch (13.46 cm) length and it is made of polypropylene which has excellent chemical resistance and a maximum service temperature upto 200°F. This mixer provides an overlapping baffled passage forcing the fluid to encounter flow reversal and swirling regions. The mixer well was placed below the clear Polycarbonate observation section (after the test section), and before the gas-liquid separator liquid storage tank (refer to Figure 3.1). Since the cross sectional flow passage of the mixing is substantially smaller than the test section, it has the potential of increasing the system back-pressure. Thus, in order to reduce the potential back-pressure problem which might affect the flow pattern inside of the test section, the mixing well was placed below and after the test and the clear observation sections. The outlet bulk temperature was measured immediately after the mixing well.

3.1.6 Voltmeter and DC Ammeter

A HP 3468B digital multimeter was used to measure the actual voltage drop across the test section. The range for voltage measurement is 1 microvolt to 300 volts with an accuracy of 1% of the reading, and a resolution of 10 microvolts.

The current passing through the test section wall was measured with a Cole-Parmer Clamp Power Meter/Datalogger placed on one of the welding cables. Then, the power meter was connected to the CIO-AD08 A/D board using an RS-232 interface. The accuracy is about $\pm 2\%$ of the reading.

3.1.7 Heat Exchanger

An ITT Standard model BCF 4036 one shell and two tube pass heat exchanger was used to cool the test fluid to an allowable and steady-state bulk temperature. The cooling water was provided from a city water tap through an OMEGA FL-9028 rotameter. The heat exchanger was 39.6 inches (1 m) in length.

3.1.8 Pumps

For low flow rates, a pump (refer to Pump1 in Figure 3.1) manufactured by Oberdorfer Pumps, model SKH35FN193T was used. It produces a flow rate of 11 GPM at 3450 rpm using a General Electric 1/3 HP motor. For high flow rates, Armstrong series 4270 with 4.33 inch impeller centrifugal pump (refer to Pump2 in Figure 3.1) procured from Federal Corporation, Oklahoma City, OK was used. The motor was rated 1 HP producing about 30 GPM at 3500 rpm for 68 ft head. It should be noted here that during the air-water two-phase experiments, the limit of the water amount was much reduced since the water was mixed together with gas at the mixer and delivered into the test section. Due to the high pressure of the mixed air, the capability of delivering water by those pumps were quite reduced.

One inch and 1.5 inch diameter of schedule 40 PVC pipes were used for the inlets of those pumps from the reservoir tank to eliminate cavitation and the frictional loss, and flexible hoses were connect to the pump upstream to prevent vibrations to be transmitted to the calming and test sections.

A schematic view of how these pumps were connected to the test loop is shown in Figure 3.7. Since those pumps were operated at a constant rpm, a separate by-pass line

was placed just after the pumps and before the filter. To regulate the flow rate, the valve at the by-pass line opened or closed, and the pumps were always operated with a constant speed.

In order to remove dirt and dust particles from the liquid in the test flowline, an Aqua-Pure Filter Housing (model AP12) double cartridge filter system was used with two filter cartridges (model AP110 H/C), which can remove 5 micron diameter dust particles. Those filter cartridge and filters were procured from CUNO Inc., Meriden, CT.

3.1.9 Liquid Turbine Meters and Frequency Meter

For small flow rates up to about 3 GPM, a Cole-Parmer P-33110-00 Polypropylene impeller flow meter (0.05 to 5 GPM) was used over a frequency range of 3 to 65 Hz, giving flow rates from 0.25 to 3.3 GPM. Following the manufacture's installation guide, this flow meter was installed within a straight run of pipe having more than five pipe diameter long on the inlet side of the flow meter placed before the gas-liquid mixer (refer to Turbine Meter 2 in Figure 3.1). It has $\pm 1\%$ full scale accuracy and linearity, and $\pm 0.5\%$ full scale repeatability. The maximum allowable pressure limit is 150 psi, and recommended operating temperature is about up to 160 °F (71°C).

For large flow rates, a 0.5 inch Halliburton turbine flow meter with 1 inch threaded NPT (refer to Turbine Meter 1 in Figure 3.1) was used over a frequency range of 700 to 2000 Hz for flow rates approximately from 3.2 to 9 GPM. This turbine meter has an accuracy of $\pm 1\%$ of reading and repeatability of $\pm 0.05\%$ of reading. Operating temperature range is from -67 to 250°F (-55 to 121°C), and maximum allowable pressure is about 200 psi.

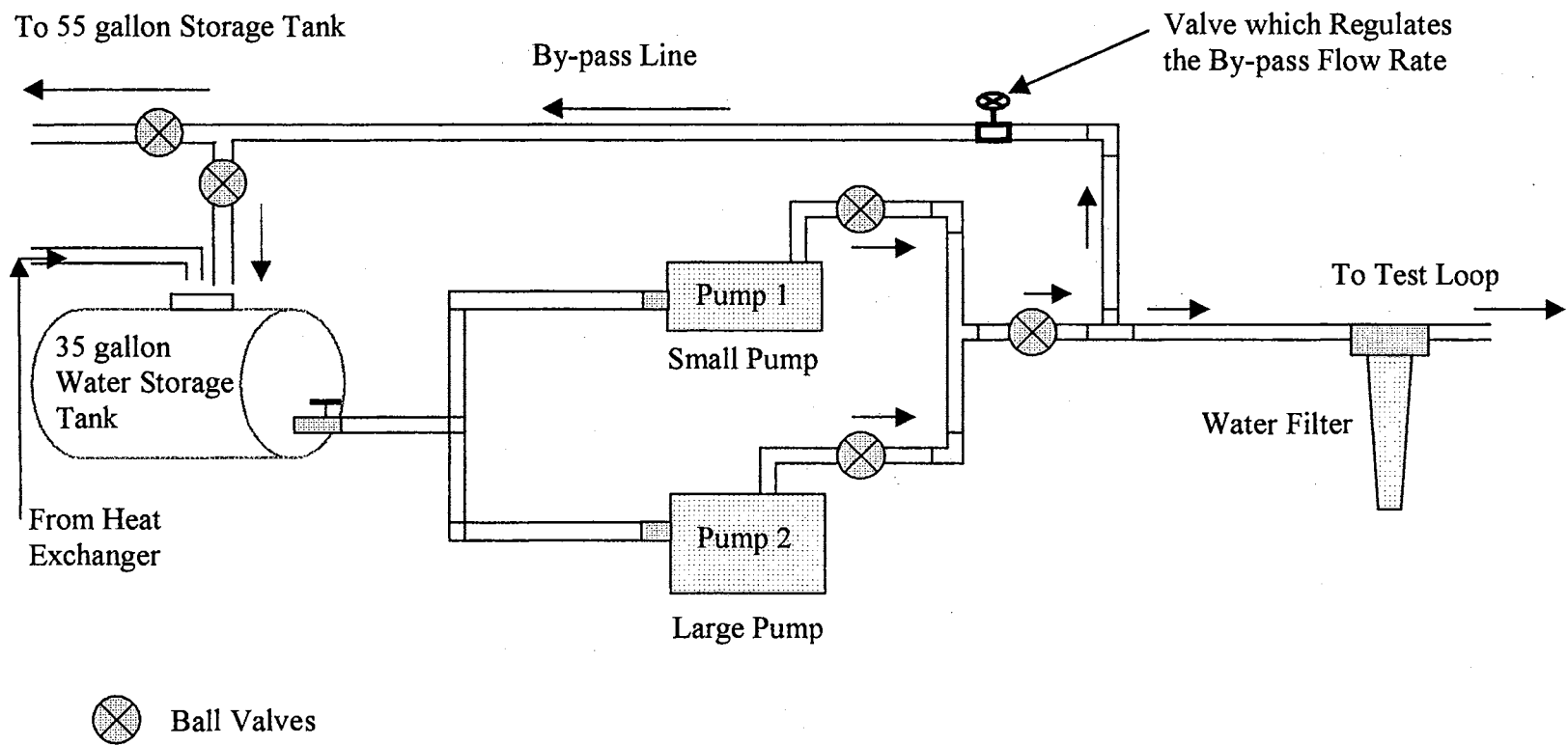


Figure 3.7 Pumps and By-pass Line

The outputs of the turbine meters were connected to an OMEGA DPF701 6-digit rate meter (Totalizer) with an OMEGA DPF700-A analog output board. The pulse (frequency) generated from the turbine meter was measured by this rate meter and converted to analog input into the analog output board. Then, this analog output was sent to the A/D board installed inside of a PC. The rate meter could accommodate a range of input frequencies from 0.5 Hz to 30 kHz.

3.1.10 Gas Flowmeter and Absolute Pressure Transducer

In order to measure the volumetric flow rate of the gas supplied to the system flow line, a Cole-Parmer P-32915-15 0.25 inch NPT flowmeter was used. The amount of gas (liters/min) supplied to the system could be monitored through a 3-digit LCD display. It has $\pm 2\%$ of full scale accuracy, $\pm 1\%$ of full scale repeatability, and 10 msec response time. The recommended operating temperature is 0 to 50°C and the maximum allowable pressure limit is 100 psi. Using the Mini-Din connector, the flow meter provided a 5.0 Vdc output span. This voltage was in the range of 0.010 Vdc for zero flow and 5.0 Vdc for full scale flow. The output voltage was linear over the entire range and connected to the CIO-AD08 A/D board.

In order to calculate gas density and the mass flow rate of the supplied gas, the knowledge of the gas absolute pressure was required. For this, an OMEGA PX137 pressure transducer was used. It has silicone pressure sensor in conjunction with stress free packing technique to provide more accurate and temperature compensated pressure readings. This pressure transducer featured 0 to 100 psia pressure range, $\pm 0.1\%$ of full scale linearity, hysteresis, and repeatability, 0 to 70°C operating temperature, three times

of full scale proof pressure reading, and five times of full scale burst pressure. The voltage output from 0 to 4.5 Vdc was connected to the CIO-AD08 A/D board.

3.1.11 Water Reservoirs

Two cylindrical polyethylene tanks (55 and 35 gallons) were used to separate air and water after the test section, and supply water into the inlet of the calming section. The 55 gallon (208.2 liters) tank was placed after the mixing well to separate air and water from the system line, and this stored water was transported to the other water tank using a 1/3 HP rating centrifugal pump producing 11 GPM at 3450 rpm (refer to Pump 3 in Figure 3.1). The 35 gallon tank was used to store and supply water into the test section.

In order to automatically adjust the amount of the water inside of the 35 gallon storage tank, an OMEGA LV621-P pump up/down level control switch with LV600-CW counterweight was installed inside of the storage tank. Depending on whether LV621-P float is a specified up or down position adjusted by the cable length of the switch, the 15 amp relay inside of the float changes the state of the pump (Pump 3), on or off the pump.

3.1.12 Data Acquisition System

For the heat transfer measurements in the test section, a Cole-Parmer MAC-14 ninety-six channel input data logger was interfaced with a personal computer to provide digital data acquisition for the temperature measurements. The data acquisition system accepts input voltages from 0.3 micro-volts to 10 volts, has an accuracy of $\pm 0.02\%$ of volts, and has 16 bit resolution. Connection to the computer is through shielded cable to an RS232 port, and to the printer via the printer port. Menu driven software (MS) procured from Cole Parmer was used in conjunction with signal conditioning (SC), real time graphics (RTG), and printer driver (PD) software to handle data input and output.

An IBM compatible personal computer with 80386 CPU, a 80 MB hard drive, dual floppy disk drives, a VGA monitor, a 8087 coprocessor was connected with the Cole-Parmer MAC-14 data logger. This computer was only used for data logging and data storage of the temperatures. Another IBM compatible personal computer featured AMD Pentium 233 MHz processor and 4.3 GB hard drive with to the CIO-AD08 A/D computer board was used for the measurements of gas and liquid flow rates, gas absolute pressure, system pressure, the pressure drops from the test section, and the current passing through the test section wall.

3.2 Experimental Calibration

Upon completing the experimental setup construction and acquiring the monitoring equipment, calibration of all equipment was required. In the experimental setup used, six key instruments were calibrated. They are (1) thermocouples (2) liquid turbine meter, (3) gas flow meter, (4) system pressure transducer, (5) liquid differential pressure transducer, and (6) gas pressure transducer. The calibration processes of the equipment will be presented here.

3.2.1 Thermocouples

For the MAC-14 data acquisition system, no calibration was required. However the thermocouples connected to the system were calibrated by means of a constant temperature bath. The constant temperature bath system used was a FTS system (Model RC-00180-A FTS Systems Inc., New York), which uses HT-30 fluid to maintain a constant temperature. For this experiment, we made 56 thermocouples, out of which 44

were used during the actual experimental test. The 56 thermocouples were tested on the FTS system initially to check that they worked properly.

A Model 5100 data logger (manufactured by Electronics Controls Design, Inc., Milwaukie, Oregon) was used to take temperature readings from the 56 thermocouples. The thermocouples were tested for a temperature range from 10 °C to 65 °C at 5 °C intervals. Two sets of thermocouples were used while testing, since the maximum input for the 5100 data logger was only 40. The first set contained 32 thermocouples, and the second set contained 24 thermocouples. After collecting the data for the two sets of thermocouples for the temperature range from 10 °C to 65 °C, the data sets were then used to determine the maximum, minimum, and average temperatures for each thermocouple.

A sample calibration curve for thermocouple 1 is shown in Figure 3.8. The calibration curves for all of the other thermocouples used for this test setup were almost identical to Figure 3.8. It was observed that almost all of the thermocouples behaved well (within ± 0.4 °C temperature reading differences), before they were actually placed on the test section. Defective thermocouples were removed during the test runs. Two thermocouples were found to be operating defectively after they were placed on the test section. They were then replaced by well-behaved thermocouples.

The calibration was performed with respect to the constant bath temperature. Although there are slight deviations in the constant bath temperatures (± 0.1 °C), the bath temperature was assumed to be accurate. The calibration was done at several values of temperatures (10 °C to 65 °C) as explained above (see Figure 3.8). These calibration curves were straight lines, which clearly showed that the thermocouples behaved well at

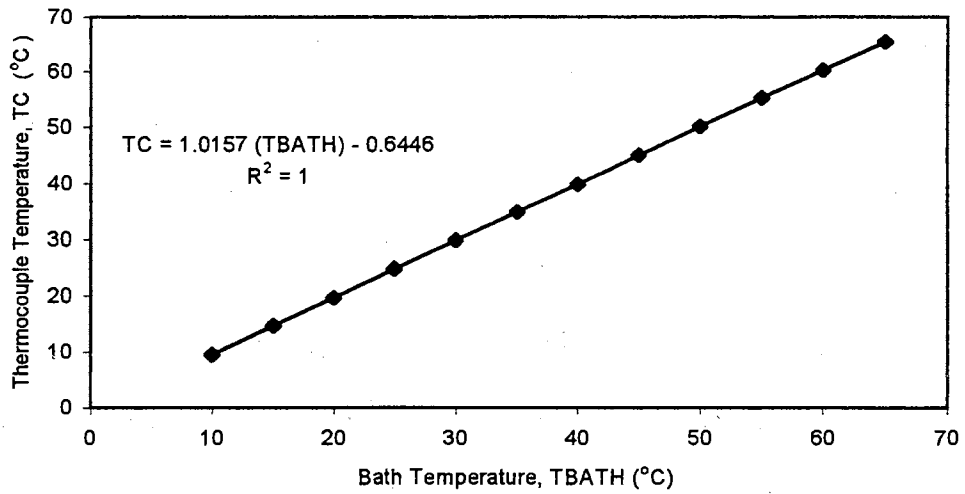


Figure 3.8 Calibration Curve for Thermocouple 1

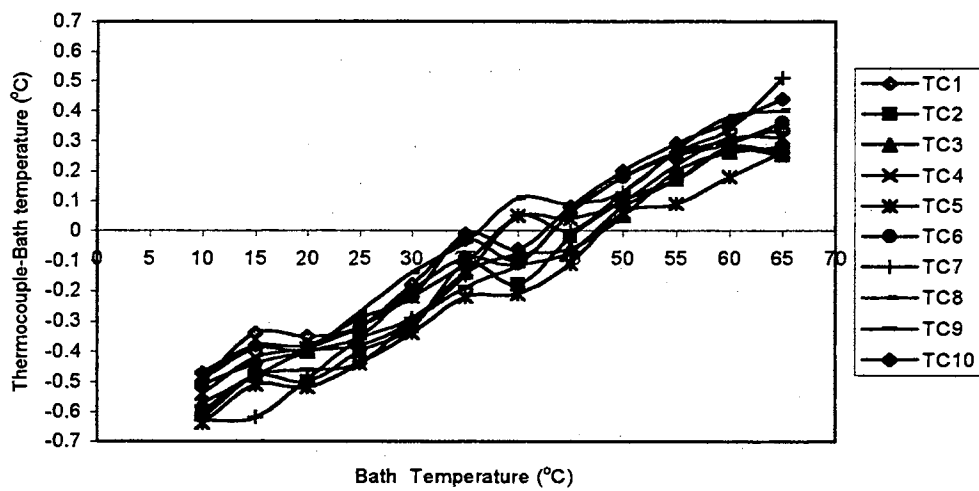


Figure 3.9 Trend of Temperature Differences Between Thermocouple and Bath vs. Bath Temperatures

all of the temperatures ranging from 10 °C to 65 °C.

Similarly the thermocouple and the thermocouple probe measuring the bulk inlet and outlet temperatures were also calibrated in the same way, with the help of the temperature bath. The calibration curves for both of the thermocouples and the probe were almost identical to Figure 3.8.

To investigate the behavior of the difference between the thermocouple readings and the bath temperature as the temperature of the bath changed, Figure 3.9 was plotted. From this graph, it is evident that, although there was a bias in the temperature readings as the bath temperature increased, the thermocouples were working well enough to carry out the experiment. Similar plots like Figure 3.9 for all of the other 46 thermocouples were also obtained.

Figure 3.10 shows isothermal temperature measurements using those tested thermocouples attached to the test section. Water (4.4 gallons/min) was used as the test fluid. A total of 40 thermocouple readings (4 thermocouples at 10 stations, refer to Figure 3.3) obtained over approximately a time period of 20 minutes with a time interval of one minute. Figure 3.10 (a) shows that the temperature difference among those 40 thermocouples were within ± 1 °C at the beginning and at the end of the measurement. This figure also shows temperature rises of the thermocouples with time due to the friction between inside wall of the test section and the fluid. Figure 3.10 (b) shows the measurements of the fluid's bulk inlet, bulk outlet and storage tank temperatures. The bulk temperatures were quite dependent on the variation of the water temperature in the storage tank. As can be seen from Figures 3.10 (a) and (b), all those thermocouples installed on the outside of the test section, the thermocouples for bulk fluid inlet and water

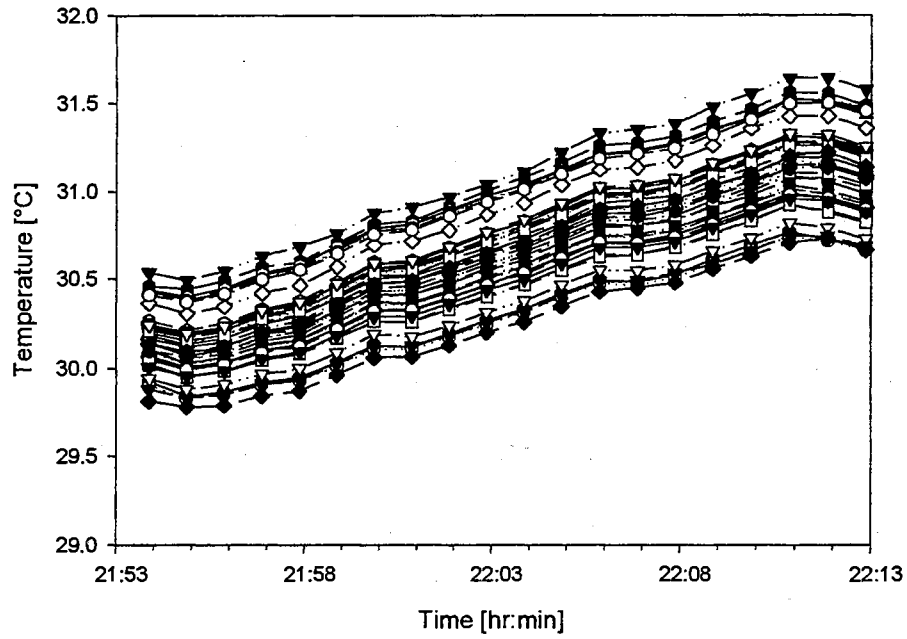


Figure 3.10 (a) Temperature Readings from 40 Thermocouples along the Test Section Based on the Time Variation

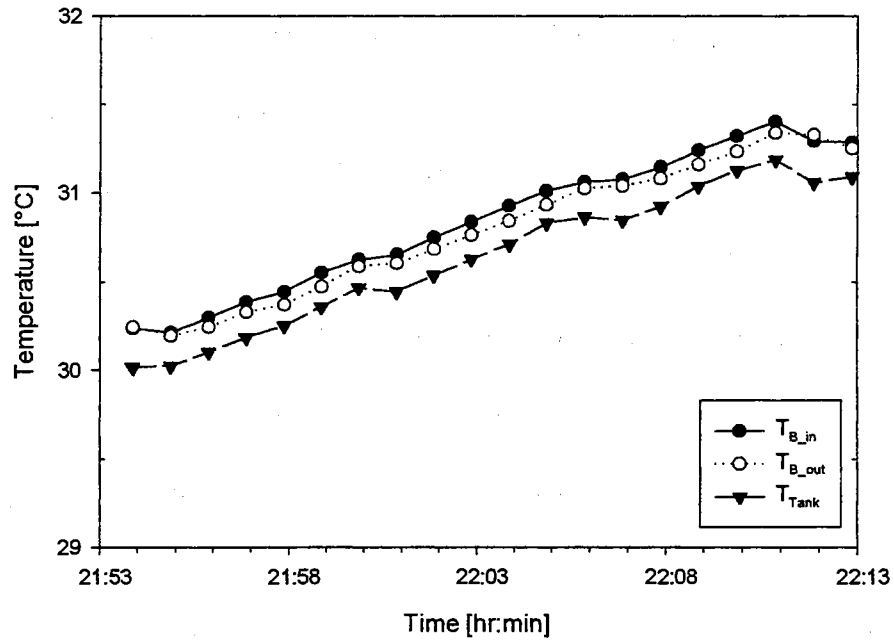


Figure 3.10 (b) Temperatures of Bulk Inlet (T_{B_in}) and Outlet (T_{B_out}) of the Fluid and Water Temperature of the Storage Tank (T_{Tank})

in the storage tank, and the thermocouple probe for the bulk fluid outlet measured temperatures accurately and reasonably well compared with each other.

After the isothermal runs, test runs were done with uniform heat flux applied to the test section (479 amps with a 3.8 volts of voltage drop across the test section). Water (3 gallons/min) was used as the test fluid. At least 50 such runs were done to see how the thermocouples responded with heat applied to the test section. Figure 3.11 shows how the thermocouples behaved with uniform heat flux on the test section. Figure 3.11 (a) shows 40 thermocouple readings from the 10 stations of the test section after reaching steady-state condition. All of the temperature readings were consistent over the run period of 15 minutes. Figure 3.11 (b) shows the time averaged wall temperatures from the 10 stations and the bulk fluid inlet and outlet temperatures. This figure indicates that after station number 4, a thermally fully developed condition was obtained along the test section based on the observation of constant temperature difference between the wall temperature at each station and the fluid bulk temperature.

Each thermocouple measurement on the test section was carefully studied during these test runs, and it was found that the thermocouples needed no further calibration or replacements. Although the thermocouples worked well over 100 °C, it was made sure that the temperatures were not raised above 100 °C, since the water would start boiling.

3.2.2 Calibration of Liquid Turbine Meter

The liquid flow rate through the two turbine meters was calibrated against the frequency of impeller rotation. The calibration required an OMEGA DPF700 rate meter

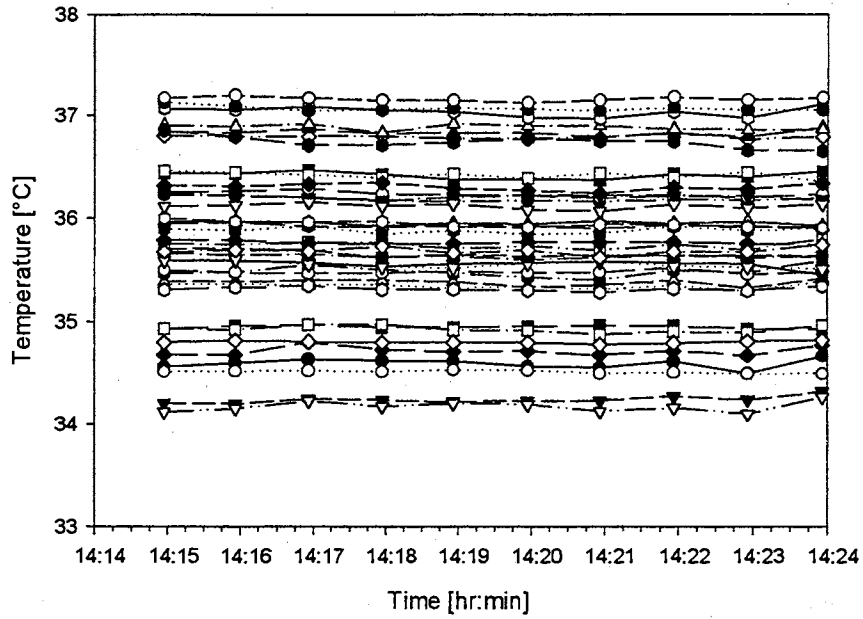


Figure 3.11 (a) Temperature Readings from 40 Thermocouples along the Test Section Based on the Time Variation

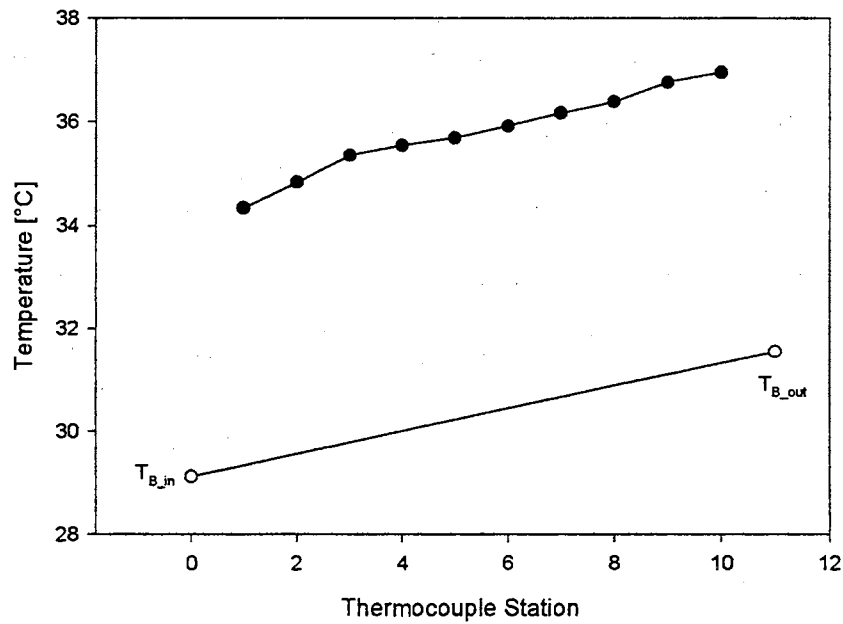


Figure 3.11 (b) Averaged Wall Temperatures of the Thermocouple Stations and Bulk Inlet ($T_{B,in}$) and Outlet ($T_{B,out}$) Temperatures of the Fluid

(Totalizer) for the turbine meter frequency input, the CIO-AD08 A/D board for the frequency and time recordings by a simple computer code, and a five gallon tank for a graduated liquid container. The pump was switched on and the fluid passed through the turbine meter. The frequency of the impeller rotation from the turbine meter was recorded using the Totalizer and A/D board while the fluid was retrieved by the five gallon container. When five gallons of fluid was collected, the simple computer code measured the period of time elapsed and averaged the recorded frequency. In order to measure one data point of the frequency at a specific time, one thousand frequency measurements were averaged using the CIO-AD08 A/D board that has a 50kHz maximum sampling rate. The volumetric flow rate was then calculated for the specific frequency. The procedure was repeated at representative values over the available frequency range.

The data of volumetric flow rate versus averaged frequency was curve-fitted to a linear equation. Figure 3.12 shows the collected data and the correlated linear fits for Halliburton 1/2 inch turbine meter and Cole-Parmer P-33110-00 turbine meter. During the data taking process, Halliburton turbine meter was used for the ranges of liquid flow rate from 3 to 8 GPM and Cole-Parmer turbine meter was used for the ranges of liquid flow rate below 3 GPM in order to measure liquid flow rate reliably.

3.2.3 Calibration of Gas Flow Meter

The voltage generated from the gas flow meter, Cole Parmer Model 32915, was calibrated against the gas volumetric flow rate [liters/min] displayed on the LCD display in the gas flow meter. The gas flow meter provided a 5.0 Vdc output span. This voltage was usually in the range of 0.010 Vdc for zero flow and 5.0 Vdc for full scale flow. The output voltage was linear over the entire range and was available through Mini Din connector,

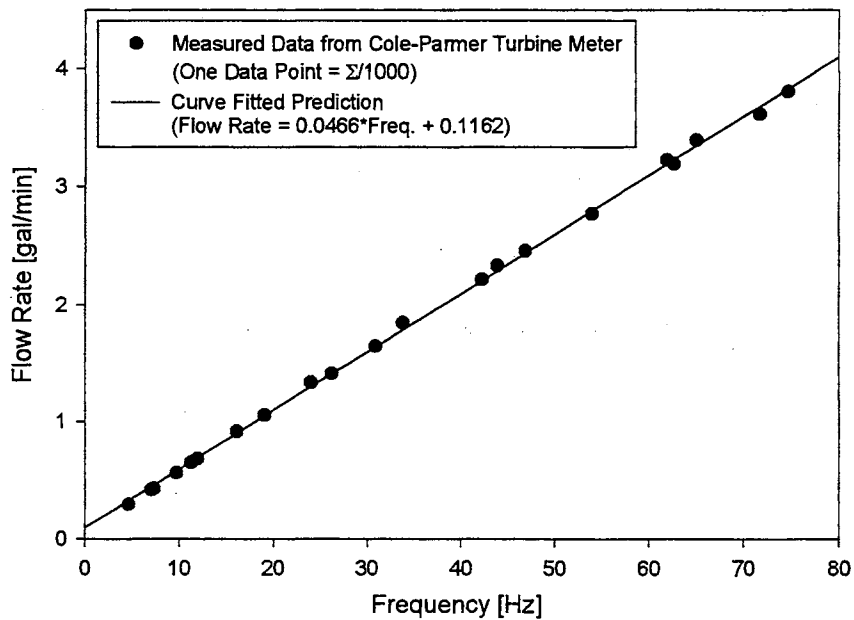
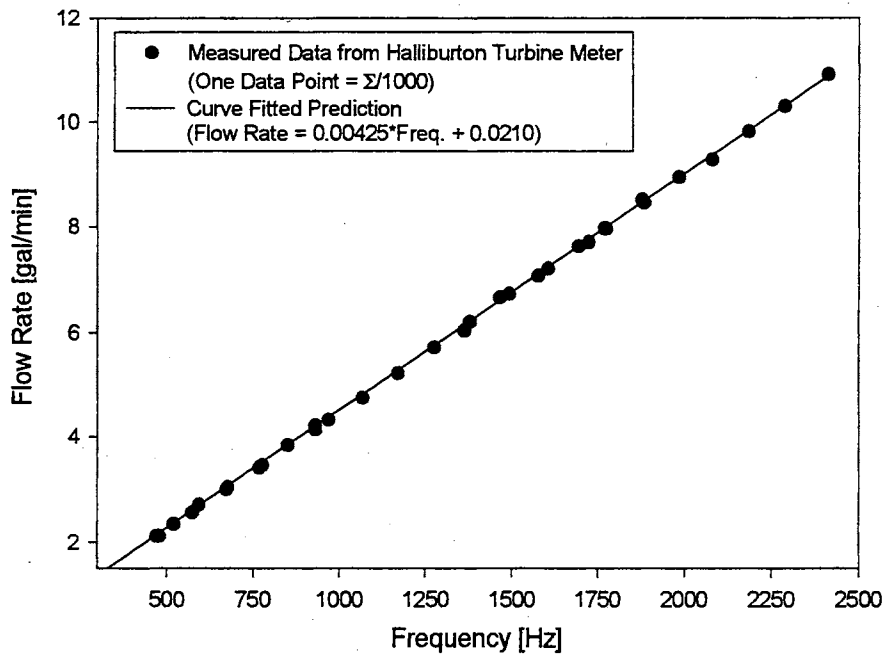


Figure 3.12 Calibrations of Liquid Turbine Meters

which was connected to the CIO-AD08 A/D computer board using a RS-232 cable. In order to measure one data point of the voltage, one thousand voltage measurements were averaged using the maximum 50kHz A/D board. Then, the gas volumetric flow rate was decided for the specific voltage. The procedure was repeated at representative values over the available gas flow range. The data of gas volumetric flow rate versus averaged voltage was curve-fitted to a linear equation. Figure 3.13 shows the collected data and the correlated linear fit. The curve-fitted equation was used to calculate the gas volumetric flow rate [liters/min] in the data taking process.

3.2.4 Calibration of System Pressure Transducer

In order to measure the test section gage pressure, an OMEGA Model PX242-060G pressure transducer was calibrated using the air supplied from the building as a pressurized device against the U-tube mercury manometer. The pressure transducer needed 10Vdc excitation and provided 1.25 to 7.5 Vdc output. Also, the pressure transducer has $\pm 1.5\%$ full scale linearity, $\pm 0.25\%$ of full scale hysteresis and repeatability, and operable over pressure of minimum two times full scale. The pressure readings from the manometer were recorded versus the voltage readings from the pressure transducer as shown in Figure 3.14. In order to measure one data point of the voltage, one thousand voltage measurements were averaged using the CIO-AD08 A/D board. A linear equation was fitted to the pressure [psig] and the voltage reading.

3.2.5 Calibration of Differential Pressure Transducer

To calibrate the wet-wet DP15 differential pressure transducer, an inverted U-tube manometer was used for the differential pressure reading, and the test section was used for a pressure source. The DP15 pressure transducer was connected to both the test section

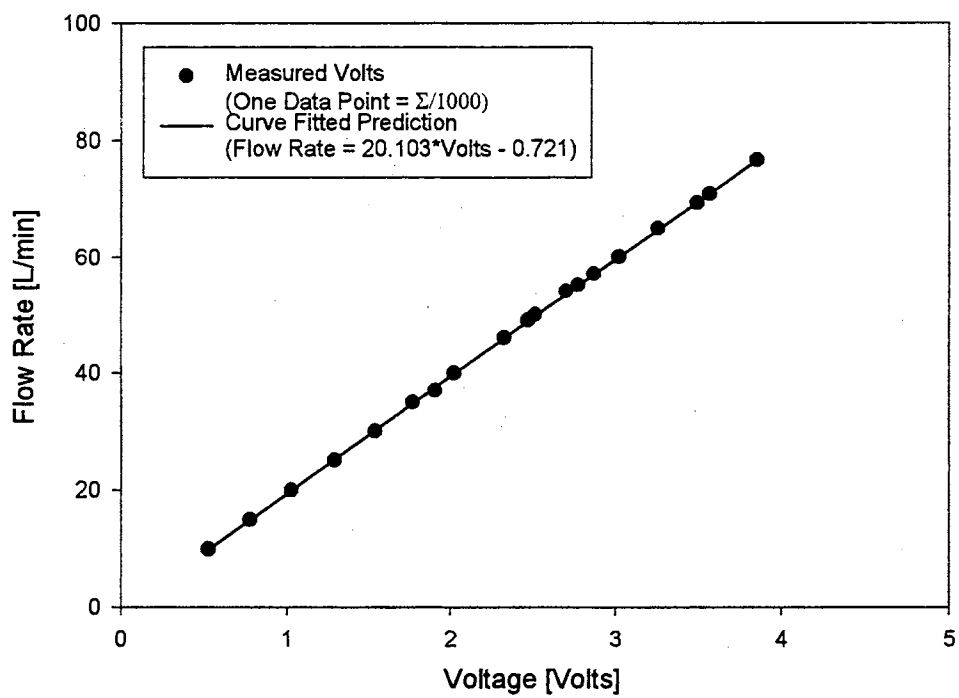


Figure 3.13 Calibration of Gas Flow Meter

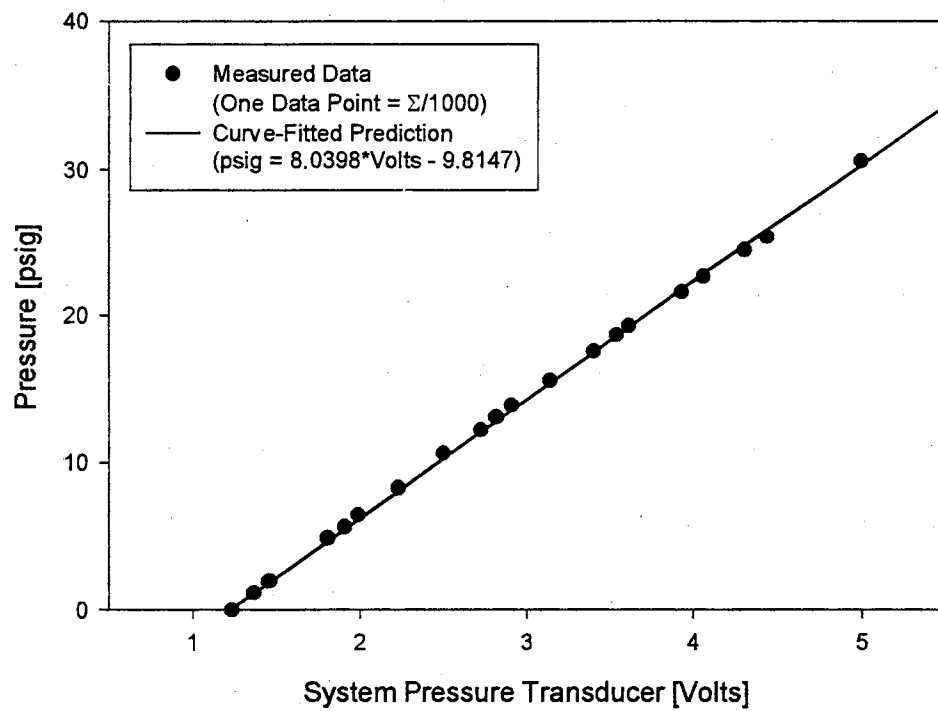


Figure 3.14 Calibration of System Pressure Transducer

and the inverted U-tube manometer. In order to measure the voltage drop from the differential pressure transducer, Validyne CD15 sine wave carrier demodulator was connected to both the pressure transducer and the CIO-AD08 A/D board. For the 0 differential pressure, the carrier demodulator was set to 1 Vdc output. Figure 3.15 shows the data collected from the calibration and the correlated linear fit.

3.2.6 Calibration of Gas Pressure Transducer

In order to measure the gas inlet absolute pressure, voltage generated from an OMEGA PX137-100AV absolute pressure transducer was calibrated against a mercury U-tube manometer. Air supplied from the building was used as a pressurized device and U-tube mercury manometer was used for the pressurized reading. Since the pressure transducer was for an absolute pressure, atmosphere pressure reading from a barometer was needed in addition to the pressure reading from the mercury U-tube manometer. A 5 volt DC power source was connected as an excitation voltage, and the CIO-AD 08 A/D board was used for the output voltage measurement for the pressure transducer. The measured voltage from the transducer showed a linear relationship with the gas inlet absolute pressure, and Figure 3.16 shows the data collected and the linear fit correlated.

3.3 Data Reduction Programs

The experimental procedure for a uniform wall heat flux boundary condition consists of measuring the tube outside wall surface temperatures at discrete locations and the inlet and outlet bulk temperatures in addition to other measurements such as gas and liquid flow rates, room temperature, voltage drop across the test section, and current

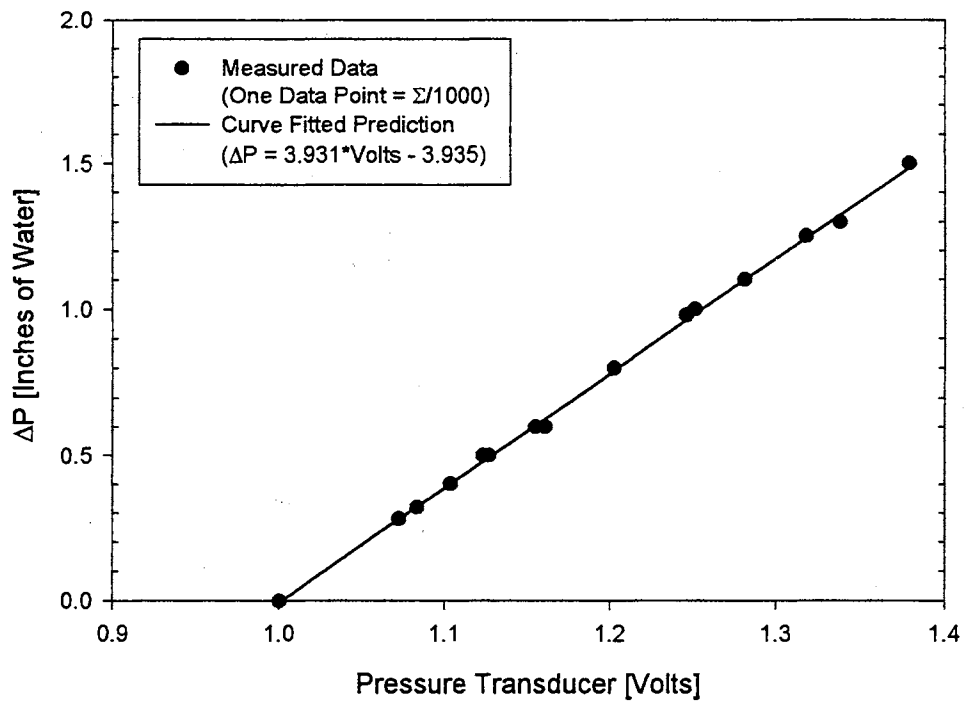


Figure 3.15 Calibration of Differential Pressure Transducer

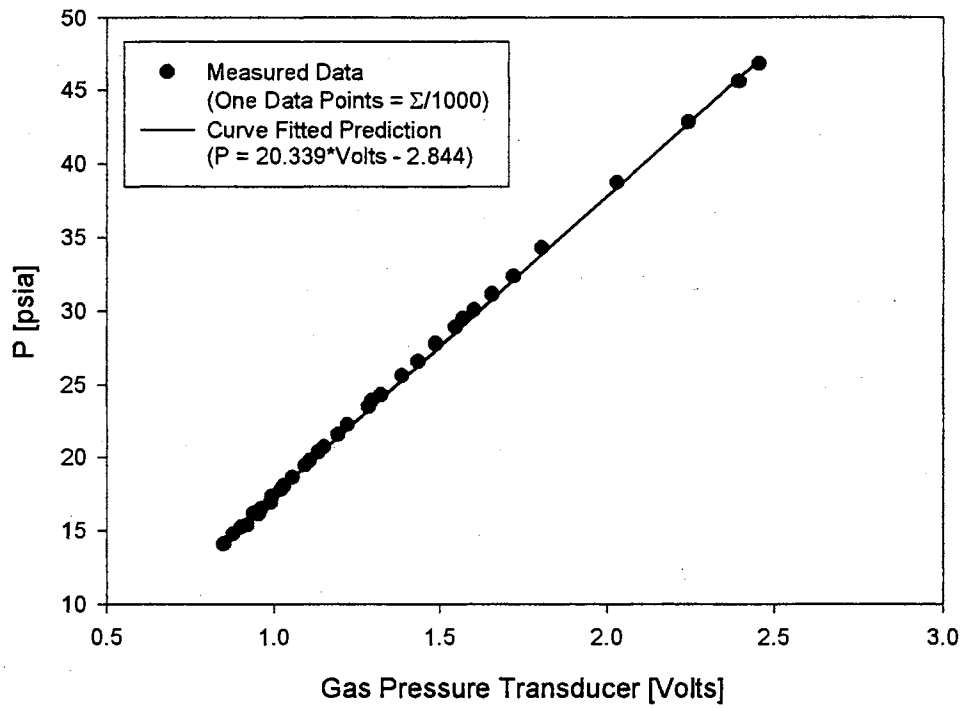


Figure 3.16 Calibration of Gas Absolute Pressure Transducer

carried by the test section. The peripheral heat transfer coefficient (local average) and the Nusselt number thereafter were calculated based on the knowledge of the pipe inside wall surface temperature. Because measurement of the inside wall temperature was difficult, it was calculated from the measurements of the outside wall temperature, the heat generation within the pipe wall, and the thermophysical properties of the pipe material (electrical resistivity and thermal conductivity).

Ghajar and Zurigat (1991) developed an interactive computer program to calculate the local inside wall temperatures and local peripheral heat transfer coefficients from local outside wall temperatures measured at different axial locations along an electrically heated horizontal circular tube. The test fluids used were water and mixtures of ethylene glycol and water. The main ideas of Ghajar and Zurigat's (1991) program was adapted to this study and will be introduced as follows.

The computer program called RHt99F (see Appendix B for computer code listing) consisted of four segments, the input data, the finite-difference formulations, the physical properties and the output.

3.3.1 Input Data

The inputs of this program included the type of test fluid used, the voltage drop across the tube, the current carried by the tube, the volumetric flow rates, the bulk fluid temperatures at the inlet and exit, and the outside wall temperature data for all locations. This input data file was obtained in a specified format by another interactive computer program called Dated99F which directly read all those necessary information from the experimental measurement devices including the outside wall temperature data using the A/D board and the data logger.

3.3.2 Finite-Difference Formulations

The numerical solution of the conduction equation with internal heat generation and variable thermal conductivity and electrical resistivity was based on the following assumptions:

- Steady state condition exist.
- Peripheral and radial wall conduction exist.
- Axial conduction is negligible.
- The electrical resistivity and thermal conductivity of the tube wall are functions of temperature.

Based on the above assumptions, the expressions for calculation of the local inside wall temperatures, heat flux, and local and average peripheral heat transfer coefficients are presented next.

a. Calculation of the local inside wall temperature and the local inside wall heat flux

The heat balance on a segment of the tube wall at any particular station is given by (see Figure 3.17):

$$Q_g = Q_1 + Q_2 + Q_3 + Q_4 \quad (3.1)$$

From Fourier's law of heat conduction in a given direction n we know that

$$Q = -kA \frac{dT}{dn} \quad (3.2)$$

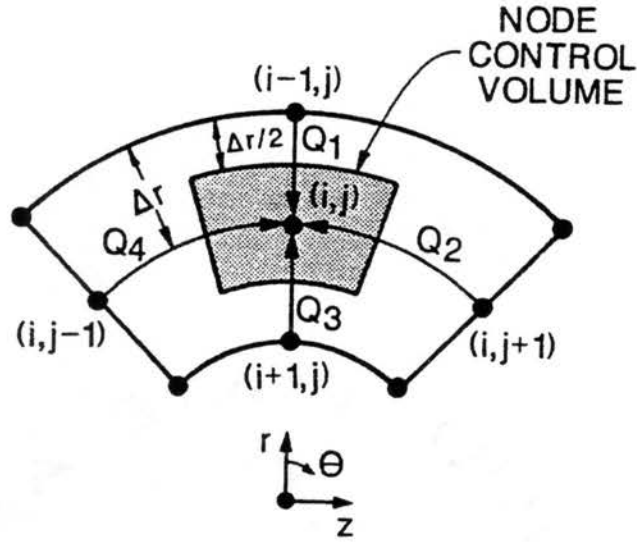


Figure 3.17 Finite-Difference Grid Arrangement (Ghajar and Zurigat, 1991)

Now substituting Fourier's law and applying the finite-difference formulation for the radial (i) and peripheral (j) directions in Equation (3.1) we obtain:

$$Q_1 = \frac{(k_{i,j} + k_{i-1,j})}{2} \frac{2\pi \left(r_i + \frac{\Delta r}{2} \right) \Delta z}{N_{TH}} \frac{(T_{i,j} - T_{i-1,j})}{\Delta r} \quad (3.3)$$

$$Q_2 = \frac{(k_{i,j} + k_{i,j+1})}{2} (\Delta r \Delta z) \frac{(T_{i,j} - T_{i,j+1})}{\left(\frac{2\pi r_i}{N_{TH}} \right)} \quad (3.4)$$

$$Q_3 = \frac{(k_{i,j} + k_{i+1,j})}{2} \frac{2\pi \left(r_i - \frac{\Delta r}{2} \right) \Delta z}{N_{TH}} \frac{(T_{i,j} - T_{i+1,j})}{\Delta r} \quad (3.5)$$

$$Q_4 = \frac{(k_{i,j} + k_{i,j-1})}{2} (\Delta r \Delta z) \frac{(T_{i,j} - T_{i,j-1})}{\left(\frac{2\pi r_i}{N_{TH}} \right)} \quad (3.6)$$

where

- k = thermal conductivity
- r_i = tube inside radius
- Q = rate of heat transfer
- T = temperature
- Δz = length of element
- Δr = incremental radius
- N_{TH} = number of finite-difference sections in the θ -direction (peripheral)
which is equal to the number of thermocouples at each station.
- i and j = the indices of the finite-difference grid points, i is the radial direction starting from the outside surface of the tube and j is the peripheral direction starting from top of the tube and increasing clockwise.

Heat generated at i,j element volume is given by:

$$Q_g = I^2 R \quad (3.7)$$

where

- I = Current
- R = $\gamma l / A$ = resistance
- γ = electrical resistivity of the element
- l = Δz = length of the element
- A = $(2\pi r_i / N_{TH})\Delta r$ = cross-sectional area of the element

Substituting the above definitions into Equation (3.7) gives:

$$Q_s = I^2 \frac{\gamma \Delta z}{\left(\frac{2\pi r_i}{N_{TH}} \right) \Delta r} \quad (3.8)$$

Substitution of Equations (3.3) to (3.6) and (3.8) into Equation (3.1) and solving for $T_{i+1,j}$ gives:

$$T_{i+1,j} = T_{i,j} - \left\{ \frac{I^2 \gamma N_{TH}}{(2\pi r_i \Delta r)} - \frac{(k_{i,j} + k_{i-1,j}) \pi \left(r_i + \frac{\Delta r}{2} \right)}{\Delta r N_{TH}} (T_{i,j} - T_{i-1,j}) \right. \\ \left. - (k_{i,j} + k_{i,j+1}) \frac{\Delta r N_{TH}}{4\pi r_i} (T_{i,j} - T_{i,j+1}) - (k_{i,j} + k_{i,j+1}) \frac{\Delta r N_{TH}}{4\pi r_i} (T_{i,j} - T_{i,j+1}) \right\} \quad (3.9) \\ \left\{ \frac{\Delta r N_{TH} (k_{i,j} + k_{i+1,j})}{\pi \left(r_i - \frac{\Delta r}{2} \right)} \right\}$$

Equation (3.9) was used to calculate the temperature of the interior nodes. In this equation the thermal conductivity and electrical resistivity of each node control volume were determined as a function of temperature from the following equations for 316 stainless steel (Ghajar and Zurigat, 1991):

$$k = 7.27 + 0.0038T \quad (3.10)$$

$$\gamma = 27.67 + 0.0213T \quad (3.11)$$

where T in $^{\circ}\text{F}$, k in $\text{Btu/hr-ft-}^{\circ}\text{F}$, and γ in micro-ohm-in.

Once the local inside wall temperatures were calculated from Equation (3.9), the local peripheral inside wall heat flux could be calculated from the heat balance equation, see Equation (3.1).

b. Calculation of the local peripheral and local average heat transfer coefficients

From the local inside wall temperature, the local peripheral inside wall heat flux and the local bulk fluid temperature, the local peripheral heat transfer coefficient could be calculated as follows:

$$h_i = \dot{q}_i'' / (T_{wi} - T_b) \quad (3.12)$$

where

- h_i = local peripheral heat transfer coefficient
- \dot{q}_i'' = local peripheral inside wall heat flux
- T_{wi} = local inside wall temperature
- T_b = bulk fluid temperature at the thermocouple station

Note that in these analysis it was assumed that the bulk fluid temperature increases linearly from the inlet to the outlet according to the following equation:

$$T_b = T_{in} + (T_{out} - T_{in}) X/L \quad (3.13)$$

Where

- T_{in} = bulk inlet temperature
- T_{out} = bulk outlet temperature
- X = distance from the pipe inlet to the thermocouple station
- L = total length of the test section

The local average heat transfer coefficient at each station could be calculated by the following equation:

$$\bar{h}_i = \bar{q}_i'' / (\bar{T}_{wi} - T_b) \quad (3.14)$$

where

\bar{h}_i = local average heat transfer coefficient

\bar{q}_i'' = average peripheral inside wall heat flux at a station

\bar{T}_{wi} = average inside wall temperature at a station

3.3.3 Physical Properties of the Fluids

The correlation equations for the fluids which were used in this study are based on the following information given in Table 3.1:

Table 3.1 Physical Properties of the Fluids used in This Study

Fluid	Equation for the Physical Property (T = Temperature in °F except where noted)	Range of Validity & Accuracy	Source
Air	ρ (lbm/ft ³) = P/RT where P in lbf/ft ² , T in °R, and R = 53.34 ft-lbf/lbm°R C_p (Btu/lbm-°F) = 7.540x10 ⁻⁶ T + 0.2401 μ (lbm/ft-hr) = -2.673x10 ⁻⁸ T ² + 6.819x10 ⁻⁵ T + 0.03936 k (Btu/hr-ft-°F) = -6.154x10 ⁻⁹ T ² + 2.591x10 ⁻⁵ T + 0.01313	P ≤ 150 psi -10 ≤ T ≤ 242, 0.2% -10 ≤ T ≤ 242, 0.1% -10 ≤ T ≤ 242, 0.2%	Vijay (1978)
Water	ρ (lbm/ft ³) = {2.101x10 ⁻⁸ T ² - 1.303x10 ⁻⁶ T + 0.01602} ⁻¹ C_p (Btu/lbm-°F) = 1.337x10 ⁻⁶ T ² - 3.374x10 ⁻⁴ T + 1.018 μ (lbm/ft-hr) = {1.207x10 ⁻⁵ T ² + 3.863x10 ⁻³ T + 0.09461} ⁻¹ k (Btu/hr-ft-°F) = 4.722x10 ⁻⁴ T + 0.3149 σ (lbf/ft) = 5.52288x10 ⁻¹² T ³ - 8.05936x10 ⁻⁹ T ² - 4.75886x10 ⁻⁶ T + 5.346x10 ⁻³ T	32 ≤ T ≤ 212, 0.1% 32 ≤ T ≤ 212, 0.3% 32 ≤ T ≤ 212, 1.0% 32 ≤ T ≤ 176, 0.2% 68 ≤ T ≤ 150	Vijay (1978)

3.3.4 Output

Figure 3.18 shows a sample output data file using the Computer Program, RHt99F. The output data file starts with the run number for a quick reference and a summary of some of the important information about the experimental run such as mass flow rate, mass flux, fluid velocity, room temperature, inlet and outlet temperatures, averaged Reynolds and Prandtl numbers, current and voltage drop across the test section, average heat flux, and heat balance error. Then, the calculated inside wall temperatures and the liquid superficial Reynolds numbers based on the inside wall temperature are listed. Next, the inside surface peripheral heat fluxes and the peripheral heat transfer coefficients for each thermocouple station along the pipe are listed. Finally, for each station, superficial liquid Reynolds number, liquid Prandtl number, its location from the tube entrance, liquid viscosity at the local bulk temperature, liquid viscosity at the local inside wall temperature, fluid bulk temperature, inside wall temperature, liquid density, and the local average Nusselt number are listed.

The main ideas of the interactive data reduction computer program called RHt99F have been described in this section. This computer program was developed in conjunction with another interactive computer program called Datared99F which directly read all the necessary information from the experimental measurement devices using the A/D board and the data logger. Also, this interactive computer program (Datared99F) controlled all the necessary measurement devices and generated the specified input data file which were used by the data reduction program.

In the next section, the experimental procedures for warming up the instruments, data collection, and shut down of the experimental setup will be introduced.

-----*
 RUN NUMBER 5104
 TEST FLUID IS DISTILLED WATER
 -----*

VOLUMETRIC FLOW RATE = 3.02 GPM
 MASS FLOW RATE = 1504.7 LBM/HR
 MASS FLUX = 229256 LBM/(SQ.FT-HR)
 FLUID VELOCITY = 1.02 FT/S
 ROOM TEMPERATURE = 73.66 F
 INLET TEMPERATURE = 84.53 F
 OUTLET TEMPERATURE = 88.87 F
 AVERAGE RE NUMBER = 10954
 AVERAGE PR NUMBER = 5.39
 CURRENT TO TUBE = 478.5 AMPS
 VOLTAGE DROP IN TUBE = 3.82 VOLTS
 AVERAGE HEAT FLUX = 2517 BTU/(SQ.FT-HR)
 Q=AMP*VOLT = 6236 BTU/HR
 Q=M*C*(T2-T1) = 6518 BTU/HR
 HEAT BALANCE ERROR = -4.51 %

OUTSIDE SURFACE TEMPERATURES - DEGREES F

	1	2	3	4	5	6	7	8	9	10
1	94.29	94.92	95.62	96.13	96.17	96.67	97.14	97.56	98.23	98.66
2	94.14	94.87	95.68	95.86	96.33	96.72	97.22	97.55	98.30	98.71
3	93.65	94.51	95.88	96.00	96.37	96.59	97.18	97.35	98.39	98.89
4	93.53	94.66	95.57	95.98	96.24	96.69	97.02	97.58	98.11	98.07

INSIDE SURFACE TEMPERATURES - DEGREES F

	1	2	3	4	5	6	7	8	9	10
1	92.95	93.57	94.27	94.78	94.82	95.32	95.79	96.21	96.88	97.31
2	92.79	93.52	94.33	94.51	94.98	95.37	95.87	96.20	96.95	97.36
3	92.30	93.16	94.53	94.65	95.02	95.24	95.83	96.00	97.04	97.55
4	92.17	93.31	94.22	94.63	94.89	95.34	95.67	96.23	96.76	96.71

REYNOLDS NUMBER AT THE INSIDE TUBE WALL

	1	2	3	4	5	6	7	8	9	10
1	11771	11854	11947	12015	12020	12087	12150	12206	12296	12355
2	11750	11847	11955	11978	12042	12094	12161	12205	12306	12361
3	11685	11799	11982	11997	12047	12076	12155	12178	12318	12386
4	11668	11819	11940	11995	12029	12090	12133	12209	12280	12273

INSIDE SURFACE HEAT FLUXES BTU/HR/FT2

	1	2	3	4	5	6	7	8	9	10
1	2332	2341	2347	2342	2351	2350	2349	2350	2351	2345
2	2340	2341	2349	2353	2346	2346	2348	2348	2352	2353
3	2349	2352	2340	2346	2346	2352	2348	2356	2346	2339
4	2356	2347	2352	2350	2349	2347	2353	2347	2357	2370

PERIPHERAL HEAT TRANSFER COEFFICIENT BTU/(SQ.FT-HR-F)

	1	2	3	4	5	6	7	8	9	10
1	287	281	272	269	282	279	277	277	269	268
2	293	282	270	279	276	277	274	277	267	268
3	314	297	263	273	275	282	276	285	264	260
4	320	290	274	274	279	278	282	276	274	291

-----*
 RUN NUMBER 5104
 SUMMARY
 -----*

ST	RE	PR	X/D	MUB	MUW	TB	TW	DENS	NU
1	10713.09	5.52	6.4	1.956	1.788	84.82	92.55	62.17	78.42
2	10766.51	5.49	15.5	1.947	1.772	85.24	93.39	62.16	74.39
3	10820.04	5.46	24.6	1.937	1.753	85.66	94.34	62.16	69.85
4	10873.67	5.43	33.7	1.927	1.747	86.07	94.64	62.15	70.74
5	10927.40	5.40	42.8	1.918	1.741	86.49	94.93	62.15	71.83
6	10981.24	5.37	52.0	1.909	1.734	86.91	95.32	62.14	72.05
7	11035.17	5.34	61.1	1.899	1.725	87.33	95.79	62.14	71.56
8	11089.21	5.31	70.2	1.890	1.718	87.74	96.16	62.13	71.94
9	11143.35	5.29	79.3	1.881	1.704	88.16	96.91	62.13	69.23
10	11197.58	5.26	88.4	1.872	1.698	88.58	97.23	62.13	69.94

NOTE: TBULK IS GIVEN IN DEGREES FAHRENHEIT
 MUB AND MUW ARE GIVEN IN LBM/(FT*HR)

Figure 3.18 A Sample Output Data File from the Computer Program RHt99F

3.4 Experimental Procedures

The system warm up, data collection, and shut off procedures were conceived with consideration for accuracy, repeatability, safety, and ease of performance.

3.4.1 Testing the Loop

Before each experiment, a quick check of all apparatus and equipment was performed to ensure no leaks nor failed components were present in the system. When decision about desired flow rates of the gas and liquid and heat input had been made the warm up procedure was instituted.

3.4.2 Warm Up

The warm up procedure is as follows:

1. Make the connection between the frequency meter and either Halliburton turbine flow meter for large liquid flow rate from 3 to 9 GPM or Cole-Parmer impeller liquid flow meter for small flow rates up to about 3 GPM.
2. Turn on all of the electrical instruments such as the data acquisition system for the temperature measurement (MAC-14), frequency meter for the liquid flow rate, gas flow meter for the gas flow rate, power supplies for the air pressure transducer and the Scanni valve, CD15 carrier demodulator for the pressure transducer, and voltmeter for the voltage drop measurement across the test section.

3. Set the liquid control valves after the pump assembly in correct position such that the correct pump will provide liquid flow to the system, either large or small pump.
4. Switch on the pump.
5. Set the inlet and by-pass control valves of the test section such that right amount of the liquid is provided to the test section.
6. Adjust the gas control valve before the mixer to attain the desired gas flow rate.
7. If necessary, fine tune the liquid control valves including the by-pass valve to attain the desired liquid flow rate after mixed with the gas.
8. Check the welder cable and all connections to ensure their integrity and proper fitting.
9. Switch the welder on and adjust the current output to the near desired value on the welder ammeter. Check the DC ammeter for the current across the test section and re-adjust the welder current until this meter is reading the desired value.
10. After approximately 15 minutes (depending on the flow rates of gas and liquid) of operation turn on the heat exchanger coolant. The coolant flow rate through the heat exchanger is set such that the inlet bulk temperature of steady state operation is in the desired vicinity of operation.

3.4.3 Data Collection and Shut Down

After the test section reaches a steady-state condition, the initiation of data collection begins. The data collection procedure and shutdown is common for all the different experimental test runs. By monitoring the inlet bulk temperature, exit bulk

temperature, the first thermocouple section, and the last thermocouple section, a decision as to when steady-state conditions are reached can be made. The procedure is as follows:

1. On the temperature measurement computer bring up the RTG software monitoring the MAC-14 data logger output. Set the data logger to print data on the screen every minute.
2. Re-adjust the heat exchanger coolant flow rate such that inlet bulk temperature is in the desired vicinity (within $\pm 0.5^{\circ}\text{C}$).
3. When the first thermocouple station, the last thermocouple station, and the inlet and the exit bulk temperatures all indicate less than 0.3°C deviation in five minutes, assume steady state condition has been reached.
4. Record the frequency of the flow meter, the voltage at the digital voltmeter, and amperage on the ammeter.
5. Set the MAC-14 logging parameters through RTG software such that disk storage of data occurs for all the channels. Monitor all equipment during operation and discontinue data collection on the MAC-14 until desired number of samples (75-100) stored.
6. When the data collection period is complete, repeat step 4 for all final values. Disable all data recording devices.
7. Turn off the DC welder, voltmeter, amplifier, and/or frequency meter. When the inlet and exit bulk temperatures approach room temperature shut off the coolant water to the heat exchanger and the reservoir mixer.
8. Turn off the pump, close the flow control valve and the inlet and exit test section valves. Switch off the MAC-14, and the computer.

9. Inspect the test section apparatus and ensure that no leaks have become evident.
10. It is always advisable not to take the runs continuously as it may build up considerable heat in the welder.
11. Provide at least a gap of 1 hour between any two consecutive test runs. This will also help to return the bulk temperatures to room temperature.

In this section, the details of the experimental procedures have been discussed. In the next chapter, the experimental results of flow pattern and heat transfer measurements will be introduced.

CHAPTER IV

RESULTS AND DISCUSSION

This chapter deals with the heat transfer results of the present investigation. First, the single-phase heat transfer results are presented and compared with five well-known correlations. Next, the flow pattern data of the two-phase flow are presented. Then, the identified flow pattern data are compared with the well known flow pattern map. Finally, two-phase flow heat transfer data are presented and appropriate two-phase heat transfer correlations are recommended.

4.1 Single-Phase Heat Transfer Results

To help in determining whether the test setup was working well enough to carry out two-phase heat transfer experiments, first, single-phase heat transfer data were taken and compared with predictions of five well established correlations. Based on the agreements between the single-phase experimental data and the predictions from the selected heat transfer correlations, the current apparatus was proven to be reliable. Details of the comparisons are introduced in this section. More information of the single-phase heat transfer experimental data can be found in Ryali (1999) and Kim (2000).

4.1.1 Nusselt Numbers Along the Test Section

After the flow had traveled through the tube to a point far from the inlet, the velocity and thermal profiles became fully developed. The distance from the inlet to this fully developed point is known as the entrance length. Siegel et al. (1958) defined the thermal entrance region as the length required for the local heat transfer coefficient to approach to within a few percent of the fully developed value of the coefficient. Others such as Shah (1978) defined thermal entry length as it related to Nusselt number; and because the Nusselt number is a dimensionless heat transfer coefficient, the criteria for thermal entrance effect can be related to heat transfer coefficient [or the Nusselt number] deviation equally well. Figure 4.1 shows an example of Nusselt number variation with dimensionless axial distance for test runs which covered a wide range of Reynolds number. This figure demonstrates that the Nusselt number over the Reynolds number range (2600 to 16400) showed a steady decrease from the inlet of the test section, and gradually became constant after x/D was about 40. This indicated that the fluid attained a fully developed flow after x/D equal to about 40. Hence station 6 ($x/D = 52.0$ refer to Figure 3.3 in Chapter III) was considered to be an ideal station where the fluid was said to be fully developed; and thus all of the Nusselt number comparisons with selected correlations have been performed at this station.

4.1.2 Comparison of Available Correlations with Experimental Data

Using the data accumulated throughout this single-phase heat transfer study, it was desirable to consider how accurately the data could be predicted by conventional well-known correlations. To accomplish this goal, the single-phase heat transfer correlations were compared with the data conforming to the respective correlation

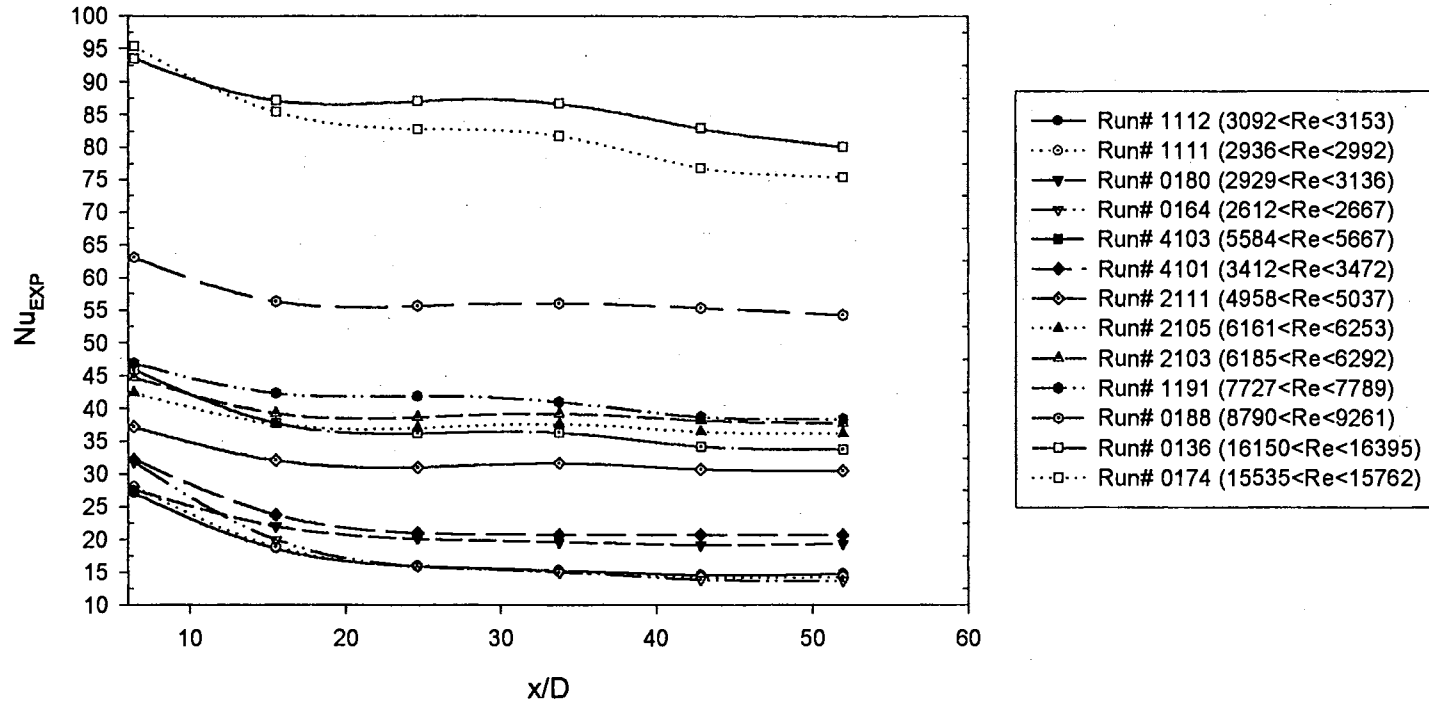


Figure 4.1 Experimental Nusselt Number vs. Dimensionless Axial Distance for All Types of Test Runs

limitations (and sometimes outside of the ranges of those correlations in order to see the robustness of data vs. correlation). The Nusselt number was calculated using data at station 6, at which the flow was considered to be fully developed. From Figure 4.1, it was observed that the Nusselt number at station 6 ($x/D = 52.0$) appeared to be fully developed. A deviation of $\pm 20\%$ between experimental data and prediction was considered to be a good test run, and all of the following graphs have been drawn with $\pm 20\%$ or $\pm 10\%$ deviation reference lines.

As mentioned at the beginning of this section, five correlations were chosen to compare the predictions with the experimental Nusselt numbers. Those correlations are as follows:

Colburn (1933) correlation:

$$Nu = 0.023 Re^{0.8} Pr^{1/3} \quad (4.1)$$

where $Re \geq 10,000, 0.6 \leq Pr \leq 160$

Sieder and Tate (1936) correlation:

$$Nu = 0.023 Re^{0.8} Pr^{1/3} (\mu_b / \mu_w)^{0.14} \quad (4.2)$$

where $Re \geq 10,000, 0.7 \leq Pr \leq 16,700$

Gnielinski [1] (1976) correlation:

$$Nu = \frac{(c_f / 2)(Re - 1000)Pr}{1 + 12.7(c_f / 2)^{1/2}(Pr^{2/3} - 1)} \quad (4.3)$$

where $\frac{1}{\sqrt{c_f}} = 1.58 \ln Re - 3.28$; Filonenko Correlation

$$0.5 \leq Pr \leq 2,000, 2,300 \leq Re \leq 5 \times 10^6$$

Gnielinski [3] (1976) correlation:

$$Nu = 0.012(Re^{0.87} - 280)Pr^{0.4} \quad (4.4)$$

where $1.5 \leq Pr \leq 500, 3,000 \leq Re \leq 1 \times 10^6$

Ghajar and Tam (1994) correlation:

$$Nu = 0.023 Re^{0.8} Pr^{0.385} (x/D_i)^{-0.0054} (\mu_b/\mu_w)^{0.14} \quad (4.5)$$

where $3 \leq x/D_i \leq 192, 7000 \leq Re \leq 49000$

$4 \leq Pr \leq 34, 1.1 \leq \mu_b/\mu_w \leq 1.7$

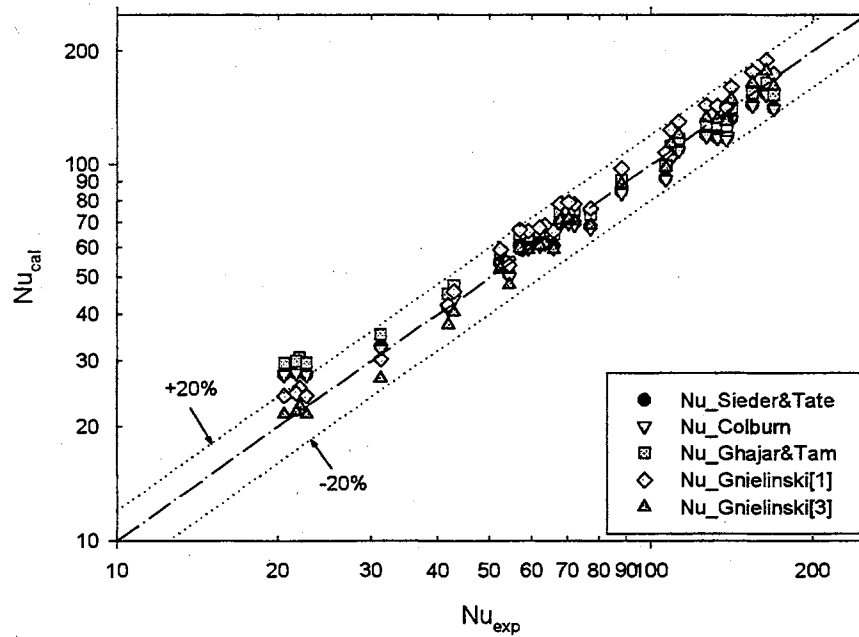


Figure 4.2 Comparison of Nu_{exp} vs. Nu_{cal} from Selected Correlations at Thermocouple Station No. 6 ($3,000 < Re < 30,000$)

The predicted Nusselt numbers using the above correlations were compared with the experimental Nusselt numbers. The results of the comparison (without concern for the recommended parameter ranges) for each of the five correlations are shown in Figures 4.2 and 4.3. As shown in those figures, the experimental Nusselt numbers were in good

agreement with the calculated Nusselt numbers, and all of them were within a $\pm 20\%$ error band except for Colburn, Sieder and Tate, and Ghajar and Tam correlations in the low Reynolds number ($Re < 5,000$) regime. A detailed comparison for each correlation follows.

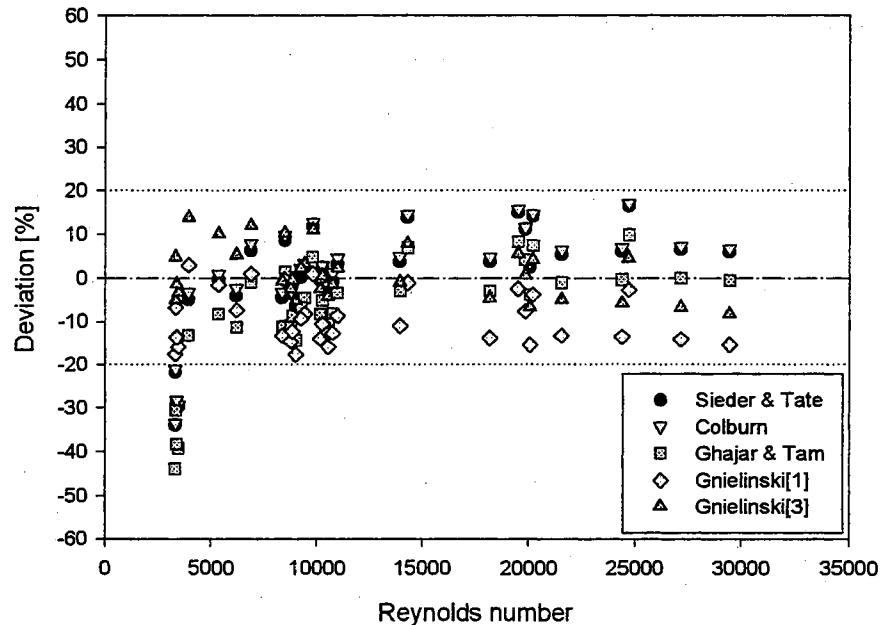


Figure 4.3 Deviations of Nu_{cal} Referenced to Nu_{exp} vs. Reynolds Number at Thermocouple Station No. 6 ($3,000 < Re < 30,000$)

Colburn (1933): Figure 4.4 shows the comparison of experimental Nusselt numbers with the calculated Nusselt numbers by using the Colburn correlation. As shown in Eq. (4.1), the lower recommended Reynolds number range of the Colburn correlation is 10,000. Among the all of 31 data points in Figs. 4.2 and 4.3, a total of 23 data points ($Re > 8,000$) were used to predict the Colburn correlation. Within the recommended range of Reynolds number, most of the 23 data points fell within a $\pm 10\%$ deviation band as can be seen from Fig. 4.4, which shows a very good agreement between the experimental Nusselt numbers and the predictions from the Colburn correlation. Table

4.1 shows the minimum and maximum values of the experimental ranges of Re, Pr, Nu_{EXP} , Nu_{CAL} , and percent deviations for Colburn correlation. A maximum deviation of 16.99 % and a minimum deviation of -5.49 %, and a mean deviation of 5.76 % with an rms deviation of 8.55 % is achieved by using the Colburn correlation.

Table 4.1 Ranges of Reynolds, Prandtl, and Nusselt Numbers, and % Deviations for Colburn (1933) Correlation (23 Data Points)

	Re	Pr	Nu_{EXP}	Nu_{CAL}	Deviation [%] (1- Nu_{CAL}/Nu_{EXP}) \times 100
Minimum	8351	5.02	52.38	54.09	-5.49
Maximum	29443	6.64	164.12	153.25	16.99
Mean	18987	-	-	-	5.76

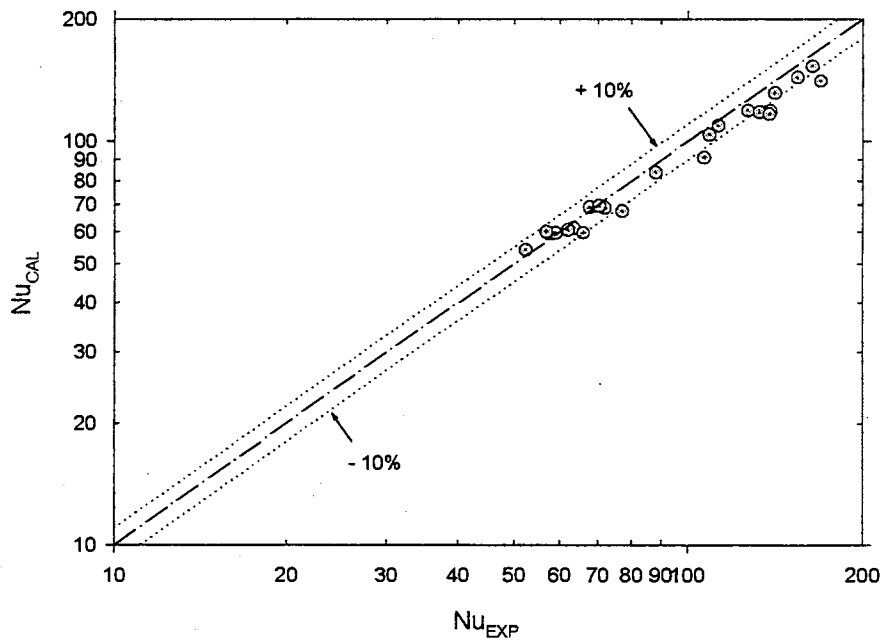


Figure 4.4 Nu_{EXP} vs. Nu_{CAL} – Colburn (1933) Correlation

Sieder and Tate (1936): Since the lower recommended Reynolds number was 10,000 by the Sieder and Tate correlation, a total of 23 data points having Reynolds

numbers greater than 8,000 were used for the Sieder and Tate correlation. As shown in Figure 4.5, the results were very similar to those produced by the Colburn (1933) correlation due to the fact that the Sieder and Tate correlation added the viscosity ratio term to the Colburn correlation. From this aspect, we can see that the viscosity ratio term is not very significant for single-phase water heat transfer. As can be seen from Table 4.2, there was a maximum deviation of 16.45 %, a minimum deviation of -6.75 %, and a mean deviation of 4.81 % with an rms deviation of 8.08 %. Most of data points fell into a ± 10 % deviation band, which showed a very good Nusselt number comparison.

Table 4.2 Ranges of Reynolds, Prandtl, and Nusselt Numbers, and % Deviations for the Sieder and Tate (1936) Correlation (23 Data Points)

	Re	Pr	Nu _{EXP}	Nu _{CAL}	Deviation [%] (1-Nu _{CAL} /Nu _{EXP})×100
Minimum	8351	5.02	52.38	54.73	-6.75
Maximum	29443	6.64	164.12	154.31	16.45
Mean	-	-	-	-	4.81

Ghajar and Tam (1994): The Ghajar and Tam correlation applies several limitations as shown in Eq. (4.5). Among those limitations, Reynolds number and viscosity ratio were concerned since the rest of the limitations were sufficiently satisfied. A total of 16 data points ($1.06 \leq \mu_b/\mu_w \leq 1.151$, $Re \geq 6,000$) were predicted with the Ghajar and Tam correlation. The results shown in Table 4.3 and Fig. 4.6 indicate that the experimental Nusselt numbers agreed well with the predictions of the Ghajar and Tam correlation. Most of data fell into the ± 10 % deviation band, having a maximum

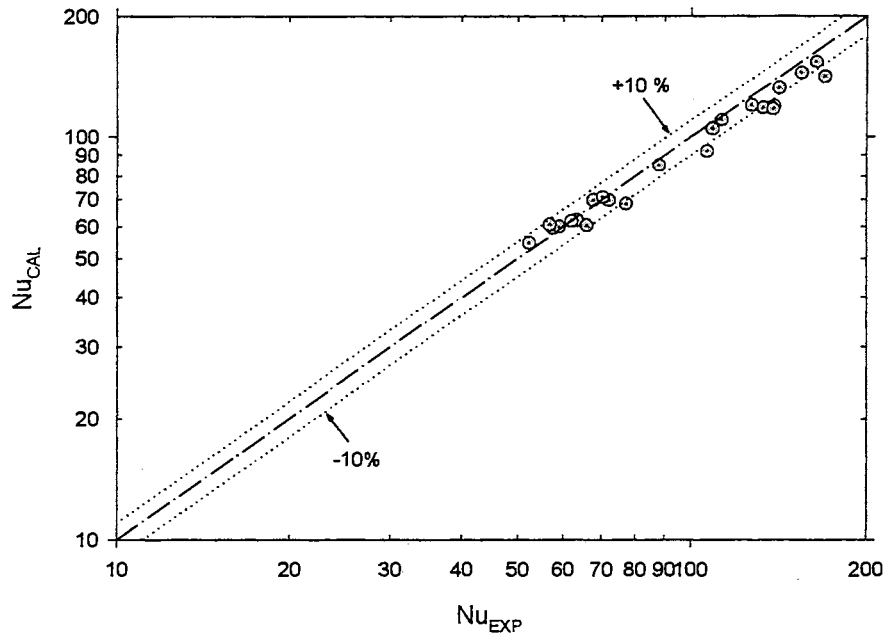


Figure 4.5 Nu_{EXP} vs. Nu_{CAL} - Sieder and Tate (1936) Correlation

deviation of 6.91 %, a minimum deviation of -14.36 %, and a mean deviation of -4.28 % with an rms deviation of 6.90 %. From this result, it can be concluded that the current data is reasonably accurate since the proven Ghajar and Tam (1994) correlation predictions agree very well with the data presented herein.

Table 4.3 Ranges of Reynolds, Prandtl, and Nusselt Numbers, and % Deviations for the Ghajar and Tam (1994) Correlation (16 Data Points)

	Re	Pr	μ_B/μ_W	Nu_{EXP}	Nu_{CAL}	Deviation [%] (1- Nu_{CAL}/Nu_{EXP}) \times 100
Minimum	6176	5.02	1.06	42.83	47.65	-14.36
Maximum	21522	6.64	1.151	126.92	128.29	6.91
Mean	-	-	-	-	-	-4.28

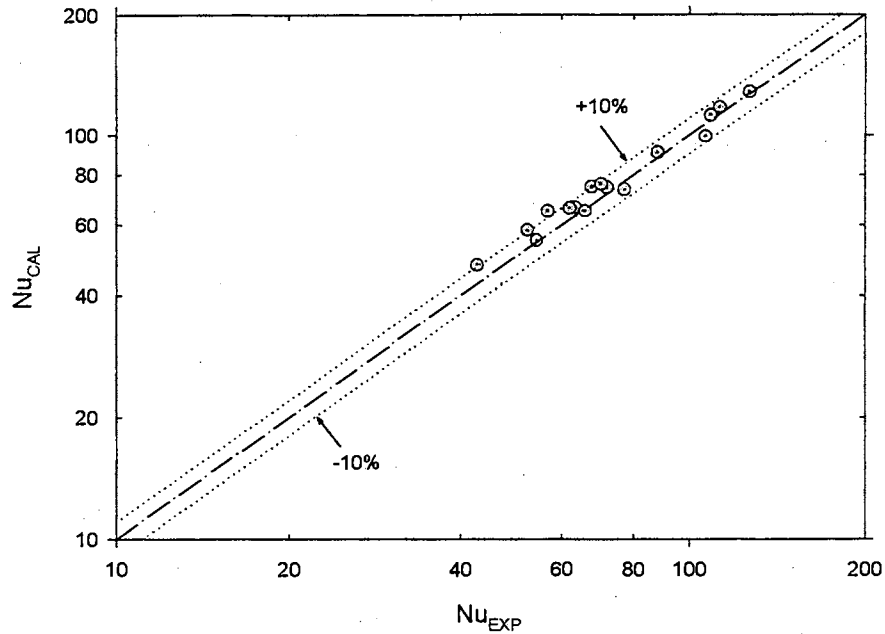


Figure 4.6 Nu_{EXP} vs. Nu_{CAL} - Ghajar and Tam (1994) Correlation

Gnielinski (1976) proposed three correlations for different parameter ranges. The first Gnielinski [1] correlation employed the friction factor (f) and was used for transitional and turbulent flows. The second and third correlations do not require friction factor. The second Gnielinski [2] correlation is used for low Prandtl number ($0.5 \leq Pr \leq 1.5$) and fully turbulent flow ($10^4 \leq Re \leq 5 \times 10^6$). The third Gnielinski [3] correlation was used for transitional and turbulent flow regions without the use of friction factor. In this study, Gnielinski [1] and [3] were used to compare the experimental Nusselt numbers with the calculated Nusselt numbers.

Gnielinski [1] (1976): Since the lower limit of recommended Reynolds number is 2300, 13 transitional ($3,000 < Re < 9,000$) and 18 fully turbulent ($Re \geq 9,000$) experimental data points were predicted with the Gnielinski [1] correlation. The calculation of friction coefficients for these predictions employed the Filonenko

correlation which was used by Gnielinski (1976) himself to develop the correlation. As shown in Table 4.4 and Fig. 4.7, the results of the comparison using the Gnielinski [1] correlation were sufficiently acceptable. The calculated Nusselt numbers using the Gnielinski [1] correlation has a maximum deviation of 2.97 %, a minimum deviation of -17.60 %, and a mean deviation of -9.16 % with an rms deviation of 11.02 %. All 31 data points fell into a ± 20 % deviation band as shown in Fig. 4.7.

Table 4.4 Ranges of Reynolds, Prandtl, and Nusselt Numbers, and % Deviations for the Gnielinski [1] (1976) Correlation (31 Data Points)

	Re	Pr	Nu _{EXP}	Nu _{CAL}	Deviation [%] (1-Nu _{CAL} /Nu _{EXP})×100
Minimum	3286	5.02	20.57	24.17	-17.60
Maximum	29443	6.64	164.12	189.35	2.97
Mean	-	-	-	-	-9.16

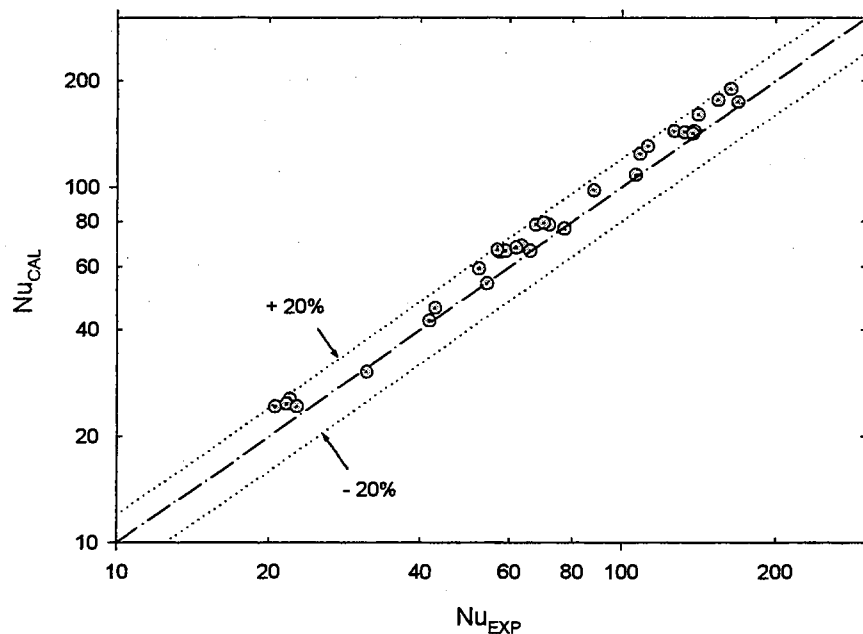


Figure 4.7 Nu_{EXP} vs. Nu_{CAL} - Gnielinski [1] (1976) Correlation

Gnielinski [3] (1976): As with the Gnielinski [1] correlation, the Gnielinski [3] correlation covered transitional and fully turbulent ($3,000 \leq Re \leq 10^6$) flows. Thus, the 13 transitional and 18 fully turbulent flow heat transfer data points could be examined. Unlike the Gnielinski [1] correlation, the Gnielinski [3] does not employ the friction coefficient and predicts Nusselt number using only Reynolds and Prandtl numbers. As shown in Figure 4.8 and Table 4.5, the comparison of the experimental Nusselt numbers with the calculated ones using the Gnielinski [3] correlation showed very good agreement between the experimental and the predicted values. The results with the Gnielinski [3] correlation has a maximum deviation of 13.82 % and a minimum deviation of -8.18 %, and a mean deviation of 1.20 % with an rms error of 6.49 %. Most of the data fell into a ± 10 % deviation band as shown in Fig. 4.8.

Table 4.5 Ranges of Reynolds, Prandtl, and Nusselt Numbers, and % Deviations for the Gnielinski [3] (1976) Correlation (31 Data Points)

	Re	Pr	Nu _{EXP}	Nu _{CAL}	Deviation [%] (1-Nu _{CAL} /Nu _{EXP})×100
Minimum	3286	5.02	20.57	21.59	-8.18
Maximum	29443	6.64	164.12	177.55	13.82
Mean	-	-	-	-	1.20

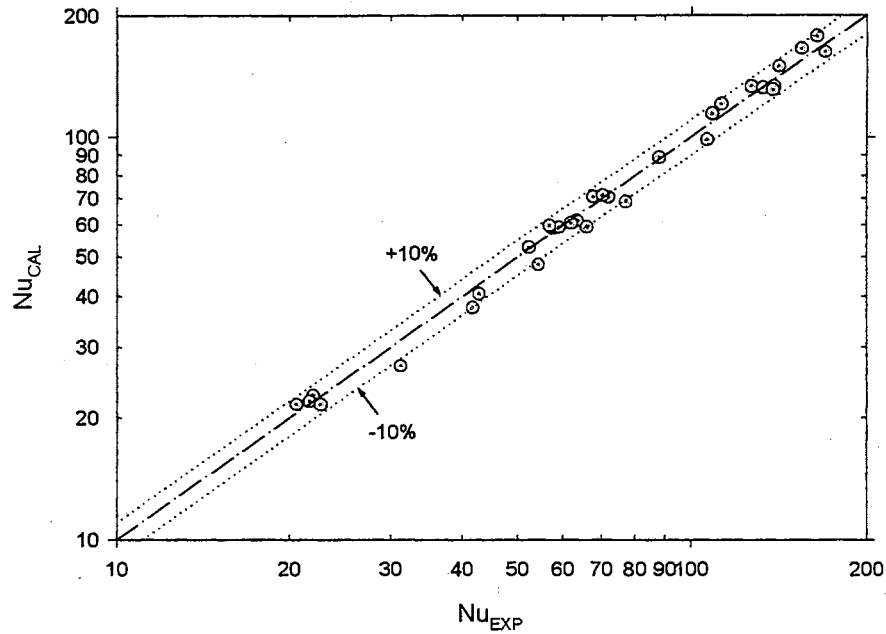


Figure 4.8 Nu_{EXP} vs. Nu_{CAL} - Gnielinski [3] (1976) Correlation

The data obtained from this test setup compared well with these well-established single-phase correlations. The experimental Nusselt numbers agreed well with those predicted by the correlations. Therefore, based on the overall comparisons of those correlations with the experimental data, it is concluded that the test data is good enough to prove that the test setup can properly handle single-phase flows. In the following section, the flow pattern criteria for two-phase horizontal pipes and the observed flow patterns will be described.

4.2 Presentation of Flow Patterns

Because of the multitude of flow patterns and the various interpretations accorded to them by different investigators, no uniform procedure exists at present for describing

and classifying them. However, in recent years, some attempts have been made to standardize the description and terminology of the flow patterns (Breber et al., 1980, Govier and Aziz, 1973, Griffith and Wallis, 1961, Hewitt and Hall-Taylor, 1970, Taitel and Dukler, 1976). Among those standardization efforts, the characterization and description proposed by Taitel and Dukler (1976) appears to be the best and most common for a horizontal pipe flow.

In Section 1.2.2, the descriptions and equations of the flow patterns presented by Carey (1992) which used the flow pattern map of Taitel and Dukler (1976) was described. In this study, the flow pattern identification for the experimental data was based on the procedures suggested by Taitel and Dukler (1976), Breber et al. (1980), and visual observation as appropriate. In this section, experimentally observed flow patterns, the detailed procedures of the flow pattern identification using the well known flow pattern map, and finally the ranges of different flow patterns will be presented.

4.2.1 Flow Pattern Observations

The two-phase flow leaving the mixer entered the calming section (refer to Figure 3.1 in Chapter III), which consisted of a clear polycarbonate tube of a 1 inch (2.54 cm) I.D. and 96 inches (244 cm) in length ($L/D = 96$). All observations for the flow pattern judgements were made at two locations, just before the test section (about $L/D = 93$ in the calming section) and right after the test section (see Figure 3.1 for 'Observation Section' after the test section). Leaving the liquid flow rate fixed, flow patterns were observed for various air flow rates. The liquid flow rate was then adjusted and the process was repeated. If the observed flow patterns differed before and after the test section,

experimental data were not taken and the flow rates of gas and liquid were readjusted for consistent flow pattern observations.

Table 4.6 shows a summary of the two-phase flow pattern experimental data taken. This table shows the flow patterns observed; number of data points taken in each flow pattern; minimum, maximum, and averaged values of the mass flow rates of liquid and gas along with their superficial velocities and Reynolds numbers; Martinelli parameter (X); temperature and pressure of gas-liquid mixture; two-phase pressure drop along the test section (ΔP); supplied gas pressure (P_G); void fraction (α); and Prandtl numbers of liquid and gas.

Some of the basic flow patterns (stratified, wavy, and slug) described in Section 1.2.2 in a horizontal pipe, and several transitional flow patterns (wavy/slug, annular/wavy, annular/bubbly, annular/bubbly/slug, and bubbly/slug) were observed. Flow patterns that simultaneously showed characteristics of the basic flow patterns described in Section 1.2.2 were classified as transitional flow patterns. Those visually observed flow patterns were photographed by means of a high speed still camera (Nikon, F3) using three high intensity discharge lamps (one 300 watts and two 150 watts lamps) without the aid of a stroboscope.

Representative photographs of the various flow patterns that were observed are given in Figure 4.9. Figure 4.9a illustrates the observed stratified flow pattern in which liquid flowing in the bottom of the pipe was separated from gas in the upper portion of the pipe by a relatively smooth interface. Figure 4.9b shows the observed wavy flow pattern. After the flow rate and/or the quality was increased in the stratified flow pattern, the interface became unstable, whereupon the interface became wavy. In wavy flow

Table 4.6 Summary of the Two-Phase Flow Pattern Experimental Data

	\dot{m}_L [lbm/hr]	V_{SL} [ft/sec]	Re_{SL}	\dot{m}_G [lbm/hr]	V_{SG} [ft/sec]	Re_{SG}	X	T_{MIX} [°C]	P_{MIX} [psi]	ΔP [inH ₂ O]	P_G [psi]	α	Pr_L	Pr_G
Stratified Flow Pattern (13 data points)														
Min.	86.72	0.07	709.38	1.58	1.08	539.26	0.34	26.00	0.23	0.03	0.01	0.74	5.18	0.71
Max.	187.76	0.15	1359.7	12.53	6.49	4272.3	2.92	32.20	1.17	0.17	5.67	0.91	5.99	0.71
Avg.	124.11	0.10	974.82	6.35	3.75	2169.9	1.08	30.24	0.67	0.09	1.81	0.85	5.42	0.71
Wavy Flow Pattern (9 data points)														
Min.	84.57	0.07	628.69	12.63	6.47	4341.9	0.21	25.30	0.25	0.37	4.71	0.85	5.26	0.71
Max.	319.23	0.26	2424.0	32.61	8.21	11179.	0.79	31.50	1.38	1.37	25.77	0.92	6.09	0.71
Avg.	184.78	0.15	1369.3	23.97	7.68	8206.6	0.48	27.36	0.62	0.69	16.43	0.89	5.81	0.71
Wavy/Slug Flow Pattern (7 data points)														
Min.	317.18	0.26	2276.9	9.20	5.38	3113.0	0.96	25.60	0.39	1.08	2.71	0.75	5.36	0.71
Max.	977.10	0.80	7153.4	20.26	7.47	6982.2	2.30	30.70	0.86	2.58	12.32	0.84	6.05	0.71
Avg.	525.98	0.43	4026.7	13.88	6.56	4736.1	1.59	28.53	0.55	1.88	6.30	0.80	5.64	0.71
Slug Flow Pattern (46 data points)														
Min.	319.36	0.26	2425.0	1.61	1.10	546.76	1.64	25.60	0.24	0.10	0.03	0.29	5.38	0.71
Max.	5461.9	4.47	43068.	20.82	7.46	7087.5	36.85	30.50	7.16	18.15	16.54	0.80	6.05	0.71
Avg.	2046.9	1.67	15534.	8.51	4.20	2895.9	9.49	28.30	1.68	5.09	4.35	0.59	5.67	0.71
Wavy/Annular Flow Pattern (14 data points)														
Min.	82.31	0.07	662.55	42.63	8.13	14430.	0.13	25.90	0.82	0.51	37.34	0.77	5.26	0.71
Max.	925.90	0.76	7000.8	77.88	9.51	26361.	1.50	31.50	3.73	9.27	69.82	0.94	6.01	0.71
Avg.	380.63	0.31	2882.3	59.28	8.93	20093.	0.57	28.66	1.87	4.04	53.12	0.87	5.63	0.71
Annular/Bubbly or Annular/Bubbly/Slug Flow Pattern (12 data points)														
Min.	1243.7	1.02	9564.4	41.95	8.16	14308.	1.67	26.20	3.04	8.60	37.36	0.60	5.52	0.71
Max.	3785.5	3.10	29480.	76.41	9.60	25996.	4.27	29.40	10.50	24.52	66.67	0.74	5.96	0.71
Avg.	2155.5	1.76	16220.	59.61	8.88	20248.	2.74	27.74	6.06	16.09	53.66	0.68	5.75	0.71
Bubbly/Slug Flow Pattern (12 data points)														
Min.	905.99	0.74	6762.9	24.31	7.08	8291.9	1.74	25.80	1.56	4.55	17.58	0.52	5.39	0.71
Max.	4888.0	4.00	35707.	79.57	9.65	27070.	9.07	30.40	12.86	24.36	70.75	0.76	6.02	0.71
Avg.	3242.8	2.65	23971.	41.36	8.08	14052.	4.95	27.05	6.94	16.94	36.07	0.61	5.84	0.71

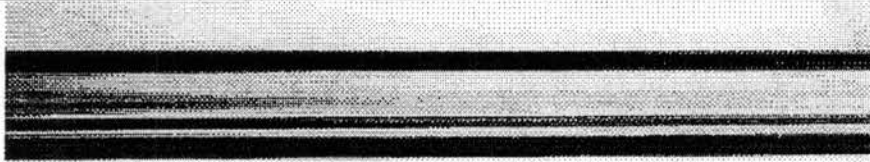


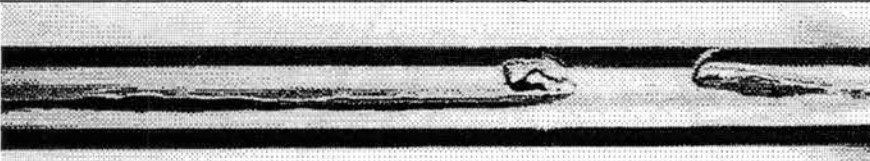


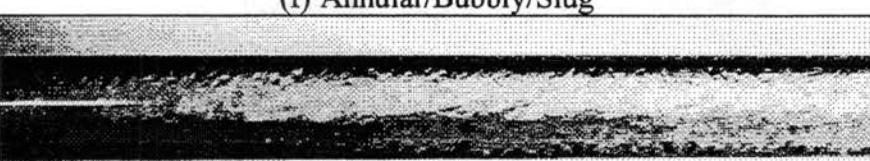
 <p>(a) Stratified</p>	$\dot{m}_L = 139.4$ [lbm/hr] $\dot{m}_G = 2.7$ [lbm/hr] $f = 8 @ 1/2000$ [sec]
 <p>(b) Wavy</p>	$\dot{m}_L = 185.7$ [lbm/hr] $\dot{m}_G = 18.8$ [lbm/hr] $f = 8 @ 1/2000$ [sec]
 <p>(c) Wavy/Slug</p>	$\dot{m}_L = 600.4$ [lbm/hr] $\dot{m}_G = 16.5$ [lbm/hr] $f = 8 @ 1/2000$ [sec]
 <p>(d) Slug</p>	$\dot{m}_L = 1069.2$ [lbm/hr] $\dot{m}_G = 2.8$ [lbm/hr] $f = 8 @ 1/2000$ [sec]
 <p>(e) Annular/Wavy</p>	$\dot{m}_L = 412.9$ [lbm/hr] $\dot{m}_G = 68.1$ [lbm/hr] $f = 8 @ 1/2000$ [sec]
 <p>(f) Annular/Bubbly/Slug</p>	$\dot{m}_L = 2311.9$ [lbm/hr] $\dot{m}_G = 74.0$ [lbm/hr] $f = 8 @ 1/2000$ [sec]
 <p>(g) Bubbly/Slug</p>	$\dot{m}_L = 4021.3$ [lbm/hr] $\dot{m}_G = 74.0$ [lbm/hr] $f = 8 @ 1/2000$ [sec]

Figure 4.9 Photographs of Representative Flow Patterns

pattern, the velocity of the gas was sufficient to cause waves to form but not enough to cause waves to reach the top of the pipe surface.

In Fig. 4.9c, those waves caused by the gas flow under conditions where the velocity of the gas was sufficient for the rapid wave growth, were reached to top of the inside pipe surface. This type of flow was categorized as wavy/slug transitional flow pattern. In Fig. 4.9d, as the liquid rate was increased, the liquid level rose and the wave was formed so that the crest spans the entire width of the pipe, effectively forming large slug-type bubbles. The slugs of gas flowing along the tube, because of their buoyancy, tended to skew toward the upper portion of the pipe.

In Fig. 4.9e, wavy type of liquid film at the bottom side of the pipe together with the liquid annulus along the inside pipe wall were observed. At high gas velocities and moderate liquid flow rates, there was insufficient liquid flow to maintain and form liquid bridge, and the liquid in the wave was swept up around the tube to form a liquid annulus with some entrainment. For such conditions, buoyancy effects tended to thin the liquid film on the top portion of the pipe wall and thicken it at the bottom. Butterworth (1972) has demonstrated this mechanism for annular film formation. This transitional type of flow pattern was classified as that from wavy to annular transition flow pattern.

In Fig. 4.9f, liquid film annulus together with frothy type of bubble slugs were observed. In these conditions, buoyancy effects still tended to thin the liquid film on the top portion of the pipe wall and thicken it at the bottom resulting in slightly thicker liquid film at the bottom side of the pipe wall than the liquid film at the top. With relatively high gas and liquid flow rates, much less liquid annulus than Fig. 4.8f with frothy type of bubble slugs were observed in Fig. 4.9g. In this condition, the gas flow was invariably

turbulent and strong lateral Reynolds stresses and the shear resulting from secondary flows might serve to distribute the liquid more evenly around the tube perimeter against the tendency of gravity to stratify the flow. This type of observed flow pattern was classified as bubbly/slug transitional flow pattern. In the next section, all those observed flow patterns will be compared with the Taitel and Dukler (1976) flow pattern map.

4.2.2 Experimental Data on Taitel and Dukler (1976) Flow Pattern Map

In this section, in order to build a solid flow pattern criteria, measured experimental data having variety of different flow patterns judged by appropriate visual observation along with the description of Carey (1992) are plotted on the flow pattern map of Taitel and Dukler (1976). Some of the equations introduced in Section 1.2.2 for flow pattern criteria will be repeated in this section for convenience.

In Figs. 4.10 to 4.16, observed flow patterns are compared with their calculated positions on the Taitel & Dukler map using the equations (Eqs. 1.34 to 1.36) described in Section 1.2.2. The map proposed by Taitel & Dukler, which attempted to account for the different combinations of physical parameters that affect different regime transitions on the map, is shown in Fig. 1.5 in Section 1.2.2. The horizontal coordinate on the map is the Martinelli parameter (X) that fixes the horizontal position on the map regardless of the flow regime. However, the vertical coordinates of the dimensionless parameters used to determine the flow regime vary depending on the specific transition being considered (Eqs. 1.34 to 1.36).

For stratified flow to wavy flow transition, the vertical position of the corresponding point in Fig. 1.5 is specified in terms of the parameter K_{TD} , defined as

$$K_{TD} = \left[\frac{\rho_G V_{SG}^2 V_{SL}}{\nu_L (\rho_L - \rho_G) g \cos \Omega} \right]^{0.5} \quad (1.34)$$

where ν_L is the kinematic viscosity of the liquid and Ω is the angle of inclination between the tube axis and the horizontal. Wavy to annular and wavy to intermittent (plug or slug) transitions in Fig. 1.5 are evaluated in terms of X and the parameter F_{TD} , defined as

$$F_{TD} = \left[\frac{\rho_G V_{SG}^2}{(\rho_L - \rho_G) D g \cos \Omega} \right]^{0.5} \quad (1.35)$$

where D is the tube diameter. Intermittent flow to bubbly flow transition is specified in terms of X and the parameter T_{TD} , defined as

$$T_{TD} = \left[\frac{-(dP/dz)_L}{(\rho_L - \rho_G) g \cos \Omega} \right]^{0.5} \quad (1.36)$$

where $-(dP/dz)_L$ is specified by the following relationship, Equation (4.8).

$$-(dP/dz)_L = \frac{4C_L}{D} \left(\frac{V_{SL} D}{\nu_L} \right)^{-0.2} \frac{\rho_L V_{SL}^2}{2} \quad (4.8)$$

The transition between intermittent and annular flow or bubbly to annular flow simply corresponds to $X = 1.6$ on the map.

The steps for identifying the flow pattern using the above equations can be summarized as follows:

- Stratified flow pattern: if the observed flow pattern data on the Taitel and Dukler map are below the stratified flow to wavy flow (stratified wavy, SW) transition line of the calculated K_{TD} values (Eq. 1.34), then the observed flow pattern is stratified flow pattern.

- Wavy flow pattern: if the observed flow pattern data are above the stratified flow to wavy flow transition line of the calculated K_{TD} values (Eq. 1.34) and the flow pattern data are below the wavy to annular and wavy to intermittent transition line of the calculated F_{TD} values (Eq. 1.35), then the observed flow pattern is wavy flow pattern.
- Intermittent (plug or slug) flow pattern: if the observed flow pattern data are above the wavy to annular and wavy to intermittent transition line of the calculated F_{TD} values (Eq. 1.35), and the flow pattern data are below the intermittent to bubbly transition line of the calculated T_{TD} values (Eq. 1.36), and the values of the Martinelli parameter (X) of the flow pattern data are greater than the intermittent to annular transition value of $X = 1.6$, then the observed flow pattern data are intermittent flow pattern data.
- Annular flow pattern: if the observed flow pattern data are above the wavy to annular and wavy to intermittent transition line of the calculated F_{TD} values (Eq. 1.35) and the values of the Martinelli parameter (X) of the flow pattern data are smaller than the intermittent to annular flow or bubbly to annular flow transition value of $X = 1.6$, then the observed flow pattern data are annular flow pattern data.
- Bubbly flow pattern data: if the observed flow pattern data are above the intermittent to bubbly transition line of the calculated T_{TD} values (Eq. 1.36) and the values of the Martinelli parameter (X) of the flow pattern data are greater than the intermittent to annular flow or bubbly to annular flow transition value of $X = 1.6$, then the observed flow pattern is bubbly flow pattern.

In Figure 4.10, observed stratified flow pattern data points were compared with their calculated positions on the Taitel & Dukler map. All of the observed data points (13

data points) were below the stratified wavy (SW) curve. Thus, we can conclude from this result that the observed flow pattern is stratified flow pattern.

Figures 4.11 show the comparisons of Taitel & Dukler map with the observed wavy flow pattern data. Figure 4.11 (a) shows that some of the observed wavy flow pattern data were on the stratified wavy (SW) curve. Thus, the comparison of the observed flow pattern data and the K_{TD} curve did not provide enough information for the flow pattern judgement. Figure 4.11 (b) shows the calculated F_{TD} values of the wavy to annular and wavy to intermittent (plug or slug) transitions for the observed wavy flow pattern data. All of the observed data points (13 data points) were below the line of F_{TD}

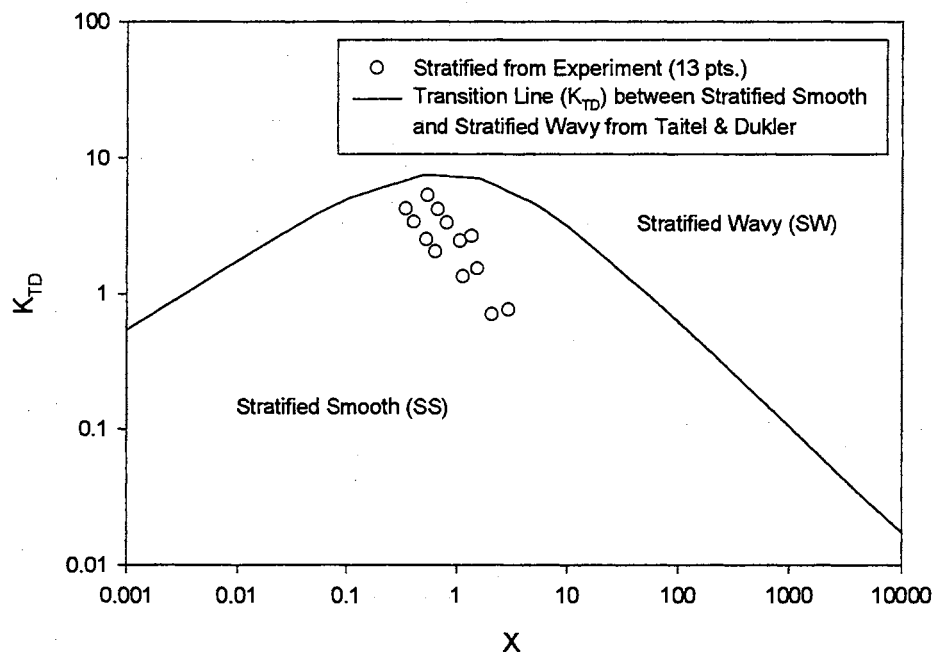
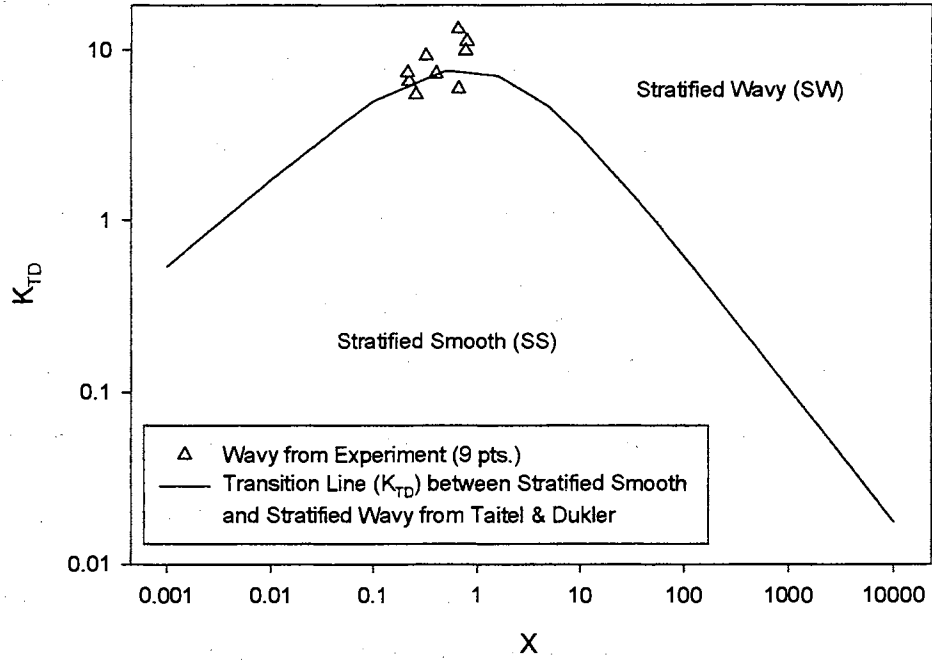
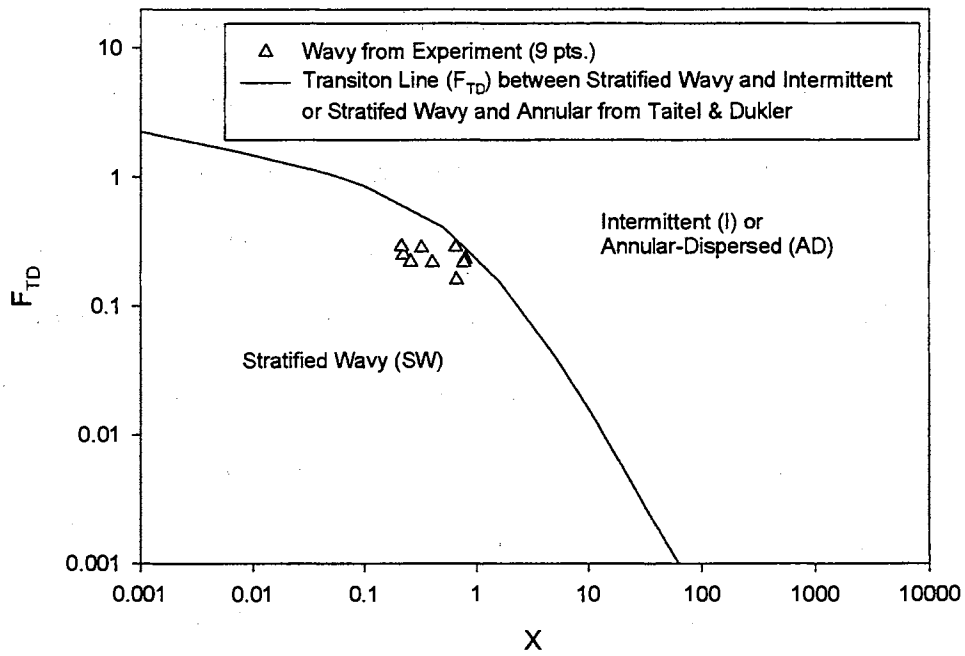


Figure 4.10 Comparison of Taitel & Dukler Map with Stratified Flow Pattern Data



(a)



(b)

Figure 4.11 Comparisons of Taitel & Dukler Map with Wavy Flow Pattern Data

transition values. Therefore, from this result, we can confirm that the observed flow pattern is wavy flow pattern.

Experimentally observed wavy/slug transition flow pattern data is compared with the calculated position on the Taitel and Dukler map in Figure 4.12. As can be seen from this figure, three of seven data points were just below the line of wavy to annular and wavy to intermittent (plug or slug) transitions, and three of seven data points for F_{TD} values were close to the transition line of wavy to intermittent (plug or slug) transition curve. Thus, we can conclude that the observed flow pattern is wavy to intermittent (plug or slug) transition flow pattern.

Comparisons of Taitel and Dukler map with experimentally observed slug flow pattern data are plotted on Figures 4.13. Figure 4.13 (a) shows that some of the observed slug flow pattern data were just below the line of stratified flow to wavy flow transition values, K_{TD} , and others were above the K_{TD} line. Thus, we could not judge the observed flow pattern from this comparison. The observed flow pattern was compared with the wavy to annular and wavy to intermittent transition line of F_{TD} in Figure 4.13 (b). Again, some of the observed slug flow pattern data were just below the line of wavy to annular and wavy to intermittent flow pattern transition values of F_{TD} , and others are above the F_{TD} line. Thus, we could not judge the observed flow pattern from this comparison. Figure 4.13 (c) shows the comparison of the observed flow pattern with the intermittent (slug or plug) to dispersed bubbly flow pattern transition (T_{TD}) and intermittent to annular dispersed flow pattern transition ($X = 1.6$). As can be seen from this comparison, all of the observed flow pattern data were below the line of intermittent to dispersed bubble transition, T_{TD} , and greater than the line value of the intermittent to annular dispersed

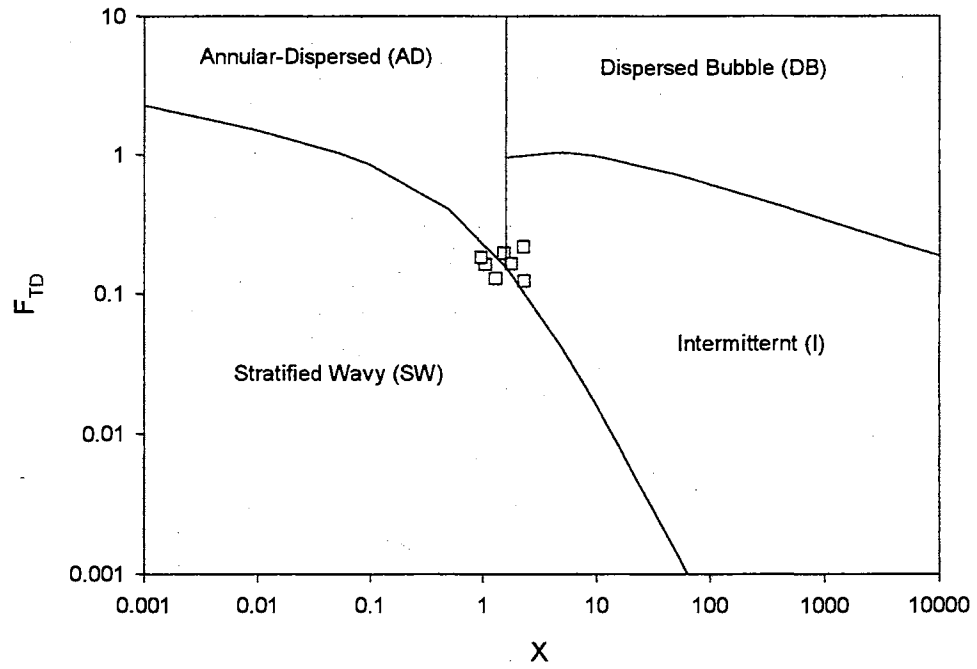


Figure 4.12 Comparison of Taitel & Dukler Map with Wavy/Slug Transition Flow Pattern Data

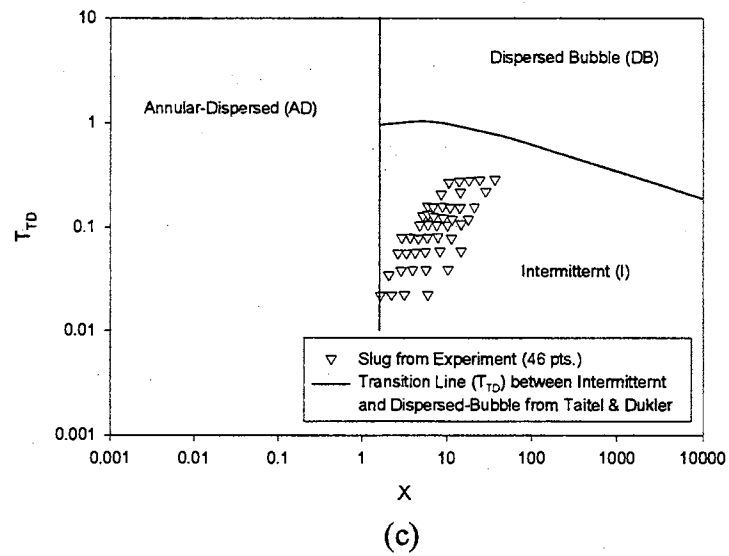
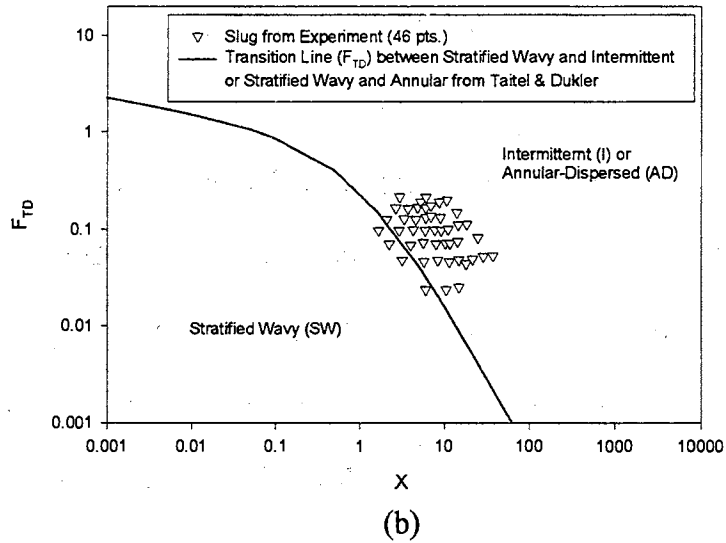
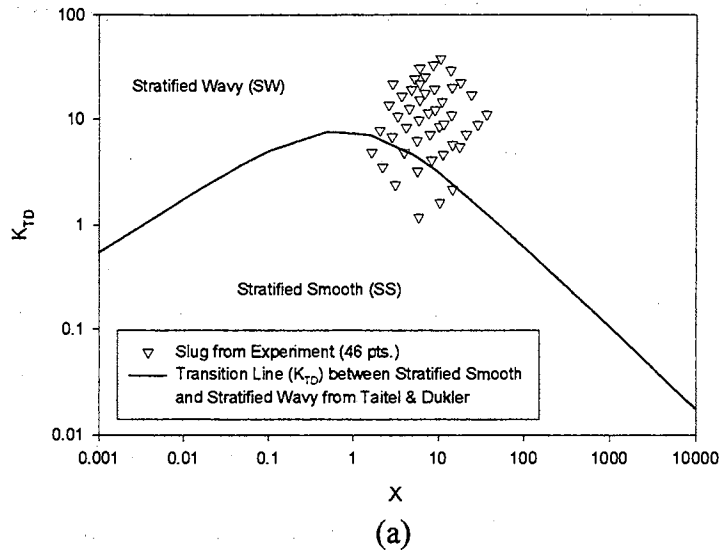


Figure 4.13 Comparisons of Taitel & Dukler Map with Slug Flow Pattern Data

flow transition ($X = 1.6$). Therefore, we can conclude that the observed flow pattern is slug flow pattern.

Figure 4.14 shows the comparison of observed 14 data points of wavy/annular transition flow pattern data with their calculated position on Taitel & Dukler map. Some of the observed flow pattern data were just below the line of stratified wavy to annular-dispersed transition, some of them were on the line, and rest of them were slightly above the transition curve of F_{TD} . Also, all of the observed flow pattern data were less than the line value of the annular dispersed to intermittent flow transition ($X = 1.6$). Therefore, we can confirm from this comparison that the observed flow pattern is wavy to annular transition flow pattern.

In Figures 4.15, observed annular/bubbly and annular/bubbly/slug flow pattern data were compared with their calculated positions on Taitel and Dukler map. As can be seen from Figure 4.15 (a) all of the observed flow pattern data were above the line of stratified wavy to annular-dispersed and stratified wavy to intermittent transition, F_{TD} . Thus, the right flow pattern can not be decided from this comparison. Figure 4.15 (b) shows the comparison between the observed flow pattern and the calculated positions (T_{TD}) on intermittent to annular-dispersed transition line ($X = 1.6$) and intermittent to dispersed bubble transition line, T_{TD} . All of the observed flow pattern data were well below the transition line of intermittent to dispersed bubbly flow patterns, and were slightly larger than the value of $X = 1.6$ for intermittent to annular-dispersed flow pattern transition line. From these comparisons, we may conclude that the observed flow pattern is either annular/bubbly or annular/bubbly/slug transition flow pattern.

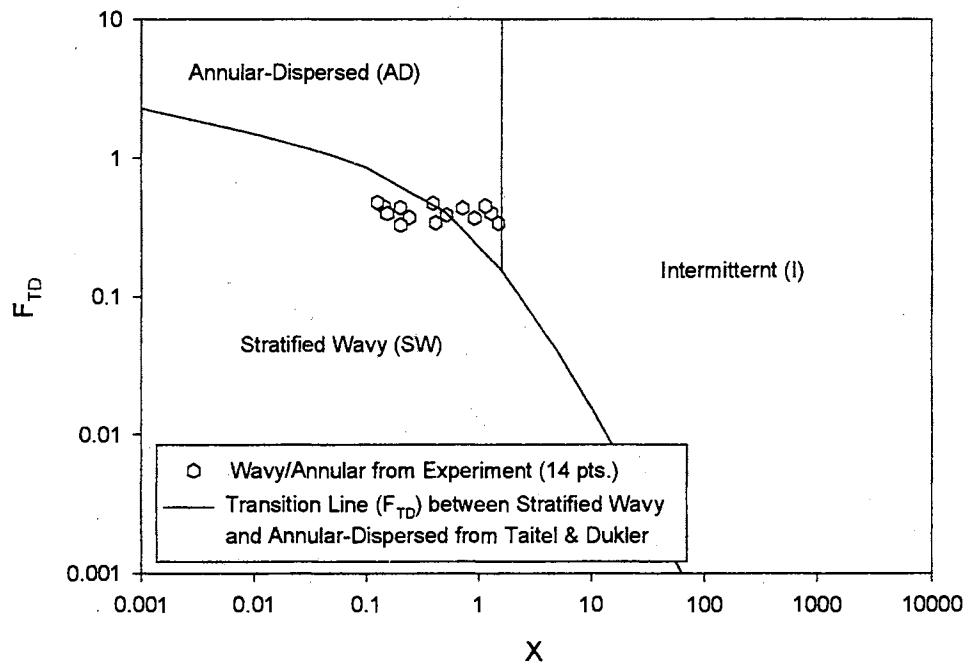


Figure 4.14 Comparison of Taitel & Dukler Map with Annular/Wavy Transition Flow Pattern Data

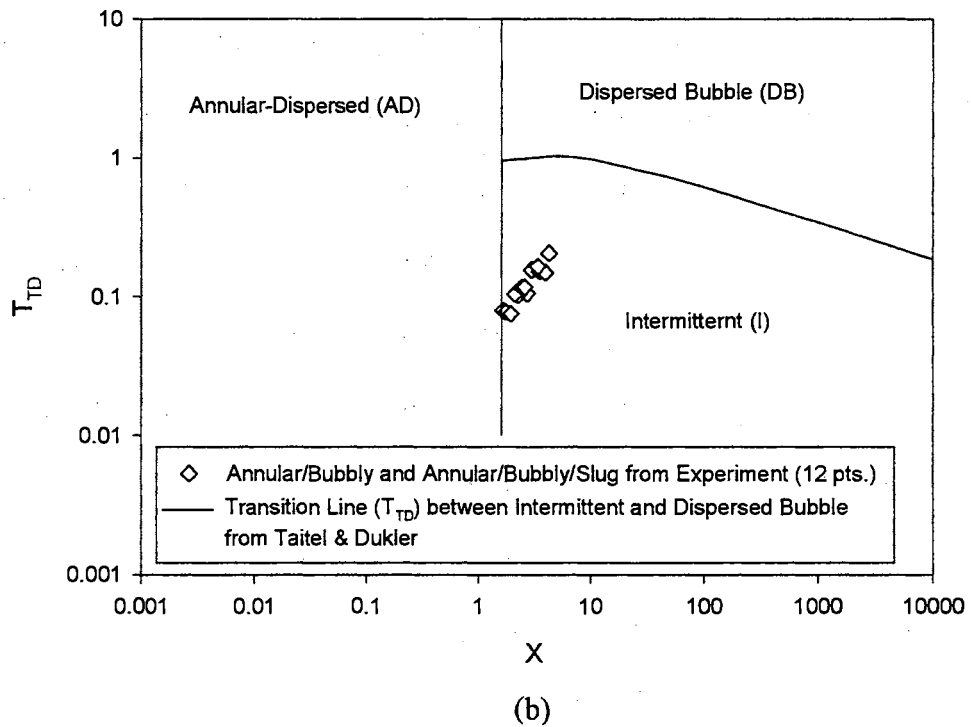
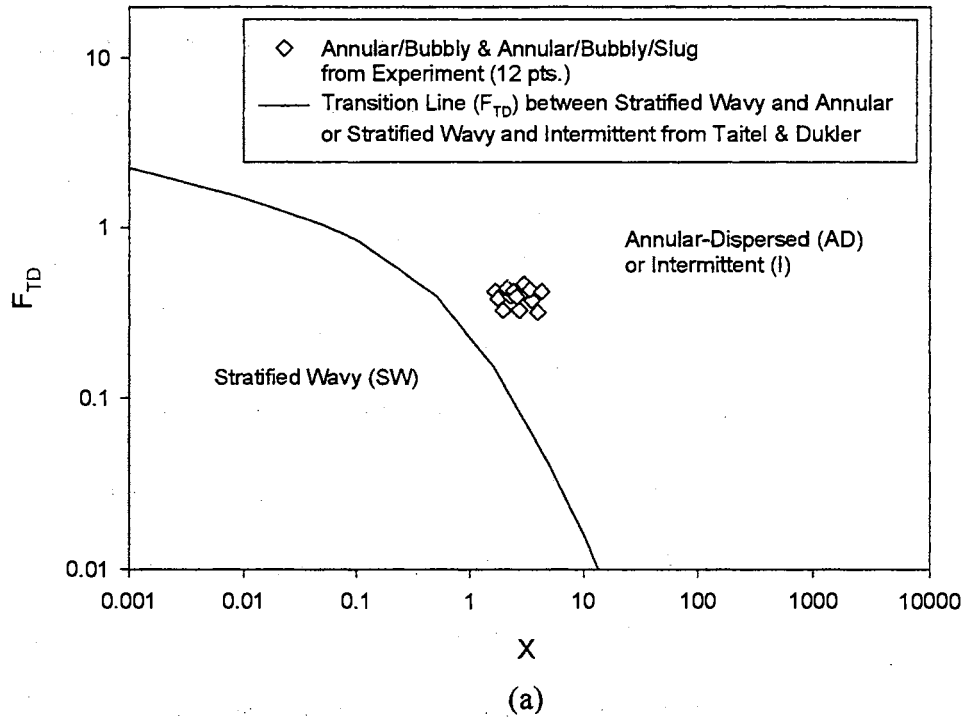


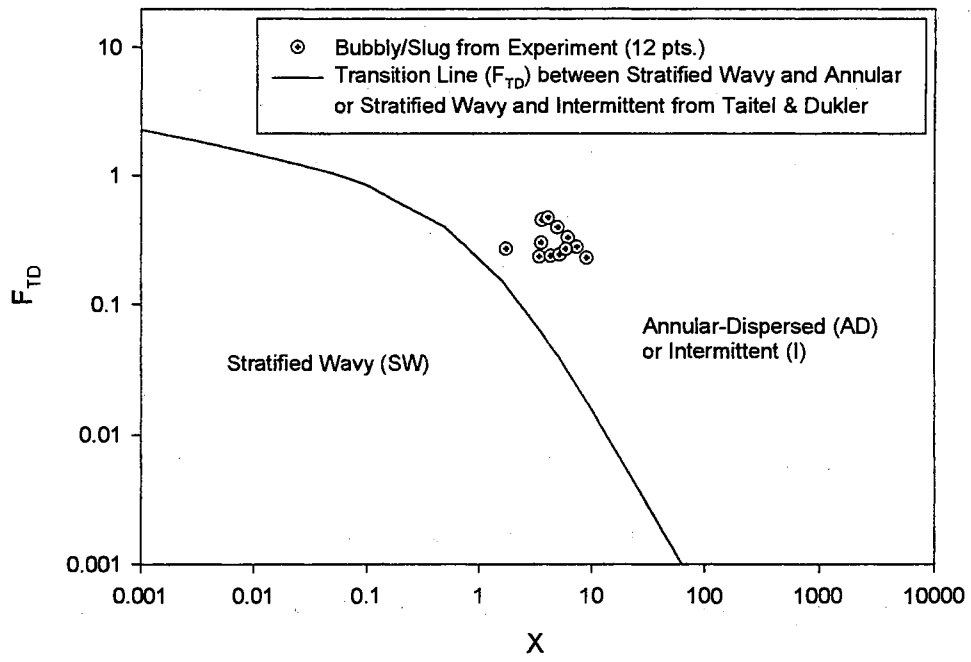
Figure 4.15 Comparisons of Taitel & Dukler Map with Annular/Bubbly and Annular/Bubbly/Slug Flow Pattern Data

In Figures 4.16, observed bubbly/slug flow pattern data were compared with their calculated positions on Taitel & Dukler map. As can be seen from Figure 4.16 (a) all of the observed flow pattern data were above the line of stratified wavy to annular-dispersed and stratified wavy to intermittent transition, F_{TD} . Thus, we can not decide the right flow pattern from this comparison. Figure 4.16 (b) shows the comparison between the observed flow pattern and the calculated positions (T_{TD}) on intermittent to annular-dispersed transition line ($X = 1.6$) and intermittent to dispersed bubble transition line. All of the observed flow pattern data were quite below the transition line of intermittent to dispersed bubbly flow patterns, and were larger than the value of $X = 1.6$ for intermittent to annular-dispersed flow pattern transition line. From these comparisons, we may conclude that the observed flow pattern is bubbly/slug transition flow pattern.

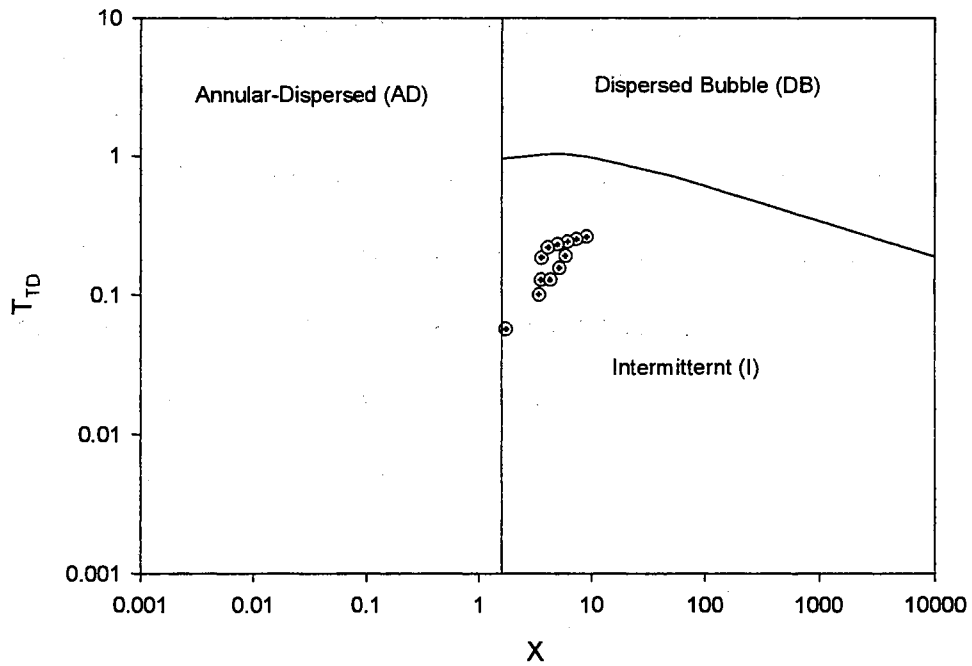
Next, all of the measured flow pattern data will be plotted along with the mass flow rates of air and water. Based on this plot, an attempt to classify each different flow pattern using the values of the mass flow rates will be introduced.

4.2.3 Flow Pattern Classification Using the Mass Flow Rates of Air and Water

Experimentally observed flow pattern data were plotted on their corresponding values of mass flow rates of air and liquid in Figure 4.17. Shaded lines in diagonal direction show possible flow pattern transitions. Under the conditions of small amounts of air and liquid mass flow rates, stratified flow patterns were observed. At moderate gas flow rates with the low liquid flow rates, wavy flow patterns were observed. Also, with the low liquid flow rates together with relatively high air flow rates, annular/wavy transitional flow patterns were observed. Next, with moderate to relatively high liquid flow rates together with low to moderate air flow rates, slug flow patterns were observed.



(a)



(b)

Figure 4.16 Comparisons of Taitel & Dukler Map with Bubbly/Slug Flow Pattern Data

With relatively moderate mass flow rates of both air and water, wavy/slug transitional flow patterns were observed. With relatively high liquid flow rates mixed with high air flow rates, either bubbly/slug or annular/bubbly/slug transitional flow patterns were observed. However, it was very difficult to clearly distinguish the location of either bubbly/slug or annular/bubbly/slug flow patterns on the mass flow rate flow pattern map of Figure 4.17.

Table 4.7 shows the minimum and maximum values of air and water mass flow rates according to the different flow pattern classifications. These minimum and maximum values are based on the rectangular shapes which were plotted on Figure 4.17. The rectangles were constructed by connecting more than three data points at which same flow patterns were observed. With these rectangular shapes, a desired flow pattern can be easily controlled by taking the amounts of air and liquid inside the minimum and maximum straight lines in the rectangle. This way the ambiguity in judging the right flow pattern can be avoided.

Table 4.7 also shows the number of experimental data points that has been obtained for the two-phase heat transfer experiments. Those numbers are based on the area occupied in Figure 4.17. Due to the large area and the shape of the slug flow pattern on Figure 4.17, two rectangles were plotted on this figure for slug flow and two different minimum and maximum values of air and liquid mass flow rates are suggested in Table 4.7. It should be mentioned that due to the small area of wavy/slug flow pattern and the difficulty of clearly controlling the mass flow rates of air and liquid based on the irregular shape of the boundaries on Figure 4.17, no number of data points for the wavy/slug flow pattern was assigned in Table 4.7. The suggested limits for the mass flow rates of air and

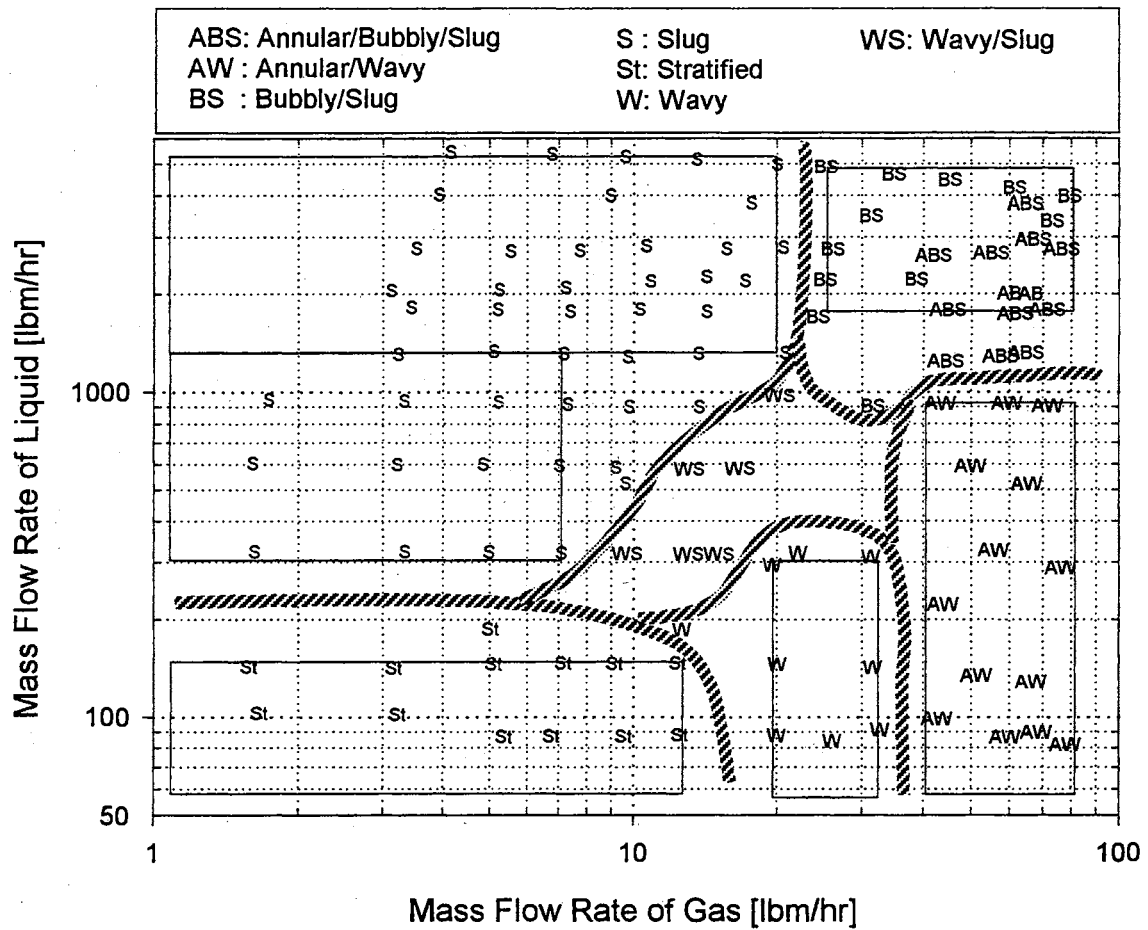


Figure 4.17 Observed Flow Pattern Data as a Function of the Corresponding Mass Flow Rates of Air and Water

Table 4.7 Minimum and Maximum Values of the Air and Water Mass Flow Rates According to the Different Flow Patterns and Number of Experimental Data Points Taken

\dot{m}_G [lbm/hr]		\dot{m}_L [lbm/hr]		Expected Flow Pattern	Prospective Number of Data Points
Min.	Max.	Min.	Max.	All of the Flow Patterns	150
0	12	0	147	Stratified	-
0	7	300	1300	Slug	25
0	20	1300	5460	Slug	30
20	32	0	310	Wavy	20
10	30	300	800	Wavy/Slug	-
24	80	1080	4890	Bubbly/Slug or Annular/Bubbly/Slug	35
43	80	0	925	Annular/Wavy	40

water in wavy/slug flow pattern in Table 4.7 are somewhat arbitrary and the mass flow rates of air and water should be carefully adjusted in order to generate clear wavy/slug transitional flow pattern. Also, due to the difficulty of applying low wall heat flux (< 350 amperes) to the test section, no heat transfer measurement in stratified flow pattern was obtained. Since, both of the gas and liquid flow rates are relatively quite small, there was the strong possibility of boiling due to the continuous increase of the top surface temperature of the inside pipe wall. This situation could cause damage to the test section. Thus, no heat transfer measurement in stratified flow pattern was assigned in Table 4.7.

Through out this section, the observed flow patterns, comparisons of the observed flow pattern data with the Taitel and Dukler (1976) map, and an attempt to classify the flow patterns with the aid of the mass flow rates of air and water were presented. In the next section, the experimental results of air-water two-phase heat transfer measurements and comparisons of the experimental data with previous studies, and finally recommended correlations for the two-phase heat transfer coefficients in horizontal pipes will be introduced.

4.3 Two-Phase Heat-Transfer Results

In this section, the results of air-water two-phase heat transfer data covering wavy and slug flow patterns, and wavy/annular, slug/bubbly, and annular/bubbly/slug transitional flow patterns are presented. First, the ranges of the experimental data taken are described and the general behavior of the two-phase heat transfer results are discussed. Then, the data for two-phase heat transfer coefficients were compared with the data available from the open literature (refer to Table 1.14). Also, the two-phase heat transfer coefficients from the experiment were compared with previously recommended correlations (Kim et al. 1999c, Kim et al. 2000). At the end of this section, the recommended correlations for two-phase heat transfer coefficients in horizontal pipes are introduced.

4.3.1 Two-Phase Air-Water Experimental Data

Table 4.8 shows a summary of the air-water heat transfer experimental data taken under steady-state conditions with uniform wall heat flux. This table shows the flow

Table 4.8 Summary of the Air-Water Experimental Data

	\dot{m}_L	V_{SL}	Re_{SL}	\dot{m}_G	V_{SG}	Re_{SG}	X	T_{MIX}	P_{MIX}	ΔP	P_G	α	Pr_L	\bar{h}_{TP}	Q''	Heat Balance Error
	[lbm/hr]	[ft/sec]		[lbm/hr]	[ft/sec]			[°F]	[psi]	[inH ₂ O]	[psi]			[Btu/hr-ft ² °F]	[Btu/ft ² -hr]	[%]
Wavy Flow Pattern (20 data points)																
Min.	114.57	0.08	636	21.33	4.85	6754	0.32	61.45	0.27	0.66	19.73	0.83	6.63	170.25	1093	4.68
Max.	312.58	0.21	1829	31.14	5.16	9887	0.85	76.49	0.87	2.33	37.33	0.90	6.99	749.90	1664	21.49
Avg.	190.54	0.13	1098	25.38	5.02	8049	0.53	67.30	0.47	1.07	27.33	0.87	6.74	417.33	1355	13.70
Wavy- Annular Transitional Flow Pattern (41 data points)																
Min.	408.71	0.28	2163	39.53	4.82	12615	0.76	57.28	2.02	1.37	40.52	0.76	6.30	417.65	2486	-3.13
Max.	954.95	0.65	4985	60.43	6.95	19132	1.52	67.90	3.30	6.72	67.69	0.82	6.99	724.65	2899	20.02
Avg.	689.41	0.47	3611	49.45	5.89	15678	1.19	61.36	2.60	5.14	55.61	0.78	6.57	531.11	2764	8.65
Slug Flow Pattern (53 data points)																
Min.	343.74	0.23	2468	1.68	0.89	536	2.13	71.37	0.06	0.34	0.72	0.27	5.2	171.55	2202	-18.99
Max.	5179.73	3.51	35503	20.36	5.0	6448	41.59	99.76	7.6	12.93	20.11	0.78	6.98	1370.58	4643	18.43
Avg.	2269.63	1.54	15012	8.04	3.04	2545	10.74	82.54	2.14	5.30	5.77	0.56	6.26	567.51	3709	1.85

Table 4.8 Summary of the Air-Water Experimental Data - Cont'd

	\dot{m}_L	V_{SL}	Re_{SL}	\dot{m}_G	V_{SG}	Re_{SG}	X	T_{MIX}	P_{MIX}	ΔP	P_G	α	Pr_L	\bar{h}_{TP}	Q''	Heat Balance Error
	[lbm/hr]	[ft/sec]		[lbm/hr]	[ft/sec]			[°F]	[psi]	[inH ₂ O]	[psi]			[Btu/hr-ft ² °F]	[Btu/ft ² -hr]	[%]
Slug-Bubbly or Annular/Bubbly/Slug Transitional Flow Pattern (36 data points)																
Min.	1233.54	0.84	7842	21.54	4.0	6857	2.79	54.54	3.11	2.43	29.93	0.47	6.46	574.35	3425	-20.55
Max.	4602.14	3.12	26140	66.82	5.82	21213	10.13	75.65	17.96	12.93	80.73	0.68	7.8	1307.15	4539	18.26
Avg.	3156.48	2.14	17153	39.02	4.87	12436	5.76	65.31	9.48	12.12	50.47	0.57	6.94	885.36	3796	-1.65
Overall Data (150 data points)																
Min.	114.57	0.08	636	1.68	0.89	536	0.32	54.54	0.06	0.34	0.72	0.27	5.2	170.25	1093	-20.55
Max.	5179.73	3.51	35503	66.82	6.95	21213	41.59	99.76	17.96	12.93	80.73	0.9	7.8	1370.58	4643	21.49
Avg.	1773.34	1.20	10555	29.11	4.52	9242	5.58	70.58	3.80	6.33	32.99	0.66	6.57	613.82	3158	4.45

patterns observed, number of data points taken in each flow pattern, the minimum, maximum, and averaged values of the following parameters: mass flow rates of liquid and gas along with their superficial velocities and Reynolds numbers, Martinelli parameter (X), temperature and pressure of gas-liquid mixture, two-phase pressure drop along the test section (ΔP), supplied gas pressure (P_G), void fraction (α), liquid Prandtl number, mean heat transfer coefficient (\bar{h}_{TP}), applied heat flux (Q''), and the heat balance error between the applied wall heat flux and the enthalpy balance. All of the measured values of gas and liquid mass flow rates were within the range of those in Table 4.7 for each specific flow pattern. More details on the experimental data listed on Table 4.8 can be found in Appendix C.

Figure 4.18 (a) shows the measured temperatures of the fluid bulk inlet (T_{B_in}) and outlet (T_{B_out}) of the test section and the water storage tank (T_{Tank}) for one of the test runs (Run #7113) listed in Appendix C. A uniform heat flux (568 amps with a 4.56 volts of voltage drop across the test section) was applied to the test section. Figure 4.18 (a) indicates the variations of those temperatures according to the measured period of time and Figure 4.18 (b) indicates the variations of temperature difference between the inlet and outlet fluid bulk temperatures during the measurement period. As can be seen from these figures, during the measurement time period the temperature difference between the inlet and outlet fluid bulk temperatures were maintained almost constant (within $\pm 0.3^\circ\text{C}$). Thus, it can be concluded from this result that a steady-state condition was reached and maintained across the test section.

Figures 4.19 show the time averaged wall temperatures from the 10 stations, the

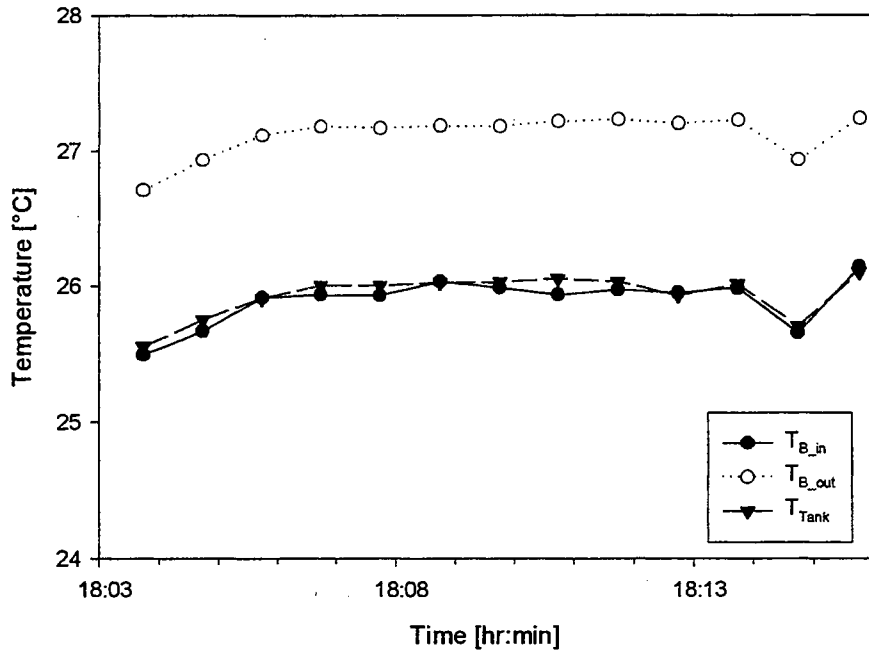


Figure 4.18 (a) Variation in Bulk Inlet (T_{B_in}) and Outlet (T_{B_out}) Temperatures of the Fluid and Water Temperature of the Storage Tank (T_{Tank}) During the Measurement Period

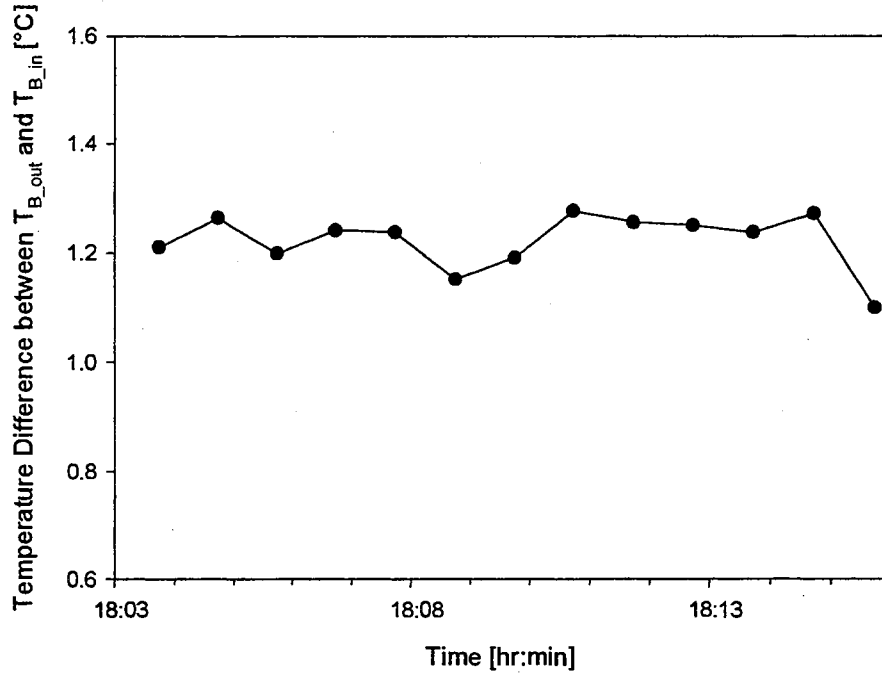


Figure 4.18 (b) Variation of Temperature Difference between Bulk Inlet (T_{B_in}) and Outlet (T_{B_out}) of the Fluid with the Measurement Time

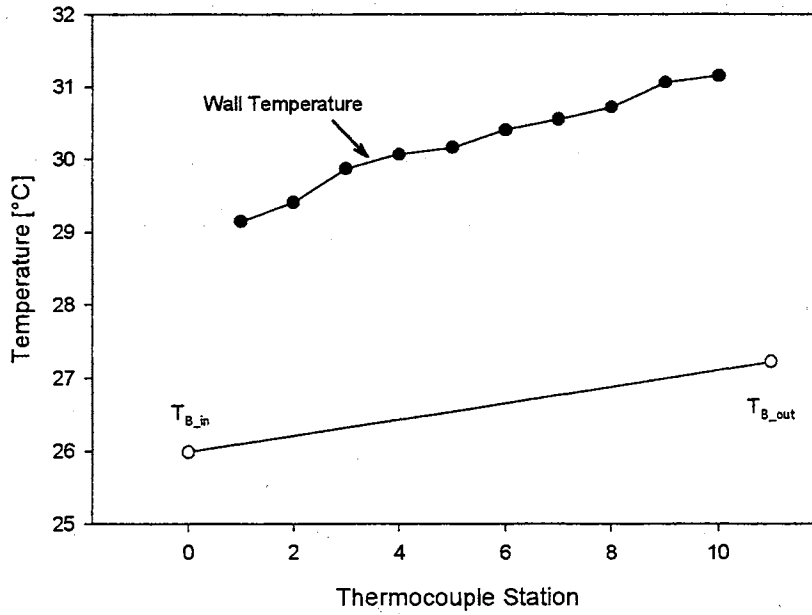


Figure 4.19 (a) Averaged Wall Temperatures of the Thermocouple Stations and Bulk Inlet (T_{B_in}) and Outlet (T_{B_out}) Temperatures of the Fluids

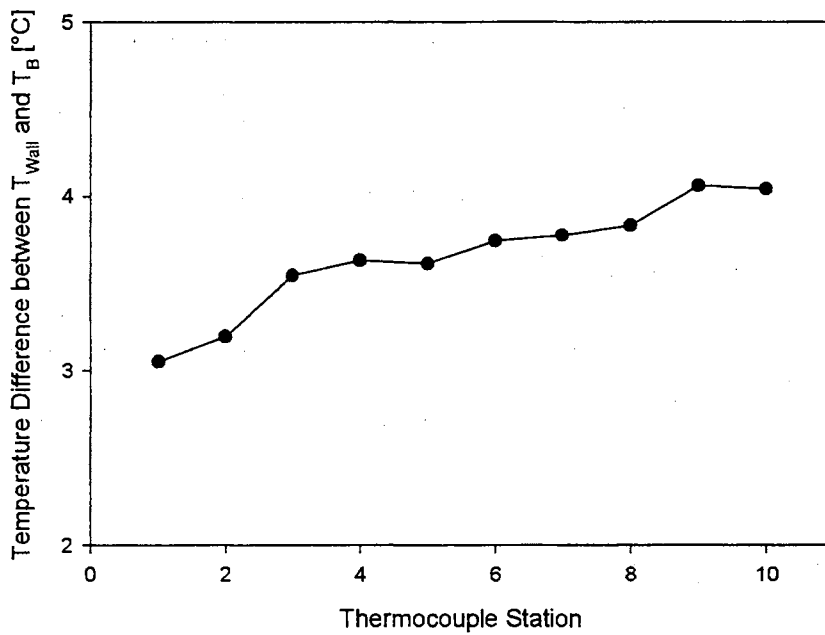


Figure 4.19 (b) Temperature Difference between the Averaged Wall (T_{wall}) and Fluid Bulk (T_B) of the Test Section

bulk fluid inlet and outlet temperatures, and the temperature difference between the wall and the fluid bulk at each station for the test Run #7113 listed in Appendix C. Figure 4.19 (b) indicates that the temperature difference between the wall and the bulk temperatures increased from the inlet to exit of the test section. Thus, it may be concluded that unlike the single-phase heat transfer results, as was shown in Figure 3.11 (b), the thermally fully developed condition cannot be established in the two-phase heat transfer runs with a uniform heat flux boundary condition. It should be mentioned here that even though the pressure drops (ΔP) across the test section were always measured during the two-phase test runs, this information will not be used and analyzed in this study and is gathered for other two-phase flow related studies.

Figure 4.20 shows the local heat transfer coefficients along the test section in slug flow pattern for those test runs listed in Table 4.8. Comparing the single-phase local heat transfer coefficient results plotted in Figure 4.1 with this figure, we may conclude from this result that the local heat transfer coefficient along the section does not decrease smoothly and there is no clear location for thermally fully developed region as can be seen from Figures 4.20. Thus, the mean heat transfer coefficient (\bar{h}_{TP}) is evaluated by averaging the local heat coefficient (h_{TP}) along the test section. This is similar to the procedures used by other two-phase flow researchers (Aggour, 1978; Rezkallah, 1986; Vijay, 1978).

Figure 4.21 shows the variation of mean heat transfer coefficients as function of superficial Reynolds numbers (Re_{SG} and Re_{SL}) for all of the air-water data points listed in Table 4.8 and Appendix C. From this figure it can be seen that, generally, as the gas superficial Reynolds number (Re_{SG}) increases for a fixed liquid superficial Reynolds

number (Re_{SL}), the heat transfer coefficient increases. Some of the previous researchers also observed the increase in two-phase heat transfer as the gas Reynolds number increases for a fixed liquid Reynolds number.

Zaidi and Sims (1986) observed from the results of their two-phase heat transfer experiment in a vertical pipe that the h_{TP} generally increased as the air flow rate was increased for each fixed liquid flow rate. Also, the increase in h_{TP} was more significant at low Re_{SL} than at high Re_{SL} . They explained the increase in h_{TP} , as suggested by Kudirka et al. (1965), by the turbulence level already present in the liquid stream. At low liquid

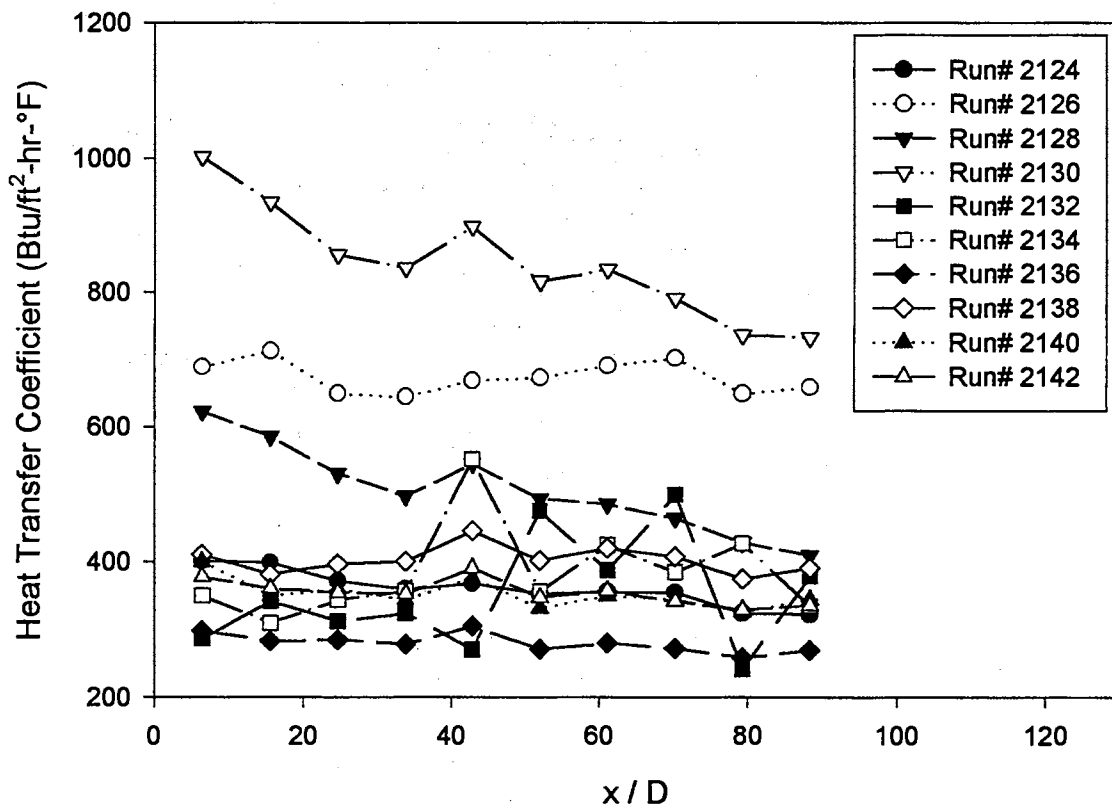


Figure 4.20 Local Heat Transfer Coefficients Along the Test Section for Test Runs Listed in Table 4.8

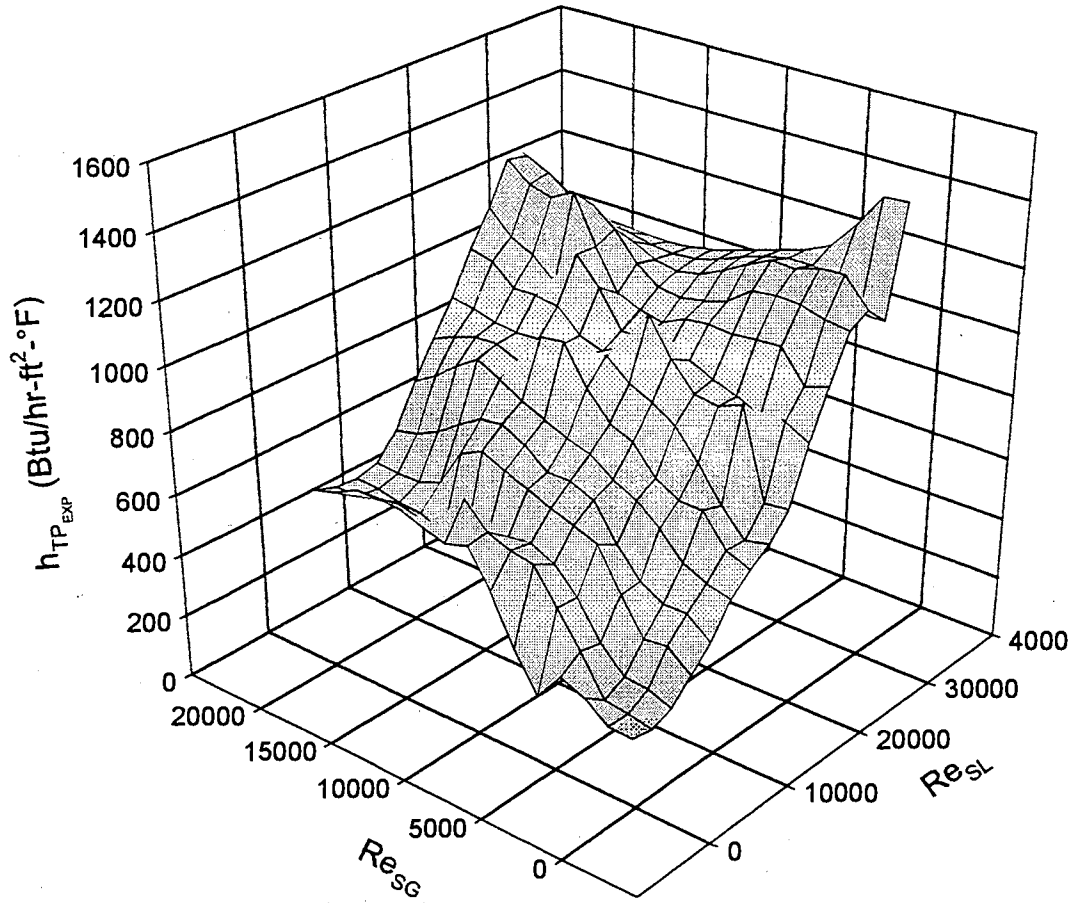


Figure 4.21 Variation of Mean Heat Transfer Coefficients with Superficial Reynolds Numbers (Re_{SL} and Re_{SG}) for All Flow Patterns Listed in Table 4.8

flow rates, the turbulence level in the liquid stream is small before being introduced into the gas stream. The introduction of gas phase into the liquid stream increases the turbulence level which results in a high heat transfer coefficient. However, at high Re_{SL} the turbulence level is already high and the effect of gas-phase on h_{TP} is not that pronounced.

Kudirka et al. (1965) observed the increase in h_{TP} caused by the addition of a gas phase into liquid flow from their air-water and air-ethylene glycol mixtures in a vertical pipe. They discussed the reasons for those increases in terms of the following possible mechanisms: liquid and mixture velocity increase due to the addition of the gas phase; increased turbulence and mixing action in the main stream due to continuous interaction of the two phases; and increased turbulence near the heated wall caused by gas bubbles, resulting in disturbance and decrease in the effective thickness of the viscous boundary sublayer by the fact that the eddies, presented in the wake of the rising bubbles, penetrate in the viscous sublayer. Groothuis and HENDAL (1959) mentioned in comparing their own air-oil and air-water results that the influence of air on heat transfer was most pronounced at the lowest Reynolds numbers because air would be more effective in promoting turbulence there.

Ravipudi and Godbold (1978) found from their experimental data of air-water and air-toluene mixtures in a vertical pipe that the introduction of air into the liquid increased the heat transfer coefficient substantially due to the reduction of the effective thickness of the viscous sublayer. They also found that h_{TP} was increased, reached a maximum and then decreased. The maximum in h_{TP} was observed to be in the transition zone between annular flow and mist flow. They explained that the highly turbulent motion of the gas-

liquid mixture with increasing amounts of air caused randomly distributed dry spots to appear on the wall and thereby decreased the heat transfer rate. Also, they attributed the decrease in h_{TP} at high Re_{SG} to the followings. First, the outlet liquid temperature decreased due to the mass transfer from liquid to air. Next, the h_{TP} did not increase in proportion to the increase in the temperature gradient. Finally, the measurement of two-phase mixture temperature was difficult.

From Fig. 4.21, we can also observe that there exists a maximum increase in h_{TP} as the Re_{SG} increases for a fixed liquid Re_{SL} . The value of this Re_{SL} is around 30000. For the Re_{SL} greater than about 30000, the increase in h_{TP} reached a maximum, then h_{TP} decreased as more air was added into the test section. Previously, Pletcher and McManus, Jr. (1968) also observed from air-water annular flow experiments in a horizontal pipe that h_{TP} passes through a maximum for a given water rate and then decreases as the air rate increases. They explained this trend as follows. As the air rate increases a countering mechanism comes into play which tends to reduce the heat transfer coefficients by depressing the final exit equilibrium temperature. As the ratio of air flow rate to water flow rate increases, more and more evaporation is possible. At some air flow rate, this latter mechanism begins to dominate. They also suggested that the decrease in h_{TP} is due to liquid entrainment at the higher air rates.

Figure 4.22 shows the trends of h_{TP} with the values of Re_{SG} and Re_{SL} in each different flow pattern. In wavy flow pattern, Fig. 4.22 (a), the h_{TP} increases relatively linearly as the Re_{SG} increases for a fixed liquid Re_{SL} . However, the h_{TP} is independent of Re_{SL} . The h_{TP} magnitude increased by about more than 5 times as Re_{SG} increased from 7000 to 10000. From these results, it can be concluded that the influence of air on heat

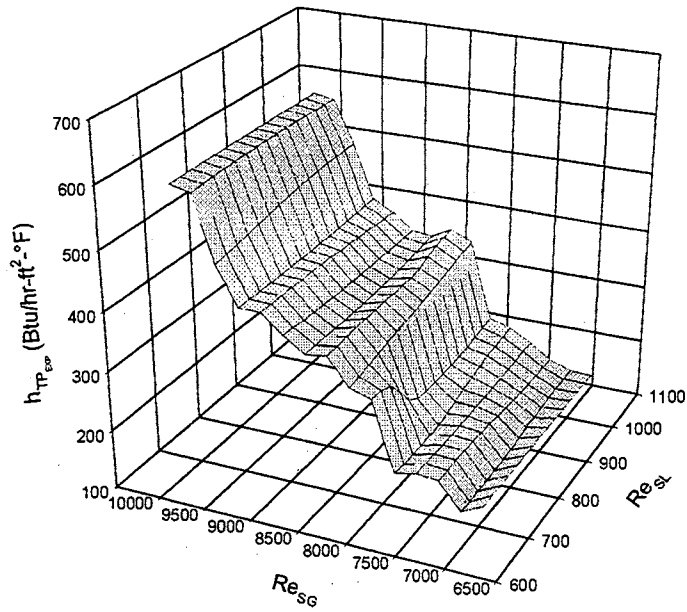


Figure 4.22 (a) Air-Water Two-Phase Heat Transfer Coefficients in Wavy Flow Pattern (20 Data Points)

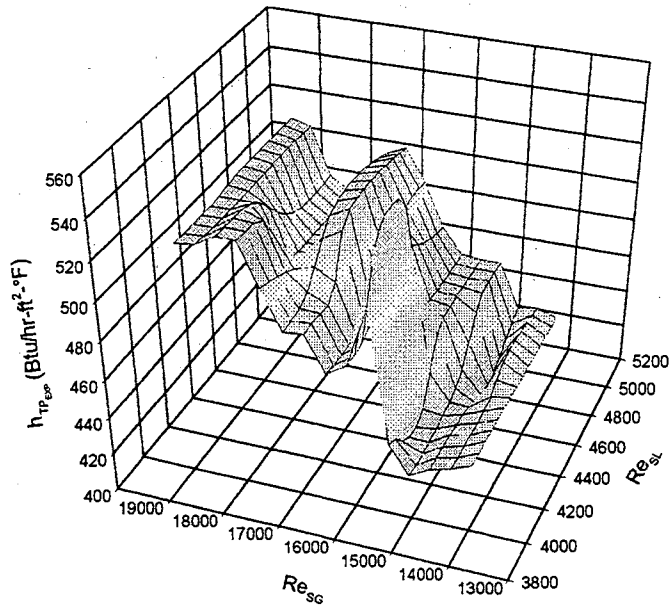


Figure 4.22 (b) Air-Water Two-Phase Heat Transfer Coefficients in Wavy/Annular Transitional Flow Pattern (41 Data Points)

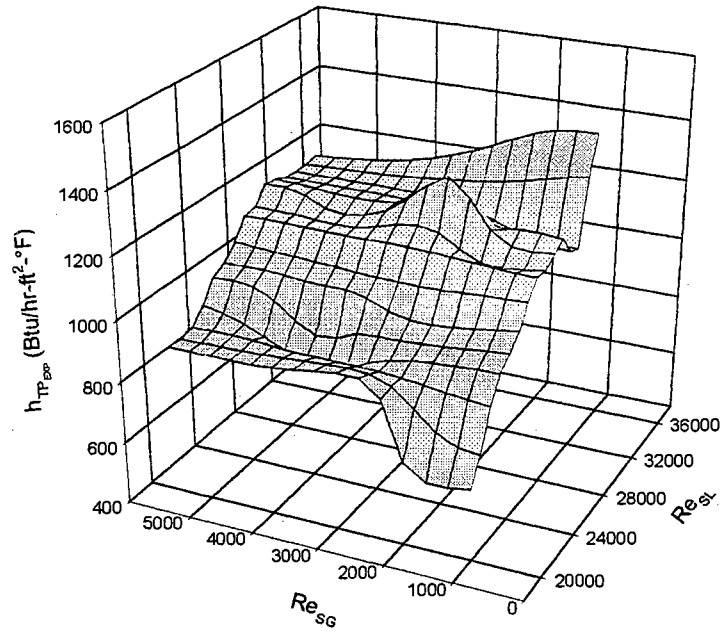


Figure 4.22 (c) Air-Water Two-Phase Heat Transfer Coefficients in Slug Flow Pattern (53 Data Points)

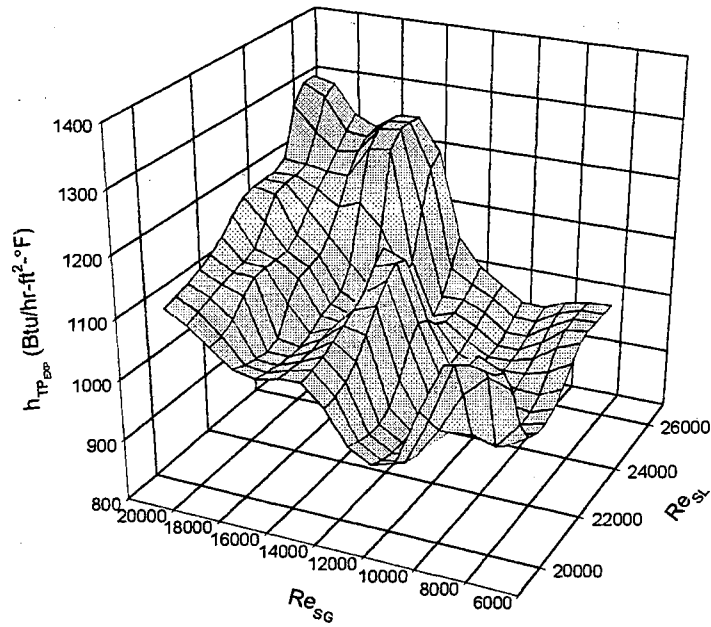


Figure 4.22 (d) Air-Water Two-Phase Heat Transfer Coefficients in Bubbly/Slug or Annular/Bubbly/Slug Transitional Flow Pattern (36 Data Points)

transfer is most pronounced at the lowest Re_{SL} because air would be more effective in promoting turbulence there. Similar observations were also made by Groothuis and Hendl (1959), Kudirka et al. (1965), and Zaidi and Sims (1986).

In wavy to annular transitional flow pattern, Fig. 4.22 (b), a relative maximum in h_{TP} exists as the Re_{SG} increases for a fixed liquid Re_{SL} . This mechanism can be explained by the following reasons suggested by Ravipudi and Godbold (1978) and Pletcher and McManus, Jr. (1968): the outlet liquid temperature decreased due to the mass transfer from liquid to air; the measurement for the two-phase mixture temperature was difficult; or the liquid entrainment at the relatively higher air rates reduced the exit mixture bulk temperature.

In slug flow pattern [Fig. 4.22 (c)] and slug to bubbly or annular/bubbly/slug transitional flow pattern [Fig. 4.22 (d)], the h_{TP} generally increases as either Re_{SG} or Re_{SL} increases. However, at high Re_{SL} in slug flow pattern the effect of gas-phase on h_{TP} is not pronounced since the turbulence level of the liquid is already high.

In this section, the trends of the mean heat transfer coefficients (\bar{h}_{TP}) evaluated from the air-water two-phase flow test runs for wavy and slug flow patterns and wavy/annular, slug/bubbly, and annular/bubbly/slug transitional flow patterns listed in Table 4.8 were presented and the supporting mechanisms for those trends were discussed. In the next section, mean heat transfer coefficients will be compared with the experimental data and correlations available from the literature. Then, at the end of the next section, recommended correlations for air-water two-phase heat transfer coefficients in a horizontal pipe are introduced.

4.3.2 Prediction of Air-Water Two-Phase Heat Transfer Experimental Data

Limited experimental data (one set of slug flow data from King, 1952 and one set of annular flow data from Pletcher, 1966) are available from the open literature. Slug flow air-water heat transfer experimental data in a horizontal pipe have been obtained from the current study and King (1952). Due to the capacity of the experimental setup in the current study, no annular flow pattern data could be achieved. It is desirable to see how well both sets of slug flow experimental data can be coincident. However, direct comparisons with King's (1952) experimental data are impossible. King's experimental range of the gas and liquid mass flow rates was much higher than that of this study. Also, his experiments were conducted under a uniform wall temperature boundary condition (steam heated test section) rather than a uniform wall heat flux boundary condition. Therefore, the next best approach would be to compare the results of predictions of these data by previously recommended heat transfer correlations.

Figure 4.23 shows the comparison of the predictions of Kim et al.'s (2000) vertical pipe correlation (see Eq. 2.11) with the 150 horizontal pipe experimental data points from current study and the 21 slug flow data points from King's (1952) horizontal pipe experiments. As shown in this figure, the previously recommended general correlation (Kim et al., 2000) for a vertical pipe regardless of flow pattern and fluid combination predicted the heat transfer coefficients quite well for the bubbly-slug and bubbly-slug-annular transitional flow data, which can be obtained in both vertical and horizontal pipes. All those predictions were within $\pm 30\%$ deviation band. However, the trend of predictions for the heat transfer coefficients in wavy flow or wavy-annular

transitional flow patterns were not correctly predicted. Since the complete separation between phases of gas and liquid occurred in the wavy flow and wavy-annular transitional flow patterns with relatively small flow rates of air and water, the heat transfer mechanism in a horizontal pipe is quite different from the heat transfer mechanism in a vertical pipe as can be seen from the heat transfer predictions for wavy flow and wavy-annular transitional flow patterns in Fig. 4.23.

It is interesting to note that there are similarities in the distribution of King's predicted results and the current study's slug flow data as shown in Fig. 4.23. Also, the predictions for both slug data are close to $\pm 30\%$ deviation band. Thus, the experimental data in only slug flow and the bubbly-slug transitional flow can be accurately predicted by the previously recommended general correlation for a vertical pipe (see Eq. 2.11) with minor adjustments of its constants.

Figure 4.24 shows the comparison of the predictions of the general form of the two-phase correlation (Eq. 2.9) with modified constants for the 21 slug experimental data points of King (1952) and 89 experimental data points of the current study. In order to predict those experimental data accurately, values of the leading coefficient (C), the exponents on the quality ratio term (m), and the void fraction term (n) were modified from the previously recommended values (Kim et al., 2000) using the least-squares method. Since the Prandtl number ratio term and the viscosity ratio term are typically used to represent large variation in physical properties and the influence of the properties of different fluids, the original vertical flow exponents were retained (refer to Table 2.12 and Table 4.9). This new recommended correlation yields a mean deviation of 0.36%, an rms deviation of 12.29%, and a deviation range of -25.17% to 31.31%. About 92% of the

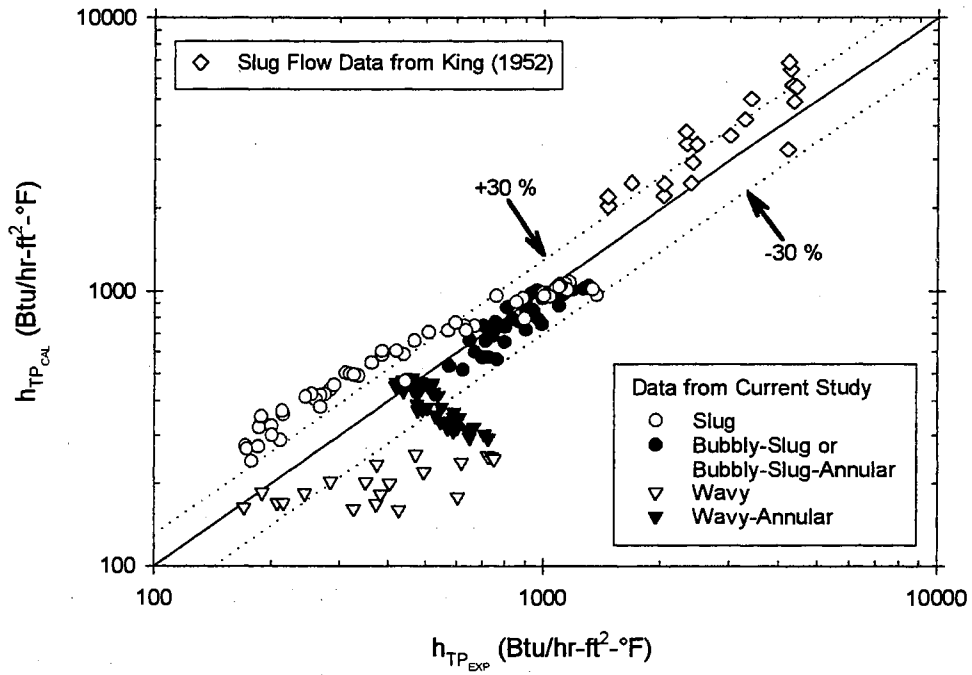


Figure 4.23 Comparison of Kim et al. (2000) Vertical Pipe Correlation with Current Horizontal Pipe Experimental Data (150 pts.) and King's (1952) Horizontal Pipe Data (21 pts.)

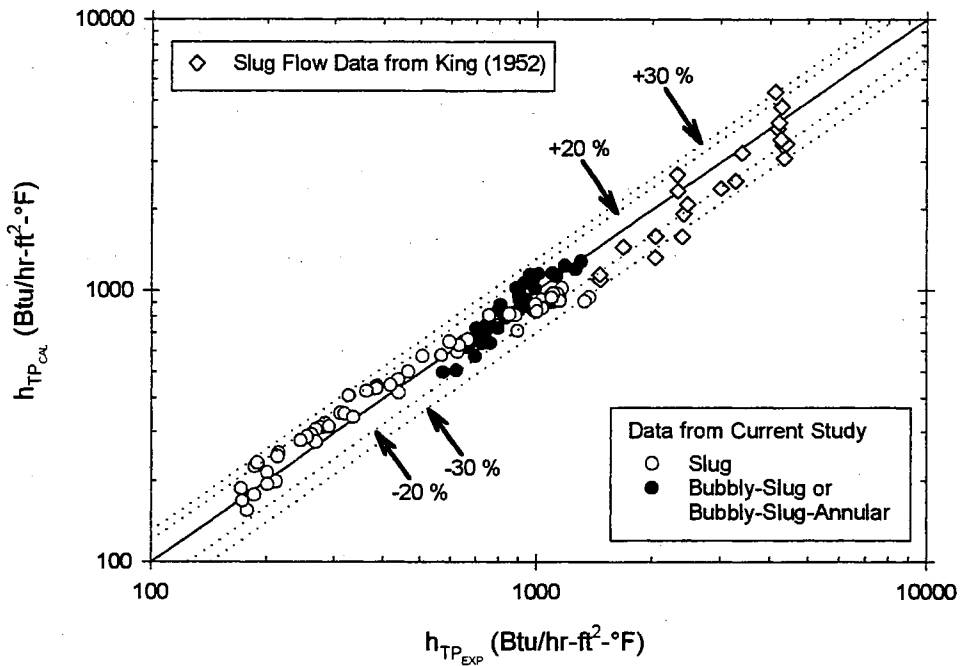


Figure 4.24 Comparison of Recommended Correlation for Slug Flow and Bubbly-Slug or Annular-Bubbly-Slug Transitional Flow with Current Horizontal Pipe Experimental Data (89 pts.) and King's (1952) Horizontal Pipe Data (21 pts.)

slug flow or its transitional flow experimental data (82 data points) were predicted with less than $\pm 20\%$ deviation. This new recommended correlation also predicted the slug flow data from King (1952) with a mean deviation of 12.79%, an rms deviation of 20.78%, and a deviation range of -31.13% to 35.13%.

A similar procedure was used for our other experimental data with wavy and wavy-annular transitional flow patterns. Table 4.9 shows the summary of the values of the leading coefficient (C) and exponents (m, n, p, q) in the recommended general form (Eq. 2.9) of the two-phase heat transfer correlation, the prediction results for each different flow pattern, and the range of each parameter in the general form of the correlation (Eq. 2.9). From this table, the following two important observations were made.

First, since the ranges of Re_{SL} for the wavy flow or wavy-annular transitional flow are lower than the suggested Re_{SL} range for the vertical heat transfer correlation (refer to Table 4.9 and Eq. 2.11), it was necessary for all of the five constants, the leading coefficient (C) and exponents (m, n, p, q) including the Prandtl number ratio term (p) and the viscosity ratio term (q), to be modified from the previously recommended values in order to predict the h_{TP} accurately. From this result, it can be concluded that the effects of the Prandtl number ratio term and the viscosity ratio term on h_{TP} in laminar flow regime of the liquid ($Re_{SL} < 4000$) are more pronounced than their effects on h_{TP} in the turbulent flow regime of the liquid. However, since the above observation is based on limited air-water experimental data in a horizontal pipe, this observation should be further verified by comparing the results with additional experimental data for different fluid combinations as they become available.

Second, since the range of the parameters for the wavy flow pattern are considerably different than those for the other flow patterns (see Table 4.9), it leads to much larger values for the recommended constants in the heat transfer correlation for this flow pattern. In particular, the difference between the relative magnitudes of the gas and liquid flow rates in this flow pattern (wavy) in comparison to other flow patterns (see Table 4.7) is mostly responsible for this large increase in the heat transfer correlation constants.

Graphical prediction results in wavy-annular transitional flow and wavy flow are also provided in Figure 4.25. From this figure, the improved predictions by the new values in Table 4.9 may be observed and compared with the previously recommended correlation for a vertical pipe (Eq. 2.11) shown in Fig. 4.23. As can be seen from this figure, the trends on h_{TP} for wavy-annular transitional flow and wavy flow are now correctly predicted (in contrast to the results in Fig. 4.23). 100% of the wavy-annular transition flow data (41 data points) and 80% of the wavy flow data (16 data points out of 20) were predicted with less than $\pm 20\%$. Figure 4.26 shows the predictions based on the recommended constants given in Table 4.9 for all of the flow pattern data from the current study. The overall deviation range of the prediction is from -25% to 34% , the overall mean deviation is about 1% , and the overall r.m.s. deviation is about 12% . 93% of all of the data (139 data points out of 150) from the current study were predicted with less than $\pm 20\%$.

Throughout this chapter, the details of the results for single-phase heat transfer, two-phase flow patterns from current horizontal experimental setup, and air-water horizontal heat transfer behavior in different flow patterns have been discussed. In the

next chapter, summary and conclusions of this study based on the current results and future recommendations will be introduced.

Table 4.9 Summary of the Values of the Leading Coefficient (C) and Exponents (m, n, p, q) in the Recommended Heat Transfer Coefficient Correlation (h_{TP}), the Results of Prediction, and the Parameter Range of the Correlation

General Form of the Two-Phase Heat Transfer Coefficient Correlation:														
$h_{TP} = (1-\alpha)h_L \left[1 + C \left(\frac{x}{1-x} \right)^m \left(\frac{\alpha}{1-\alpha} \right)^n \left(\frac{Pr_G}{Pr_L} \right)^p \left(\frac{\mu_G}{\mu_L} \right)^q \right]$														
Experimental Data	Value of C and Exponents (m, n, p, q)					Mean Dev. (%)	rms Dev. (%)	Number of Data within $\pm 20\%$	Range of Dev. (%)	Range of Parameter				
	C	m	n	p	q					Re_{SL}	$\left(\frac{x}{1-x} \right)$	$\left(\frac{\alpha}{1-\alpha} \right)$	$\left(\frac{Pr_G}{Pr_L} \right)$	$\left(\frac{\mu_G}{\mu_L} \right)$
Slug and Bubbly/Slug Bubbly/Slug/Annular 89 data points from Current Study	2.86	0.42	0.35	0.66	-0.72	0.36	12.29	82	-25.17 and 31.31	2468 and 35503	6.9×10^{-4} and 0.03	0.36 and 3.45	0.102 and 0.137	0.015 and 0.028
Slug 21 data points from King (1952)						12.79	20.78	10	-31.13 and 35.13	22500 and 119000	7.1×10^{-4} and 0.11	0.34 and 7.55	0.23 and 0.25	0.041 and 0.044
Wavy-Annular 41 data points from Current Study	1.58	1.40	0.54	-1.93	-0.09	1.15	3.38	41	-12.77 and 19.26	2163 and 4985	0.05 and 0.13	3.10 and 4.55	0.10 and 0.11	0.015 and 0.018
Wavy 20 data points from Current Study	27.89	3.10	-4.44	-9.65	1.56	3.60	16.49	16	-19.79 and 34.42	636 and 1829	0.08 and 0.25	4.87 and 8.85	0.102 and 0.107	0.016 and 0.021
All of the Data Points for Current Study (See Table 4.8) 150 data points	See Above for the Values for Each Flow Pattern					1.01	12.08	139	-25.17 and 34.42	636 and 35503	6.9×10^{-4} and 0.25	0.36 and 8.85	0.102 and 0.137	0.015 and 0.028

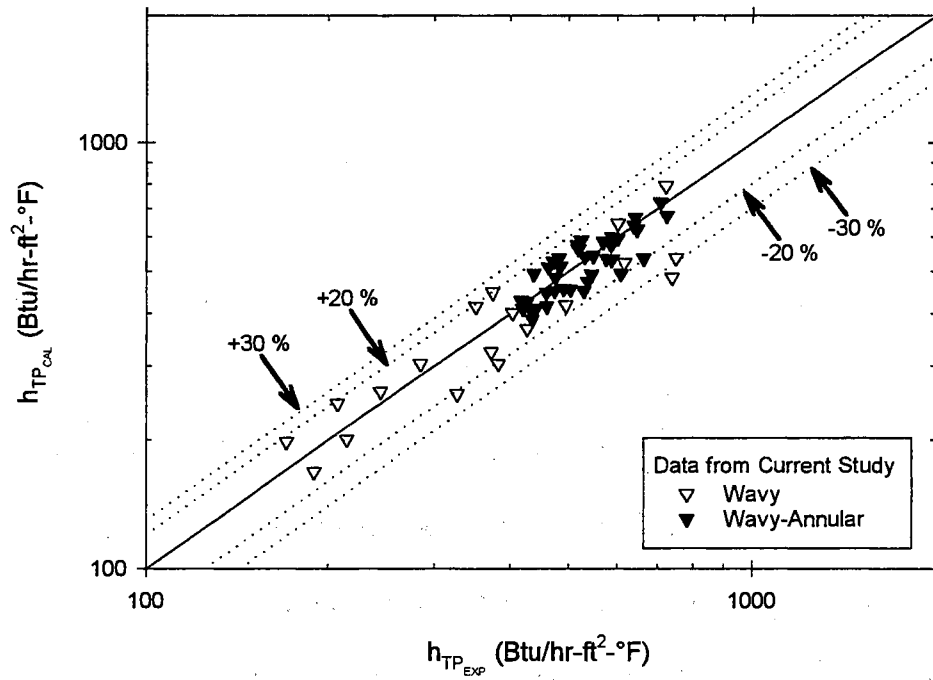


Figure 4.25 Comparison of Recommended Correlations with Wavy Flow Data (20 pts.) and Wavy-Annular Transitional Flow Data (41 pts.) from Current Study

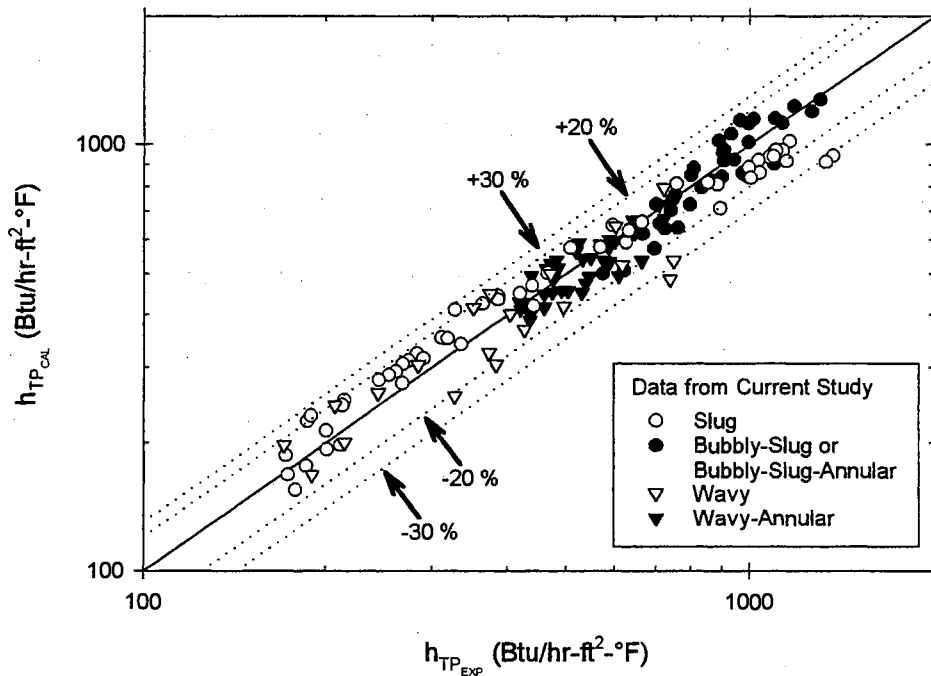


Figure 4.26 Comparison of Recommended Correlations with Data from Current Study (150 pts.)

CHAPTER V

SUMMARY, CONCLUSIONS AND RECOMMENDATIONS

To develop general two-phase heat transfer correlations which can be applied to different fluid combinations, flow patterns, and pipe orientations, an in-depth review of the current open literature was conducted, the existing two-phase heat transfer correlations were identified (Kim et al., 1999b), a robust correlation for vertical pipes was developed (Kim et al., 2000), a two-phase flow experimental setup for heat transfer and pressure drop measurements in a horizontal pipe was constructed, a flow pattern map for the flow patterns that can be observed from the present study's experimental setup was established, and the present study's air-water heat transfer experimental data in a horizontal pipe with different flow patterns were correlated using a modified version of our general vertical pipe heat transfer correlation. The results of these accomplishments were presented and discussed throughout this study. This chapter will briefly highlight these accomplishments, and recommendations for the future work will be presented.

5.1 Summary and Conclusions

This study was undertaken to develop a general two-phase heat transfer correlation(s) which is robust enough to span all or most of the fluid combinations, pipe

orientations, and flow patterns. To achieve this goal successfully, the following tasks were completed:

1. The general validity of the performance of the previously identified correlations (see Table 1.6) with and without considering the author-specified ranges of applicability was tested against the seven sets of extensive experimental data (see Table 2.1) identified from the open literature (Kim et al., 1997, Kim et al., 1999a).
2. In order to improve the applicability of the previously recommended correlations to different flow patterns and fluid combinations, each exponent of the key parameters that appeared in the previously recommended correlations was varied to investigate how critical that parameter is, and also to find out whether or not a changed exponent value can yield improved fits of the correlation to the experimental data (Kim et al., 1999b).
3. With the outcome of tasks 1 and 2 described above, a new improved two-phase heat transfer correlation was developed, and the performance of the correlation was compared against previously recommended correlations (Kim et al., 1999c, Kim et al., 2000).
4. In order to obtain a comprehensive set of two-phase heat transfer experimental data in a horizontal pipe covering several different flow patterns, an experimental setup was constructed.
5. To help in determining whether the test setup was working well enough to carry out two-phase heat transfer experiments, single-phase heat transfer data was taken and compared with predictions of well-known single-phase heat transfer correlations.

6. Based on the procedures of the flow pattern identification suggested by Taitel and Dukler (1976) and visual observation as appropriate, two-phase isothermal experimental data covering several different flow patterns was obtained and a new flow pattern identification map (Fig. 4.17) was suggested based on the gas and liquid mass flow rates of air and water in a horizontal pipe.
7. Air-water two-phase experimental data covering several different flow patterns in a horizontal pipe were obtained and the trend of the mean heat transfer coefficients was discussed based on the variation of the heat transfer coefficients with superficial Reynolds numbers (Re_{SG} and Re_{SL}).
8. The results of the mean heat transfer coefficients from the present study were compared with previously recommended correlations (Kim et al., 2000), and new heat transfer correlations for the present experimental data were suggested.

Based on the results of the completed tasks described above, the conclusions drawn may be summarized as follows:

1. In order to assess the validity of the two-phase heat transfer correlations, predictions of the identified 20 heat transfer correlations were compared with the seven sets of experimental data identified from the open literature with or without considering the restrictions of Re_{SL} and V_{SG}/V_{SL} accompanying the correlations (Kim et al., 1999a). There were no remarkable differences for the recommendations of the heat transfer correlations based on the results with or without the restrictions on Re_{SL} and V_{SG}/V_{SL} . The comparison results between those heat transfer correlations and the seven sets of experimental data are summarized in Table 2.4 for major flow patterns and in Table 2.5 for transitional flow patterns.

2. In order to improve the applicability of those recommended correlations to the available experimental data covering different flow patterns and fluid combinations, the exponent value on either one of the three key parameters (α , $1+V_{SG}/V_{SL}$, or V_{SG}/V_{SL}) which was typically added to most single-phase heat transfer correlations to account for two-phase effects on heat transfer was parametrically varied and optimized such that the final results were much improved fits of the correlations to the experimental data. The conclusions of this task may be summarized as follows:
- (a) Table 2.6 gives the summary of the optimal values for the exponent (n) of the key parameter in each of the six selected two-phase heat transfer correlations: for glycerin-air and water-freon 12 flows within vertical pipes, this study recommends the use of the Aggour (1978) correlation along with the optimal n values listed in Table 2.6 for the different fluid combinations; use of the Knott et al. (1959) correlation with the optimal n values listed in Table 2.6 for silicone-air and water-helium flows within vertical pipes and water-air slug flow within horizontal pipes; use of the Shah (1981) correlation along with the optimal n values listed in Table 2.6 for water-air flow within vertical pipes; and use of the Kudirka et al. (1965) correlation with the optimal n values for water-air annular flow within horizontal pipes.
- (b) Simplifying the modified exponent n values listed in Table 2.7 which depend on the four major flow patterns (bubbly, slug, froth, annular) in vertical pipes was successfully completed without significant loss of accuracy (see Table 2.8). The simplified exponent n values are 0.39 for the parameter $(1+V_{SG}/V_{SL})$ in the Shah (1981) correlation for predicting the water-air flow; -0.28 for the parameter $(1-\alpha)$ in

the Aggour (1978) correlation for glycerin-air flow; 0.29 for the parameter $(1+V_{SG}/V_{SL})$ in the Knott et al. (1959) correlation for silicone-air flow; 0.34 for the parameter $(1+V_{SG}/V_{SL})$ in the Knott et al. (1959) correlation for water-helium flow; and -0.82 for the parameter $(1-\alpha)$ in the correlation for water-freon 12 flow.

(c) Attempts to simplify the exponent values in the six two-phase heat transfer correlations according to the major flow patterns regardless of the fluid combinations used for predicting the five sets of two-phase heat transfer experimental data in vertical pipes were also made (see Table 2.9). Recommended exponent (n) values are 0.80 for the parameter $(1+V_{SG}/V_{SL})$ in the Shah (1981) correlation for bubbly flow; -0.60 for the parameter $(1-\alpha)$ in the Aggour (1978) correlation for slug flow; -0.43 for the parameter $(1-\alpha)$ in the Rezkallah and Sims (1987) correlation for froth flow; and 0.26 for the parameter (V_{SG}/V_{SL}) in the Ravipudi and Godbold (1978) correlation for annular flow.

(d) To further improve the predictive capabilities of the recommended correlations in predicting the two-phase heat transfer coefficient in each flow pattern, there appears to be at least one additional parameter, related to the effects of different fluid combinations on two-phase heat transfer, that might be required.

3. With the advanced knowledge accumulated from the above accomplishments using the previously introduced correlations, this study developed a new general semi-mechanistic heat transfer correlation (see Eq. 2.11), which can be applied to turbulent gas-liquid two-phase flow in vertical pipes having different fluid flow patterns and fluid combinations. The general correlation gives a very good representation of the 255 experimental data points referred to in Table 2.11 for water-air (Vijay, 1978),

silicone-air (Rezkallah, 1987), water-helium (Aggour, 1978), and water-freon 12 (Aggour, 1978) with a mean deviation of 2.54%, an rms deviation of 12.78%, and a deviation range of -64.71% to 39.55%.

4. A two-phase heat transfer experimental setup covering several different flow patterns in a horizontal pipe was built, and all of the details for the experimental setup are described in Chapter 3. From this experimental setup, flow rates of air and water, absolute pressure and temperature of air supplied, inlet and outlet of the mixture temperatures, mixture system pressure, differential pressure drops at ten pressure taps, and four local surface temperatures of the test section at ten thermocouple stations (see Fig. 4.3) could be successfully measured.
5. Single-phase heat transfer data from this experimental setup was obtained and compared with the calculated values from several well-established single-phase heat transfer correlations (see Tables 4.1 to 4.5). The experimental Nusselt numbers agreed well (within $\pm 20\%$) with those predicted by the correlations. Therefore, based on the overall comparisons of those correlations with the experimental data, it was concluded that the experimental data was sufficient to prove that the test setup can properly handle single-phase flow.
6. Two-phase flow experimental data covering several different flow patterns was collected from this experimental setup. Observed flow pattern data was compared with calculated locations on the flow pattern map suggested by Taitel and Dukler (1976). It was concluded from this comparison that all of the observed flow patterns were matched with the predicted flow patterns by Taitel and Dukler. Using the

collected experimental data, a new flow pattern map based on the mass flow rates of air and water was also introduced (see Fig. 4.17).

7. Figure 4.21 shows the variation of mean heat transfer coefficient with regard to superficial Reynolds numbers (Re_{SG} and Re_{SL}) for all of the data points in several flow patterns listed in Table 4.8. Since the introduction of the gas phase into the liquid stream increases the turbulence level and mixing action in the main stream due to continuous interaction of the two phases, the heat transfer coefficient generally increases as the Re_{SG} increases for a fixed Re_{SL} . At low liquid flow rates, since the turbulence level in the liquid stream was small before being introduced into the gas stream, the influence of air on h_{TP} was most pronounced by effectively promoting turbulence in the mixture, resulting in enhancement of the two-phase heat transfer. However, for the wavy to annular transitional flow pattern, a relative maximum in h_{TP} existed as the Re_{SG} increased for a fixed liquid Re_{SL} due to the decrease in the outlet liquid temperature caused by mass transfer from liquid to air or by liquid entrainment at the relatively higher air flow rates.
8. The general correlation developed for turbulent flow in a vertical pipe was applied to the experimental data obtained from the present study in a horizontal pipe. The general form of the correlation (Eq. 2.9) could be retained for the experimental data in a horizontal pipe since the predictions for the heat transfer coefficients for the bubbly-slug and bubbly-slug-annular transitional flow were within $\pm 25\%$ deviation without any modification of the constants of the general vertical correlation (see Fig. 4.23). However, for those flow patterns that do not exist in a vertical pipe, the constants in the general vertical correlation needed to be modified in order to predict the h_{TP}

accurately. Table 4.9 shows a summary of the values of the leading coefficient (C) and exponents (m, n, p, q) in the recommended general form (Eq. 2.9) of the two-phase heat transfer correlation. The overall deviation range of the prediction is from –25% to 34%, the overall mean deviation is about 1%, and the overall r.m.s. deviation is about 12%. 93% of all of the data (139 data points out of 150) from the current study were predicted with less than $\pm 20\%$ deviation.

9. As can be seen from Table 4.9, it was necessary for all of the five constants, the leading coefficient (C) and exponents (m, n, p, q) including the Prandtl number ratio term (p) and the viscosity ratio term (q), to be modified from the previously recommended values in order to accurately predict the h_{TP} in wavy flow and annular wavy transitional flow patterns. Thus, the effects of the Prandtl number ratio term and the viscosity ratio term on h_{TP} in the laminar flow regime of the liquid ($Re_{SL} < 4000$) are more pronounced than their effects on h_{TP} in the turbulent flow regime of the liquid. Also, as the range of the parameters for the wavy flow pattern are considerably different than those for the other flow patterns (see Table 4.9), this leads to the much larger values for the constants recommended to be used in the heat transfer correlation for this flow pattern. In particular, the difference between the relative magnitudes of the gas and liquid flow rates in this flow pattern (wavy) in comparison to other flow patterns (see Table 4.7) was mostly responsible for this large increase in the heat transfer correlation constants.

5.2 Recommendations

Throughout the present study, a robust two-phase heat transfer correlation for turbulent flow ($Re_{SL} > 4000$) in a vertical pipe with different fluid flow patterns and fluid combinations was developed. Also, with modified constants, the general form of the correlation could be successfully applied to the air-water experimental data in a horizontal pipe. However, based on the observations and conclusions made during this study, the followings are recommended:

1. Very limited two-phase heat transfer data in horizontal pipes with different flow patterns is available in the open literature (see Table 1.14). King (1952) provides data for slug flow and Pletcher (1966) for annular flow. In this study we focused on taking data for the slug related flow pattern which is more practical for the oil/gas industry and matched the capabilities of our experimental setup. In the future, heat transfer data in all of the flow patterns (see Fig. 4.17) with different fluid combinations should be collected. This would allow development of more comprehensive/robust correlation(s) for the two-phase heat transfer in horizontal pipes. To achieve this requires certain modifications to our existing experimental setup. Namely, adding a large pump (about 2 hp pump or \dot{m}_L [lbm/hr] = about 7000) for liquid flow and increasing the air compressor capacity (\dot{m}_G [lbm/hr] = about 500).
2. Presently, there is no two-phase heat transfer data in the open literature for inclined pipes as a function of inclination angle. Govier and Aziz (1973) explained that the effect of pipe inclination on pressure drop is high at relatively low gas flow rates but decreases with increasing gas flow rate. They concluded that at the lower gas and

liquid rates, the slug flow pattern is dominant in uphill flow while in the downhill case, the flow is usually in the stratified or wavy flow pattern. From these results, we can see that the two-phase heat transfer mechanisms for different pipe inclination angles may be different from those in vertical and horizontal pipes. Thus, by taking two-phase heat experimental data in inclined pipes as a function of inclination angle, the ultimate goal of developing a general correlation(s) which can be applied for different fluid combinations, flow patterns, and pipe orientations can be achieved. This type of correlation has application in the gas/oil industry.

3. While predicting the heat transfer data from present study, the general form of the correlation (Eq. 2.9) could be retained for the experimental data in the bubbly-slug and bubbly-slug-annular transitional flow patterns. However, it was necessary for all of the five constants, the leading coefficient (C) and exponents (m , n , p , q) including the Prandtl number ratio term (p) and the viscosity ratio term (q), to be modified from the previously recommended values in order to accurately predict the h_{TP} in wavy flow and annular wavy transitional flow patterns. Thus, the effects of the Prandtl number ratio term and the viscosity ratio term on h_{TP} in the laminar flow regime of the liquid ($Re_{SL} < 4000$) are more pronounced than their effects on h_{TP} in the turbulent flow regime of the liquid. Also, as the range of the parameters for the wavy flow pattern are considerably different than those for the other flow patterns (see Table 4.9), this lead to the much larger values for the constants recommended to be used in the heat transfer correlation for this flow pattern. However, since the above observations were based on limited air-water experimental data in a horizontal pipe,

these observations can be further verified by comparing the results with additional experimental data for different fluid combinations as they become available.

4. During the procedures of developing the general form of the recommended correlation, Eq. (2.9), it was assumed that the density ratio of gas to liquid in Eq. (2.7) could be canceled out with the density ratio within the velocity ratio of gas to liquid, Eq. (1.11). However, for two-phase heat transfer in a horizontal pipe, it cannot be always true since Davis and David (1964) introduced the density ratio of liquid to gas in their suggested two-phase heat transfer correlation (see Table 1.6). Thus, the following alternative form of the general correlation can be developed by applying similar procedures used in the development of Eq. (2.9).

$$h_{TP} = (1 - \alpha)h_L \left[1 + \text{Const.} \left(\frac{x}{1-x} \right)^m \left(\frac{\alpha}{1-\alpha} \right)^n \left(\frac{Pr_G}{Pr_L} \right)^p \left(\frac{\mu_L}{\mu_G} \right)^q \left(\frac{\rho_G}{\rho_L} \right)^r \right] \quad (5.1)$$

The constants in the above equation should be determined empirically.

5. Zaidi and Sims (1986) based on an experimental study of surfactant effect on two-phase flow pattern and heat transfer in a vertical pipe using water-air and surfactant solution-air, concluded that the surfactant produced very little effect on the heat transfer coefficients. However, in a horizontal pipe, due to the stratification mechanism caused by the gravitational force, the different surface tensions in gas and liquid can be important. Therefore, the influence of surface tension effect on two-phase heat transfer in horizontal pipes should be re-investigated.
6. Based on the accumulated knowledge from the procedures of identifying previously recommended correlations and improving those correlations for better fit of the existing experimental data, this study developed a new robust heat transfer correlation

for turbulent flow in a vertical pipe. However, the correlation could not cover two-phase heat transfer for laminar flow in a vertical pipe since two-phase heat transfer for laminar flow in most cases is strongly influenced by secondary flow effects. Thus, developing new heat transfer correlation(s) for laminar flow in vertical pipes can be achieved by identifying the secondary flow effects on h_{TP} .

7. As we could see from the variation of heat transfer coefficients with superficial Reynolds numbers (Re_{SG} and Re_{SL}) from Fig. 4.21, h_{TP} was increased, reached a maximum and then decreased as Re_{SG} was increased for a fixed liquid Re_{SL} . Ravipudi and Godbold (1978) also observed the same trends from their experimental data of air-water and air-toluene mixtures in a vertical pipe, and they attributed the decrease in h_{TP} at high Re_{SG} to the decrease in the outlet liquid temperature caused by mass transfer from liquid to air. Thus, two-phase heat transfer with mass transfer for horizontal pipes should be investigated.
8. During the two-phase heat transfer measurements in a horizontal pipe, the pressure drop (ΔP) across the test section was also measured. Since some researchers previously tried to correlate the two-phase heat transfer data with the relationship between two-phase pressure drop and single-phase pressure drop suggested by Lockhart and Martinelli (1949), this type of approach could also be attempted.

REFERENCES

- Aggour, M.A. (1978), "Hydrodynamics and Heat Transfer in Two-Phase Two-Component Flow," Ph.D. Thesis, University of Manitoba, Canada.
- Baker, O. (1954), "Simultaneous Flow of Oil and Gas," *Oil and Gas J.*, Vol. 53, pp. 185-195.
- Barnea, D. (1987), "A Unified Model for Predicting Flow-Pattern Transitions for the Whole Range of Pipe Inclinations," *Int. J. Multiphase Flow*, Vol. 13, No. 1, pp. 1-12.
- Barnea, D. and N. Yacoub (1983), "Heat Transfer in Vertical Upwards Gas-Liquid Slug Flow," *Int. J. Heat Mass Transfer*, Vol. 26, No. 9, pp. 1365-1376.
- Beggs, H.D. and J.P. Brill (1973), "A Study of Two-Phase Flow in Inclined Pipes," *JPT*, Vol. 607, pp. 607-617.
- Breber, G., J.W. Palen and J. Taborek (1980), "Prediction of Horizontal Tubeside Condensation of Pure Components Using Flow Regime Criteria," *J. Heat Transfer*, Vol. 102, pp. 471-476.
- Butterworth, D. (1975), "A Comparison of Some Void-Fraction Relationships for Co-Current Gas-Liquid Flow," *Int. J. Multiphase Flow*, Vol. 1, pp. 845-850.
- Carey, V.P. (1992), Liquid-Vapor Phase-Change Phenomena: An Introduction to the Thermophysics of Vaporization and Condensation Process in Heat Transfer Equipment, Taylor & Francis, Bristol.
- Chisholm, D. (1973), "Research Note: Void Fraction During Two-Phase Flow," *J. Mech. Eng. Sci.*, Vol. 15, No. 3, pp. 235-236.
- Chu, Y-C. and B.G. Jones (1980), "Convective Heat Transfer Coefficient Studies in Upward and Downward, Vertical, Two-Phase, Non-Boiling Flows," *AIChE Symp. Series*, Vol. 76, pp. 79-90.
- Colburn, A.P. (1933), "A Method of Correlating Forced Convection Heat Transfer Data and a Comparison with Liquid Friction," *Trans. Am. Inst. Chem. Engrs*, Vol. 29, pp. 174-210.

- Davis, E.J., N.P. Cheremisinoff and C.J. Guzy (1979), "Heat Transfer with Stratified Gas-Liquid Flow," *AIChE Journal*, Vol. 25, No. 6, pp. 958-966.
- Davis, E.J. and M.M. David (1964), "Two-Phase Gas-Liquid Convection Heat Transfer," *I&EC Fundamentals*, Vol. 3, No. 2, pp. 111-118.
- Davis, E.J., S.C. Hung and S. Arciero (1975), "An Analogy for Heat Transfer with Wavy/Stratified Gas-Liquid Flow," *AIChE Journal*, Vol. 21, No. 5, pp. 872-878.
- Dorresteyn, W.R. (1970), "Experimental Study of Heat Transfer in Upward and Downward Two-Phase Flow of Air and Oil Through 70 mm Tubes," *Proc. 4th Int. Heat Transfer Conf.*, Vol. 5, B 5.9, pp. 1-10.
- Dukler, A.E. and O. Shaharabany (1977), *For Multiphase Processing, Studies in Intermittent (Slug) Flow in Horizontal Tubes: Design Manual I-2*, American Institute of Chemical Engineers, New York.
- Dusseau, W. T. (1968), "Overall Heat Transfer Coefficient for Air-Water Froth in a Vertical Pipe," M. S. Thesis, Chemical Engineering, Vanderbilt University.
- Elamvaluthi, G. and N.S. Srinivas (1984), "Two-Phase Heat Transfer in Two Component Vertical Flows," *Int. J. Multiphase Flow*, Vol. 10, No. 2, pp. 237-242.
- Ewing, M. E., Weinandy, J. J. and Christensen, R. N. (1999), "Observations of Two-Phase Flow Patterns in a Horizontal Circular Channel," *Heat Transfer Engineering*, Vol. 20, No. 1, pp. 9-14.
- Fried, L. (1954), "Pressure Drop and Heat Transfer for Two-Phase, Two-Component Flow," *Chem. Eng. Prog. Symp. Series*, Vol. 50, No. 9, pp. 47 - 51.
- Frisk, D.P. and E.J. Davis (1972), "The Enhancement of Heat Transfer by Waves in Stratified Gas-Liquid Flow," *Int. J. Heat Mass Transfer*, Vol. 15, pp. 1537-1551.
- Ghajar, A.J. and Tam, T.M. (1994), "Heat Transfer Measurements and Correlation's in the Transition Region for a Circular Tube with Three Different Inlet Configurations," *Experimental Thermal and Fluid Science*, Vol. 8, pp. 79-90.
- Ghajar, A.J. and Y.H. Zurigat (1991), "Microcomputer-Assisted Heat Transfer Measurement/Analysis in a Circular Tube," *Int. J. Appl. Engng Ed.*, Vol. 7, No. 2, pp. 125-134.
- Gnielinski, V. (1976), "New Equations for Heat and Mass Transfer in Turbulent Pipe and Channel Flow," *Int. Chem. Eng.*, Vol. 16, No. 2, pp. 359-368.

- Govier, G.W. and K. Aziz (1973), The Flow of Complex Mixtures in Pipes, Van Nostrand Reinhold Company, New York.
- Griffith, P. and G.B. Wallis (1961), "Two-Phase Slug Flow," *J. Heat Transfer*, Trans. ASME, Ser. C 83, pp. 307-320.
- Groothuis, H. and W.P. Hendal (1959), "Heat Transfer in Two-Phase Flow," *Chemical Engineering Science*, Vol. 11, pp. 212-220.
- Hewitt, G.F. and N.S. Hall-Taylor (1970), Annular Two-Phase Flow, Pergamon Press Ltd., Oxford.
- Hewitt, G.F. and D.N. Roberts (1969), "Studies of Two-Phase Flow Patterns By Simultaneous X-ray and Flash Photography," AERE-M 2159, Her Majesty's Stationary Office, London.
- Hubbard, M.G. and A.E. Dukler (1975), "A Model for Gas-Liquid Slug Flow in Horizontal and Near Horizontal Tubes," *Ind. Eng. Che. Fund.*, Vol. 14, No. 4, pp. 337-347.
- Hughmark, G.A. (1965), "Holdup and Heat Transfer in Horizontal Slug Gas Liquid Flow," *Chem. Engng. Sci.*, Vol. 20, pp. 1007-1010.
- Johnson, H. A. (1955), "Heat Transfer and Pressure Drop for Viscous-Turbulent Flow of Oil-Air Mixtures in a Horizontal Pipe," *ASME Trans.*, Vol. 77, pp. 1257-1264.
- Johnson, H. A. and A. H. Abou-Sabe (1952), "Heat Transfer and Pressure Drop for Turbulent Flow of Air-Water Mixture in a Horizontal Pipe," *ASME Trans.*, Vol. 74, pp. 977-987.
- Khoze, A.N., S. V. Dunayev, and V. A. Sparin (1976), "Heat and Mass Transfer in Rising Two-Phase Flows in Rectangular Channels," *Heat Transfer Soviet Research*, Vol. 8, No. 3, pp. 87 - 90.
- Kim, D., Y. Sofyan, A.J. Ghajar and R.L. Dougherty (1997), "An Evaluation of Several Heat Transfer Correlations for Two-Phase Flow with Different Flow Patterns in Vertical and Horizontal Tubes," *Fundamentals of Bubble and Droplet Dynamics: Phase Change and Two-Phase Flow*, S. G. Kandlikar, C. H. Amon, M. E. Ulucakli, and J. O'Brien, eds., HTD-Vol. 342, ASME, New York, pp. 119-130.
- Kim, D., A.J. Ghajar, R.L. Dougherty and V.K. Ryali (1999a), "Comparison of Twenty Two-Phase Heat Transfer Correlations with Seven Sets of Experimental Data, Including Flow Pattern and Tube Orientation Effects," *Heat Transfer Engineering*, Vol. 20, No. 1, pp. 15-40.

- Kim, D., A.J. Ghajar and R.L. Dougherty, (1999b), "Development of Improved Two-Phase Two-Component Pipe Flow Heat Transfer Correlations From Existing Correlations and Published Data," *Proc. of the 5th ASME/JSME Joint Thermal Engineering Conference*, AJTE-99-6122, March 15-19, San Diego, California.
- Kim, D., A.J. Ghajar and R.L. Dougherty, (1999c), "A Heat Transfer Correlation for Turbulent Gas-Liquid Two-Phase Flow of Several Fluid Combinations and Different Flow Patterns in Vertical Pipes," *Proc. of the 33rd National Heat Transfer Conference*, HTD99-141, August 15-17, 1999, Albuquerque, New Mexico.
- Kim, D., A.J. Ghajar and R.L. Dougherty, (2000), "Robust Heat Transfer Correlation for Turbulent Gas-Liquid Flow in Vertical Pipes," *Journal of Thermophysics and Heat Transfer*, Vol. 14, No. 3, July-September (in press).
- Kim, J. (2000) "Construction and Performance Testing of a Uniform Heat Flux Two-Phase Gas-Liquid Experimental Setup Using a Horizontal Circular Tube," M.S. Thesis, Oklahoma State University.
- King, C.D.G. (1952), "Heat Transfer and Pressure Drop for an Air-Water Mixture Flowing in a 0.737 Inch I.D. Horizontal Tube," M.S. Thesis, University of California.
- Kline, S. J. and McClintock, F. A. (1953), "Describing Uncertainties in Single-Sample Experiments," *Mech. Engr.*, Vol. 1, pp. 3-8.
- Knott, R.F., R.N. Anderson, A. Acrivos and E.E. Petersen (1959), "An Experimental Study of Heat Transfer to Nitrogen-Oil Mixtures," *Ind. and Engineering Chemistry*, Vol. 51, No. 11, pp. 1369-1372.
- Kudirka, A.A., R. J. Grosh and P.W. McFadden (1965), "Heat Transfer in Two-Phase Flow of Gas-Liquid Mixtures," *I & EC Fundamentals*, Vol. 4, No. 3, pp. 339-344.
- Lockhart, R. and R.C. Martinelli (1949), "Proposed Correlation of Data for Isothermal Two-Phase, Two-Component Flow in Pipes," *Chem. Eng. Prog.*, Vol. 45, No. 1, pp. 39-48.
- Mandhane, J.M., G.A. Gregory and K. Aziz (1974), "Flow Pattern Map for Gas-Liquid Flow in Horizontal Pipes," *Int. J. Multiphase Flow*, Vol. 1, pp. 537-553.
- Martin, B. W. and G. E. Sims (1971), "Forced Convection Heat Transfer to Water With Air Injection in a Rectangular Duct," *Int. J. Heat Mass Transfer*, Vol. 14, pp. 1115-1134.

- Niu, T. (1976), "Heat Transfer During Gas-Liquid Slug Flow in Horizontal Tubes," M.Sc. Thesis, University of Houston.
- Novosad, Z. (1955), "Heat Transfer in Two-Phase Liquid - Gas Systems," *Collection Czechoslov. Chem. Commun.*, Vol. 20, pp. 477- 499.
- Oliver, D. R. and S. J. Wright (1964), "Pressure Drop and Heat Transfer in Gas-Liquid Slug Flow in Horizontal Tubes," *British Chem. Engrg.*, Vol. 9, No. 9, pp. 590 - 596.
- Oliver, D.R. and A. Young Hoon (1968), "Two-Phase Non-Newtonian Flow. Part II: Heat Transfer," *Trans. INSTN Chem. Engrs.*, Vol. 46, pp. T116-T122.
- Pletcher, R.H. (1966), "An Experimental and Analytical Study of Heat Transfer and Pressure Drop in Horizontal Annular Two-Phase, Two-Component Flow," Ph.D. Thesis, Cornell University.
- Pletcher, R.H. and H.N. McManus, Jr. (1968), "Heat Transfer and Pressure Drop in Horizontal Annular Two-Phase, Two-Component Flow," *Int. J. Heat Mass Transfer*, Vol. 11, pp. 1087-1104.
- Porteus, A. (1969), "Prediction of the Upper Limit of the Slug Flow Regime," *Brit. Chem. Eng.*, Vol. 14, No. 9, pp. 117-119.
- Radovcich, N.A. and R. Moissis (1962), "The Transition from Two-Phase Bubble Flow to Slug Flow," Report No. 7-7673-22, Mechanical Engineering Department, MIT, Cambridge, MA.
- Ravipudi, S.R. and T.M. Godbold (1978), "The Effect of Mass Transfer on Heat Transfer Rates for Two-Phase Flow in a Vertical Pipe," *Proc. 6th Int. Heat Transfer Conf.*, Toronto, Vol. 1, pp. 505-510.
- Rezkallah, K.S. (1986), "Heat Transfer and Hydrodynamics in Two-Phase Two-Component Flow in a Vertical Tube," Ph.D. Thesis, University of Manitoba, Canada.
- Rezkallah, K.S. and G.E. Sims (1987), "An Examination of Correlations of Mean Heat Transfer Coefficients in Two-Phase and Two-Component Flow in Vertical Tubes," *AIChE Symp. Series*, Vol. 83, pp. 109-114.
- Ryali, V. (1999), "Design, Construction and Testing of a Single-Phase and Two-Phase Fluid Flow System in a Horizontal Circular Tube with Constant Heat Flux," M.S. Thesis, Oklahoma State University.

- Seigel, R. E.M. Sparrow and T.M. Hallman (1958), "Steady Laminar Heat Transfer in a Circular Tube with Prescribed Wall Heat Flux," *Appl. Sci. Res., Sec. A*, Vol. 7, pp. 386-392.
- Serizawa, A., I. Kataoka and I. Michiyoshi (1975), "Turbulence Structure of Air-Water Bubbly Flow-III. Transport Properties," *Int. J. Multiphase Flow*, Vol. 2, pp. 247-259.
- Shah, R.K. (1978), "A Correlation for Laminar Hydrodynamic Entry Length Solutions for Circular and Non-Circular Ducts," *J. Fluids Engineering, Trans. ASME*, Vol. 100, pp. 177-179.
- Shah, M.M. (1981), "Generalized Prediction of Heat Transfer During Two Component Gas-Liquid Flow in Tubes and Other Channels," *AIChE Symp. Series*, Vol. 77, No. 208, pp. 140-151.
- Shaharabanny, O. (1976), "Experimental Investigation of Heat Transfer in Slug Flow in Horizontal Tubes," M.Sc. Thesis, University of Houston.
- Shaharabanny, O., Y. Taitel and A.E. Dukler (1978), "Heat Transfer During Intermittent/Slug Flow in Horizontal Tubes: Experiments," *Proceedings of the 2nd CSNI Specialists Meeting*, June 12-14, Paris, pp. 627-649.
- Shoham, O., A.E. Dukler and Y. Taitel (1982), "Heat Transfer During Intermittent/Slug Flow in Horizontal Tubes," *Ind. Eng. Chem. Fundam.*, Vol. 21, pp. 312-319.
- Sieder, E.N. and G.E. Tate (1936), "Heat Transfer and Pressure Drop of Liquids in Tubes," *Ind. Eng. Chem.*, Vol. 28, No. 12, p. 1429.
- Spalding, D.B. (1964), "Contribution to the Theory of Heat Transfer Across a Turbulent Boundary Layer," *Int. J. Heat Mass Transfer*, Vol. 7, pp. 743-761.
- Taitel, Y., D. Barnea and A.E. Dukler (1980), "Modeling Flow Pattern Transitions for Steady Upward Gas-Liquid Flow in Vertical Tubes," *AIChE Journal*, Vol. 26, No. 3, pp. 345-354.
- Taitel, Y. and A.E. Dukler (1976), "A Model for Predicting Flow Regime Transitions in Horizontal and Near Horizontal Gas-Liquid Flow," *AIChE Journal*, Vol. 22, No. 1, pp. 47-54.
- Taitel, Y. and A.E. Dukler (1977), "Flow Regime Transitions for Vertical Upward Gas-Liquid Flow: A Preliminary Approach through Physical Modeling," Paper Presented at Session on *Fundamental Research in Fluid Mechanics at the 70th AIChE Annual Meeting*, New York.

- Ueda, T. and M. Hanaoka (1967), "On Upward Flow of Gas-Liquid Mixtures in Vertical Tubes: 3rd. Report, Heat Transfer Results and Analysis," *Bull. JSME*, Vol. 10, pp. 1008-1015.
- Vijay, M.M. (1978), "A Study of Heat Transfer in Two-Phase Two-Component Flow in a Vertical Tube," Ph.D. Thesis, University of Manitoba, Canada.
- Vijay, M.M., M.A. Aggour and G.E. Sims (1982), "A Correlation of Mean Heat Transfer Coefficients for Two-Phase Two-Component Flow in a Vertical Tube," *Proceedings of 7th Int. Heat Transfer Conference*, Vol. 5, pp. 367-372.
- Wallis, G.B. (1965), One-Dimensional Two-Phase Flow, Wiley, New York.
- Yoo, S.S. (1974), "Heat Transfer and Friction Factors for Non-Newtonian Fluids in Turbulent Pipe Flow," Ph.D. Thesis, University of Illinois at Chicago Circle.
- Zaidi, A.J. (1981), "Hydrodynamics and Heat Transfer in Two-Phase Two-Component Flow in a Vertical Tube," M.Sc. Thesis, University of Manitoba, Canada.
- Zaidi, A.J. and G.E. Sims (1986), "The Effect of a Surfactant on Flow Patterns, Pressure Drop and Heat Transfer in Two-Phase Two-Component Vertical Flow," *Proc. 8th International Heat Transfer Conference*, San Francisco, CA, C.L. Tien, V.P. Carey, and J.K. Ferrell, Editors, Hemisphere Publishing Corp., Vol. 5, pp. 2283-2288.

APPENDIX A
UNCERTAINTY ANALYSIS

APPENDIX B

UNCERTAINTY ANALYSIS

The probable error involved in the experimental measurements of the two-phase heat transfer is presented in this appendix. Calculation of the uncertainties is based on the method proposed by Kline and McClintock (1953).

The heat transfer coefficient is defined as:

$$h = \frac{\dot{q}''}{T_{wi} - T_B} \quad (\text{B-1})$$

where T_{wi} is the inside wall temperature.

The percent probable error for h (U_h) is given by:

$$U_h = \left[\left(\frac{d\dot{q}''}{\dot{q}''} \right)^2 + \left(\frac{dT}{\Delta T} \right)^2 \right]^{1/2} \quad (\text{B-2})$$

The heat flux (\dot{q}'') is the product of the voltage drop (V) across the test section and the current (I) carried by the tube. Therefore, the heat flux can be written as:

$$\dot{q}'' = \frac{V I}{\pi D_i L} \quad (\text{B-3})$$

The uncertainty in the heat flux ($U_{\dot{q}''}$) can then be calculated using the following equation:

$$U_{\dot{q}''} = \left[\left(\frac{dV}{V} \right)^2 + \left(\frac{dI}{I} \right)^2 + \left(\frac{dD_i}{D_i} \right)^2 + \left(\frac{dL}{L} \right)^2 \right]^{1/2} \quad (\text{B-4})$$

The uncertainty of each variable was estimated as follows:

- dV The voltmeter has an accuracy of 1% of reading. The two-phase flow heat transfer experimental data had a voltage range of 2.57 to 5.45 volts, and it gives an average error of 0.0401 volt.
- dI The ammeter had an error of 2% of reading. The two-phase flow heat transfer experimental data had a current range of 309 to 643 amps, and it gives an average error of 9.52 amps.
- dD_i The inside diameter of the test section was measured accurately to 0.001 inch using a caliper, and the inside diameter was 1.097 inches.
- dL The heated length of the test section was 110 inches and was measured to within 0.0625 inch.

To evaluate the inside wall temperature, T_{wi} , the heat diffusion equation is solved by using the appropriate boundary conditions.

$$T_{wi} = T_{wo} - \left(\frac{\dot{q}}{2\pi \frac{(D_o^2 - D_i^2)}{4} k_s L} \right) \left[D_o^2 \ln\left(\frac{D_o}{D_i}\right) - \left(\frac{D_o^2 - D_i^2}{2}\right) \right] \quad (B-5)$$

The bulk temperature at the desired location x is determined by using the following equation:

$$T_B = T_{B,out} - [(T_{B,out} - T_{B,in})(L - x)]/L \quad (B-6)$$

where

$T_{B,in}$ = bulk inlet temperature

$T_{B,out}$ = bulk outlet temperature

The uncertainty associated with the quantity $(T_{wi} - T_B)$, U_T , can be estimated from the following equation:

$$U_T = \left[\left(\frac{|dT_{w_o}| + |dT_B| + |dT_1| + |dT_2|}{T_{w_i} - T_B} \right)^2 \right]^{1/2} \quad (B-7)$$

where

$$T_1 = - \left(\frac{\dot{q}}{2\pi \frac{(D_o^2 - D_i^2)}{4} k_s L} \right) \left[D_o^2 \ln \left(\frac{D_o}{D_i} \right) - \left(\frac{D_o^2 - D_i^2}{2} \right) \right] \quad (B-8)$$

$$T_2 = (T_{B,out} - T_{B,in})(L - x)/L \quad (B-9)$$

For this analysis, the following uncertainties of each term are as follows:

dT_{w_o} The assumed error in the outside wall temperature (T_{w_o}) was estimated to be 0.5 °F within a range of 59 to 104 °F, which was within the temperature variation during the test run, from the calibration runs for the thermocouples.

dT_B The average bulk temperature deviation was assumed to be 0.5 °F within a range of 59 to 104 °F, which was within the temperature variation during the test run, from the calibration runs for the thermocouple (inlet) and thermocouple probe (outlet).

dT_2 The deviation ratio, dT_2/T_2 was assumed to be 0.05.

dT_1 The deviation ratio, dT_1/T_1 was assumed to be 0.05.

Applying one of the test runs for the two-phase flow heat transfer (at thermocouple station no. 6 of Rn8171):

$$\dot{q} = 6159 \text{ Btu/hr}$$

$$\dot{q}'' = 2486 \text{ Btu/ft}^2\text{-hr}$$

$$V = 3.89 \text{ volts}$$

$$I = 464.0 \text{ amps}$$

$$T_{B,in} = 63.69 \text{ }^\circ\text{F}$$

$$T_{B,out} = 71.83 \text{ }^\circ\text{F}$$

$$D_o = 1.136 \text{ inches}$$

$$D_i = 1.097 \text{ inches}$$

$$T_{w_o} = 78.81 \text{ }^\circ\text{F}$$

$$k_s = 7.596 \text{ Btu/hr-ft-}^\circ\text{F}$$

$$x = 4.75 \text{ ft (57 inches)}$$

$$L = 9.167 \text{ ft (110 inches)}$$

Substituting all of the above values into the proper equations, we have

$$T_1 = -0.995 \text{ }^\circ\text{F}$$

$$T_2 = 3.922 \text{ }^\circ\text{F}$$

$$(T_{w_i} - T_B) = 9.907 \text{ }^\circ\text{F}$$

These values result in the expected experimental uncertainties of:

$$\begin{aligned} U_T &= \{[(0.5 + 0.5 + 0.05 + 0.05)/9.907]^2\}^{1/2} \\ &= 0.111 \end{aligned}$$

$$\begin{aligned} U_q &= [(0.04/3.89)^2 + (9.52/464.0)^2 + (0.001/1.097)^2 + (0.0625/110)^2]^{1/2} \\ &= 0.023 \end{aligned}$$

$$U_h = [(0.111)^2 + (0.023)^2]^{1/2}$$

Finally, the uncertainty for heat transfer coefficient calculations is

$$U_h = 11.34 \%$$

From the uncertainty analysis, it can be seen that the maximum error corresponding to the experimental heat transfer coefficient is approximately 11.5%. As shown in this analysis, the uncertainty in heat transfer coefficient is dominated by the maximum error in the measurements of temperatures.

APPENDIX B
COMPUTER CODE LISTING FOR RHt99F

```

C *****
C *
C *           " RHT99F "
C *
C *   A PROGRAM TO CALCULATE THE INSIDE WALL TEMPERATURES AND
C *   LOCAL HEAT TRANSFER COEFFICIENTS FOR GIVEN OUTSIDE WALL
C *   TEMPERATURES FOR SINGLE PHASE HEAT TRANSFER STUDIES IN
C *   HORIZONTAL TUBES.  THE PROGRAM ALSO CALCULATES THE PERTINENT
C *   FLUID FLOW & HEAT TRANSFER DIMENSIONLESS NUMBERS.
C *
C *   THE MATHEMATICAL ALGORITHM OF THIS PROGRAM HAS BEEN DEVELOPED
C *   BY THE STUDENTS OF DR. J.D. PARKER & DR. K.J. BELL OF
C *   OKLAHOMA STATE UNIVERSITY.
C *
C *   THE PROGRAM WAS MODIFIED BY:
C *
C *           Y. H. ZURIGAT  (APRIL 1989)
C *
C *   AND REMODIFIED FOR A SPECIFIC PURPOSE BY:
C *
C *           DONGWOO KIM    (AUGUST 1999)
C *
C *   UNDER THE SUPERVISION OF: DR. A.J. GHAJAR
C *                               SCHOOL OF MECHANICAL &
C *                               AEROSPACE ENGINEERING
C *                               OKLAHOMA STATE UNIVERSITY
C *                               STILLWATER, OK 74078
C *
C *****
C
C *****
C *
C *           SUBROUTINE LISTING
C *
C *   NAME          FUNCTION
C *   -----
C *   GEOM          Prompts for pipe dimensions and
C *                calculates geometry for finite
C *                differencing
C *
C *   BET           Calculates fluid Thermal Expansion Coefficient
C *
C *   CONDFL        Calculates fluid Thermal Conductivity
C *
C *   DENS          Calculates fluid Density
C *
C *   MEW           Calculates fluid Viscosity

```

```

C *
C *      PRNUM          Calculates fluid Prandtl Number          *
C *
C *      SPHEAT        Calculates fluid Specific Heat           *
C *
C *      PRNT          Prints calculated data to output files    *
C *
C *****
C
C *****
C *
C *                  MAIN PROGRAM                               *
C *
C *****

      CHARACTER INFILE*36, SUMFILE*11, FNAME*4, RUN*4
      DIMENSION TCHCK1(8), TCHCK2(8), QAVG(31), DELX(10),
+             CONDK(31,8), RSVTY(31,8)
      INTEGER   RSWT, STN
      COMMON/STATION/STN

      COMMON /PRINT/ IPICK, REN(31,8), TBULK(31), VEL, REYNO, PRNO, GW,
+             HTCOFF(31,8), H(31), RENO(31), GRNO(31), PR(31),
+             SNUS(31), VISBW(31), SHTHB(32), QFLXID(31,8), QFLXAV,
+             QGEXPT, QBALC, QPCT, IPMAX, TAVG(31), VISCA(31),
+             VISWLA(31), ROWA(31)
+             /INPUT/ TROOM, VOLTS, TAMP, RMFL, MFLUID, X2, FLOWRT, NRUN, VFLOW,
+             TIN, TOUT, TOSURF(31,8), TISURF(31,8), IP(32), KST(32)
+             /TEMP1/ TWALL(31,8), AMPS(31,8), RESIS(31,8), POWERS(32),
+             TPOWER
+             /MAIN1/ IST, KOUNT, NSTN
+             /GEOM1/ XAREA(31), R(31), LTP(32), LTH(32), DELZ(31), LHEAT,
+             LTEST, LOD(31), DOUT, DIN, DELR, NODES, NSLICE, PI

      REAL*4 LTH, LTP, LTEST, LHEAT, H, HTCOFF, LOD, LENGTH
      DATA DELX/6.75, 16.75, 26.75, 36.75, 46.75, 56.75, 66.75, 76.75, 86.75
+             , 96.75/

C      DELX, LENGTH WERE CREATED BY RYALI TO CALCULATE THE TBULK FOR HIS
C      SETUP
      LENGTH=103.5D0
C -----
C ----- INITIALIZE OUTPUT DATA ARRAYS TO ZERO -----
C -----
      WRITE(*,*) 'ENTER THE STATION NUMBER TO CALCULATE'
      READ(*,*) STN

```

```
OPEN(8, FILE="STN.DAT")
1200 WRITE(*,*)
```

```
1 DO 101 I=1,8
  DO 101 J=1,31
    TOSURF(J,I)=0.
    TISURF(J,I)=0.
    REN(J,I)=0.
    QFLXID(J,I)=0.
101   HTCOFF(J,I)=0.
```

```
G=32.174
```

```
C -----
C ----- ASSIGN FOR INPUT DATA FILE NAME -----
C -----
```

```
PRINT*, ' '
PRINT*, ' '
PRINT*, 'Enter the file number.'
READ(*,1003) RUN
```

```
DO 2 J=1,18
2 INFILE='RN'//RUN//'.DAT'
OPEN(5, FILE=INFILE)
```

```
READ(5,1003) FNAME
REWIND 5
```

```
C -----
C ----- ASSIGN FILE NAMES TO VARIABLES AND OPEN OUTPUT FILES -----
C -----
```

```
SUMFILE='RN'//FNAME//'.HTI'
OPEN(6, FILE=SUMFILE)
SUMFILE='RN'//FNAME//'.CMP'
OPEN(7, FILE=SUMFILE)
```

```
C -----
C ----- ASSIGN FOR UNITS INPUT -----
C -----
```

```
7 IPICK = 1
```

```
C -----
C ----- READ RUN NUMBER AND # STATIONS FROM INPUT FILE -----
C -----
```

```
8 READ(5,1004) NRUN,NSTN
```



```

C -----
C ----- CHECK FOR END OF FILE -----
C -----

      IF (NRUN .EQ. 0) GO TO 99

C -----
C ----- READ DATA FROM INPUT FILE -----
C -----

      X2=0.0
      IPMAX=0
      READ(5,1005)MFLUID,X2, FLOWRT, TAMPS, VOLTS, TIN, TOUT, TROOM
      Write(*,*) 'Tin =', Tin

      IF(X2.LT.0.0.OR.X2.GT.1.0)THEN
      WRITE(*,*) ' WARNING : MASS CONCENTRATION IS OUT OF RANGE '
      STOP
      END IF

      DO 9 IST=1,NSTN
      READ(5,1006)KST(IST),IP(IST),LTH(IST),
+      (TOSURF(IST,IPR),IPR=1,IP(IST))
      IF(IST.NE.1)THEN
      IF(IP(IST).GE.IPMAX)IPMAX=IP(IST)
      ELSE
9      ENDIF

      VFLOW=FLOWRT

C -----
C -----CALCULATION OF MASS FLOW RATE IN LBM/HR -----
C -----

      CALL DENS(TIN,MFLUID,X2,ROW)
      RMFL=VFLOW*0.133666*60.0*ROW

C -----
      CALL GEOM
C -----

      NNODE=NODES-1

C -----
C ----- START SOLUTION WITH STATION 1 -----
C -----

```

```

DO 30 IST=1,NSTN
  IPP= IP(IST)
  DO 10 IPR=1,IPP
10      TCHCK1(IPR)=0.0

```

```

C -----
C ----- SET ALL RADIAL TEMPERATURES EQUAL -----
C ----- TO THE OUTSIDE SURFACE TEMPERATURES -----
C -----

```

```

DO 11 ISL=1,NODES
  DO 11 IPR=1,IPP
11      TWALL(ISL,IPR)=TOSURF(IST,IPR)
      KOUNT=1

```

```

C -----
C ----- CALCULATE THERMAL CONDUCTIVITY OF STAINLESS STEEL -----
C ----- FOR EACH NODE IN BTU/(HR-FT-DEGF) -----
C -----

```

```

12 DO 13 ISL=1,NODES
  DO 13 IPR=1,IPP
      CONDK(ISL,IPR)=7.27+0.0038*TWALL(ISL,IPR)
13 CONTINUE

```

```

C -----
C ----- CALCULATE ELECTRICAL RESISTIVITY OF STAINLESS STEEL -----
C ----- FOR EACH NODE IN OHMS-SQIN/IN -----
C -----

```

```

DO 14 ISL=1,NODES
  IPP= IP(IST)
  DO 14 IPR=1,IPP
      RSVTY(ISL,IPR)=(27.67+0.0213*TWALL(ISL,IPR))/1.E6
14 CONTINUE

```

```

C -----
C ----- CALCULATE RESISTANCE FOR EACH SEGMENT, ALSO -----
C ----- CALCULATE EQUIVALENT RESISTANCE FOR PARALLEL CIRCUITS -----
C -----

```

```

DELR = (DOUT-DIN)/2.0/NSLICE
R(1) = DOUT/2.0
DO 15 I=1,NSLICE
15    R(I+1)=R(I)-DELR

```

```

IPP= IP(IST)
XAREA(1)=(R(1)-DELR/4.0)*PI*DELR/IPP
XAREA(NODES)=(R(NODES)+DELR/4.0)*PI*DELR/IPP
DO 16 I=2,NSLICE
16   XAREA(I)= 2.0*R(I)*PI*DELR/IPP

RINV = 0.0
DO 17 ISL=1,NODES
  DO 17 IPR=1,IPP
    RESIS(ISL,IPR) = RSVTY(ISL,IPR)*DELZ(IST)/XAREA(ISL)
    RINV = RINV +1.0/RESIS(ISL,IPR)
17 CONTINUE

```

```

C -----
C ----- CALCULATE CURRENT FOR EACH SEGMENT -----
C -----

```

```

OHMS = 1.0/RINV
AMP=0.0
DO 18 ISL=1,NODES
  DO 18 IPR=1,IPP
    AMPS(ISL,IPR) = TAMPS*OHMS/RESIS(ISL,IPR)
    AMP=AMP+AMPS(ISL,IPR)
18 CONTINUE

```

```

C -----
C ----- CALCULATE TEMPERATURES AT NODE 2 -----
C ----- TEMPERATURES AT NODE 1 ARE OUTSIDE WALL TEMPERATURES -----
C -----

```

```

ISL=1
DO 20 IPR=1,IPP
  ITHCTL=IPP
  IMINS=IPR-1
  IPLUS=IPR+1
  NMINS = ISL - 1
  NPLUS = ISL + 1
  IF(IMINS.EQ.0 .AND. IPP.EQ. ITHCTL) IMINS=ITHCTL
  IF(IPLUS.EQ.(ITHCTL+1) .AND. IPP.EQ. ITHCTL) IPLUS=1
  A= 3.41214*12.0*AMPS(ISL,IPR)*AMPS(ISL,IPR)
  +   *RSVTY(ISL,IPR)/XAREA(ISL)
  B = IPP*DELR*(CONDK(ISL,IPR)+CONDK(ISL,IPLUS))
  +   *(TWALL(ISL,IPR)-TWALL(ISL,IPLUS))/(8.0*PI*R(ISL))
  C = IPP*DELR*(CONDK(ISL,IPR)+CONDK(ISL,IMINS))
  +   *(TWALL(ISL,IPR)-TWALL(ISL,IMINS))/(8.0*PI*R(ISL))
  X = PI*(R(ISL)-DELR/2.0)*(CONDK(ISL,IPR)+CONDK(NPLUS,IPR))
  +   /(IPP*DELR)

```

```

20      TWALL(NPLUS, IPR) = TWALL(ISL, IPR) - (A-B-C)/X

C -----
C ----- CALCULATE REMAINING NODAL TEMPERATURES -----
C -----

      DO 21 ISL=2, NNODE
      DO 21 IPR=1, IPP
      ITHCTL=IPP
      IMINS=IPR-1
      IPLUS=IPR+1
      NMINS=ISL-1
      NPLUS=ISL+1
      IF(IMINS.EQ.0 .AND. IPP .EQ. ITHCTL) IMINS=ITHCTL
      IF(IPLUS.EQ.(ITHCTL+1) .AND. IPP .EQ. ITHCTL) IPLUS=1
      A= 3.41214*12.0*AMPS (ISL, IPR) *AMPS (ISL, IPR)
      +      *RSVTY (ISL, IPR) /XAREA (ISL)
      B =PI*(R (ISL)+DELR/2.)*(CONDK (ISL, IPR)+CONDK (NMINS, IPR))
      +      *(TWALL (ISL, IPR)-TWALL (NMINS, IPR)) / (IPP*DELR)
      C = IPP*DELR*(CONDK (ISL, IPR)+CONDK (ISL, IPLUS))
      +      *(TWALL (ISL, IPR)-TWALL (ISL, IPLUS)) / (4.0*PI*R (ISL))
      D = IPP*DELR*(CONDK (ISL, IPR)+CONDK (ISL, IMINS))
      +      *(TWALL (ISL, IPR)-TWALL (ISL, IMINS)) / (4.0*PI*R (ISL))
      X =PI*(R (ISL)-DELR/2.)*(CONDK (ISL, IPR)+CONDK (NPLUS, IPR))
      +      / (IPP*DELR)
21      TWALL (NPLUS, IPR) = TWALL (ISL, IPR) - (A-B-C-D) /X

C -----
C ----- CHECK FOR THE CONVERGENCE OF THE WALL TEMPERATURES -----
C -----

      TCHCK = 0.0
      DO 22 IPR=1, IPP
      TCHCK2 (IPR)=TWALL (NODES, IPR)
22      TCHCK = TCHCK + ABS (TCHCK2 (IPR) -TCHCK1 (IPR))
      IF (TCHCK .GT. 0.001) GO TO 23
      GO TO 26
23      DO 24 IPR=1, IPP
24      TCHCK1 (IPR) = TCHCK2 (IPR)
      KOUNT = KOUNT+1
      GO TO 12
      WRITE (6, 1007) IST, KOUNT
26      DO 27 IPR=1, IPP
27      TISURF ( IST , IPR) =TWALL (NODES, IPR)

C -----
C ----- CALCULATE POWER GENERATED IN EACH SEGMENT IN BTU/HOUR -----

```

```

C -----
POWER =0.0
DO 28 ISL=1,NODES
  DO 28 IPR=1,IPP
    POWER=POWER+AMPS (ISL, IPR) *AMPS (ISL, IPR) *RESIS (ISL, IPR)
28  CONTINUE

POWERS (IST) =POWER*3.41214

C -----
C ----- CALCULATE HEAT FLUX AT INSIDE SURFACE -----
C -----

ISL=NODES
IPP= IP (IST)
ITHCTL=IPP
DO 29 IPR=1,IPP
  IPLUS=IPR+1
  IMINS=IPR-1
  IF (IMINS.EQ.0 .AND. IPP .EQ. ITHCTL) IMINS=ITHCTL
  IF (IPLUS.EQ. (ITHCTL+1) .AND. IPP.EQ. ITHCTL) IPLUS=1
  Q1 = PI* (CONDK (ISL-1, IPR) +CONDK (ISL, IPR) ) * (R (ISL-1) -DELR/2.0) *
+      (TWALL (ISL, IPR) -TWALL (ISL-1, IPR) ) / (IPP*DELR)
  Q2 = IPP* (CONDK (ISL, IPLUS) +CONDK (ISL, IPR) ) *DELR
+      * (TWALL (ISL, IPR) -TWALL (ISL, IPLUS) ) / (PI*R (ISL) *8.0)
  Q4 = IPP* (CONDK (ISL, IPR) +CONDK (ISL, IMINS) ) *DELR
+      * (TWALL (ISL, IPR) -TWALL (ISL, IMINS) ) / (PI*R (ISL) *8.0)
  QGEN=3.41214*12.0*AMPS (ISL, IPR) *AMPS (ISL, IPR)
+      *RSVTY (ISL, IPR) /XAREA (ISL)
29  QFLXID (IST, IPR) = (QGEN-Q1-Q2-Q4) *IPP*12.0/ (2.0*PI*R (ISL) )

30 CONTINUE

C -----
C ----- CALCULATE REYNOLDS NUMBERS AT INSIDE TUBE SURFACE -----
C -----

DO 40 IST=1,NSTN
  IPP= IP (IST)
  DO 40 IPR=1,IPP
    TR=TISURF (IST, IPR)
    CALL MEW (TR, MFLUID, X2, VISS)
    REN (IST, IPR) =RMFL*48.0/ (PI*DIN*VISS)

40 CONTINUE

```

```

C -----
C ----- CALCULATE TOTAL POWER GENERATED IN BTU/HOUR -----
C -----

      TPOWER=0.0
      DO 45 IST=1,NSTN
45    TPOWER=TPOWER+POWERS(IST)

C -----
C ----- CALCULATE BULK FLUID TEMPERATURE AT EACH STATION,DEG.F -----
C -----

      TBULK(1)=TIN+(TOUT-TIN)*LTP(1)/LTEST
      DO 50 IST =2,NSTN
50    TBULK(IST) = TBULK(IST-1) + (TOUT-TIN)*LTP(IST)/LTEST

C -----
C ----- CALCULATION OF INPUT AND OUTPUT HEAT TRANSFER RATE,BTU/HR -----
C ----- AND OVERALL AVERAGE REYNOLDS AND PRANDTL NUMBERS -----
C -----

      QGCALC=TPOWER
      QGEXPT =TAMPS*VOLTS*3.41214
      QIN=QGEXPT
      QFLXAV=QIN/(3.1416*DIN/12.0*(LHEAT/12.0))

C ----- CALCULATE FLUID PROPERTIES AT TAVE -----

      T=(TOUT+TIN)/2.0
      CALL SPHEAT(T,MFLUID,X2,SPHT)
      CALL MEW(T,MFLUID,X2,VISC)
      CALL CONDFL(T,MFLUID,X2,COND)

      QBALC=RMFL*SPHT*(TOUT-TIN)
      QPCT=(QIN-QBALC)*100.0/QIN
      AID=PI*DIN*DIN/4.0/144.0
      GW=RMFL/AID
      REYNO=GW*DIN/12.0/VISC
      PRNO=VISC*SPHT/COND

C -----
C ----- CALCULATION OF PERIPHERAL HEAT TRANSFER COEFFICIENT -----
C ----- FROM EXPERIMENTAL DATA,BTU/(HR-SQ.FT-DEG.F) -----
C -----

      DO 55 IST=1,NSTN
      IPP= IP(IST)

```

```

DO 55 IPR=1, IPP
HTCOFF (IST, IPR) =QFLXID (IST, IPR) / (TISURF (IST, IPR) -TBULK (IST) )
55 CONTINUE

```

```

C -----
C ----- CALCULATE RATIO OF TOP/BOTTOM HEAT TRANSFER COEFFICIENTS -----
C -----

```

```

DO 65 IST=1, NSTN
IPP= IP (IST)
IF (IPP.EQ. 4) GO TO 60
SHTHB (IST) =HTCOFF (IST, 1) /HTCOFF (IST, 2)
GO TO 65
60 SHTHB (IST) =HTCOFF (IST, 1) /HTCOFF (IST, 3)
65 CONTINUE

```

```

C -----
C ----- CALCULATION OF OVERALL HEAT TRANSFER COEFFICIENT -----
C -----

```

```

DO 75 IST=1, NSTN
QQ=0.0
TT=0.0
IPP= IP (IST)
DO 70 J=1, IPP
TT=TT+TISURF (IST, J)
QQ=QQ+QFLXID (IST, J)
70 CONTINUE
TAVG (IST) =TT/IPP
QAVG (IST) =QQ/IPP
H (IST) =QAVG (IST) / (TAVG (IST) -TBULK (IST) )
75 CONTINUE

```

```

C -----
C ----- CALCULATE FLUID PROPERTIES -----
C -----

```

```

DO 85 IST=1, NSTN
T=TBULK (IST)
CALL MEW (T, MFLUID, X2, VISC)
CALL SPHEAT (T, MFLUID, X2, SPHT)
CALL CONDFL (T, MFLUID, X2, COND)
CALL DENS (T, MFLUID, X2, ROW)
CALL BET (T, MFLUID, X2, BETA)
VISCA (IST) =VISC
ROWA (IST) =ROW

```

```

PR(IST) = VISC*SPHT/COND
RENO(IST) = GW*DIN/(12.0*VISC)
GRNO(IST)=G*BETA*ROW**2*(DIN/12)**3*(TAVG(IST)-TBULK(IST))
+      /VISC**2 *3600.0**2
TIS=0.0
IPP= IP(IST)
DO 80 IPR=1,IPP
80      TIS=TIS+TISURF(IST,IPR)
T=TIS/IPP
CALL MEW(T,MFLUID,X2,VISWL)
VISWLA(IST) = VISWL
VISBW(IST) = VISC/VISWL
SNUS(IST)=H(IST)*DIN/(12.0*COND)
TWALL(IST,1)=TAVG(IST)
85 CONTINUE

```

```

C -----
C ----- CALCULATE FLUID VELOCITY IN FT/SEC -----
C -----

```

```

      VEL = VFLOW/(2.462557*DIN*DIN)

```

```

C -----
C ----- PRODUCE OUTPUT -----
C -----

```

```

      CALL PRNT

```

```

C -----
C ----- PROMPT USER FOR PROGRAM TERMINATION OR CONTINUATION -----
C -----

```

```

      WRITE(*,*) 'WANT TO PROCEED PRESS 1 ELSE 0'
      READ(*,*) RSWT

```

```

      IF(RSWT.EQ.1) THEN
      GOTO 1200
      ENDIF

```

```

      KEEP = 2
      GO TO 8

```

```

99 STOP

```

```

1002 FORMAT(A36)
1003 FORMAT(A4)
1004 FORMAT(I4,I3)

```



```

1005 FORMAT(I2,F5.2,F8.4,5F8.2)
1006 FORMAT(I3,I3,F9.2,8F8.2)
1007 FORMAT(/5X,'TEMPERATURES AT STATION',I3,' DO NOT CONVERGE AFTER',
+         I3,' ITERATIONS. JUMP TO NEXT STATION')
1008 FORMAT(//////////,6X,'DATA REDUCTION COMPLETED FOR RUN # ',I4,
+         //////////)
        CLOSE(6)
        CLOSE(7)
        END

```

```

C *****
C *
C *
C *
C *
C *
C *
C *
C *****

```

```

SUBROUTINE GEOM

```

```

COMMON /MAIN1/ IST,KOUNT,NSTN
+       /GEOM1/ XAREA(31),R(31),LTP(32),LTH(32),DELZ(31),LHEAT,
+       LTEST,LOD(31),DOUT,DIN,DELR,NODES,NSLICE,PI

```

```

REAL*4 LTH,LTP,LTEST,LHEAT,LOD

```

```

NSLICE=10
NODES= NSLICE + 1

```

```

C -----
C ----- PROMPT FOR PIPE SIZE -----
C -----

```

```

1 IPSO = 2

```

```

DOUT=1.315
DIN=1.097
LHEAT=103.5

```

```

C -----
C ----- CALCULATE GEOMETRY FOR FINITE DIFFERENCING -----
C -----

```

```

2 PI = 3.141592654
LTEST = LHEAT+0.5

```

```

DO 3 I=1,NSTN
3   LOD(I)=LTH(I)/DIN

```

```

LTH(NSTN+1)=LHEAT
LTP(1)=LTH(1)
SUM=LTP(1)
DO 4 I=2,NSTN
LTP(I) = LTH(I)-LTH(I-1)
4 SUM=SUM+LTP(I)
LTP(NSTN+1)=LHEAT-SUM
DELZ(1) = LTH(1)+( LTH(2)-LTH(1))/2.0
DO 5 I=2,NSTN
5 DELZ(I) = ( LTH(I+1)-LTH(I-1))/2.0
RETURN
END

```

```

C *****
C *
C * SUBROUTINE BET *
C *
C * CALCULATES THE THERMAL EXPANSION COEFFICIENT (BETA) FOR PURE *
C * WATER AND ANY CONCENTRATION OF ETHYLENE GLYCOL/WATER SOLUTION. *
C * THE INPUT IS TEMPERATURE IN DEGREES F AND THE OUTPUT IS 1/F. *
C *
C *****

```

```

SUBROUTINE BET(TF,MFLUID,X,BETA)

```

```

T = (TF-32.0)/1.8

```

```

C ----- PURE WATER -----

```

```

IF(MFLUID.GT.1)GO TO 1

```

```

PDRT=0.0615-0.01693*T+2.06E-4*T**2-1.77E-6*T**3+6.3E-9*T**4

```

```

GO TO 2

```

```

C ----- ETHYLENE GLYCOL -----

```

```

1 PDRTA = -1.2379*1.E-4 - 9.9189*1.E-4*X +4.1024*1.E-4*X*X

```

```

PDRTB = 2.*((-2.9837E-06*T+2.4614E-06*X*T -9.5278E-8*X*X*T))

```

```

PDRT=(PDRTA+PDRTB)*1000.

```

```

2 CALL DENS(TF,MFLUID,X,ROW)

```

```

ROW=ROW/.062427

```

```

BETAC= -(1.0/ROW)*(PDRT)

```

```

BETAF =(1.0/BETAC)*1.8

```

```

BETA = 1.0/BETAF

```

```

RETURN

```

```

END

```

```

C *****

```



```

AD(2,3)= 4.1024E-04
AD(3,1)=-2.9837E-06
AD(3,2)= 2.4614E-06
AD(3,3)= -9.5278E-08

DO 2 I=1,3
  DO 2 J=1,3
2   D(I,J)=AD(I,J)*X**(J-1)*T**(I-1)
  SUM=0.0
  DO 3 I=1,3
    DO 3 J=1,3
3   SUM=SUM+D(I,J)
  SUM=SUM*1.E6/1000.0
  ROW=SUM*0.062427

4 RETURN
END

```

```

C *****
C *
C *          SUBROUTINE MEW
C *
C *          CALCULATES THE DYNAMIC VISCOSITY (VISC) FOR PURE WATER
C *          AND ANY CONCENTRATION OF ETHYLENE GLYCOL/WATER SOLUTION.
C * THE INPUT IS TEMPERATURE IN DEGREES F AND THE OUTPUT IS LB/HR.FT.
C *
C *          TEMPERATURE RANGE:
C *          PURE WATER          10 - 100 C
C *          E.G. MIXTURES      0 - 150 C
C *
C *****

```

```

SUBROUTINE MEW(TF,MFLUID,X,VISC)
DIMENSION V(3,3),AV(3,3),V2(3)

```

```

T=(TF-32.0)/1.8
IF(MFLUID.GT.1) GO TO 1

```

```

C ----- PURE WATER -----

```

```

IF(T.LT.10..OR.T.GT.115.0)THEN
  WRITE(*,*)' TEMPERATURE IS OUT OF RANGE IN SUBROUTINE MEW'
  STOP
END IF

```

```

VISC=2.4189*1.0019*10.0**((1.3272*(20.0-T)-0.001053*(20-T)
+ **2)/(T+105.0))

```

GO TO 4

C ----- ETHYLENE GLYCOL -----

```
1 IF(T.LT.0..OR.T.GT.150.0) THEN
  WRITE(*,*) ' TEMPERATURE IS OUT OF RANGE IN SUBROUTINE MEW'
  STOP
END IF
```

```
AV(1,1)=0.55164
AV(1,2)=2.6492
AV(1,3)=0.82935
AV(2,1)=-0.027633
AV(2,2)=-0.031496
AV(2,3)= 0.0048136
AV(3,1)= 6.0629E-17
AV(3,2)= 2.2389E-15
AV(3,3)= 5.879E-16
```

```
DO 2 I=1,2
DO 2 J=1,3
  V(I,J)=AV(I,J)*X**(J-1)*T**(I-1)
2   V2(J)=AV(3,J)*X**(J-1)
```

```
SUM=0.0
DO 3 I=1,3
3  SUM=SUM+V2(I)
  V3=SUM**0.25*T*T
  VISC=V3 + V(1,1)+V(1,2)+V(1,3)+V(2,1)+V(2,2)+V(2,3)
VISC=EXP(VISC)*2.4189
```

```
4 RETURN
END
```

```
C *****
C *
C *          SUBROUTINE PRNUM          *
C *
C *          CALCULATES THE PRANDTL NO. (PRN) FOR PURE WATER          *
C *          AND ANY CONCENTRATION OF ETHYLENE GLYCOL/WATER SOLUTION.  *
C *          THE INPUT IS TEMPERATURE IN DEGREES F.                    *
C *
C *          TEMPERATURE RANGE:                                          *
C *          PURE WATER          10 - 100 C                              *
C *          E.G. MIXTURES      0 - 150 C                               *
C *
C *****
```

```
SUBROUTINE PRNUM(TF,MFLUID,X,PRN)
DIMENSION P(3,3),AP(3,3),P2(3)
```

```
T=(TF-32.0)/1.8
IF(MFLUID.GT.1) GO TO 1
```

```
C ----- PURE WATER -----
```

```
IF(T.LT.10.OR.T.GT.115.0)THEN
WRITE(*,*)' TEMPERATURE IS OUT OF RANGE IN SUBROUTINE PRNUM'
STOP
END IF
```

```
CALL SPHEAT(TF,MFLUID,X,SPHT)
CALL MEW(TF,MFLUID,X,VISC)
CALL CONDFL(TF,MFLUID,X,COND)
PRN=SPHT*VISC/COND
RETURN
```

```
C ----- ETHYLENE GLYCOL -----
```

```
1 IF(T.LT.0.0.OR.T.GT.150.0)THEN
WRITE(*,*)' TEMPERATURE IS OUT OF RANGE IN SUBROUTINE PRNUM'
STOP
END IF
```

```
AP(1,1)=2.5735
AP(1,2)=3.0411
AP(1,3)=0.60237
AP(2,1)=-0.031169
AP(2,2)=-0.025424
AP(2,3)= 0.0037454
AP(3,1)= 1.1605E-16
AP(3,2)= 2.5283E-15
AP(3,3)= 2.3777E-16
```

```
DO 2 I=1,2
```

```
DO 2 J=1,3
```

```
P(I,J)=AP(I,J)*X**(J-1)*T**(I-1)
```

```
2 P2(J)=AP(3,J)*X**(J-1)
```

```
SUM=0.0
```

```
DO 3 I=1,3
```

```
3 SUM=SUM+P2(I)
```

```
P3=SUM**0.25*T*T
```

```

PRN=P3+P(1,1)+P(1,2)+P(1,3)+P(2,1)+P(2,2)+P(2,3)
PRN=EXP(PRN)

```

```

RETURN
END

```

```

C *****
C *
C *          SUBROUTINE SPHEAT
C *
C *          CALCULATES THE SPECIFIC HEAT (SPHT) FOR PURE WATER
C *          AND ANY CONCENTRATION OF ETHYLENE GLYCOL/WATER SOLUTION.
C *          THE INPUT IS TEMPERATURE IN DEGREES F
C *          AND THE OUTPUT IS IN BTU/(LBM-DEGF) .
C *
C *          TEMPERATURE RANGE:
C *          PURE WATER          0 - 100 C
C *          E.G. MIXTURES      0 - 150 C
C *
C *****

```

```

SUBROUTINE SPHEAT(TF,MFLUID,X,SPHT)

```

```

T=(TF-32.0)/1.8
IF(MFLUID .GT. 1.0)GO TO 1

```

```

C ----- PURE WATER -----

```

```

IF(T.LT.0.0.OR.T.GT.115.0)THEN
WRITE(*,*)' TEMPERATURE IS OUT OF RANGE IN SUBROUTINE SPHT'
STOP
END IF

```

```

SPHT=-1.475E-7*T**3+3.66E-5*T*T-.0022*T+4.216
SPHT=SPHT/4.1868

```

```

RETURN

```

```

C ----- ETHYLENE GLYCOL -----

```

```

1 IF(T.LT.0.0.OR.T.GT.150.0)THEN
WRITE(*,*)' TEMPERATURE IS OUT OF RANGE IN SUBROUTINE SPHT'
STOP
END IF

```

```

CALL MEW(TF,MFLUID,X,VISC)
CALL CONDFL(TF,MFLUID,X,COND)

```



```

CALL PRNUM(TF,MFLUID,X,PRN)
SPHT = PRN*COND/VISC
RETURN
END

```

```

C *****
C *
C *          SUBROUTINE PRINT-OUT          *
C *
C *          PRINTS DATA TO OUTPUT FILES:  *
C *
C *          "RN(run #).SUM"      - Device #6 *
C *          "RN(run #).DAT"      - Device #9 *
C *
C *****

```

SUBROUTINE PRNT

```

INTEGER IREN(31,8),IDFLX(31,8),hHAU(10,4),hSDT(10,4)
INTEGER STN
COMMON /PRINT/ IPICK,REN(31,8),TBULK(31),VEL,REYNO,PRNO,GW,
+             HTCOFF(31,8),H(31),RENO(31),GRNO(31),PR(31),
+             SNUS(31),VISBW(31),SHTHB(32),QFLXID(31,8),QFLXAV,
+             QGEXPT,QBALC,QPCT,IPMAX,TAVG(31),VISCA(31),
+             VISWLA(31),ROWA(31)
+             /INPUT/ TROOM,VOLTS,TAMPS,RMFL,MFLUID,X2,FLOWRT,NRUN,VFLOW,
+             TIN,TOUT,TOSURF(31,8),TISURF(31,8),IP(32),KST(32)
+             /TEMP1/ TWALL(31,8),AMPS(31,8),RESIS(31,8),POWERS(32),
+             TPOWER
+             /MAIN1/ IST,KOUNT,NSTN
+             /GEOM1/ XAREA(31),R(31),LTP(32),LTH(32),DELZ(31),LHEAT,
+             LTEST,LOD(31),DOUT,DIN,DELR,NODES,NSLICE,PI

REAL*4 LTH,LTP,LTEST,LHEAT,H,HTCOFF,LOD
REAL*8 muW(10),Twl(10),muB(10),Tb1(10),kL(10),nHAU(10),nSDTT(10)
+      ,aPTP,fPTP,fGNL,ndTB(10),nPTP(10),nGNL(10),nCLB(10),
+      nSDTL(10),TMP,AmBmW,fCHR,nCHRL,nCHRT,nCHR(10),nGHJL(10),
+      nGHJT(10),cPTP
REAL*8 LovD,DovL,IHCOF(31,8)
COMMON/STATION/STN
LovD=94.80401d0
DovL=0.010548d0
AmBmW=0.0
DO 5000 IST=1,10
nGNL(IST)=0.0
nGHJt(IST)=0.0
nPTP(IST)=0.0

```

```

5000 CONTINUE
C -----
C ----- SET FLAG FOR STATION OUTPUT CONTROL -----
C -----

      ATST=NSTN/11.
      IFST=INT(ATST)+1

C -----
C ----- PRINT RUN NUMBER & TUBE DATA -----
C -----

C ----- ENGLISH UNITS -----

      WRITE(6,2001)NRUN

C ----- PRINT FLUID-TYPE DESCRIPTION -----

      IF(MFLUID.EQ.1) THEN
        WRITE(6,2003)
      ELSE
        WRITE(6,2004)X2
      ENDIF

C ----- PRINT TUBE DATA -----

      IGW=GW
      IREYN=REYNO
      IFXA=QFLXAV
      IQEX=QGEXPT
      IQBL=QBALC

      WRITE(6,2016)VFLOW,RMFL,IGW,VEL,TROOM,TIN,TOUT,IREYN,PRNO,
+          TAMP, VOLTS, IFXA, IQEX, IQBL, QPCT

C -----
C ----- PRINT TUBE OUTSIDE SURFACE TEMPERATURES -----
C -----

C ----- ENGLISH UNITS -----

      DO 5 K=1,NSTN
      IF(IP(K).EQ.2) THEN
        TOSURF(K,3)=TOSURF(K,2)
        TOSURF(K,2)=0.0
        TOSURF(K,4)=0.0
      ELSE

```

```

5  ENDIF

      WRITE (6,2005)
      DO 7 ICNT=1,IFST
cc     KMIN=1+(ICNT-1)*9
cc     KMAX=KMIN+8
      KMIN=1+(ICNT-1)*10
      KMAX=KMIN+9
      IF (NSTN.LT.KMAX) KMAX=NSTN
      DO 6 IPR=1,IPMAX
      IF (IPR.EQ.1) WRITE (6,2006) (KST(K),K=KMIN,KMAX)
cc     IF (IPR.EQ.1 .AND. KMAX.LT. (KMIN+8)) WRITE (6,2007)
      IF (IPR.EQ.1 .AND. KMAX.LT. (KMIN+9)) WRITE (6,2007)
      WRITE (6,2008) IPR, (TOSURF (IST, IPR), IST=KMIN, KMAX)

6     CONTINUE
7     CONTINUE

C -----
C ----- PRINT INSIDE SURFACE TEMPERATURES TO OUTPUT FILE -----
C -----

C ----- ENGLISH UNITS -----

      DO 14 K=1,NSTN
      IF (IP(K).EQ.2) THEN
      TISURF (K, 3) =TISURF (K, 2)
      TISURF (K, 2) =0.0
      TISURF (K, 4) =0.0
      ELSE
14  ENDIF

      WRITE (6,2010)
      DO 16 ICNT=1,IFST
      KMIN=1+(ICNT-1)*10
      KMAX=KMIN+9
      IF (NSTN.LT.KMAX) KMAX=NSTN
      DO 15 IPR=1,IPMAX
      IF (IPR.EQ.1) WRITE (6,2006) (KST(K),K=KMIN,KMAX)
      IF (IPR.EQ.1 .AND. KMAX.LT. (KMIN+9)) WRITE (6,2007)
      WRITE (6,2008) IPR, (TISURF (IST, IPR), IST=KMIN, KMAX)

15  CONTINUE
16  CONTINUE

      DO 151 IST=1,10
      Twl (IST) = (TAVG (IST) -32.0) /1.8

```

```

      Tbl (IST) = (TBULK (IST) - 32.0) / 1.8
      muB (IST) = 2.4189 * 1.0019 * 10.0 ** ( (1.3272 * (20.0 - Tbl (IST)) -
+          0.001053 * (20 - Tbl (IST)) ** 2) / (Tbl (IST)
+          + 105.0) )
      muW (IST) = 2.4189 * 1.0019 * 10.0 ** ( (1.3272 * (20.0 - Twl (IST)) -
+          0.001053 * (20 - Twl (IST)) ** 2) / (Twl (IST) + 105.0) )

      kL (IST) = (0.56276 + 1.874E-3 * Tbl (IST) - 6.8E-6 * Tbl (IST) ** 2) * 0.5778D0
      AmBmW = AmBmW + (muB (IST) / muW (IST))

151  CONTINUE
      AmBmW = AmBmW / 10

C -----
C ----- PRINT REYNOLDS NUMBERS TO OUTPUT FILE -----
C -----

22  DO 29 K=1, NSTN
      IF (IP (K) .EQ. 2) THEN
          IREN (K, 1) = INT (REN (K, 1))
          IREN (K, 3) = INT (REN (K, 2))
          IREN (K, 2) = 0
          IREN (K, 4) = 0
      ELSE
          DO 28 L=1, IPMAX
28      IREN (K, L) = INT (REN (K, L))
29  ENDIF

      WRITE (6, 2014)
      DO 31 ICNT=1, IFST
          KMIN = 1 + (ICNT - 1) * 10
          KMAX = KMIN + 9
          IF (NSTN .LT. KMAX) KMAX = NSTN
      DO 30 IPR=1, IPMAX
          IF (IPR .EQ. 1) WRITE (6, 2006) (KST (K), K=KMIN, KMAX)
          IF (IPR .EQ. 1 .AND. KMAX .LT. (KMIN + 9)) WRITE (6, 2007)

              WRITE (6, 2015) IPR, (IREN (IST, IPR), IST=KMIN, KMAX)
30      CONTINUE
31      CONTINUE

C -----
C ----- PRINT INSIDE HEAT FLUXES TO OUTPUT FILE -----
C -----

C ----- ENGLISH UNITS -----

```

```

DO 35 K=1,NSTN
IF (IP (K) .EQ.2) THEN
  IDFLX (K, 1) =INT (QFLXID (K, 1) )
  IDFLX (K, 3) =INT (QFLXID (K, 2) )
  IDFLX (K, 2) =0
  IDFLX (K, 4) =0
ELSE
  DO 34 L=1, IPMAX
34   IDFLX (K, L) =INT (QFLXID (K, L) )
35 ENDIF

WRITE (6, 2020)
DO 37 ICNT=1, IFST
  KMIN=1+ (ICNT-1) *10
  KMAX=KMIN+9
  IF (NSTN.LT.KMAX) KMAX=NSTN
DO 36 IPR=1, IPMAX
  IF (IPR.EQ.1) WRITE (6, 2006) (KST (K) , K=KMIN, KMAX)
  IF (IPR.EQ.1 .AND. KMAX.LT. (KMIN+9) ) WRITE (6, 2007)
    WRITE (6, 2021) IPR, (IDFLX (IST, IPR) , IST=KMIN, KMAX)
36  CONTINUE
37  CONTINUE

```

```

C -----
C ---- PRINT PERIPHERAL HEAT TRANSFER COEFFICIENTS ----
C -----

```

```

  WRITE (6, 2017)NRUN
C ----- ENGLISH UNITS -----

```

```

DO 46 K=1,NSTN
IF (IP (K) .EQ.2) THEN
  IHCOF (K, 1) =HTCOFF (K, 1)
  IHCOF (K, 3) =HTCOFF (K, 2)
  IHCOF (K, 2) =0
  IHCOF (K, 4) =0
ELSE
  DO 45 L=1, IPMAX
45   IHCOF (K, L) =HTCOFF (K, L)
46 ENDIF

```

```

WRITE (6, 2023)
DO 48 ICNT=1, IFST
  KMIN=1+ (ICNT-1) *10
  KMAX=KMIN+9
  IF (NSTN.LT.KMAX) KMAX=NSTN
DO 47 IPR=1, IPMAX

```



```

+      /18X, 'FLUID VELOCITY', 7X, '=', F9.2, 3X, 'FT/S',
+      /18X, 'ROOM TEMPERATURE', 5X, '=', F9.2, 3X, 'F',
+      /18X, 'INLET TEMPERATURE', 4X, '=', F9.2, 3X, 'F',
+      /18X, 'OUTLET TEMPERATURE', 3X, '=', F9.2, 3X, 'F',
+      /18X, 'AVERAGE RE NUMBER', 4X, '=', I9,
+      /18X, 'AVERAGE PR NUMBER', 4X, '=', F9.2,
+      /18X, 'CURRENT TO TUBE', 6X, '=', F9.1, 3X, 'AMPS',
+      /18X, 'VOLTAGE DROP IN TUBE =', F9.2, 3X, 'VOLTS',
+      /18X, 'AVERAGE HEAT FLUX', 4X, '=', I9, 3X, 'BTU/(SQ.FT-HR)'
+      /18X, 'Q=AMP*VOLT', 11X, '=', I9, 3X, 'BTU/HR',
+      /18X, 'Q=M*C*(T2-T1)', 8X, '=', I9, 3X, 'BTU/HR',
+      /18X, 'HEAT BALANCE ERROR', 3X, '=', F9.2, 3X, '%'
2017 FORMAT(/ /31X, '*', 15('-',) , '*', /32X, 'RUN NUMBER ', I4, /31X, '*',
+      15('-',) , '*')
2020 FORMAT(/ /22X, 'INSIDE SURFACE HEAT FLUXES BTU/HR/FT2')
2021 FORMAT(3X, I1, 10I8)
2023 FORMAT(/14X, 'PERIPHERAL HEAT TRANSFER COEFFICIENT BTU/',
+      '(SQ.FT-HR-F)')
2028 FORMAT(/ /31X, '*', 15('-',) , '*', /32X, 'RUN NUMBER ', I4, /36X,
+      'SUMMARY', /31X, '*', 15('-',) , '*')
2029 FORMAT(/1X, 'ST', 6X, 'RE', 7X, 'PR', 5X, 'X/D', 5X, 'MUB', 5X, 'MUW',
+      5X, 'TB', 6X, 'TW', 5X, 'DENS', 6X, 'NU', /)
2030 FORMAT(1X, I2, 3X, F8.2, 2X, F5.2, 3X, F5.1, 3X, F5.3, 3X, F5.3,
+      2(2X, F6.2) , 3X, F5.2, 3X, F6.2)
2032 FORMAT(/, 20X, 'NOTE: TBULK IS GIVEN IN DEGREES FAHRENHEIT', /,
+      26X, 'MUB AND MUW ARE GIVEN IN LBM/(FT*HR)')

END

```

APPENDIX C
AIR-WATER EXPERIMENTAL DATA

Run #	\dot{m}_L [lbm/hr]	V_{SL} [ft/sec]	Re_{SL}	\dot{m}_G [lbm/hr]	V_{SG} [ft/sec]	Re_{SG}	X	T_{MX} [°F]	P_{MX} [psi]	ΔP [inH ₂ O]	P_G [psi]	α	Pr_L	\bar{h}_{TP} [Btu/hr-ft ² °F]	Q'' [Btu/ft ² -hr]	Heat Balance Error [%]
Annular-Wavy Transitional Flow Pattern (41 data points)																
8187	869.36	0.59	4533	60.43	6.95	19132	1.25	60.95	3.26	6.72	57.43	0.77	6.46	518.92	2772	2.31
8186	899.30	0.61	4660	56.85	6.89	17952	1.33	60.52	3.12	6.47	54.06	0.77	6.46	484.63	2813	1.46
8185	879.85	0.60	4640	49.56	6.73	15651	1.40	61.79	2.63	5.38	46.68	0.77	6.46	459.90	2810	2.31
8184	880.14	0.60	4696	45.69	6.66	14430	1.45	62.64	2.34	5.10	42.43	0.77	6.46	441.75	2806	-1.53
8183	875.01	0.59	4658	44.90	6.65	14180	1.45	62.47	2.26	4.88	41.53	0.77	6.46	434.83	2828	-1.69
8182	918.22	0.62	4838	44.37	6.69	14013	1.52	61.60	2.29	4.89	40.52	0.76	6.46	435.15	2836	-3.13
8181	954.95	0.65	4985	48.21	6.79	15225	1.51	61.09	2.67	5.70	44.48	0.76	6.46	460.15	2823	0.25
8180	876.87	0.60	4569	46.31	6.71	14624	1.43	61.11	2.34	4.53	42.77	0.77	6.46	419.88	2793	0.96
8179	833.60	0.57	4355	47.05	6.74	14857	1.36	61.02	2.31	4.77	43.44	0.77	6.46	426.55	2780	-1.42
8178	843.59	0.57	4219	48.43	6.78	15335	1.35	58.83	2.40	5.29	44.64	0.77	6.46	417.65	2778	-0.12
8177	776.18	0.53	4073	53.30	6.75	16877	1.21	61.56	2.55	5.38	50.80	0.78	6.46	483.78	2785	0.57
8176	776.36	0.53	4097	49.25	6.71	15635	1.26	61.97	2.36	5.05	46.06	0.78	6.63	437.70	2811	2.97
8175	757.28	0.51	4061	51.04	6.71	16203	1.21	63.20	2.41	5.34	48.22	0.78	6.63	471.58	2820	1.68

Run #	\dot{m}_L [lbm/hr]	V_{SL} [ft/sec]	Re_{SL}	\dot{m}_G [lbm/hr]	V_{SG} [ft/sec]	Re_{SG}	X	T_{MIX} [°F]	P_{MIX} [psi]	ΔP [inH ₂ O]	P_G [psi]	α	Pr_L	\bar{h}_{TP} [Btu/hr-ft ² -°F]	Q'' [Btu/ft ² -hr]	Heat Balance Error [%]
Annular-Wavy Transitional Flow Pattern (41 data points - Cont'd)																
8174	783.29	0.53	4064	53.73	6.69	17055	1.22	60.51	2.65	5.59	51.76	0.78	6.63	482.00	2775	1.45
8173	812.52	0.55	4177	52.57	6.62	16689	1.28	60.23	2.69	5.52	50.96	0.77	6.63	463.80	2767	5.63
8172	768.62	0.52	4026	57.27	6.65	18230	1.18	61.20	2.91	6.09	56.32	0.78	6.63	523.98	2720	5.10
8171	791.79	0.54	4533	53.48	5.98	17024	1.31	67.90	3.16	6.55	59.14	0.77	6.63	518.28	2486	-2.22
8170	866.91	0.59	4383	59.96	6.67	19034	1.28	58.91	3.23	1.37	59.76	0.77	6.63	516.75	2727	3.78
8169	823.04	0.56	4202	50.13	5.58	15913	1.44	59.38	3.17	1.45	59.71	0.76	6.63	537.90	2713	3.96
8168	697.79	0.47	3556	52.79	5.36	16760	1.24	59.44	3.30	1.43	66.95	0.77	6.63	548.48	2703	12.95
8167	694.61	0.47	3728	44.09	5.10	13995	1.36	63.00	2.66	1.37	56.88	0.76	6.63	503.75	2701	8.78
8166	717.91	0.49	3734	45.26	5.33	14368	1.36	60.54	2.61	5.77	55.68	0.77	6.63	474.70	2839	7.15
8165	684.29	0.46	3383	46.29	5.30	14694	1.29	57.28	2.66	6.01	57.65	0.77	6.63	491.13	2821	6.86
8164	662.13	0.45	3366	47.17	5.32	14976	1.24	58.95	2.68	5.73	58.84	0.77	6.63	476.38	2822	13.24
8163	628.31	0.43	3209	48.34	5.27	15387	1.18	59.39	2.76	6.00	60.99	0.78	6.80	531.93	2788	12.83
8162	595.01	0.40	3126	50.33	5.28	16021	1.11	61.54	2.85	6.23	64.00	0.78	6.80	588.55	2837	12.80

Run #	\dot{m}_L [lbm/hr]	V_{SL} [ft/sec]	Re_{SL}	\dot{m}_G [lbm/hr]	V_{SG} [ft/sec]	Re_{SG}	X	T_{MIX} [°F]	P_{MIX} [psi]	ΔP [inH ₂ O]	P_G [psi]	α	Pr_L	\bar{h}_{TP} [Btu/hr-ft ² -°F]	Q'' [Btu/ft ² -hr]	Heat Balance Error [%]
Annular-Wavy Transitional Flow Pattern (41 data points - Cont'd)																
8161	651.43	0.44	3639	43.65	5.01	13931	1.31	66.09	2.65	5.77	57.05	0.77	6.98	589.23	2877	11.69
8160	586.27	0.40	2958	47.93	5.26	15176	1.11	58.87	2.68	5.96	61.03	0.78	6.46	609.90	2861	20.02
8159	595.09	0.40	3086	45.93	5.21	14504	1.15	60.63	2.57	5.68	58.88	0.78	6.30	530.05	2862	14.45
8158	535.60	0.36	2809	51.13	5.33	16189	0.99	61.49	2.71	6.05	65.12	0.79	6.46	585.00	2851	17.23
8157	539.52	0.37	2825	48.32	5.23	15300	1.03	61.23	2.58	5.81	62.13	0.79	6.46	576.88	2851	17.81
8156	547.96	0.37	2837	45.83	5.16	14511	1.07	60.26	2.44	5.49	59.09	0.79	6.46	545.35	2753	15.86
8155	490.70	0.33	2556	50.66	5.29	16040	0.92	61.03	2.60	5.83	64.95	0.80	6.46	601.53	2556	18.91
8154	495.58	0.34	2583	48.01	5.18	15240	0.96	61.06	2.41	5.47	62.03	0.80	6.63	569.50	2744	17.32
8153	478.38	0.32	2566	47.78	5.14	15208	0.94	62.77	2.36	5.35	62.13	0.80	6.80	640.53	2830	17.84
8152	514.50	0.35	2944	39.53	4.82	12615	1.12	67.62	2.06	4.80	52.75	0.79	6.98	664.75	2899	13.60
8151	459.41	0.31	2413	53.38	5.52	16901	0.83	61.41	2.46	5.59	65.71	0.81	6.46	643.60	2723	17.73
8150	422.43	0.29	2227	54.83	5.54	17359	0.76	61.76	2.43	5.58	67.69	0.82	6.46	708.90	2690	19.58
8149	455.96	0.31	2376	47.80	5.36	15134	0.88	61.12	2.16	5.09	59.43	0.81	6.46	587.58	2626	18.30

Run #	\dot{m}_L [lbm/hr]	V_{SL} [ft/sec]	Re_{SL}	\dot{m}_G [lbm/hr]	V_{SG} [ft/sec]	Re_{SG}	X	T_{MIX} [°F]	P_{MIX} [psi]	ΔP [inH ₂ O]	P_G [psi]	α	Pr_L	\bar{h}_{TP} [Btu/hr-ft ² °F]	Q'' [Btu/ft ² -hr]	Heat Balance Error [%]
Annular-Wavy Transitional Flow Pattern (41 data points - Cont'd)																
8148	417.45	0.28	2192	46.86	5.30	14875	0.82	61.59	2.02	4.72	58.65	0.82	6.63	647.90	2542	19.04
8147	408.71	0.28	2163	49.05	5.32	15570	0.79	61.84	2.13	4.93	61.70	0.82	6.63	724.65	2497	18.49
Min.	408.71	0.28	2163	39.53	4.82	12615	0.76	57.28	2.02	1.37	40.52	0.76	6.30	417.65	2486	-3.13
Max.	954.95	0.65	4985	60.43	6.95	19132	1.52	67.90	3.30	6.72	67.69	0.82	6.99	724.65	2899	20.02
Avg.	689.41	0.47	3611	49.45	5.89	15678	1.19	61.36	2.60	5.14	55.61	0.78	6.57	531.11	2764	8.65

Run #	\dot{m}_L [lbm/hr]	V_{SL} [ft/sec]	Re_{SL}	\dot{m}_G [lbm/hr]	V_{SG} [ft/sec]	Re_{SG}	X	T_{MIX} [°F]	P_{MIX} [psi]	ΔP [inH ₂ O]	P_G [psi]	α	Pr_L	\bar{h}_{TP} [Btu/hr-ft ² °F]	Q'' [Btu/ft ² -hr]	Heat Balance Error [%]
Bubbly-Slug or Bubbly-Slug-Annular Transitional Flow Pattern (36 data points)																
8113	4339.83	2.94	24147	65.28	5.82	20834	5.70	65.73	17.45	12.93	77.69	0.54	6.98	1186.08	4019	6.56
8112	4528.40	3.07	23554	36.33	5.07	11533	7.99	60.90	12.54	12.93	44.79	0.50	6.80	932.60	3735	-2.45
8111	4602.14	3.12	24265	45.93	5.41	14580	7.15	61.83	14.81	12.93	55.72	0.51	6.80	964.75	3880	-5.57
8110	4564.06	3.10	25820	24.95	4.32	7921	10.13	66.93	10.83	12.93	33.25	0.47	6.80	995.25	3811	-13.07
8109	4358.09	2.96	26140	66.82	5.80	21213	5.66	71.30	17.96	12.93	80.73	0.53	6.80	1307.15	3564	-20.55
8108	4488.11	3.04	23492	47.27	5.31	15047	6.99	61.34	15.03	12.93	58.82	0.51	6.98	1131.75	3531	-3.36
8107	4553.43	3.09	25581	52.25	5.36	16722	6.79	66.41	15.91	12.93	65.27	0.51	7.18	1266.35	3875	-5.42
8106	4454.92	3.02	23197	51.60	5.47	16381	6.59	61.00	15.39	12.93	63.49	0.52	6.80	1014.20	3621	-16.96
8105	4261.79	2.89	22011	28.57	4.71	9093	8.66	60.38	9.84	12.93	35.40	0.50	6.98	902.38	3745	8.88
8104	3809.78	2.58	19589	26.91	4.66	8565	8.06	60.13	8.54	12.93	32.95	0.52	6.98	809.75	3505	9.51
8103	4160.49	2.82	21518	38.51	5.03	12324	7.28	60.54	10.83	12.93	48.08	0.52	6.98	889.93	3483	4.38
8102	4123.59	2.80	21439	56.08	5.50	17899	5.94	60.88	15.44	12.93	69.16	0.53	6.98	994.45	3810	1.42
8101	4032.47	2.74	22314	60.18	5.50	19258	5.67	65.30	16.15	12.93	75.03	0.54	6.98	1101.63	4048	0.45

Run #	\dot{m}_L [lbm/hr]	V_{SL} [ft/sec]	Re_{SL}	\dot{m}_G [lbm/hr]	V_{SG} [ft/sec]	Re_{SG}	X	T_{MIX} [°F]	P_{MIX} [psi]	ΔP [inH ₂ O]	P_G [psi]	α	Pr_L	\bar{h}_{TP} [Btu/hr-ft ² -°F]	Q'' [Btu/ft ² -hr]	Heat Balance Error [%]
Bubbly-Slug or Bubbly-Slug-Annular Transitional Flow Pattern (36 data points - Cont'd)																
7199	4055.16	2.75	20007	27.94	4.69	8940	8.47	57.30	9.25	12.93	34.26	0.51	7.80	1098.85	4539	-18.75
7196	3483.27	2.36	16496	53.66	5.18	17171	5.38	54.54	13.85	12.93	70.23	0.55	7.37	906.65	3854	12.40
7195	3720.04	2.52	18852	34.49	4.67	11036	7.16	59.13	10.56	12.93	45.94	0.52	7.18	942.88	3721	13.62
7194	3672.10	2.49	17699	38.76	4.95	12371	6.59	55.77	10.87	12.93	49.85	0.54	7.58	906.85	4018	-1.32
7193	3181.73	2.16	15358	25.40	4.53	8107	7.12	55.78	6.41	12.93	31.50	0.54	6.98	754.63	3946	1.07
7192	2814.66	1.91	13941	46.28	4.95	14770	4.80	57.59	9.84	12.93	62.30	0.58	6.98	801.15	3989	3.11
7191	2978.41	2.02	16406	32.45	4.52	10384	6.11	65.00	7.74	12.93	44.26	0.56	7.18	866.48	3924	-9.78
7190	2962.32	2.01	16937	37.33	4.64	11944	5.67	67.70	8.99	12.93	51.37	0.56	7.18	972.98	3859	-11.67
7189	3051.29	2.07	16834	26.83	4.55	8564	6.69	65.06	6.35	12.93	33.92	0.55	6.98	834.33	3908	-14.84
7188	2503.46	1.70	13919	49.78	4.92	15889	4.21	65.84	9.65	12.93	68.61	0.60	6.98	901.73	3817	-5.62
7187	2663.37	1.81	15779	40.69	4.72	12988	4.92	70.40	8.70	12.93	56.30	0.58	6.98	993.13	3907	0.88
7186	2506.04	1.70	13560	33.23	4.73	10549	5.04	63.66	6.21	12.93	43.59	0.59	6.80	746.73	3847	-0.69
7185	2589.45	1.76	14749	26.40	4.71	8380	5.70	67.35	5.34	12.60	31.84	0.58	6.80	703.28	3685	-13.90

Run #	\dot{m}_L [lbm/hr]	V_{SL} [ft/sec]	Re_{SL}	\dot{m}_G [lbm/hr]	V_{SG} [ft/sec]	Re_{SG}	X	T_{MIX} [°F]	P_{MIX} [psi]	ΔP [inH ₂ O]	P_G [psi]	α	Pr_L	\bar{h}_{TP} [Btu/hr-ft ² -°F]	Q'' [Btu/ft ² -hr]	Heat Balance Error [%]
Bubbly-Slug or Bubbly-Slug-Annular Transitional Flow Pattern (36 data points - Cont'd)																
7184	2017.52	1.37	11763	43.25	4.85	13730	3.69	69.19	6.50	12.93	59.28	0.63	6.98	796.93	3666	0.29
7183	2197.20	1.49	13028	32.15	4.70	10207	4.56	70.44	5.26	12.75	42.01	0.61	6.98	741.60	3525	-9.24
7182	2064.29	1.40	12121	27.29	4.64	8686	4.63	69.90	4.29	10.77	33.97	0.62	6.98	647.20	3425	-10.63
7181	2015.70	1.37	12138	29.31	4.58	9353	4.44	71.57	4.48	10.79	38.07	0.62	6.98	711.60	3602	-9.19
7180	1488.42	1.01	9441	30.99	4.69	9837	3.25	75.48	3.75	8.45	40.24	0.66	6.63	698.15	3717	-4.37
7179	1406.43	0.95	8700	21.54	4.00	6857	3.86	73.41	3.11	2.43	29.93	0.65	6.63	574.35	3833	13.96
7178	1698.92	1.15	10230	31.76	4.41	10109	3.72	72.17	4.61	10.91	44.84	0.64	6.46	668.40	3835	9.21
7177	1572.87	1.07	9475	40.71	4.52	12958	3.11	71.71	5.55	12.13	59.72	0.65	6.46	725.68	3846	10.20
7176	1480.16	1.00	9178	45.24	4.64	14399	2.79	73.81	6.00	12.71	65.88	0.66	6.46	761.08	3750	18.26
7173	1233.54	0.84	7842	28.59	4.45	9101	2.90	75.65	3.14	6.44	38.51	0.68	6.46	622.00	3817	3.84
Min.	1233.54	0.84	7842	21.54	4.0	6857	2.79	54.54	3.11	2.43	29.93	0.47	6.46	574.35	3425	-20.55
Max.	4602.14	3.12	26140	66.82	5.82	21213	10.13	75.65	17.96	12.93	80.73	0.68	7.80	1307.15	4539	18.26
Avg.	3156.48	2.14	17153	39.02	4.87	12436	5.76	65.31	9.48	12.12	50.47	0.57	6.94	885.36	3796	-1.65

Run #	\dot{m}_L [lbm/hr]	V_{SL} [ft/sec]	Re_{SL}	\dot{m}_G [lbm/hr]	V_{SG} [ft/sec]	Re_{SG}	X	T_{MIX} [°F]	P_{MIX} [psi]	ΔP [inH ₂ O]	P_G [psi]	α	Pr_L	\bar{h}_{TP} [Btu/hr-ft ² °F]	Q'' [Btu/ft ² -hr]	Heat Balance Error [%]
Slug Flow Pattern (53 data points)																
7162	1266.47	0.86	8029	3.47	1.85	1093	10.53	75.31	0.37	1.16	1.06	0.55	5.32	283.70	3484	4.69
7161	1236.75	0.84	8299	5.75	2.91	1811	6.70	79.88	0.55	1.91	1.90	0.62	5.20	311.13	3492	11.96
7160	1149.22	0.78	8559	5.76	2.93	1815	6.26	88.86	0.48	1.99	1.83	0.63	5.32	318.83	3469	15.72
7159	1095.80	0.75	8136	3.09	1.67	973	10.17	88.31	0.29	1.06	0.87	0.55	5.20	275.18	3456	7.94
7158	1038.42	0.71	7965	3.18	1.72	1003	9.45	91.38	0.30	1.14	0.88	0.57	5.32	268.88	3451	10.36
7157	986.92	0.67	8132	6.76	3.33	2131	4.81	97.77	0.45	2.22	2.36	0.67	5.44	335.95	3464	7.27
7156	955.28	0.65	7347	5.67	2.88	1791	5.39	91.77	0.45	1.83	1.78	0.66	5.44	290.55	3398	11.09
7155	953.20	0.65	7419	3.37	1.81	1065	8.39	92.64	0.26	1.22	0.91	0.59	5.71	261.63	3425	0.39
7154	873.22	0.59	6864	3.18	1.71	1006	8.19	93.52	0.25	1.15	0.82	0.59	5.85	268.45	3822	10.23
7153	846.51	0.58	6363	5.69	2.91	1794	4.83	89.87	0.36	1.65	1.74	0.67	5.85	255.08	3529	13.73
7152	793.49	0.54	6090	5.79	2.95	1824	4.48	91.38	0.40	1.67	1.76	0.68	5.71	245.48	3572	11.24
7151	776.79	0.53	5853	3.30	1.78	1040	7.09	90.10	0.23	1.22	0.85	0.62	5.85	214.95	3544	-0.83
7150	674.30	0.46	5065	2.91	1.58	919	6.99	89.53	0.19	0.87	0.72	0.62	5.99	186.38	3555	-2.53

Run #	\dot{m}_L [lbm/hr]	V_{SL} [ft/sec]	Re_{SL}	\dot{m}_G [lbm/hr]	V_{SG} [ft/sec]	Re_{SG}	X	T_{MIX} [°F]	P_{MIX} [psi]	ΔP [inH ₂ O]	P_G [psi]	α	Pr_L	\bar{h}_{TP} [Btu/hr-ft ² -°F]	Q" [Btu/ft ² -hr]	Heat Balance Error [%]
Slug Flow Pattern (53 data points - Cont'd)																
7149	664.35	0.45	4964	5.41	2.78	1714	4.06	89.08	0.26	1.49	1.53	0.70	5.99	213.58	3590	6.64
7148	603.01	0.41	4446	5.68	2.90	1799	3.58	87.98	0.27	1.48	1.66	0.71	5.99	188.98	3641	2.60
7147	577.46	0.39	4056	2.92	1.57	927	6.11	83.46	0.18	0.82	0.73	0.64	6.14	211.58	4270	15.44
7146	498.24	0.34	4186	5.34	2.76	1687	3.17	99.76	0.24	1.18	1.57	0.73	5.99	200.55	3725	10.44
7145	482.10	0.33	3800	3.11	1.67	985	4.91	93.90	0.10	0.72	0.85	0.67	6.14	171.55	3693	-3.13
7144	417.11	0.28	3292	6.19	3.13	1961	2.39	94.01	0.16	1.14	1.84	0.76	6.14	200.83	3705	2.24
7143	406.44	0.28	3172	4.31	2.28	1363	3.17	92.95	0.09	0.90	1.13	0.73	6.14	185.25	3852	3.98
7142	343.74	0.23	2586	3.84	2.05	1217	3.01	89.35	0.06	0.77	0.97	0.74	6.30	177.98	4080	10.63
7141	351.80	0.24	2468	5.86	3.02	1847	2.13	83.64	0.19	0.34	1.67	0.78	6.14	172.98	3886	9.88
7140	4832.33	3.28	29975	13.69	4.14	4324	13.84	73.88	6.47	12.93	12.95	0.46	6.80	1103.18	3912	7.97
7139	5014.48	3.40	31186	8.53	3.17	2687	19.78	74.11	5.16	10.92	7.95	0.40	6.80	1077.65	3878	7.35
7138	5179.73	3.51	33107	4.10	1.74	1296	36.93	76.27	3.98	6.81	5.11	0.29	6.98	1033.50	3862	4.51
7137	4741.96	3.22	30464	17.37	4.42	5484	11.98	76.63	7.60	12.93	18.14	0.47	6.80	1167.00	3803	2.61

Run #	\dot{m}_L [lbm/hr]	V_{SL} [ft/sec]	Re_{SL}	\dot{m}_G [lbm/hr]	V_{SG} [ft/sec]	Re_{SG}	X	T_{MIX} [°F]	P_{MIX} [psi]	ΔP [inH ₂ O]	P_G [psi]	α	Pr_L	\bar{h}_{TP} [Btu/hr-ft ² -°F]	Q'' [Btu/ft ² -hr]	Heat Balance Error [%]
Slug Flow Pattern (53 data points - Cont'd)																
7136	4833.58	3.28	30603	12.66	3.98	4008	14.59	75.50	6.07	12.93	11.86	0.45	6.80	1134.63	3816	-5.02
7135	4827.72	3.28	29753	9.47	3.36	3007	17.72	73.38	5.25	12.57	8.74	0.42	6.46	1152.03	4015	-1.19
7134	5064.16	3.44	35503	3.47	1.48	1105	41.59	83.74	3.69	6.17	4.72	0.27	6.38	1370.58	4594	7.37
7133	4421.10	3.00	28742	16.73	4.43	5295	11.35	77.57	6.39	12.93	16.85	0.48	6.38	1107.05	3857	6.33
7132	4405.22	2.99	29048	13.64	4.16	4331	12.71	78.73	5.72	12.91	12.64	0.47	6.63	1096.73	3978	11.79
7131	4508.54	3.06	30470	8.92	3.29	2840	17.30	80.76	4.65	10.90	7.85	0.43	6.63	1335.98	4643	6.32
7130	4511.66	3.06	29543	6.16	2.60	1944	22.57	78.16	3.77	8.14	5.25	0.38	6.63	1040.03	3973	7.26
7129	3953.70	2.68	25561	15.86	4.49	5021	10.45	77.18	5.35	12.75	14.81	0.51	6.71	997.50	3842	18.43
7128	3933.43	2.67	25398	11.69	4.04	3710	12.37	77.07	4.48	11.13	9.43	0.49	6.54	1004.33	4094	18.06
7126	3998.08	2.71	25112	9.68	3.72	3050	14.15	74.87	3.94	10.06	7.29	0.47	6.80	885.63	3937	-7.92
7125	3389.30	2.30	21607	18.10	4.78	5702	8.35	76.08	4.90	12.66	17.15	0.54	6.63	853.95	3842	-10.78
7121	3153.93	2.14	20947	8.77	2.84	2790	13.54	79.37	2.76	7.85	10.94	0.47	6.38	895.50	4426	-4.56
7120	2324.03	1.58	14796	20.36	4.88	6448	5.63	76.01	3.32	10.17	20.11	0.61	6.80	665.70	3691	-6.20

Run #	\dot{m}_L [lbm/hr]	V_{SL} [ft/sec]	Re_{SL}	\dot{m}_G [lbm/hr]	V_{SG} [ft/sec]	Re_{SG}	X	T_{MIX} [°F]	P_{MIX} [psi]	ΔP [inH ₂ O]	P_G [psi]	α	Pr_L	\bar{h}_{TP} [Btu/hr-ft ² -°F]	Q" [Btu/ft ² -hr]	Heat Balance Error [%]
Slug Flow Pattern (53 data points - Cont'd)																
7119	2120.84	1.44	13791	14.19	4.71	4493	6.09	77.58	2.23	6.80	10.48	0.61	6.63	568.73	3652	-12.71
7118	2307.78	1.57	15233	12.26	4.45	3890	7.17	78.86	2.24	6.63	8.29	0.59	6.63	626.45	3931	-2.45
7117	2156.20	1.46	13903	19.86	4.86	6287	5.32	76.92	3.33	8.96	19.41	0.62	6.63	632.53	3537	-10.04
7116	2008.87	1.36	13240	7.97	3.58	2532	8.38	78.79	1.28	4.39	3.92	0.58	6.63	466.55	3674	-11.16
7115	1891.14	1.28	12644	1.68	0.89	536	29.59	79.84	0.61	1.31	1.03	0.35	6.54	441.53	4188	-7.87
7114	1442.09	0.98	9145	16.83	5.00	5328	3.91	75.67	1.70	4.76	13.46	0.68	6.80	439.20	3627	-3.27
7113	1783.80	1.21	12047	5.41	2.71	1708	10.06	80.80	0.91	2.71	2.14	0.55	6.38	385.75	3567	-7.62
7112	1651.26	1.12	10848	8.90	3.90	2824	6.44	78.43	1.27	4.16	4.39	0.62	6.63	419.05	3768	-4.73
7110	1520.96	1.03	10093	9.91	4.40	3120	5.37	79.24	1.20	3.80	4.36	0.65	6.46	385.25	3594	-7.44
7109	1729.91	1.17	12164	3.84	2.04	1208	12.87	83.97	0.73	1.74	1.27	0.51	5.99	363.40	3545	-13.39
7107	3718.28	2.52	24429	12.07	4.42	3813	11.07	78.47	3.87	11.63	8.28	0.51	6.38	757.80	3409	2.18
7104	3232.66	2.19	20604	5.20	2.44	1643	18.40	76.03	2.14	5.30	3.22	0.43	6.46	596.33	2774	-18.13
7102	2706.09	1.84	16995	5.76	2.73	1829	14.25	74.83	1.76	4.68	2.91	0.49	6.46	508.10	2844	-8.80

Run #	\dot{m}_L [lbm/hr]	V_{SL} [ft/sec]	Re_{SL}	\dot{m}_G [lbm/hr]	V_{SG} [ft/sec]	Re_{SG}	X	T_{MIX} [°F]	P_{MIX} [psi]	ΔP [inH ₂ O]	P_G [psi]	α	Pr_L	\bar{h}_{TP} [Btu/hr-ft ² -°F]	Q'' [Btu/ft ² -hr]	Heat Balance Error [%]
Slug Flow Pattern (53 data points - Cont'd)																
5120	1937.12	1.31	11626	2.68	1.44	845	19.77	71.37	0.65	1.52	1.40	0.43	6.63	327.18	2202	-18.99
Min.	343.74	0.23	2468	1.68	0.89	536	2.13	71.37	0.06	0.34	0.72	0.27	5.20	171.55	2202	-18.99
Max.	5179.73	3.51	35503	20.36	5.00	6448	41.59	99.76	7.60	12.93	20.11	0.78	6.98	1370.58	4643	18.43
Avg.	2269.63	1.54	15013	8.04	3.04	2545	10.74	82.54	2.14	5.30	5.77	0.56	6.26	567.51	3709	1.85

Run #	\dot{m}_L [lbm/hr]	V_{SL} [ft/sec]	Re_{SL}	\dot{m}_G [lbm/hr]	V_{SG} [ft/sec]	Re_{SG}	X	T_{MIX} [°F]	P_{MIX} [psi]	ΔP [inH ₂ O]	P_G [psi]	α	Pr_L	\bar{h}_{TP} [Btu/hr-ft ² °F]	Q'' [Btu/ft ² -hr]	Heat Balance Error [%]
Wavy Flow Pattern (20 data points)																
8141	117.04	0.08	647	24.64	4.97	7800	0.35	65.25	0.35	0.91	26.61	0.90	6.63	327.48	1097	16.48
8140	118.18	0.08	674	22.28	5.03	7055	0.37	66.30	0.30	0.66	22.18	0.90	6.63	170.25	1102	8.0
8138	114.57	0.08	636	28.43	4.96	9000	0.32	65.19	0.48	0.95	33.01	0.90	6.63	426.38	1093	21.49
8137	126.38	0.09	688	27.02	5.01	8556	0.36	64.89	0.43	1.07	30.21	0.89	6.63	372.53	1164	15.49
8135	126.28	0.09	697	24.16	5.05	7650	0.38	65.78	0.34	0.69	25.17	0.89	6.63	207.28	1207	14.56
8134	126.64	0.09	692	22.74	5.09	7199	0.38	65.28	0.29	0.80	22.48	0.89	6.63	214.85	1211	15.93
8133	150.45	0.10	815	24.79	5.05	7848	0.43	63.96	0.38	0.78	26.22	0.88	6.63	244.45	1399	11.42
8132	151.28	0.10	828	21.33	5.16	6754	0.46	65.07	0.27	0.66	19.73	0.88	6.63	189.53	1384	6.13
8131	148.41	0.10	827	26.13	5.06	8272	0.42	64.95	0.41	1.18	28.29	0.88	6.63	382.53	1380	17.30
8130	145.48	0.10	811	31.14	5.04	9887	0.39	66.04	0.60	1.21	36.58	0.89	6.80	602.10	1331	20.48
8128	187.25	0.13	1034	23.20	5.08	7366	0.54	65.94	0.35	0.74	23.22	0.87	6.80	284.93	1477	7.20
8127	185.03	0.13	995	26.02	5.00	8260	0.52	63.21	0.43	0.99	28.53	0.87	6.80	403.75	1495	11.03
8126	186.78	0.13	1024	25.87	5.01	8236	0.52	65.23	0.45	0.99	28.00	0.87	6.80	351.10	1511	9.01

Run #	\dot{m}_L [lbm/hr]	V_{SL} [ft/sec]	Re_{SL}	\dot{m}_G [lbm/hr]	V_{SG} [ft/sec]	Re_{SG}	X	T_{MIX} [°F]	P_{MIX} [psi]	ΔP [inH ₂ O]	P_G [psi]	α	Pr_L	\bar{h}_{TP} [Btu/hr-ft ² -°F]	Q'' [Btu/ft ² -hr]	Heat Balance Error [%]
Wavy Flow Pattern (20 data points - Cont'd)																
8125	306.78	0.21	1717	31.02	4.93	9875	0.77	66.50	0.86	2.33	37.33	0.83	6.80	722.60	1664	14.19
8124	312.58	0.21	1829	25.08	4.85	7983	0.85	69.98	0.67	1.56	28.07	0.83	6.80	470.88	1611	4.68
8121	283.70	0.19	1811	24.51	5.06	7780	0.77	75.72	0.56	1.06	25.49	0.84	6.80	739.38	1486	16.73
8120	270.83	0.18	1733	25.35	5.09	8025	0.73	76.49	0.56	1.56	26.75	0.84	6.80	749.90	1572	19.88
8119	257.54	0.17	1646	25.35	5.07	8048	0.70	75.41	0.55	1.05	26.78	0.85	6.80	617.35	1578	14.18
8116	237.69	0.16	1259	26.57	4.98	8411	0.64	61.45	0.58	1.42	29.76	0.85	6.80	495.13	1199	11.21
8114	257.96	0.17	1601	21.91	4.95	6973	0.75	73.26	0.45	0.87	21.93	0.84	6.98	374.28	1131	18.60
Min.	114.57	0.08	636	21.33	4.85	6754	0.32	61.45	0.27	0.66	19.73	0.83	6.63	170.25	1093	4.68
Max.	312.58	0.21	1829	31.14	5.16	9887	0.85	76.49	0.87	2.33	37.33	0.90	6.99	749.90	1664	21.49
Avg.	190.54	0.13	1098	25.38	5.02	8049	0.53	67.30	0.47	1.07	27.33	0.87	6.74	417.33	1355	13.70

VITA 2

Dongwoo Kim

Candidate for the degree of

Doctor of Philosophy

Thesis: AN EXPERIMENTAL AND EMPIRICAL INVESTIGATION OF
CONVECTIVE HEAT TRANSFER FOR GAS-LIQUID TWO-PHASE FLOW
IN VERTICAL AND HORIZONTAL PIPES

Major Field: Mechanical Engineering

Biographical:

Personal Data: Born in Seoul, Korea, on August 23, 1965, the son of Sangok Kim and Yunok Koo.

Education: Graduated from Baemoon high school, Seoul, Korea in February 1984; received Bachelor of Science degree in Mechanical Engineering from Soongsil University, Seoul, Korea in February 1988; received the Master of Science degree in Mechanical Engineering from Oklahoma State University, Stillwater, Oklahoma in July 1994. Completed the requirements for the Doctor of Philosophy degree at Oklahoma State University in July 2000.

Experience: School of Mechanical and Aerospace Engineering as a graduate research assistant; Oklahoma State University, School of Mechanical and Aerospace Engineering, 1995 to 2000. School of Mechanical and Aerospace Engineering as a teaching assistant; Oklahoma State University, School of Mechanical and Aerospace Engineering, 1995 to 1999.

Professional Membership: American Society of Mechanical Engineers (ASME), Korean Scientists and Engineers in America (KSEA).